

Fall 2003

Statistically Designed Spheronization and Scale-Up of Ibuprofen Microparticulates Using the Rotor Disk Fluid-Bed Technology: Coating for Prolonged Release and Hard Gelatin Encapsulation of Microparticulates

Beatrice Chukwumezie

Follow this and additional works at: <https://dsc.duq.edu/etd>

Recommended Citation

Chukwumezie, B. (2003). Statistically Designed Spheronization and Scale-Up of Ibuprofen Microparticulates Using the Rotor Disk Fluid-Bed Technology: Coating for Prolonged Release and Hard Gelatin Encapsulation of Microparticulates (Doctoral dissertation, Duquesne University). Retrieved from <https://dsc.duq.edu/etd/407>

This Immediate Access is brought to you for free and open access by Duquesne Scholarship Collection. It has been accepted for inclusion in Electronic Theses and Dissertations by an authorized administrator of Duquesne Scholarship Collection. For more information, please contact phillips@duq.edu.

STATISTICALLY DESIGNED SPHERONIZATION AND SCALE-UP
OF IBUPROFEN MICROPARTICULATES USING THE ROTOR DISK FLUID-BED
TECHNOLOGY: COATING FOR PROLONGED RELEASE AND HARD GELATIN
ENCAPSULATION OF MICROPARTICULATES

A Dissertation

Presented to the Graduate School of Pharmaceutical Sciences

Duquesne University

In Partial Fulfillment of the
Requirements for the Degree
of
Doctor of Philosophy

By

Sr. Beatrice Nkem Chukwumezie, D.M.M.M.

August, 2003

©Copyright by

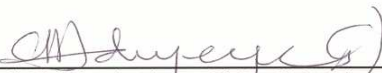
Sr. Beatrice Nkem Chukwumezie, D.M.M.M.

2003


All rights reserved

DISSERTATION EXAMINATION FORM


Sr. Beatrice Nkem. Chukwumezie was examined in an oral defense of her dissertation in partial fulfillment of the degree of doctor of philosophy and we, the undersigned, find that she (has/~~has not~~) presented an adequate report and (is/~~is not~~) satisfactorily familiar with the facts related to the dissertation signed this the Nineteenth day of August, Two Thousand and Three.




Moji Christianah Adeyeye, Ph.D., Chair, Dissertation Committee
Professor of Pharmaceutics
Graduate School of Pharmaceutical Sciences, Duquesne University
Pittsburgh, PA




James K. Drennen III, Ph.D., Associate Professor of Pharmaceutics and
Division Head of Pharmaceutics Sciences
Graduate School of Pharmaceutical Sciences, Duquesne University
Pittsburgh, PA



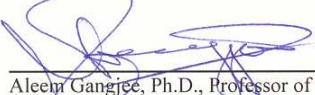
David A. Johnson, Ph.D., Associate Professor of Pharmacology-Toxicology
Graduate School of Pharmaceutical Sciences, Duquesne University
Pittsburgh, PA




Frank J. D'Amico, Ph.D., Professor of Mathematics
McAnulty College & Graduate School of Liberal Arts, Duquesne University
Pittsburgh, PA



N. K. Ebube, Ph.D., Research & Development Manager
Wyeth Consumer Healthcare, Richmond, Virginia



Aleem Gangjee, Ph.D., Professor of Medicinal Chemistry
Mylan School of Pharmacy Distinguished Professor
Director, Graduate School of Pharmaceutical Sciences, Duquesne University
Pittsburgh, PA



R. Pete Vanderveen, Ph.D., Dean and Professor
Mylan School of Pharmacy and the Graduate School of Pharmaceutical Sciences
Duquesne University, Pittsburgh, PA

APPROVAL PAGE

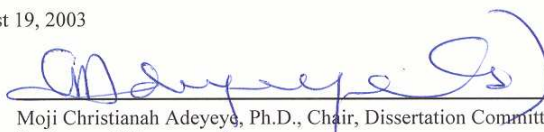
Name: Sr. Beatrice Nkem. Chukwumezie

Dissertation: Statistically Designed Spheronization and Scale-up of Ibuprofen
Microparticulates Using the Fluid-bed Rotor Disk Technology: Coating for
Prolonged Release and Hard Gelatin Encapsulation of Microparticulates

Degree: Doctor of Philosophy

Date: August 19, 2003

APPROVED



Moji Christianah Adeyeye, Ph.D., Chair, Dissertation Committee
Professor of Pharmaceutics
Graduate School of Pharmaceutical Sciences, Duquesne University
Pittsburgh, PA

APPROVED



James K. Drennen III, Ph.D., Associate Professor of Pharmaceutics and
Division Head of Pharmaceutical Sciences
Graduate School of Pharmaceutical Sciences, Duquesne University
Pittsburgh, PA

APPROVED




David A. Johnson, Ph.D.
Associate Professor of Pharmacology-Toxicology
Graduate School of Pharmaceutical Sciences, Duquesne University
Pittsburgh, PA

APPROVED



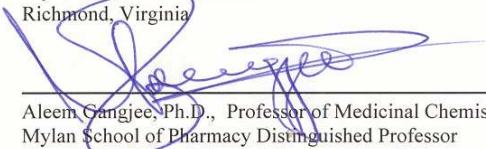
Frank T. D'Amico, Ph.D., Professor of Mathematics
McAnulty College & Graduate School of Liberal Arts
Duquesne University, Pittsburgh, PA

APPROVED



N. K. Ebube, Ph.D., Research & Development Manager,
Wyeth Consumer Healthcare
Richmond, Virginia

APPROVED &
ACCEPTED



Aleem Gangjee, Ph.D., Professor of Medicinal Chemistry
Mylan School of Pharmacy Distinguished Professor
Director, Graduate School of Pharmaceutical Sciences
Duquesne University, Pittsburgh, PA

APPROVED &
ACCEPTED



R. Pete Vanderveen, Ph.D., Dean and Professor
Mylan School of Pharmacy and the
Graduate School of Pharmaceutical Sciences, Duquesne University
Pittsburgh, PA

To My late dad, Chief Sir Anthony N. Chukwumezie

and

Our late Father Founder, Rt. Rev. Dr. Anthony G. Nwedo, C.S.S.P.

and

My natural family members, especially my mum and my sister Njide

and

My religious family members, especially Rev. Mothers M. Assumpta and M. Paul

ACKNOWLEDGEMENTS

I would like to thank my advisor Dr. Moji Christianah Adeyeye for her consistent guidance and encouragement in my academic and personal life.

I would like to thank my dissertation defense committee members Dr. Frank D'Amico, Dr. James K. Drennen, Dr. David Johnson, and Dr. N. K. Ebube for their useful suggestions. I also acknowledge with gratitude Dr. D'Amico's guidance with the statistical part of the work. I am grateful to the workers at VPS Corporation, Cranbury and Vector Corporation, Iowa for the use of their fluid-bed machines, especially Mr. Mark Wojcik and Mr. Paul Malak for their help with the operation of the machines. I am grateful to the workers at Romaco Incorporation, particularly Ms. B. Smith, Mr. Kyle and Mr. R. Engenhardt for the use of the encapsulation machine, to Mr. H. Piekema for his assistance with the operation of the machine. A special gratitude to the Dean, faculty and administrative staff of the Pharmacy Department, particularly Drs. Adeyeye, Drennen and Ganjee for their understanding during my very difficult moment.

I am grateful to Albemarle Corporation, LA, and FMC Corporation, NJ, for their generous supply of ibuprofen and Avicel[®] respectively. I thank Rohm Technical Inc., MA, and Colorcon, PA, for their kind supply of Eudragit[®] and Surelease[®] respectively. I am also grateful to Dan, Dave and Andrew as well as Derby, Nancy, Jackie, Wayne and Mr. Morrison of Duquesne University for their technical and administrative services respectively. I thank Mr. Al Stewart of University of Pittsburgh for his assistance with the scanning electron microscopy.

I would like to thank all my colleagues, especially Dr. Mohamed Ghorab, Dr. Ashwin Jain and Ms Sabitha Katpally as well as Ms Betty Katondo for their moral support.

I am immensely grateful to my sister Njide for her profound support and for being there for me. I am also grateful to my mum and other siblings especially my sister Pat, brother Kanayo and In-laws Martins and Nkechi for all their support. I am indebted to the sisters of my religious order, especially Rev. Mothers Assumpta and Paul for their understanding, as well as Srs. Valen and Leta. I would like to thank the Knorr's family of K-7 garage, Mr. & Mrs. J. Goethals, Mr. & Mrs. M. Manjoine, Mr. & Mrs. Scales, Mr. & Mrs Haasl, Sr. Rosalie & community, Sr. Monica & community, McNerny's family, M. Janosko, J. DeCrosta, P. Bolea, K. Wade, and Fr. Hogan (C.S.Sp.) for their support. My gratitude goes to my friends, Rev. Frs. Joe, Wence, Chidi, Hil, Nwokedi, John, Goddy, and Pat Isichei for their encouragement.

To God Almighty I owe my profound gratitude for my life and humble accomplishment, while trusting in His mercy for the repose of the gentle soul of my darling father, the souls of our father founder, Mrs R. Dike and Auntie Lila, and for my future.

TABLE OF CONTENTS

	Page
APPROVAL PAGE	ii
DEDICATION	iii
ACKNOWLEDGEMENTS	iv
TABLE OF CONTENTS	v
LIST OF TABLES	xvi
LIST OF FIGURES	xxii
I. INTRODUCTION	1
A. Statement of the problem	1
B. Literature review	4
1. Ibuprofen	4
a. Therapeutic uses and side effects	4
b. Dosage form/Dosing	6
c. Solubility and flowability	7
2. Excipients	8
a. Microcrystalline Cellulose/Sodium Carboxymethyl Cellulose	8
b. Sodium Lauryl Sulfate	10
3. Microparticulate Drug Delivery Systems and Spheronization	11
a. Microparticulate drug delivery systems	11
b. Spheronization process	14
1. Mechanism of pellet formation	14

	Page
2. Extrusion/spheronization	18
i. Granulation	18
ii. Extrusion	19
iii. Spheronization	19
iv. Drying	20
3. Fluidized bed processes	21
i. Traditional fluid-bed technology	21
ii. Rotor disk fluid-bed	24
1. Equipment and components of the rotor disk fluid-bed	24
2. Rotor disk fluid-bed process	26
3. Factors affecting the rotor disk fluid-bed process	28
4. Optimization of equipment and process variables	34
a. Factorially designed experiments	34
b. Scale-up	36
1. The principles of geometric similarity	38
2. Reynolds' and Froude's number	39
3. Scale-up parameters	41
i. Rate of addition and amount of liquid binder in powder bed	41
ii. Fluidization air volume	42
iii. Rotational speed, centrifugal force and plate radius	43
5. Product variables and drug release	44
a. Product variables	44

	Page
1. Drug particle size	44
2. Drug load	45
b. Drug release	46
1. Immediate release of drugs	46
2. Drugs suitable for sustained drug delivery formulations	49
i. Drugs with short half-lives	49
ii. Drugs with high toxicity and low therapeutic index	50
3. Pellets and sustained drug release	51
4. Sustained release of drug	52
i. Sustained release delivery systems or devices	54
1. Dissolution-controlled products	55
2. Diffusion-controlled products	55
ii. Comparison of dissolution profiles	57
6. Polymeric membranes and sustained drug release	59
a. Surelease [®]	60
b. Poly(ethylacrylat-methylmethacrylat (Eudragit [®] NE 30D)	62
7. Hard gelatin encapsulation technology	65
a. Hard gelatin encapsulation	65
b. Hard gelatin capsule technology	67
c. Capsule filling machine instrumentation	68
d. Types of automatic capsule filling machines	69
1. Tamping filling machine	69

	Page
2. Dosator filling machine	72
3. Comparison of the tamp and dosator capsule filling machines	73
e. Stages of Hard gelatin encapsulation process	75
1. Rectification	75
2. Separation	75
3. Filling	76
4. Joining and ejection	76
f. Comparison of hard gelatin encapsulation of various dosage forms	76
1. Powder	76
2. Liquids and semi-liquids	77
3. Tablets	78
4. Pellets	78
II. EXPERIMENTAL	83
A. Materials and Equipment	83
B. Methodology	85
1. Feasibility studies in the spheronization and scale-up of ibuprofen microparticulates	85
a. Blending and spheronization	85
1. Spheronization of 0.75 kg trial batch	85
2. Spheronization of 1 kg batches	88
3. Spheronization of Pilot scale batches (5 kg and 10 kg batches)	92

	Page
b. Physical Characteristics of Developed Microparticulates	94
1. Yield of microparticulates	94
2. Particle size distribution	94
3. Density of the granules	95
4. Drug content and HPLC assays	96
5. Dissolution	97
6. Flowability	98
7. Granule friability test	99
8. Sphericity and roundness of granules	99
9. Scanning Electron Microscope (SEM)	100
c. Statistical analysis	100
2. Optimization of the developed process and product variables using statistically designed factorial experiment	100
a. Experimental design	100
b. Blending and spheronization	104
c. Physical characterization of spheroids	104
d. Statistical analysis	105
3. Evaluation of the effects of drug loading, particle size effects and scale-up to intermediate scale using the fluid-bed rotor-disk technology	106
a. Effects of drug particle size and drug loading on the characteristics of ibuprofen microparticulates	106
1. Experimental design	106

	Page
2. Blending and spheronization	109
3. Physical characterization of spheroids	111
4. Statistical analysis	112
b. Effects of intermediate size scale-up on the characteristics of ibuprofen microparticulates	112
1. Experimental design	112
2. Blending and spheronization	114
3. Physical characterization of spheroids	117
4. Statistical analysis	118
4. Coating and encapsulation of spheronized ibuprofen microparticulates using hard gelatin capsules	118
a. Polymer film coating of spheroids	118
1. Preliminary studies using Glatt fluid-bed	118
2. Experimental design for rotor-disk fluid-bed coating	119
3. Rotor disk fluid-bed coating	120
i. Coating of spheroids with Surelease [®] polymer	120
ii. Coating of spheroids with Eudragit [®] NE 30D polymer	123
4. Physical characterization of spheroids	123
i. Comparison of dissolution profiles	124
ii. Mathematical modeling of drug release	125
5. Statistical analysis	126

	Page
b. Hard Gelatin Encapsulation of Spheroids	126
1. Experimental design	126
2. Pellet encapsulation	129
3. Physical characterization	130
i. Fill weight and coefficient of fill variation	130
ii. Dissolution test	130
4. Statistical analysis	131
III. RESULTS AND DISCUSSIONS	132
1. Feasibility studies in the spheronization and scale-up of ibuprofen microparticulates	129
a. Drying time	132
b. Physical characteristics of developed microparticulates	133
1. Yield of microparticulates	133
i. Yield of one kilogram batches	133
ii. Yield of pilot scale-up batches	137
2. Density, Carr's index and Flowability	138
3. Drug content and Dissolution analyses	138
4. Friability	142
5. Sphericity and morphology of the granules	142
6. Size distribution of granules	145

	Page
2. Optimization of the developed process and product	
variables using statistically designed factorial experiment	148
a. Experimental design	148
b. Physical characterization of spheroids	154
1. Scanning electron microscopy	154
2. Moisture content determination (Loss on drying)	154
3. Yield and usable fractions of spheroids	162
4. Drug content	163
5. Friability	164
6. True density and compressibility	164
7. Sphericity of the granules	166
8. Size distribution of granules	167
9. Ibuprofen release from granules	169
3. Effects of drug particle size, drug loading and intermediate size	
scale up on the characteristics of ibuprofen microparticulates	170
a. Effects of drug particle size and drug loading	170
1. Experimental design	170
2. Physical characterization of spheroids	173
i. Scanning electron microscopy	173
ii. Moisture content/Loss on drying analyses	174
iii. Yield and usable fractions of spheroids	177
iv. Drug content	178

	Page
v. Friability	178
vi. True density and compressibility	179
vii. Flowability	179
viii. Sphericity of the granules	180
ix. Size distribution of granules	180
x. Ibuprofen release from granules	180
b. Effects of intermediate size scale-up on the characteristics of ibuprofen microparticulates	182
1. Experimental design	182
2. Physical characterization of spheroids	185
i. Scanning electron microscopy	185
ii. Moisture content/Loss on drying analyses	188
iii. Yield and usable fractions of spheroids	189
iv. Drug content	190
v. Friability	190
vi. True density and compressibility	190
vii. Flowability	191
viii. Sphericity of the granules	191
ix. Size distribution of granules	191
x. Ibuprofen release from granules	192

	Page
4. Coating and encapsulation of spheronized ibuprofen	
microparticulates using hard gelatin capsules	193
a. Effects of coating	193
1. Experimental design	193
2. Physical characterization of spheroids	196
i. Scanning electron microscopy	196
ii. Yield and usable fractions of spheroids	197
iii. Drug content	200
iv. Friability	200
v. Densities	201
vi. Flowability	201
vii. Sphericity of the granules	202
viii. Size distribution of granules	202
ix. Ibuprofen release from pellets	203
x. Kinetics of drug release	205
xi. Comparison of in vitro dissolution profiles using difference and similarity factors	210
b. Effect of encapsulation on the physical characteristics of ibuprofen microparticulates	212
1. Experimental design and Physical characteristics of pellets	212
i. Formulation type	212
ii. Operational speed	215

	Page
iii. Shuttle speed	216
iv. Drug content	218
v. Ibuprofen release from granules	218
vi. Drug release kinetics	220
vii. Comparison of in vitro dissolution profiles using difference and similarity factors	221
IV. CONCLUSIONS	225
V. APPENDIX	228
VI. BIBLIOGRAPHY	260
VII. ABSTRACT	291

LIST OF TABLES

		Page
Table I:	Characteristics of Fluid-bed Granulation and Coating Processes	25
Table II:	List of Materials	83
Table III:	List of Equipment	84
Table IV:	Spheronization Conditions and Process Parameters	87
Table VA:	Formulation Variables	90
Table VB:	Process Variables	90
Table VI:	Variables Utilized in the Preliminary Trial Batches	91
Table VII:	Experimental Design Matrix for Optimization Studies	102
Table VIII:	Experimental Design for Optimization Studies	103
Table IX:	Experimental Design Matrix for Drug Particle Size and Drug Load Effects on Spheroid Characteristics	107
Table X:	Experimental Design for Drug Particle Size and Drug Load Effects on Spheroid Characteristics	108
Table XI:	Binder and Time Conditions During Spheronization and Drying Processes	110
Table XII:	Experimental Design Matrix for Intermediate Size Scale-up Effect on the Characteristics of Ibuprofen Microparticulates	113
Table XIII:	Experimental Design for Intermediate Size Scale-up Effect on the Characteristics of Ibuprofen Microparticulates	114
Table XIV:	Spheronization Conditions of Scale-up Batches	116

	Page
Table XV: Binder and Time Conditions for Spheronization and Drying Processes of Intermediate Batch Size Ibuprofen Microparticulates	117
Table XVI: Experimental Design for the Coating of Spheronized Ibuprofen Microparticulates	120
Table XVII: Conditions and Process Parameters Used for the Coating of 700 g Ibuprofen Spheroids	121
Table XVIII: Formulation of the Aqueous Dispersions Used for the Coating of 700 g Ibuprofen Spheroids	122
Table XIX: Experimental Design Matrix for Encapsulation of Coated and Uncoated Ibuprofen Microparticulates	128
Table XXA: Physical Characteristics of 1 kg Batches	133
Table XXB: Physical Characteristics of Scale-up Batches	134
Table XXI: Accuracy and precision of HPLC Assay	140
Table XXII: Physical Characteristics of Optimized Ibuprofen Spheroids	157
Table XXIII: <i>P</i> -values of Independent Variables for the Optimized Ibuprofen Spheroids	159
Table XXIV: Summary of the Optimized Ibuprofen Spheroid Qualities	160
Table XXV: Physical Characteristics of Drug Micron Size/Drug Load Batches	175
Table XXVI: <i>P</i> -values of Independent Variables of Drug Micron Size/Drug Load Batches	176
Table XXVII: Physical Characteristics of Batch Size/Drug Load Batches	186

	Page
Table XXVIII: <i>P</i> -values of Independent Variables of Batch Size/Drug Load Batches	187
Table XXIX: Physical Characteristics of Coated Ibuprofen Spheroids	198
Table XXX: <i>P</i> -values of Independent Variables of Coated Ibuprofen Spheroids	199
Table XXXI: Results of Regression Equations for Drug Release from Uncoated and Coated Pellets According to Different Kinetic Models	208
Table XXXII: Mean Percent Dissolution of Ibuprofen Spheroids at the Specified Time Points	210
Table XXXIII: Values of Difference and Similarity Factors for Coated and Uncoated Pellets	211
Table XXXIV: Effects of Encapsulation Variables on Encapsulated and Unencapsulated (Uncoated and Coated) Ibuprofen Spheroids	213
Table XXXV: <i>P</i> -values of Independent Variables of Encapsulated and Unencapsulated Ibuprofen Spheroids	214
Table XXXVI: Results of Regression Equations for Drug Release from Encapsulated and Unencapsulated (Uncoated and Coated) Pellets According to Different Kinetic Models	220
Table XXXVII: Mean Percent Dissolution of Encapsulated Ibuprofen Spheroids at the Specified Time Points	222
Table XXXVIII: Values of of Difference and Similarity Factors for Encapsulated (Coated and Uncoated) Pellets	223

	Page
Table XXXIX: Sphericity Analysis of SS/Sm/1 kg (Trial 4) Batch from Feasibility Studies	231
Table XL: Sphericity Analysis of SS/Sm/5 kg (Trial 12) Batch from Feasibility Studies	232
Table XLI: Sphericity Analysis of SS/Sm/10 kg (Trial 13) Batch from Feasibility Studies	233
Table XLII: Sphericity Analysis of Tef/Waf/1 kg (Trial 7) Batch from Feasibility Studies	234
Table XLIII: Sphericity Analysis of Tef/Waf/5 kg (Trial 14) Batch from Feasibility Studies	235
Table XLIV: Sphericity Analysis of Tef/Waf/10 kg (Trial 15) Batch from Feasibility Studies	236
Table XLV: Dissolution Data for Ibuprofen Release of Pilot Size Scale-up Replicated Batches from Feasibility Studies	237
Table XLVI: Sphericity Analysis of LbHSSS-sm (Formulation 5) Spheroids from Experimentally Designed Batches	239
Table XLVII: Sphericity Analysis of HbLsSS-sm (Formulation 11) Spheroids from Experimentally Designed Batches	240
Table XLVIII: Dissolution Data for Ibuprofen Release of Experimentally Designed Replicated Batches	241

	Page
Table XLIX. Sphericity Analysis of Ibuprofen Spheroids from Drug Load/Drug Particle Size Replicated Batches (1kg, 20 Micron Size, 65% Drug Load)	243
Table L: Sphericity Analysis of Ibuprofen Spheroids from Drug Load/Drug Particle Size Replicated Batches (1kg, 40 Micron Size, 65% Drug Load)	244
Table LI: Dissolution Data for Ibuprofen Release of Drug Load/Drug Particle Size Replicated Batches	245
Table LII: Sphericity Analysis of Intermediate Scale-up Ibuprofen Replicated Batch (20 Micron, 50% Drug Load, 50kg Batch Size)	247
Table LIII: Sphericity Analysis of Intermediate Scale-up Ibuprofen Replicated Batch (20 Micron, 65% Drug Load, 50 kg Batch Size)	248
Table LIV: Dissolution Data for Ibuprofen Release of Intermediate Batch size (Replicated Batches)	249
Table LV: Sphericity Analysis of SR 12.5% Coated Ibuprofen Spheroids Replicated Batches)	251
Table LVI: Sphericity Analysis of EUD15.5% Coated Ibuprofen Spheroids (Replicated Batches)	252
Table LVII: Dissolution Data for Ibuprofen Release Coated Replicated Batches	253
Table LVIII: Fill Weight and Statistical Parameters of Uncoated Ibuprofen Spheroids Encapsulated at 75 rpm and 280 msecs	254

	Page
Table LVIX: Fill Weight and Statistical Parameters of Uncoated Ibuprofen Spheroids Encapsulated at 75 rpm and 300 msec	255
Table LX: Fill Weight and Statistical Parameters of Coated Ibuprofen Spheroids Encapsulated at 75 rpm and 280 msec	256
Table LXI: Fill Weight and Statistical Parameters of Coated Ibuprofen Spheroids Encapsulated at 75 rpm and 300 msec	257
Table LXIIA: Dissolution Data for Ibuprofen Release of Encapsulated and Unencapsulated (Uncoated) Spheroids	258
Table LXIIB: Dissolution Data for Ibuprofen Release of Encapsulated and Unencapsulated (Coated) Spheroids	259

LIST OF FIGURES

	Page
Figure 1: Structure of ibuprofen	4
Figure 2: The destructive nucleation growth mechanism of high shear pelletisation	16
Figure 3: Mechanisms of pellet formation in traditional spheronization methods	20
Figure 4: Fluid-bed equipment	22
Figure 5: Fluidized bed processes	24
Figure 6: Rotor disk fluid-bed product container with rotor disk insert and spray gun	26
Figure 7: Schematic representation of rotor disk technology using tangential spray gun	27
Figure 8: Types of dosage forms	48
Figure 9: Drug levels in the blood with immediate and sustained release profiles	49
Figure 10: Delivery of drug from typical matrix and reservoir devices	55
Figure 11: Release profiles of ibuprofen from tablets in dissolution media	61
Figure 12: Coating of potassium chloride crystals with Eudragit [®] NE 30 D	63
Figure 13: Capsules as versatile container for different pharmaceutical dosage forms	66
Figure 14: Capsules showing approximate sizes and typical fill weight	68

	Page
Figure 15: Tamp capsule filling machine	74
Figure 16: Tamping pellet filling system	79
Figure 17: Components of Vector FL-Multi 1 equipment	86
Figure 18: Components of the Vector FLM-15 equipment	88
Figure 19: Rotor-disk plates for fluid bed machines	93
Figure 20: Components of the Vector FLN-120 equipment	115
Figure 21: Cross-section of pellet feeder assembly	127
Figure 22: Calibration curve for HPLC analyses	139
Figure 23: Profiles of small and pilot scales ibuprofen batches	141
Figure 24: Scanning electron micrographs (x30) of small and pilot scales ibuprofen batches	144
Figure 25: Scanning electron micrographs (x200) of small and pilot scales ibuprofen batches	144
Figure 26: Geometric mean diameter of small and pilot scales ibuprofen batches	146
Figure 27: Pareto plots of effects of main factors on some product qualities (experimentally designed batches)	149
Figure 28: Interaction plots of the effects of main factors on specified qualities (experimentally designed batches)	153
Figure 29: Scanning electron micrographs (30x) of experimentally designed ibuprofen granules	155

	Page
Figure 30: Scanning electron micrographs (100x) of experimentally designed ibuprofen granules	156
Figure 31: Geometric mean diameters of experimentally designed replicated batches	167
Figure 32: Dissolution profiles of experimentally designed replicated batches	169
Figure 33. Pareto plots of effects of main factors on some product qualities (drug particle size/drug load batches)	171
Figure 34. Interaction plots of the effects of main factors some qualities of drug particle size/drug load batches	173
Figure 35: Scanning electron micrographs (30x) of 20 μm ibuprofen formulations (drug particle size/drug load batches)	174
Figure 36: The moisture content-time profile of 20 micron ibuprofen	177
Figure 37: Geometric mean diameters of drug particle size/drug load batches	181
Figure 38: Dissolution profiles of drug particle size/drug load batches	181
Figure 39: Pareto plots of effects of main factors on some product qualities (batch size/drug load batches)	183
Figure 40: Interaction plots of the effects of main factors on specified qualities (batch size/drug load batches)	184
Figure 41: Scanning electron micrographs (30x) of ibuprofen formulations (batch size/drug load batches)	185
Figure 42: The moisture content-time profile of scale-up batches	189

	Page
Figure 43: Geometric mean diameters of batch size/drug load batches	192
Figure 44: Dissolution profiles of batch size/drug load batches	192
Figure 45: Pareto plots of effects of main factors on some product qualities (Coated pellets)	194
Figure 46: Interaction plots of the effects of main factors on some product qualities (Coated pellets)	195
Figure 47: Scanning electron micrographs (30x) of ibuprofen granules (Coated pellets)	196
Figure 48: Scanning electron micrographs (100x) of ibuprofen granules (Coated pellets)	197
Figure 49: Geometric mean diameters of coated and uncoated ibuprofen pellets (Coated pellets)	203
Figure 50: Dissolution profiles of ibuprofen pellets (Coated pellets)	204
Figure 51: Mathematically modeled drug release of uncoated and coated ibuprofen pellets	207
Figure 52: First order release profiles from uncoated and coated ibuprofen pellets	209
Figure 53: Pareto plots of effects of main factors on some product qualities (Encapsulated pellets)	214
Figure 54: Average fill weight (\pm SD) of ibuprofen pellets	216
Figure 55: Percent coefficient variations of fill weight of ibuprofen pellets	217

	Page
Figure 56: Dissolution profiles of encapsulated and unencapsulated ibuprofen spheroids	219
Figure 57: Log-probability profiles for sieve analysis of 1 kg replicated batches from feasibility studies	229
Figure 58: Log-probability profiles for sieve analysis of pilot size scale-up (1 kg, 5kg and 10 kg) replicated batches from feasibility studies	230
Figure 59: Log-probability profiles for sieve analysis of experimentally designed replicated batches	238
Figure 60: Log-probability profiles for sieve analysis of drug load/drug particle size replicated batches	242
Figure 61: Log-probability profiles for sieve analysis of intermediate size scale-up replicated batches	246
Figure 62: Log-probability profiles for sieve analysis of uncoated and coated ibuprofen spheroids (replicated batches)	250

I. INTRODUCTION

A. Statement of the Problem

Ibuprofen is a prototypical nonsteroidal anti-inflammatory (NSAI) agent, used for the treatment of rheumatoid arthritis, post-operative pains, pains associated with common colds, etc. (1). The drug has also been shown to attenuate the effects of modulators of inflammation which are implicated in the pathogenesis of Alzheimer's disease (2,3).

Ibuprofen is a poorly water-soluble drug with poor flow and compressibility properties (4,5). Poor compressibility and flowability have continued to present considerable challenges in pharmaceutical unit processes such as tableting and filling of hard gelatin capsules. Flowability problems also result in poor content uniformity. Co-processing of ibuprofen with an excipient into ready-to-use microparticulates (spheroids) could potentially be useful to improve flowability, friability, compressibility and content uniformity of the drug (6,7). Moreover, co-processing with less number of excipients would reduce the problem of bulkiness usually associated with the multicomponent commercial formulations. In addition, spheroids have been shown to possess lower level of gastric irritation and fewer dose-dumping accidents (8).

In the development of spherical microparticulates or spheroids, extrusion spheronization has been the method of choice. However, it involves four major steps, and the process is difficult to optimize, reproduce and scale-up (9,10). In contrast, rotor-disk fluid-bed technology is a one-step closed process that utilizes a rotor, which can also be used for spheronization, drying, drug layering and coating. Moreover, the rotor-disk

fluid-bed can be automated, which enhances scalability, batch-to-batch reproducibility and reduction of process time and cost (6,11,12). The fluidization of the particles can also lead to cost-effective product with desirable content uniformity.

The fluid-bed operation is a multivariable process and optimization and scale-up of the process are difficult to accomplish (13,14). This is due to interplay of the variables and their influence on obtaining products with desirable qualities. Moreover, achieving desirable batch size, drug loading and the use of different particle sizes of the same drug to obtain good spheroid qualities were reported as major draw backs of the rotor-disk spheronization process, thus limiting the utility of the technology (15,16). Reports on this are limited especially on the optimization and scale-up of rotor-disk fluid-bed technology. This is possibly due to the fact that many companies could have proprietary information that are inaccessible to the general public. Therefore, optimization of the process through statistically designed experiments would lead to understanding of interplay or interaction of variables and their effects on formulation and subsequent scale-up.

In addition, ibuprofen, being a rapidly absorbed drug with high bioavailability (>80%) and short biologic half-life (1.5 - 2 hrs; 17), there is high probability for lack of patient compliance. Therefore, a sustained release formulation will alleviate this problem through reduction in dosing.

Ibuprofen is a potent non-specific cyclooxygenase and prostaglandin inhibitor which makes it amenable to significant adverse effects, including gastrointestinal tract irritation, following the large conventional oral delivery (18). The adverse gastrointestinal side effects of ibuprofen could occur both by local or systemic drug contact (19,20). This effect might be eliminated by coating for sustained release delivery

as well as encapsulation of the coated and uncoated microparticulates, which will ensure that less drug is in contact with the gastric mucosa per unit time (20,21), and also yield effective, safe and stable delivery systems for use in humans.

Several studies have shown the efficacy of sustained release ibuprofen tablets over conventional dosage forms (22-25). Brufen Retard[®], a sustained release ibuprofen that is marketed in Europe has also been shown to be effective as anti-inflammatory and analgesic agents at the recommended dose (26). However, no sustained release ibuprofen formulation has been found to exist in the market in the United States.

Therefore, the specific aims of this research are as follows:

- 1) Development of spheroids using the one pot rotor-disk fluid-bed technology, ibuprofen as the model drug, Avicel[®] as the major excipient and spheronization enhancer, sodium lauryl sulfate as lubricant and water as binder.
- 2) Optimization of the formulation and process variables using statistically designed factorial experiment.
- 3) Evaluation of the effects of drug particle size, different drug loads and scale-up up to intermediate production batch size on the the developed and optimized ibuprofen spheroids using the rotor-disk fluid-bed technology.
- 4) Polymer coating and encapsulation of coated and uncoated microparticulates using hard gelatin capsules for comparative evaluation of controlled and immediate release delivery systems.

B. Literature Review

1. Ibuprofen

a. Therapeutic uses and side effects

Ibuprofen (Figure 1) is an acidic drug with a pKa of 4.8 and a molecular weight of 206. It is a potent cyclooxygenase and prostaglandin inhibitor, an NSAID agent having anti-inflammatory, antipyretic and analgesic activity in both animals and humans. It is developed in 1960s and has been used for the treatment of rheumatoid arthritis, osteoarthritis, post-operative pains, pains associated with common colds, etc. (1). It has recently been implicated in Alzheimer's disease (2,3).

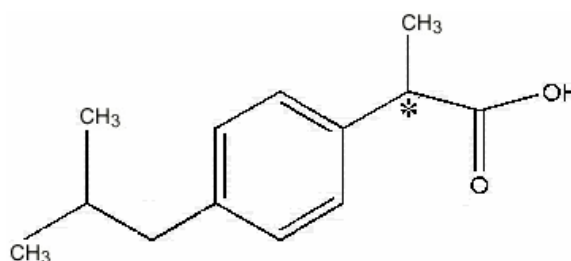


Figure 1: Structure of ibuprofen (27).

*: Chiral center constituting the R and S isomers of ibuprofen

As an antiinflammatory agent, ibuprofen inhibits cyclooxygenase (COX) enzymes, thereby inhibiting prostaglandin production (18,19). Two COX enzymes are known to be involved in prostaglandin synthesis, COX-1 and COX-2. COX-1 generates prostaglandins that maintain normal function in several organ systems, and are involved in the protection of gastrointestinal mucosa. COX-2 generates prostaglandins that mediate inflammatory

stimulus, and thereby cause inflammation and pain. The adverse gastrointestinal side effects of NSAIDs like ibuprofen are therefore related to COX-1 inhibition. Although the therapeutic efficacy of ibuprofen outweighs the severity of its side-effects (28), studies have shown an increased tendency of NSAIDs toward gastric irritation at higher doses (29). This effect could be regulated by coating and encapsulation of the drug, which will minimize the amount of drug that would be in contact with the gastric mucosa per unit time (20,21).

Ibuprofen has been implicated in the antiinflammatory modulation of Alzheimer's disease (2,3). Alzheimer's lesion is characterized by the development of β -amyloid protein deposits and neurofibrillary tangles. The protein deposits stimulate inflammation in the brain, which activates the immune cells and consequently elicit harmful substances. These include inflammatory cytokines, proteases and complement proteins that destroy nerve cells. Ibuprofen has been shown to interrupt this sequence, and thereby lessen the abnormal accumulation of β -amyloid (2,3,30).

Ibuprofen is also used in the prevention of *patent ductus arteriosus* (PDA; 31). The *ductus arteriosus* is a connection between the aorta and the pulmonary artery. It is part of the fetal pathway that helps to distribute oxygen from the mother to the baby's organs. Thus it facilitates blood flow and by-passes the lungs, which do not require high blood flow at this time of the fetal development. At birth, the lungs expand, the baby's blood vessels relax to accept more flow, and the *ductus arteriosus* usually closes on its own within the first 15 hours of life. However, sometimes the *ductus arteriosus* does not close on its own; a condition referred to as a *patent (open) ductus arteriosus*. This condition is prevalent in premature babies and can also occur in full term infants.

For newborns, NSAID such as indomethacin drug is normally administered which helps to constrict the muscle in the wall of the PDA in order to close it. Because of the potential side effects of indomethacin that includes a decline in cerebral blood flow and cerebral oxygen delivery, surgery is sometimes preferred to tie off the open duct. Some physicians also prefer to use ibuprofen instead of indomethacin, as the former has been shown to constrict the duct and also reduce the incidence of PDA in preterm infants, without the complications of indomethacin (32,33).

b. Dosage Forms/Dosing

Ibuprofen is a high dose drug with a short biologic half-life (1.5 - 2 hrs) and is therefore administered several times a day orally (34). For the immediate release products, the usual prescribed adult dose is 400 - 800 mg three or four times daily, with the maximum daily dose not exceeding 3.2 g. For the sustained release formulation, Brufen Retard[®], the recommended once or twice daily dosage (1600 mg) has been shown to provide effective control of arthritic symptoms for different patient groups compared to baseline, with significant overall improvements in pain and stiffness (34). Ibuprofen pediatric dosage form exist as tablets and suspensions, which range between 5 and 50 mg/kg daily with the maximum daily dose not exceeding 2.4 g (34).

For adults, ibuprofen is available (tablets and caplets) as oral immediate release solid dosage form. The most commercially available dosage form is the regular tablets (e. g. Motrin[®], Advil[®]), although chewable tablets, liquigel, oral drops and oral suspensions exist (35). Commercially available ibuprofen consist of not less than twelve excipients, which often lead to increased bulkiness of the oral dosage form, reduced

amount of the active and therefore increased frequency of intake. These factors could consequently reduce patient compliance. Intravenous ibuprofen injection also exists but as orphan drug (Children's Motrin[®]) for the treatment or prevention of *patent ductus arteriosus* (PDA; 31).

b. Solubility and flowability

Ibuprofen powder has a slight characteristic odor and is practically insoluble in water. It also shows poor dissolution and tableting behavior due to its hydrophobic structure (5). It is also very cohesive and exhibits poor flow characteristics (36). The physicochemical properties of ibuprofen have been improved by changes in its crystallinity and in surface properties (37). Also drug dissolution has been improved by various complexation techniques e.g. with cyclodextrines (38), and by the use of various excipients (22), including spray-drying of the drug particles with microcrystalline cellulose (MCC; 39). In the latter study, x-ray diffraction indicated that ibuprofen exists as very fine crystals on cellulose particles, which is facilitated by the rapid evaporation of the solvent during spray drying. This restricted crystal growth led to improved dissolution (39).

In a previous study (40), the incorporation of sodium carboxymethyl cellulose (NaCMC) to piroxicam- Avicel[®] PH-101 formulation (formulation A), or as a co-processed blend with MCC (Avicel[®] CL-611; formulation B) enhanced the release of piroxicam at 45 min from 30% (formulation A) to 95% (formulation B). The use of Avicel[®] RC-581 in a spheronization process has been shown to add plasticity to powder blend, thereby facilitating the formation of spherical pellets, and improving the

flowability of the formulation (41,42). Therefore, excipients such as MCC or MCC co-processed with polymers such as NaCMC, have shown good promise in granulation processes and could be useful in improving ibuprofen flowability, as well as in the development of ibuprofen microparticulates.

2. Excipients

a. Microcrystalline cellulose/Sodium carboxymethyl cellulose (Avicel®)

Microcrystalline cellulose/Sodium carboxymethyl cellulose (Avicel®) products are colloidal co-processed mixtures of microcrystalline cellulose (MCC) and sodium carboxymethyl cellulose (NaCMC). They are dispersible in water, and produce thixotropic gels at concentrations of >1.2% solids (43,44). They are also insoluble in organic solvents and dilute acids, and partially soluble in both dilute alkali and water. They consist of the RC and CL types in which the amount of carboxymethyl cellulose present can vary between 8.3 - 18.8% w/w. The RC-581 grade has lower concentration of NaCMC than the CL-611 grade. Both polymers are mostly used in solid dosage forms as diluents, lubricants, spheronization enhancers and/or binders (45,46).

Several studies (including our previous report in which RC-581 and CL-611 were co-processed with ibuprofen; 47) have shown that when used in solid dosage forms, there are no significant differences in granule quality obtained from both grades (44). Major differences have nevertheless been observed when used in suspensions due to their end product viscosity/gel strength and methods of dispersion required for complete activation, and where they exhibit a high degree of thixotropy (43,44). Additionally, differences

have been observed when compared with other Avicel[®] types (grades that do not contain NaCMC), even in solid dosage forms (48). Garcia, *et al.* showed that in the formulation of glipizide microparticulate spheres and tablet dosage forms, the former, containing Avicel[®] PH-101 gave higher drug release than spheres of the same composition but prepared with Avicel[®] RC-581 (48). On the contrary, tableted spherical formulations containing Avicel[®] RC-581 gave higher release rate constants than the formulations of the same composition prepared with Avicel[®] PH-101. These were attributed to differences in porosity of the formulations. Spheres prepared with Avicel[®] PH-101 had more pores than spheres of the same composition prepared with Avicel[®] RC-581, that resulted in swelling of RC-581 and slower drug release. It is also possible that milling of the spheroids required for tableting as well as tablet compression affected the normal packing of the polymer in the tablets. This will affect the porosity of the formulations and also play a role in determining their amount of water retention, and might have led to higher drug release of tablets produced using RC-581.

Microcrystalline cellulose (e.g. RC-581) has been used as a processing aid in traditional extrusion spheronization. The MCC acts like a molecular sponge, absorbing considerable amount of water and facilitate binding and lubrication of the moistened powder mass during extrusion (49-51). It has also been shown that incorporation of surfactants, for example, sodium lauryl sulfate (SLS), to a spheronization system can improve particle-particle and particle-liquid interactions, as well as flowability of the granules produced (52,53). These observations justified the continued use of Avicel[®] and SLS in spheronization process.

b. Sodium Lauryl Sulfate

Sodium lauryl sulfate is an anionic surfactant that has been extensively used to reduce the surface tension of pharmaceutical systems. It has been utilized as anionic emulsifier at 0.5 - 2.5%, tablet lubricant and wetting agent at 1 - 2%. It has been used widely in traditional extrusion-spheronization as a wetting agent (53,54), and to impart plasticity to extrudates (55). Studies have shown that the presence of a liquid binder in the formulation is necessary for the formation of pellets by the extrusion/spheronization technique (51,56). The spreading of the liquid can be influenced by viscosity and surface tension. The latter affects possible changes in accessibility of the pore structure within the powder bed. Both viscosity and surface tension can influence the consistency of the wet powder mass, and thereby affect the ability to produce spherical pellets.

Incorporation of a surfactant to a spheronization system has been shown to reduce the contact angle between the solid and liquid, which enhances the interaction between the liquid and powder (56). Also, the addition of surfactants extends the period of constant water level slightly, as well as eases the spreading of liquid to a greater extent. Larger pellets with narrow size distribution are produced due to particle-particle interaction when surfactants are present. The packing of the particles within the pellets is also influenced by the presence of surfactants, which results from liquid/solid interactions. Although SLS had such commendable influence on water movement, it was observed to have less effect on porosity of the granules (56).

The effects of three surfactants, namely, sorbitan monolaurate (SML), sorbitan monododecanoate (SMD), and sodium lauryl sulfate (SLS) on the physicochemical properties of sulfadimidine tablets have been studied (57). Tablets were compressed

from granules processed by the fluid-bed granulation method. All batches of the granulations were compressed to the same weight at constant pressure. The granulations that contained 0.50 SML, 0.20 or 0.50% SMD produced compressed tablets with high friability, in contrast to the granulations containing SLS. With regard to their efficiency to improve both tablet disintegration and dissolution, the surfactants were ranked as follows: SLS > SML > SMD.

In another study using a solution of 0 to 3% polyoxyethylene 20 oleate as a granulation liquid, mechanically strong, free flowing pellets were produced with a decrease in the amount of fines (58). There was also an increase in the over-sized pellets. The shape and the surface characteristics of the pellets were also improved. For instance, the pellets became rounder up to 1% addition of the surfactant, with negligible improvement after this concentration. The roughness of the pellet surfaces also decreased with an increase in the concentration of the nonionic surfactant. The results suggest that the addition of nonionic surface-active agent improves the wetting and thereby the rounding of pellets containing MCC and native maize starch as a co-filler.

3. Microparticulate Drug Delivery Systems and Spheronization

a. Microparticulate drug delivery systems

Microparticulates are drug-loaded small polymeric particles (erodible, non-erodible or ion-exchange resins) that could be delivered as solids or suspended in a liquid carrier medium. They include microspheres, spheroids and/or pellets. Microparticulates have been employed in different medical and engineering applications (59-64). In the

field of medicine, this delivery system (especially in radiolabeled form) has been used in different disorders in form of diagnostic tools for functional imaging of lungs, reticuloendothelial system, gastrointestinal system, inflammatory lesions and tumors (59).

Several distinct approaches have been used to formulate drugs as microparticulate delivery system for oral, intraocular and topical applications. These include erodible microparticulates, swelling mucoadhesive particulates, pH responsive microparticulates, nanoparticles/latex systems, ion-exchange resins, etc. (60). In ophthalmology, ocular delivery of microparticulates has been shown to improve bioavailability at the target site, and reduce the potential for ocular and systemic side effects (61). In this regard, the delivery system was used topically as controlled drug delivery in vitreoretinal disorders (some of the major causes of blindness in the developed world), to reduce frequency of intravitreal application (via injection) and optimize intraocular drug levels. This minimizes the risk of complications that can occur from frequent intravitreal injection (62). Microparticulates are used therapeutically mostly as spheroids for immediate and sustained release drug delivery (59,63,64).

Spheroids/pellets are spherical microparticulates of varying diameter depending on the application and the goal of the formulator (7). Pellets can be manufactured in different ways. These include drug layering (spraying a solution or suspension of a binder and a drug onto inert core), hot-melt (hardening of the molten droplets), spray congealing, spray-drying a solution or suspension of the drug with subsequent formation of the pellets due to the evaporation of the fluid phase, and spraying a binder solution into a whirling powder using a fluidized bed (65,66). The most popular method of producing pellets is by

extrusion-spheronization technique. This entails the simultaneous control of several formulation and process variables.

Spheroids/pellets manufactured in the pharmaceutical industry are sized between 500 and 1500 μm and are commonly filled into hard gelatin capsules (67), but can also be compressed in to tablets (68,69). As a drug delivery system, the microparticulates offer not only therapeutic advantages such as less irritation of the gastrointestinal tract, but also important bulk material processing advantages (8,67,70). They show better flowability, produce less friable dosage form, exhibit biopharmaceutical reproducibility, a narrow particle size distribution, low percentage of fines, and are easy to coat and encapsulate (6,9). They are also suitable for dosing as multiple-unit dosage formulations (contrary to the single-unit dosage forms) because of their spherical shape, their mechanical properties and the ability to readily release their active constituents (71) from hard gelatin capsules, tablets, and sprinkles. Additionally, the chance of incomplete absorption of a dose is less. For example, if a single-unit tablet fails to disintegrate, the entire dose would be lost, however, if few units of the pellets fail to release drug at the desired site, the effect would not be altered significantly.

The roundness of spheronized pellets should always be highly considered because irregular shapes tend to indicate a process that is out of control. Spheroids with low sphericity and agglomerated pellets also have high density and low porosity, which could result in poor packaging. Confirmation that the pellets are spherical is obtained using some measures of roundness, the shape factor and aspect ratios (72).

b. Spheronization process

Granulation is the process in which primary powder particles are made to adhere together to form larger, multiparticle entities called granules. Granulation methods are normally divided into two parts: wet granulation methods in which liquid is used in the process, and dry granulation methods that use no liquid. The method and conditions of granulation affect the intergranular and intragranular pore structure by changing the degree of packing within the granules (73).

Wet granulation involves the massing of a mixture of dry primary powder particles using a granulation fluid, the latter being mostly water for economical and ecological reasons (73). Wet granulation methods include wet massing and fluidized bed processes. The latter could involve the rotor-disk module in which microparticulates are manufactured directly from dry powder by spheronization.

1. Mechanism of pellet formation

Spheronization is a form of granulation process used in pellet formation and thus shares the basic granulation mechanism. Like all granulation processes, the mechanism of pellet formation involves nucleation, coalescence, abrasion, transfer, breakage and layering (74). Several studies have been performed to study the mechanism of pellet formation using high shear mixers (Gral 10 and Gral 25; 75,76), and agglomeration by nucleation and coalescence has been found to dominate such systems. Limited information is available in literature with regard to the mechanism of pellet formation using the rotor-disk fluid-bed process.

Although the granulation process of the rotor-disk fluid-bed is different from that of the high shear mixer, it has been shown that similar process variables influence the product formulation and characteristics in both systems (75-78). In fluid-bed granulation, the moisture content in the bed and the speed of the rotating disk are the key parameters controlling the pellet qualities, especially the particle size and size distribution (9,44,79-82). Similarly, in high shear mixers, the binder concentration and impeller speed are the most important variables influencing the mean granule size and size distribution (75,76). It is therefore possible that the same mechanism of growth will be applicable to both processing systems, as discussed in the subsequent paragraphs.

The nucleation or growth mechanism of spherical pellets/spheroids has been defined in a high shear equipment using torque measurement (75). Vonk *et al.* (76), also studied growth mechanisms during liquid addition stage in high shear mixers (Figure 2). They reported that spheroid formation starts with the formation of large primary nuclei that follows particle-particle contact and adhesion due to liquid bridges (nucleation). This nucleation process was described by the comparison of the theoretical tensile strength of the nuclei and the dynamic impact pressure from the measuring system. The primary nucleus is classified as loosed agglomerate with high porosity and low tensile strength. The nucleation process is followed by the formation of small secondary nuclei due to break-up of the primary nuclei. The secondary nuclei are the starting materials for exponential growth, which starts when the solid mass is sufficiently wetted, leading to their densification. Due to densification, stronger and spherical pellets are formed that survive many collisions, and growth proceeds exponentially by coalescence. Additionally, liquid is squeezed to the pellet surface, which contributes to the growth by coalescence,

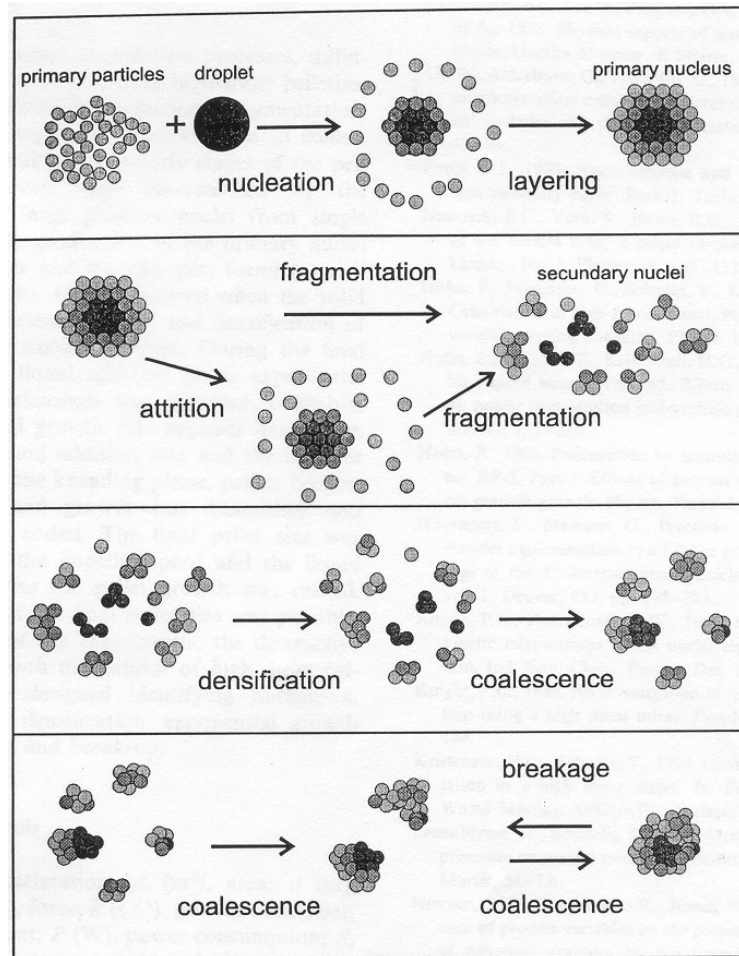


Figure 2: The destructive nucleation growth mechanism of high shear pelletisation (76)

as more particles could adhere to the already formed granule. This liquid addition stage is followed by the kneading stage (76).

During the kneading stage, net growth diminishes because no more liquid is applied, and a steady state is observed. Consequently, spheroid break-up becomes considerably important, depending on the final moisture content in the powder bed. However, at optimal conditions of binder content, the mean pellet size does not change during the final stage of the kneading phase (i.e., there is practically no break-up), which results in a well-defined, spherical product, with a reduced porosity compared to the

primary nuclei (76). It was therefore concluded that deformation and probably densification, and not fragmentation, is the dominant compression mechanisms of pellet formulation. The exponential growth and the final pellet size were linearly related to the specific liquid addition rate and the impeller speed.

Rashid *et al.* (77), have described the mechanisms of microcrystalline cellulose core formation and growth in a centrifugal granulating process as being similar to the spheronizing process of pellets. Different MCC grades were used as starting materials. In such a system, the wetting phase (nucleation region) was followed by combination of coalescence between the previously formed nuclei and the layering of the smaller fine powder over the nuclei. At a later stage, layering and abrasion became the predominant mechanisms. Majority of the formulations studied produced granules that were relatively spherical, smooth, free-flowing and had good mechanical strength, with desirable narrow range of particle size distribution.

In another study, the wetting and growth profiles of the granules were investigated using a tracer in the binder liquid and the authors reported a linear relation between tracer mass and granule mass during the agglomeration stage of the process (78). The result showed insufficient wetting and rewetting of the granules during the early kneading stages of the process respectively, which resulted in a decline of granule growth rate, and consequently to granule attrition. These growth mechanisms are applicable to those in extrusion/spheronization process and spheronization *via* rotor-disk fluid-bed processing, which will be discussed further.

2. Extrusion/spheronization

Extrusion/spheronization invented by Nakahara in 1964 has been described as the most popular method of producing pellets (6,8,79,80) and the methodology of choice in the preparation of spherical particles (71). This traditional spheronization method involves four different steps, namely, granulation (preparation of the wet mass), extrusion (shaping the mass into cylindrical form), spheronization (breaking up the extrudate and rounding of the particles into spheres) and drying of the pellets, as will be elaborated below.

i. Granulation

Different types of granulators are used to perform the mixing of the powder blend and the granulation liquid in order to produce plastic mass. The most commonly used granulator is the planetary mixer (81), although the use of high shear mixers has also been reported (82). An important problem encountered during the granulation process is the evaporation of the granulating liquid probably due to the large amount of heat introduced by most of the mixers. The liquid evaporation influences the extrusion behavior of the wet mass, especially as a homogenous distribution of the liquid phase throughout the granulated mass is highly demanded. Consequently, it was reported that the binder (mostly water) would equilibrate throughout the complete mass when the wet mass was left for 12 hr in a sealed polythene bag before the extrusion step (83). However, this measure is very time consuming.

ii. Extrusion

During extrusion, the wet plastic mass is shaped into long rods. This process is used not only in the pharmaceutical industry but also in the food, ceramic and polymer industries. Four classes of extruders exist, namely, screw, sieve and basket, roll, and ram extruders (7). The contour and position of the screens as well as method of feeding the wet mass to extruder differ in each case. Recent modifications have allowed in-process control using extrusion forces as these extrusions could be correlated to the final quality of the pellets (84). The power consumption of the motor driving the extruder can also be correlated to the pellet qualities (76).

iii. Spheronization

During spheronization, the formed cylinders are collected onto the spinning plate of the spheronizer, the friction plate, where the extrudate is broken up into smaller cylinders with a length equal to their diameter (78), and become rounded due to frictional forces from the plates. Two types of spheronization methods have been identified (7). In the first method, the process starts from a cylinder with rounded edges, to dumbbells and elliptical particles and eventually to perfect spheres (Figure 3A; 85). The second method reported by Baert and Remon (83) suggests that a twisting of the cylinders occurs after their formation resulting in rounded edges that finally results in the breaking of the cylinders into two distinct parts (Figure 3B). Both parts have a round and a flat side. Due to the rotational and the frictional forces involved in the spheronization process, the edges of the flat side fold together forming a cavity observed in certain pellets. It has been suggested that the speed in combination with the diameter of the friction plate (not the

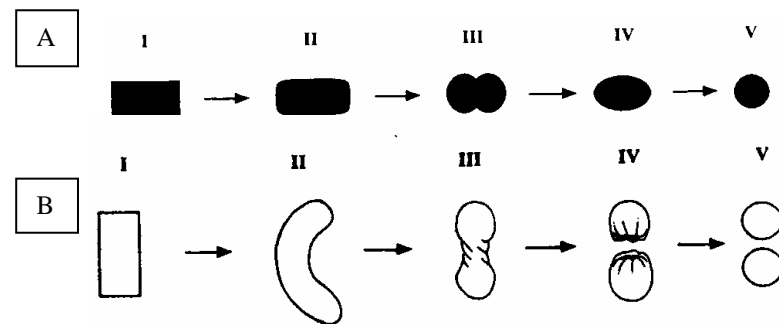


Figure 3: Mechanisms of pellet formation in traditional spheronization methods according to: (A) I. Cylinder, II. Cylinder with rounded edges, III. Dumb-bell, IV. Ellipse, V. Sphere (85). (B) I. Cylinder, II. Rope, III. Dumb-bell, IV. Sphere with a cavity outside, V. sphere (83).

absolute speed), should be used to calculate the plate peripheral velocity. These should be considered in order to obtain highly spherical pellets (86).

iv. Drying

This is the final stage in pellet formation. The pellets can be dried at room temperature (87,88), or at elevated temperature in an oven (70,89,90) or a fluidized bed (86). The use of microwave oven drying has also been reported as the final stage in the production of pellets (90,91).

Several formulation and process variables influence the final quality of the pellets derived from the spheronization process. These include the moisture content of the granulated mass, the type of liquid binder, type of extruder, extrusion speed, properties of the extrusion screen, etc. (92). It has also been shown that the success or failure of each of

these steps affects greatly the quality of the final pellets or spheres (7). Consequently, optimization, batch-to-batch reproducibility and especially scaling up to manufacturing batch size, that are the ultimate goals of industries in the development of any dosage form could be difficult to achieve with this traditional method (7). On the contrary, it has been reported that if several variables in a fluid-bed process are fully controlled, good batch-to-batch reproducibility can be obtained (7,93).

3. Fluidized bed processes

The traditional fluid-bed technology, which was developed over the past 30 years for rapid drying, was described for the first time in the pharmaceutical field by Reynolds (94) and by Conine and Hedley (68). In the 1990's, fluidized bed has been extended to rotary spheronization process as well as other routine use like agglomeration, air suspension coating, powder and solution layering (95). Nevertheless, the principles of the fluid-bed have not changed.

i. Traditional fluid-bed technology

A fluidized bed is essentially a bed of solid particles with a stream of air or gas passing through them via a slit created by a plate (inserted into the vessel) and the vessel wall. The air-flow is normally strong enough to keep the particles in motion.

The fluid-bed processing equipment generally consists of the air processing unit, the product container, and the expansion chamber for proper fluidization of the powder bed (Figure 4; 95,96). It has one or more binary nozzle(s) each comprising of a solution

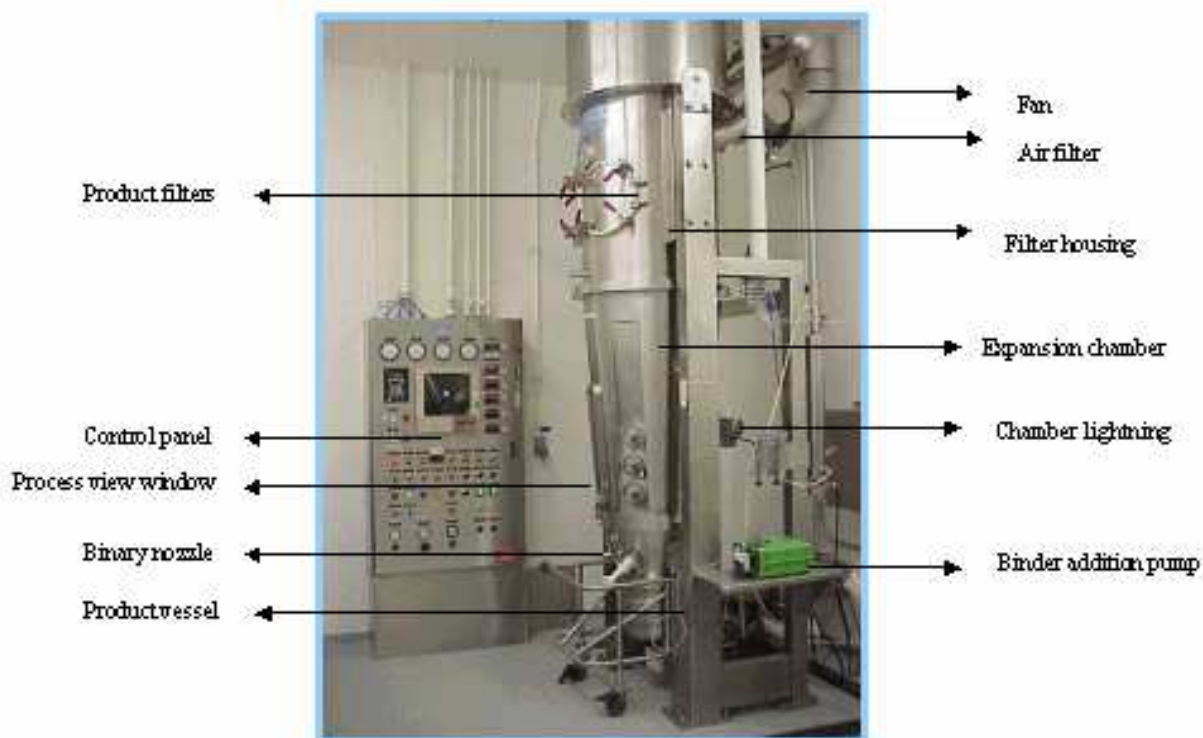


Figure 4: Fluid-bed equipment (97).

delivery system and compressed air to atomize the liquid binder, exhaust filter and blower, product temperature probe, filter housing, etc. The latter encloses cartridge filters mostly made of polyester or stainless steel materials. These filters retain products in the system, which are shaken at pre-determined time intervals to release the retained products into the product vessel for spheronization (98). The conical shape of the expansion chamber reduces the velocity of the air in the filter compartment, which helps to keep the smaller or fine particles out of the upper filter region.

The fluid-bed process has been shown to have several advantages over other granulation technologies, especially in the development of extended release products (99,100). In one study, three products were compared in the development of metoprolol tartrate extended-release matrix tablet formulations, namely directly compressible, fluid-

bed or high-shear granulated products (99). Metoprolol tartrate has a tendency to adhere to the punch surfaces and has poor flow properties, and all three processes were sufficiently sensitive to manufacturing variables. Despite the various excipients (MCC with talc or stearic acid) that were added to address the difficult physico-chemical characteristics of the drug, direct compressible materials exhibited poor flow, picking and sticking problems during tableting. High-shear granulation resulted in granules with improved granule flow and tableting characteristics but also formed hard granules that were difficult to mill. This was attributed to over-massing of the granules by this granulation process. On the other hand, the fluid-bed granulation made using various binders appeared to be satisfactory in terms of flow and tableting performance. The fluid-bed technology was therefore designated as the process of choice for further evaluation of critical and non-critical formulation and processing variables.

The fluid-bed processes include the top-spray process, the bottom-spray process and the tangential-spray process shown in Figure 5 and Table I (96,101). The three fluid-bed processes represented offer different advantages and disadvantages. They are applicable to both granulation and coating processing, however, the performance requirement of the finished product and suitable batch size of the product must be considered when selecting them for a particular product.

The top-spray process is usually used with a conventional granulator-coater, the bottom-spray process with a Wurster air-suspension column and the tangential-spray technique is used with a rotary fluid-bed granulator (101). The latter was used for this study, and will be elaborately discussed in subsequent sections.

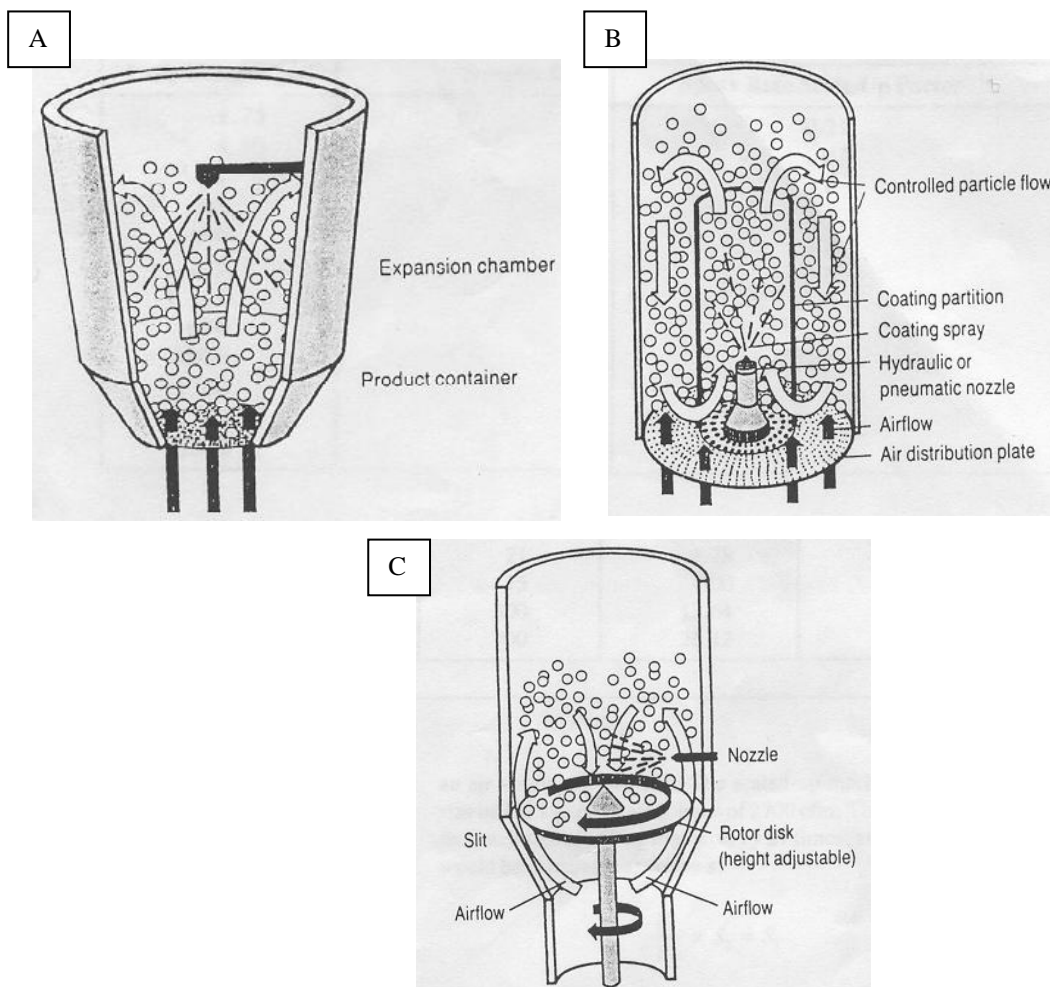


Figure 5: Fluidized bed processes. A. Top-spray method; B. Bottom-spray method; C. Tangential-spray method (101).

ii. Rotor-disk fluid-bed

1. Equipment and components of the rotor-disk fluid-bed

As previously discussed, extrusion/spheronization involves a number of successive steps such as moistening, extrusion, spheronization and drying. Rotor-disk spheronization, however, reduces the number of processing steps involved in traditional spheronization method, and thereby reduces the production time and cost, with good batch-to-batch reproducibility and consequently faster market time (11,12,102).

Table I: Characteristics of Fluid-bed Granulation and Coating Processes (96,101).

Processing Method	Advantages	Disadvantages	Applications
Top-spray coating (conventional mode) .	Accommodates large batch sizes, is simple to set up, and allows easy access to nozzle.	Limited in its applications	Hotmelt coating and aqueous enteric coatings. Not recommended for sustained release products due to inefficient coating uniformity.
Bottom-spray coating (Wurster)	Accommodates moderate batch sizes, produces uniform and reproducible film characteristics, and allows for widest application range	Tedious to set up, does not allow access to nozzles during processing, and is the tallest fluid-bed machine for coating fine particles	Sustained-release, enteric-release, and layering Poor for hotmelt coating because difficult to control and maintain required temperature
Tangential-spray coating (rotary mode)	Simple to set up, allows access to the nozzle during processing, permits higher spray rates, and is the shortest fluid-bed machine for coating fine particles	Puts mechanical stress on the product	Very good for layering, sustained-release, and enteric-coated products. Hotmelt coating possible. Not recommended for friable products because of potential for strong mechanical forces during the process.

Although rotor-disk fluid-bed comprises of set of processes that depend on each other, once optimized, each contributes to the successful transformation of the starting powder mixtures into spheroids.

The components of the fluid-bed processing equipment have been discussed previously (Figure 4). A rotor-disk, which contributes greatly to the spheronization process, is inserted in the product container of the rotor-disk fluid-bed. Figure 6 shows the product vessel with the rotor-disk insert and the spray gun facing the direction of the powder flow.



Figure 6: Rotor-disk fluid-bed product container with rotor-disk insert and spray gun (97).

2. Rotor-disk fluid-bed process Rotor-disk fluid-bed utilizes the tangential-spray process. This has been described as a method of choice for producing spheroids used for immediate release purposes, as well as for producing pellets that could be coated for controlled release applications (96,103,104). The tangential spray process is preferred

over the top- or bottom spray methods because spheroids formulated in this equipment have a surface morphology (less porous and more spherical) that is more suitable for coating than that of spheroids prepared using the other processes.

As shown in Figure 7, rotor-disk spheronization is centered around the rotor plate insert where disk rotation adds centrifugal force (F_c) to the material on it. As the powder is sprayed tangentially, it is wetted and rolls around the product vessel by the centrifugal force into a vertical moving air stream with vertical force (F_v) caused by a gap between the vessel wall and the rotor-disk insert. Because there is no force at the center of the plate, the rolling product falls back toward the center of the disk by gravitational force (F_g), thereby creating a rope-like motion (95,105). This process has been demonstrated to

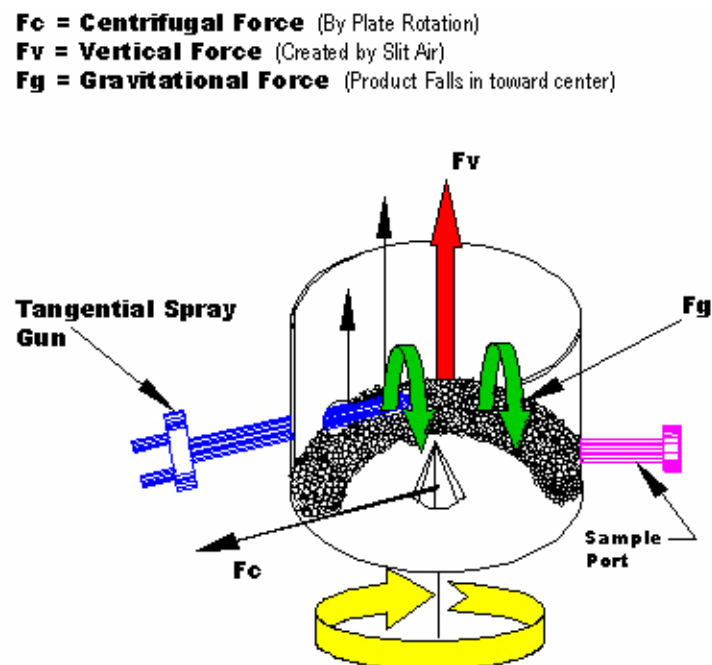


Figure 7: Schematic representation of rotor-disk technology using tangential spray gun (97).

be reproducible at the development and pilot stages, but is difficult to achieve further scale-up and optimization steps.

3. Factors affecting the rotor-disk fluid-bed process and product qualities

Several factors affect the characteristics of products produced in the fluid-bed spheronization process. These are the formulation, process and equipment variables. Formulation variables would include the amount of binder added, moisture content of the granulated mass, type of granulation liquid, and physical properties of the starting material. Process variables include inlet and outlet air temperatures, binder spray rate, spheronization speed, fluidization air velocity and volume. Equipment variables include filter shaking, scalability, plate material type and contour, etc. The amount of added binder and rotational speed have been identified as the most important variables for producing good quality spheroids (44).

Effect of type and amount of granulation liquid on the spheronization process.

In order to initiate the agglomeration and granule growth processes, an optimum amount of binder has to be introduced into the granulator (106). The nature of the powder to be agglomerated will influence the selection of binder to be used for the granulation process. Although the amount of binder used in the spheronization process has been mostly determined empirically (106), special instrumentation and procedures exist for this purpose (107).

In the spheronization process, the granulating liquid exerts a lubricant effect, which could be affected by the presence of different additives, used in most cases to

adjust its properties (108). These include surfactants and polymeric compounds, which have been shown to tailor the binder to exhibit specific behavior, thereby allowing fine-tuning of some binder properties, namely, surface wetting, viscosity, adsorption, and solid bridge strength. These directly affect both the spheronization process and the resulting product.

It has been shown that the presence of different additives could change the ease and extent with which liquids could be removed (drying) and reabsorbed (wetting) in the spheronization process (56). This was demonstrated using water, a 25% solution of glycerol in water, sodium lauryl sulfate below its critical micellar concentration, and Pluronic PF68 (a nonionic surfactant at 0.01 and 0.0001%), as granulating liquids. Lower levels of saturation were obtained with the glycerol solution and considerably increased levels of saturation with the surfactants. It has also been shown in both traditional extrusion/spheronization and rotor-disk processes, that the solubility of materials used (both drugs and fillers) plays an important role in the quantity of binder required to form satisfactory pellets and on the physical characteristics of pellets (109). These studies emphasize the importance of using minimal number of excipients in dosage formulations, as was done in the present study. Additionally, the importance of binder selection for specific products in granulation/spheronization processes is implicated.

Effects of type and amount of granulation liquid on the spheronized products qualities.

The spheronizer speed, as well as the initial and final liquid contents (at the end of spheronization process) have been shown to exhibit significant effects on the qualities of the spheroid (92,110-112). The qualities mostly affected are

sphericity, particle size distribution, and friability. These studies established a correlation between the amount of granulating liquid used in the formulation and the shape of pellets. For instance, in one of the reports in which traditional spheronization method was used (56), pellet shape, a very important spheroid characteristic was demonstrated to be highly influenced by the liquid content of the extrudate during spheronization. In addition, low levels of liquid were shown to yield elongated, non-spherical pellets while very wet blends produced larger, agglomerated pellets with a wide particle size range and a higher porosity. These were attributed to variations in water content and hence consistency.

In another report (113), it was shown that although the mean diameter of the granules was influenced by moisture contents at the final stage of spheronization, however, the effect of moisture on the granule diameter is cumulative or based on all the operational variables in granulation process. These factors were also considered as important scale-up parameters.

Influence of the spray rate of the granulating liquid on product qualities.

Liquid distribution by the nozzle influences the pellet growth (78). In addition, the spray rate and the mixing of atomization air and binder in the spray zone determine the average granule size. There is also a linear relation between the number of droplets that comprised a granule and the granule size, especially at the early stage of the process (113). Therefore, there is a requirement for nozzles that produce uniform droplets, which allow these droplets to be easily controlled in size independent of liquid- and air-flow of the nozzle. Thus, a nucleation ratio factor has been proposed as a useful parameter to

describe the binder liquid efficiency (78). This factor depends on the material properties of binder liquid and powder particles.

Effect of plate rotational speed. Spheronization speed affects spheroid qualities in both the traditional and rotary fluid-bed processing (14,114,115). In the traditional spheronization, extrudate speed influenced the size and sphericity of the pellets, with the best results obtained at intermediate spheronization velocities (116,117). In the one-step rotary process, the use of variable speeds of the rotating plate during the spheronization run has been investigated in order to achieve optimal spheroid yield (118). The study was performed due to the occurrence of material adhesion and formation of oversize particles in the product yield that was attributed to the use of a non-optimized process speed.

It was shown that when the plate speed was increased during liquid addition (spheronization process), the greater centrifugal forces generated improved liquid distribution and the mixing of the moist powder mass, resulting in a decrease in the amount of oversize particles formed (118). A "low-high-low" speed variation during rotary processing was shown to be necessary to produce spheroids with a narrow size distribution and with a minimal amount of oversize particles in the total product yield. Based on the mechanism of pellet formation already discussed, and on our practical experience, this could be translated as follows:

Low' speed at the initial stages of liquid addition when powders are still light in weight and could be easily blown into the expansion chambers and filters. This will reduce product losses. As more liquid is added to powder bed, the material gets very wet

and heavy such that 'High' speed is needed to improve powder fluidization, and also facilitate spheronization. Finally, during the drying period as the powder material bed loses its moisture and becomes lighter, 'Low' speed is needed to avoid attrition and losses into the expansion chambers and filter housing.

Effect of plate contour and plate material type

Plate contour. Rotary fluid-bed spheronization process is centered around a rotor-disk insert. The air supplied via a split between the product vessel wall and the disk, the disk rotation, and high air pressure of a pneumatic nozzle tangentially mounted on the chamber of a conventional fluidized bed granulator impart centrifugal (F_c), vertical (F_v) and the gravitational (F_g) forces on the product (Figure 7; 97,119). These create a rotating motion that leads to greater densification and spheronization of the granules than with conventional fluidized bed granulation (119,120).

The influence of disk surface and its speed on the direct pelletization with rotor technology has been previously studied in a series of experiments (98,121). For each experimental set, the process variables were kept constant within specified limits, except for the rotational speed of the disk during agglomeration and spheronization steps. Two differently textured rotating disks were used, one with smooth and the other with waffle surface. It was shown that both surface textures and rotational speed of the disk have influence on shape, surface and size of pellets, with the two textures having opposite effects on pellet qualities.

In the traditional spheronization process, pellet shape and size have been used to describe the influence of different plate geometry on pellet qualities (122). Under

constant spheronization conditions, the extrudates behaved dissimilarly on the two spheronizer plates used. The spheronizer with the rougher surface was shown to apply more mechanical energy to the extrudate and wet pellets, which reduced the water content necessary for the formation of the desired pellet qualities. Therefore, high differences were observed in the quality of the extrudates produced by the two extruders (122). These observations could be applicable to using different plate contours in the rotor-disk spheronization process (47,121).

Plate material type. Several authors have demonstrated the use of stainless steel disk material in the fluid-bed spheronization and coating processes (123,124). This plate varies in diameter and thickness depending on the size of the fluid-bed, and adds to the forces supplied to the fluidizing powder bed. The use of stainless steel disk in fluid-bed processes also facilitates product removal and cleanup. The cleanup step is more feasible with smooth textured plates than with the rough/waffle contour plates. The heat conduction of the stainless steel material makes it useful for both drying and coating processes. It has been shown that heat transfer occurs by a combination of conduction, convection and radiation, and is enhanced by vigorous mixing of the powder bed (125,126). The rate of heat transfer to the powder beds during spheronization/coating from the stainless steel plate rotor-disk insert is minimized by the addition of cold liquid binder or coating solution, which reduces the rate of evaporation of the liquid during processing at this stage. This efficient heat transfer would be difficult to be generated with other materials such as teflon, which could also be used as rotor-disk insert (47).

Using the stainless steel plate, Balakrishnan *et al.* (123), reported the coating of ascorbic acid with a 10% poly(vinylpyrrolidone) solution in ethanol by a process in which a horizontally rotating stainless steel disk was installed in the lower part of a coating tower. The latter had a circular horizontal cross-section in which hot air was blown in below the disk and was guided upwardly between the coating tower and the periphery of the disk. The flow of air above the disk and the centrifugal force of the disk supplied fluidized bed of the particle, enabling it to be efficiently coated.

A comparative study on the effects of extrusion/spheronization and rotor direct pelletization on pellet quality using a smooth disk shows similarity in physico-technological characteristics of the produced pellets (127). However, several phenomena have been shown to occur successively in the fluid-bed technology and the spheronization processes. Thus, a lot of process parameters should be controlled simultaneously during the process (14). It is therefore important to identify and control the involved process and formulation variables and conditions. This can be achieved through experimentally designed studies that identify critical and optimum conditions to obtain high quality products.

4. Optimization of Equipment and Process Variables

a. Factorially designed experiments

The effect of multiple factors such as plate contour, binder and surfactant levels can be investigated simultaneously using statistical design of experiments (14,128).

Maximum amounts of information are generated with a minimum number of

experiments, which assists to estimate the main effects of each experimental factor of the product (129). Although factorial design has been shown to be effective in predicting the properties of granulations prepared at conditions within the limits imposed by the equipment or formulation (79), there are limited reported studies on the effects of process variables on product quality and characteristics (50). Most of these were confined to studying few characteristics (128). However, none of the studies in both the traditional and non-traditional methods has statistically studied the effect of batch-to-batch reproducibility on both process variables and spheroid qualities. Additionally, apart from very few studies (9,93) most of them used beads on which drugs were layered, thus providing ready-made spheronized cores that initiated the spheronization process (129-133).

Considering the complexities of the spheronization processes, most of the processing and formulation variables, especially some critical aspects of granulating liquids, scale-up, drug loading, drug particle size, etc. need to be statistically studied and validated. This could be achieved using different process and product scales and also different aspects of the powder material qualities (129,134). Optimization studies can be based on the results of feasibility studies. Production and scaling up of spherical pellets or microparticulates will then follow (44,135).

The process variables that could affect scale-up will be discussed in this section, while the product variables will be discussed in a separate section.

b. Scale-up

The scale-up of a process or batch is studied to establish the operating conditions applicable to large scale production batches, with the goal of obtaining products of the same quality based on previously optimized laboratory scale experiments. Scale-up of processes that involve powder handling is especially difficult because the dynamic behaviors of powders are not very well understood (136). Moreover, when applied to granulation, the effects of the operational variables on powder properties and granule growth are not clearly known. Although scale-up processes of materials in the solid-state have been based on dimensional analysis, mathematical modeling and computer simulation, most of the work in this field still depends on trial and error and the principles of geometric similarity (137,138). The latter describes the interrelationships among system properties upon scale-up, thus, the ratio of some variables in a small scale equipment should be equal to that of similar variables in equivalent large scale equipment (101).

Scale-up of any chemical process is a complex science. The scale-up of fluidized bed processes is likewise complicated because it involves several scientific techniques and problems, including those involved in engineering and pharmaceutical fields (13,139). These include the problems of air-flow changes and rate (gas bypassing) and poor contact with bed particles, particle flow patterns, dissolution profiles, drug load and the physical nature of solid particles that includes the drug particle size. Although most of the work published on rotor-disk spheronization focused on small-scale equipment, fluid-bed systems are designed to maintain critical scale-up factors as constant as possible from one unit to another (13,139). Nevertheless, these studies emphasized that each fluid-bed

should operate at identical bed depths, air velocities and air changes as to simplify scale-up of products from one unit to the other. Most of these parameters have been recognized and incorporated in fluid-bed machinery.

Mehta *et al.* examined the variables that should be optimized in the scale-up of the fluid-bed coating process (101). These include, spray rate, powder bed moisture content at the end of the spraying cycle, the atomization air pressure, the inlet air temperature, the fluidization air volume, the batch size, and the type of equipment. In this study, the interplay of various processing parameters presented a great challenge in optimizing the coating process in a fluidized bed process. As such, continuing efforts to investigate and understand this interplay were reported as extremely important in order to ensure reproducible performance of the products.

Computerized techniques are becoming popular for the fluid-bed process control (140). These include fuzzy logic, neural networks, and experimental design models. In addition, engineering techniques based on particle size population balance modeling are under development for both fluid-bed and high-shear granulation processes (140). Recently, mathematical model software which utilizes a combination of classical equations for transport phenomena in conjunction with effective algorithms and actual laboratory, pilot plant, and production data, has been introduced to resolve problematic scale-up issues for the pharmaceutical engineer and formulator (141). Nevertheless, some authors have maintained that past experience is very much required in handling the numerous problems encountered during scale-up in drug development (142). Most process and formulation scale-up processes are however based on the principles of geometric similarity (138,143,144).

1. The principles of geometric similarity

Scale-up from laboratory to production batches is always problematic for the development of pharmaceuticals. Deviations in expected results in scaling-up can often be evaluated by the principle of similarity. This attempts to represent a physiological or chemical process by an unspecified relation between several dimensionless groups, one of which contains the unknown variable (138,140). If the group containing the known variables are made to have the same value on the small and large scales, then the group containing the unknown variable will also have the same values. In this form, the principle of similarity pre-supposes that the systems to be compared are geometrically similar (136).

Two methods of deriving similarity criteria are available, dimensional analysis and differential equations, the latter being preferred where applicable. Alternatively, extrapolation by means of a power law relation permits model and prototype to be compared under conditions that are not strictly similar (145).

Dimensional analysis is an algebraic treatment of variables affecting a process. This technique permits the definition of appropriate composite dimensionless numbers whose numeric values are process-specific (138). Experimental data are hereby fitted to an empirical process equation that results in scale-up being achieved more readily. This indicates that in the scaling up process, any model material system whose dimensionless material function in question is similar to that of the original material system may be chosen. Block *et al.* (141), therefore reported that scale-up may be achieved through the application of the principles of similarity, wherein effective process translation is based on the use of dimensionless ratios of measurements, forces, or velocities i.e., geometric,

mechanical, thermal, and/or chemical ratios of scale. Each of these ratios presupposes the attainment of the other similarities.

According to the theory of similarity, two processes are similar to one another if they take place in a similar geometrical space, and if all the dimensionless numbers necessary to describe the process, have the same numerical value (138,146). A complete similarity requires a geometrical, material and process-related similarities. However, according to the principles of similarity stipulated by the Center for Drug Evaluation and Research (CDER) guidelines which state that, “the equipment used to produce test batch(es) is of the same design and operating principles as those for scale-up batches. The same standard operating procedures and controls as well as the same formulation and manufacturing procedures are used on the test batch(es) and on the full-scale production batch(es)” (147).

The principle of geometric similarity is therefore the driving force when different sizes of the same processing equipment are employed in the laboratory, pilot plant, and commercial production facilities. Consequently, this principle was adapted to two dimensionless numbers of power, namely, Reynold's and Froude's, employed in the present studies.

2. Reynold's and Froude's numbers

Scale-up in fixed bowl mixer-granulators has been studied by applying the classical dimensionless numbers of power, Reynolds and Froude, and a scaling factor, to end-point prediction in a range of geometrically similar machines. When corrections are made, data from 25-, 100- and 600 L machines all fall on the same curve, allowing

predictions of optimum granulation end-point conditions to be made for production-scale equipment from measurements on laboratory-scale equipment and *vice-versa* (148,149). Reynolds' and Froude's numbers are dimensionless numbers derived directly from Navier Stoke's equations. These equations, often used as the starting point for the analysis of granular systems, mathematically describe the effect of both inertial and viscous forces on the motion of fluid elements (150). For a rotating system like the rotary fluid-bed, Reynolds' number (Re) is defined as shown in Equation 1:

$$\text{Re} = \frac{wri^2 \rho}{\mu} \quad \text{Eqn. 1}$$

where ρ and μ are respectively the density and dynamic viscosity of the granular medium, w , the angular velocity, and ri the radius to a blade tip. It is generally interpreted as the ratio of dynamic to viscous forces. The Froude's number (Fr) is defined as shown in Equation 2:

$$\text{Fr} = \frac{N^2 D}{g} \quad \text{Eqn. 2}$$

where N is the number of revolutions per minute, D the diameter or the impeller or the rotor plate (as is applicable to our study), and g the gravitational constant. This number is interpreted as the ratio of the centrifugal force generated by the equipment to the gravitational force, and is used as a criterion for dynamic similarity. The results obtained from these numbers using the high shear mixer often show that, for geometrically similar machines, it is possible to calculate the power consumption at a predefined granulation endpoint, at any given operating condition and at any scale.

In the present study, these numbers have been used to estimate scale-up effects and also to determine important scale-up factors for the rotor-disk spheronization process.

3. Scale-up parameters

i. Rate of addition and amount of liquid binder in powder bed

In granulation, an optimal amount of binder solution determined in a laboratory scale is often different than that in a production scale (111). As already discussed, the binder solution plays an essential role in the formation of granules with desired physical properties in the manufacturing process. This binder role is closely associated with the manufacturing scale. For wet granulation in high-shear mixers for instance, specific methods based on the liquid saturation and the consistency of the wet mass have been described (140,148). These two parameters can be used to quantify the characteristics of the wet granules, and they also relate well with the particle size of the end products. In practice, the power consumption of the high-shear mixer is used for monitoring of the wet granulation process. It has also been helpful to use the underlying relationship between power consumption and saturation level or wet mass consistency for scale-up purposes.

In fluid-bed granulation, the rate of binder addition, the moisture content and the air volume in the bed are the key parameters to control (140), and can be used as scale-up variables. The rate of binder addition and the moisture content in the bed can be monitored in-process through the volume or weight of the binder added per unit time interval and by near infrared probes respectively. The moisture content can also be obtained through monitoring the loss on drying or by Karl Fisher titration studies (139).

The Karl Fisher method determines the total moisture content including the residual moisture present in the product.

The scale-up ratio (SUR) involving rate of addition and amount of binder is expressed as shown in Equation 3, which could be applied to several other scale-up variables. The air volume in the bed has been mostly monitored using air-volume indicators on the fluid-bed machine, as will be discussed below.

$$SUR = \frac{\text{Amount of binder in the large equipment}}{\text{Amount of binder in the small equipment}} \quad \text{Eqn. 3}$$

ii. Fluidization air volume

Besides the rate of spraying and the amount of binder in the powder bed, several other variables are involved in the fluid-bed processes. These must be prioritized during the development stages to avoid expending excessive amounts of time during the scale-up phase. The volume of air required to give an adequate fluidization pattern on the specific machine is critical to obtain good fluidization pattern necessary to get desired product qualities. It is necessary to identify optimum operating air-flow and aeration rates accounting for gaseous emissions and bed temperatures (151), as well as for the powder bed fluidization. Consequently, air-flow parameter has been used as dimensionless factor in scale-up processes (152). The air-flow rate can be determined in two ways, in relation to the spray rate of the binder addition:

If both fluid-bed machines, the small scale size (laboratory) from which the process is being scaled and the pilot or production sizes have air volume indicators, the spray rate multiplier can be determined as the ratio of the two air volumes that are

required to give an adequate fluidization pattern in each machine. Alternatively, in cases where there are no air volume indicators, an approximation of the spray rate multiplier can be made using the ratio of the cross-sectional areas of the product bowl screens or plates. The latter method assumes however that achieving similar fluidization patterns in both pieces of equipment will require the same air velocity through the bowl screen. Therefore, the former method involving the use of air volume indicators, and which relates to the principles of geometric similarity, and is shown in Equation 4, will be applied in our scale-up processes.

$$B_2 = \frac{A_2 * B_1}{A_1} \quad \text{Eqn. 4}$$

Where A_1 and B_1 are the air volume and binder addition rate respectively of the small scale while A_2 and B_2 refer to the same parameters for subsequent scale-up batches.

iii. Rotational speed, centrifugal force and plate radius

The Froude's number defined in Equation 2 entails both a gravitational force and diameter variables, with one being inversely related to the other. The centrifugal force also relates inversely to the diameter of the impeller/plate. In the rotor-disk module, spheronization is achieved by the powder bed rotation caused by both centrifugal and gravitational forces during the densification of the powder. It has been reported that for high shear mixers, this densification could depend on the impeller rotation speed and also on the size of the mixer (140). These relationships have been adapted to the rotor-disk module with modifications, to obtain Equations 5 and 6 that formed the bases for scale-up in the present studies.

$$V = \sqrt{\frac{Fc * R}{W}} \quad \text{Eqn.5}$$

$$Fc = \frac{W * V^2}{R} \quad \text{Eqn. 6}$$

Where V is the rotational speed, Fc the centrifugal force, R the plate radius and W the weight of the powder material.

In addition to the above process variables involved in scale-up, several product variables have been shown to affect both the spheronization and scale-up processes. These include the amount of drug present in the system and its mean particle size diameter, which also affect the drug release of the products.

5. Product Variables and Drug Release

a. Product variables

1. Drug particle size

Drug particle size is an important and challenging factor in the spheronization process and therefore needs to be optimized for the success of the process (16). Studies have been performed to describe the effects of interactions observed between powder particle size and binder viscosity on the mechanisms involved in agglomerate formation and growth using high shear mixers (52,153). In such systems, agglomeration by nucleation and coalescence has been shown to dominate when agglomerating small powder particles and binders with a low viscosity. It was also observed that in order to produce spherical agglomerates (spheroids), a low viscosity binder has to be chosen when

agglomerating a powder with a small particle size, and a high viscosity binder must be applied in the agglomeration of powders with large particles. The latter requirement could be due to the low agglomerate strength of the large particle sized products that could lead to agglomerate breakage.

In another report in which three particle sizes of theophylline were used as a model drug for fluidized rotor granulation, Sienkiewicz, *et al.* (16), observed that the two finer grades of the drug were substantially more difficult to spheronize than the coarse grade of the drug. Only the latter formed the desired spherical product. Additionally, two MCC grades with different mean particle sizes were used to demonstrate the effect of their particle sizes on the spheronization process and product qualities (115). Although both MCC particle sizes gave pellets with good particle size, sphericity, and compressibility, under a wide range of spheronization conditions, pellet porosity was greater with MCC of larger particle size. It is therefore necessary that a consideration of the particle size suitable for the spheronization process should be part of the optimization studies performed at the developmental part of a project.

2. Drug load

Drug loading has been shown as a major limitation to the usefulness of the spheronization process and the spheronized dosage form, and as a challenging factor in the scaling up of fluidized bed processes (16,154). The influence of type and quantity of drugs on spheronization processes has often been studied by varying the quantity of drug with respect to the amount of lactose, pure microcrystalline cellulose or different forms of Avicel[®] (10,155). In a previous report using different loads of lactose, the effects of

loads applied to agitating powder beds on the particle size distribution was investigated (156). It was shown that at the light load (6.24 g/cm^2), smaller particles were produced while at the heavy loads (29.2 g/cm^2 and 41.9 g/cm^2), larger sized particles were produced after long mix processing. The latter observation was attributed to a quick increase of fine particles and their subsequent agglomeration to form larger particles due to the large product load. Consequently, it was assumed that there was a critical fine particle size and critical load quantity under which the physical properties of the powder bed change significantly (156).

In another study that used theophylline as the model drug, increasing the drug loading increased the geometric mean diameter of the microspheres as well as the time required to release 50% of theophylline microspheres (T_{50} ; 157). Moreover, the *in vitro* drug release of microparticles with a high drug loading has been shown to be markedly faster than those with low drug loading (158). The latter was partially attributed to a more significant initial burst-drug release of the microparticles with a high drug loading. Consequently, a proper choice of drug levels could lead to a high degree of control over the physical characteristics of products, including their drug release properties.

b. Drug Release

1. Immediate Release of drugs

Pharmaceutical preparations are formulated to release their actives as immediate release (IR) or under modified release (MR) conditions. For most immediate release drugs, including ibuprofen tablet preparations, the United States Pharmacopoeia (USP) specifies that the formulation must release at least 75% of its drug content at 30 min

(159). A single time point assessment, called Q_{20} is also used in which at least 80% of the drug is expected to be released within 20 min (160). Drug release from conventional release preparations are often described by Higuchi square root of time relationship presented in Equation 7:

$$Q = kt^{\frac{1}{2}} \quad \text{Eqn. 7}$$

where Q is the cumulative amount of drug released per unit surface area at time t and k is a constant.

Drug release is normally intended to be the rate-determining step for absorption of the drug substance into the systemic circulation (161). The release from dosage forms and subsequent absorption of the drug are controlled by the physico-chemical properties of the drug, the delivery and biologic systems. The physiological property of the latter is also a vital contributive factor. The essential drug properties for the release process include its concentration, aqueous solubility, molecular size, crystal form, protein binding and pKa (162). Consequently, it has been shown that drug release rate could be dependent on the equilibrium solubility of the drug, which in turn is dependent on the pH of its solution (23,163).

The release of drug from a delivery system involves both dissolution and diffusion factors. The release mechanisms can be one of the Higuchi matrix, zero, first or second order types, however, most drugs follow either the Higuchi matrix kinetics, the zero or

first order release kinetics (164,165). The release kinetics parameters can be calculated using the following semi empirical (Peppas) equations:

$$Mt / M = kt^n \quad \text{Eqn. 8}$$

$$\log(Mt / M) = \log k + n \log t \quad \text{Eqn. 9}$$

where Mt/M is the fraction of drug released at time t , k is a characteristic constant of the drug and n is indicative of release order. Hence, as the k value increases, the release of drug should occur faster. The n value of 1 corresponds to zero-order release kinetics, $0.5 < n < 1$ means a non-Fickian release model and $n = 0.5$ indicates Fickian diffusion drug model (first-order release kinetics). From the plot of $\log (Mt/M)$ vs. $\log t$, the kinetic parameters, n and k are calculated.

Traditionally, delivery systems do not incorporate a means of controlled release of their actives, such that with each dose of a noncontrolled-release drug (conventional), the concentration of drug available to the body immediately peaks and then declines rapidly (Figure 8). At times, the drug concentration is very high, contributing to adverse side

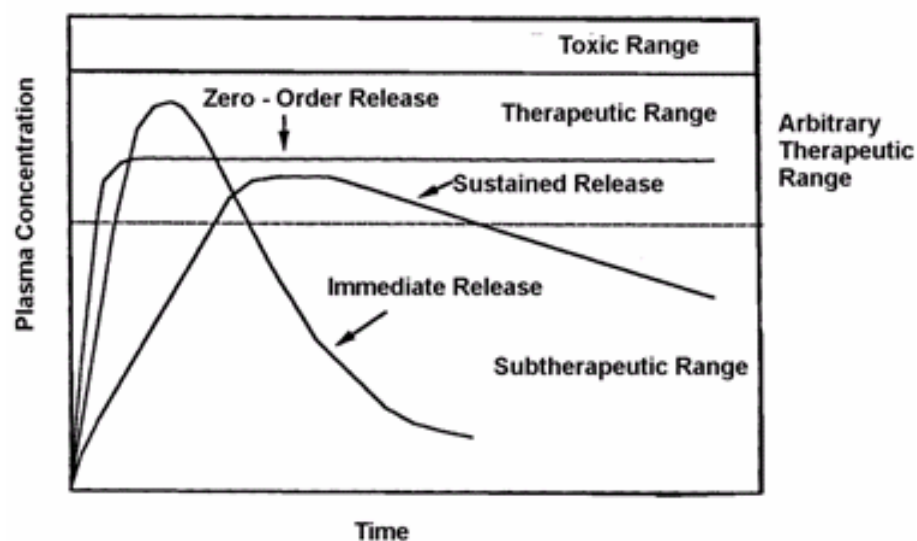


Figure 8. Types of dosage forms (166).

effects. At other times, the concentration is too low to provide therapeutic benefit (Figure 9). It is desirable to release drugs at a constant rate, thereby maintaining drug concentration within the therapeutic range and eliminating the need for frequent dosages. These and other problems have led to a shift in the drug delivery technology towards the modified/controlled release dosage forms. However, there are some characteristics associated with drugs used in sustained release formulations, as will be discussed below.

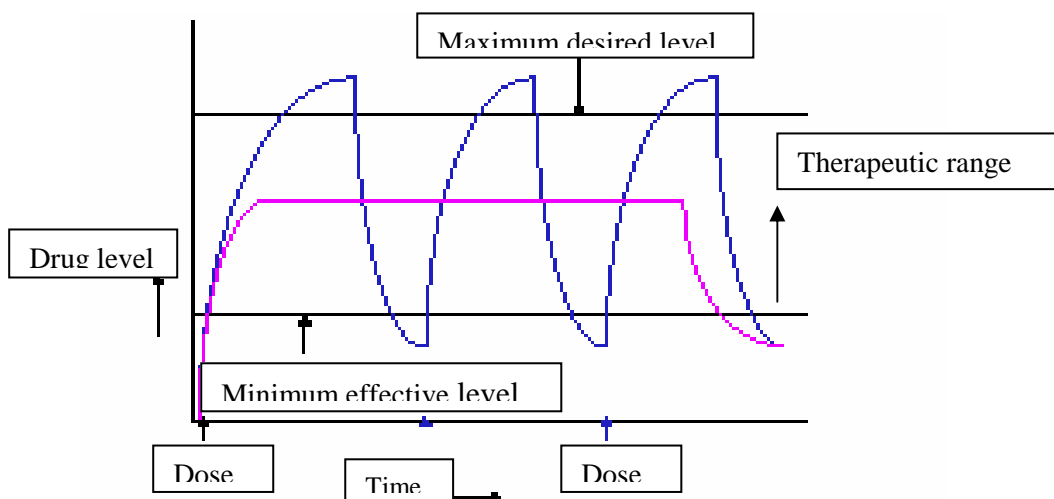


Figure 9. Drug levels in the blood with immediate (—) and sustained (—) release profiles (167).

2. Drugs suitable for sustained drug delivery formulations

i. Drugs with short half-lives.

The extent of fluctuation in drug concentration at steady state is determined by the relative magnitude of the elimination half-life and the dosing interval. If a drug is given at an interval equal to the elimination half-life, there exists a two-fold difference between the maximum and minimum concentrations at steady state, which normally affects its

effectiveness (166). Drugs with short half-lives and with a clear relationship between concentration and response, require to be dosed at regular, frequent intervals in order to maintain the concentration within the therapeutic range. These drugs are therefore suitable for sustained release delivery, as to reduce the number of daily intakes, and also maintain a steady state level that is within its therapeutic concentration. The pharmacological effects of these drugs are maintained by various mechanisms, few of which will be discussed below. Conversely, drugs with long half-lives can be given at less frequent intervals, and there is generally no advantage in formulating these drugs as sustained release formulations.

ii. Drugs with high toxicity and low therapeutic index.

As shown in Figure 8, the conventional oral route of drug administration does not provide ideal pharmacokinetic profiles. For drugs that display high toxicity and/or narrow therapeutic windows, the ideal pharmacokinetic profile will be one wherein the drug concentration reached therapeutic levels without exceeding the maximum tolerable dose, and maintains these concentrations for extended periods of time till the desired therapeutic effect is reached (Figure 9; 168). This could be achieved with sustained release preparations. Several drugs with short half-lives e.g. ibuprofen, must be dosed at frequent intervals and in high doses to achieve this aim. Such therapeutic measures may result in higher peak concentrations with the possibility of toxicity. In cases where the drugs have wide safety margins, this approach may be satisfactory because although very large fluctuations will occur within a dosing interval, no difficulty is generally encountered in view of the drugs' low toxicity (168). However, some side effects might

be deleterious to health. For this class of drugs, the use of sustained drug delivery could prevent creating unwanted side effects that occur at very high concentrations and periods of inefficiency at very low concentrations.

A wide range of drugs is now formulated in a variety of different oral extended-release dosage forms. However, only those that result in a significant reduction in dose frequency (as would apply to ibuprofen) and/or a reduction in toxicity resulting from high concentrations in the blood or gastrointestinal tract are likely to improve therapeutic outcomes. Consequently, extended release of a formulation has been broadly defined as the ability to achieve about two times reduction in dosing frequency usually used for conventional dosage form (169).

It is also worth noting that in switching a patient from an immediate-release to sustained release product, the equivalent total daily dose should generally be the same, although in most cases, an effective response has been shown to be achievable with a lower dose of the sustained release product (168). Also, in view of the complexity of extended-release products and the potential for greater variability, both inter- and intra-subject, patients should be monitored at the initial stage to ensure that the anticipated benefit of switching to such products is actually obtained.

3. Pellets and sustained drug release

Due to the regular spherical shape and the possibility of incorporation of a high drug level, pellets are often the first choice when a sustained release formulation is required. In addition, pellets offer flexibility for further release modifications (170). A membrane coat is usually used to achieve release control. Drug release by coated pellets

has been achieved by dissolution-control and mostly by drug diffusion, the latter, which is governed by the intrinsic pore network of the polymeric membrane (171). The film coat was found to be the major factor controlling the drug release, although both drug and filler solubility influenced the diffusion of drug through the membrane. In some other reports, soluble co-excipients such as calcium phosphate and lactose have been demonstrated to enhance release rates of drugs, including ibuprofen by creating osmotic forces that may break the membranous barrier, resulting in higher release rates of drugs (172,173). Such unusual results could only be explained if consideration was given to the physical characteristics of both powder and pellets (174).

In another study in which diclofenac sodium pellets were coated with Surelease[®] polymer, release was dependent on the coating level of Surelease[®] (175). At low coating level, diffusion of drug was facilitated due to the presence of more pores at the surface of the coated pellets, indicating that the rate of dissolution of the drug particles was the rate-limiting step. However, at high coating loads, drug release was mainly diffusion controlled. It has also been shown that Eudragit[®] NE 30 D was suitable for coating diclofenac sodium:alginate (1:1) microspheres (176). However, apart from the effect of increasing polymer level, the release rate of drug was affected by the size and drug load of microspheres.

4. Sustained release of drugs

Controlled drug delivery offers an excellent alternative to multiple administrations obtained with immediate release preparations. These systems are capable of delivering drugs over longer time periods than conventional formulations (175,177). Drug release is

controlled by a number of variables including drug content, polymer composition and its molecular weight, device geometry, and manufacturing process. These variables enable sustained release formulations to be fitted to the respective drug release model (178).

Modern drug technologies have facilitated the production of dosage forms that exhibit modified time of release, rate of release, or both. While numerous terms exist for defining them, the USP recognizes only two types, namely, extended release (also called sustained-, prolonged- or controlled release) and delayed release (also called modified release; 168). The delayed release system, e.g. enteric-coated products, involves the release of discrete amount(s) of drug at some time other than promptly after administration, and exhibit a lag time during which little or no absorption occurs. However, they are by definition not extended-release products.

Although both sustained and controlled drug release are generally classified as extended release preparations, some differences exist between them (168). Controlled release formulation implies a predictability and reproducibility in drug release kinetics, and is therefore rate-preprogrammed drug delivery systems. Release of drug molecules in these systems has been accomplished by system design, which controls the molecular diffusion of drug molecules. Additionally, they mostly exhibit zero order plasma release profiles (Figure 8), and Fick's law of diffusion (Equation 10) is followed (179):

$$J_b = -D_b \frac{dc}{dx} \quad \text{Eqn. 10}$$

where J_b is the bulk diffusion flux, D_b is the bulk diffusion coefficient and (c) the concentration of the species.

Sustained release products offer several advantages and also some disadvantages. The use of extended-release products maintains therapeutic concentrations over prolonged periods, thus reducing the frequency of dosing and fluctuations in blood concentration (168). In addition, adverse drug effects related to transiently high concentrations are circumvented (180-182) and patient compliance improved (168,183). On the contrary sustained release products contain a higher drug load and thus any loss of integrity of the release characteristics of the dosage form has potential toxicity problems (168). Moreover, sustained release products should never be crushed or chewed as the slow-release characteristics may be lost and toxicity may result. This is particularly important in patients unable to swallow whole tablets, a problem commonly affecting the elderly or patients with gut motility problems (183). It is therefore of importance that some drug release devices exist to minimize and/or eliminate these possible adverse situations, as will be discussed below.

i. Sustained release delivery systems or devices

Several sustained release devices exist and these include diffusion-controlled products, dissolution-controlled products, erosion products, osmotic pump systems and ion-exchange resins (168,184). Some of these systems will be discussed below.

1. Dissolution-controlled products

These include encapsulated and matrix dissolution products. In these dosage forms, the rate of dissolution of the drug (and thereby availability for absorption) is controlled by coating the dosage form with slowly dissolving polymers or by

microencapsulation. Once the coating is dissolved, the drug becomes available for dissolution. Consequently, by varying the thickness of the coat and its composition, the rate of drug release can be controlled (185,186). In some preparations a fraction of the total dose is formed as an immediate-release component to provide a pulse dose soon after administration, thus decreasing or preventing the lag time associated with sustained release formulations (187). This is followed by slow release of the remaining part of the formulation.

2. Diffusion-controlled products

In these systems, a water-insoluble polymer controls the flow of water and the subsequent diffusion of dissolved drug from the dosage form. This mechanism encompasses both reservoir and matrix systems (Figure 10; 167). In the matrix system shown in Figure 10A, the drug is homogeneously dispersed throughout a rate-controlling

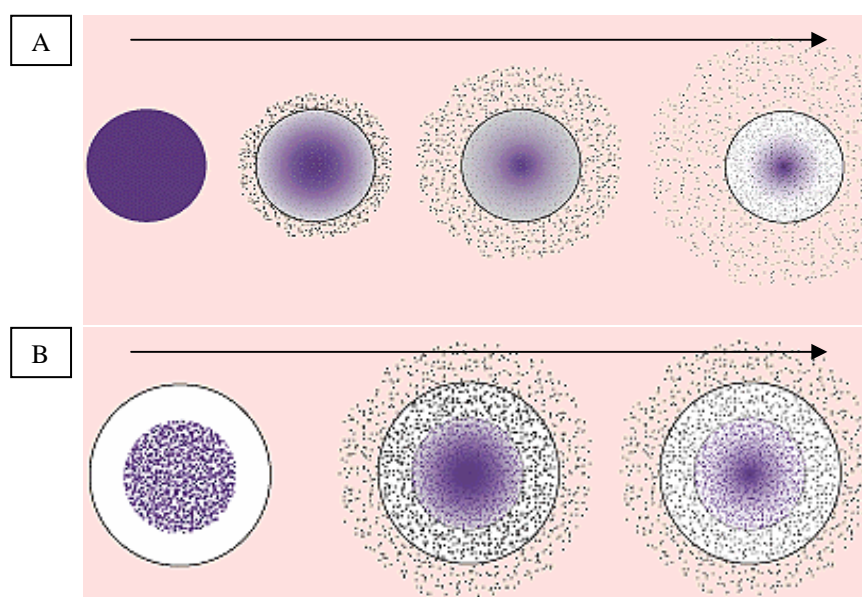


Figure 10. Delivery of drug from (A) Typical matrix drug delivery system, (B) Typical reservoir device (167). Arrows indicate the direction of drug release with time.

polymer matrix, and the rate of drug release is controlled by diffusion throughout the polymer matrix. This is described in equation 11:

$$\frac{dC}{dt} = D \frac{d^2c}{dy^2} \quad \text{Eqn. 11}$$

where y is the dimensional distance, D is the diffusion coefficient of the drug in the polymer matrix, C is the concentration of the drug at any y position and time (t).

In the reservoir device (Figure 10B) a core of drug (whether solid drug, dilute solution, or highly concentrated drug) is coated with a film or membrane of a rate-controlling material, the polymer, and the rate of drug release is controlled by its permeation through this membrane wall. Thus, because the polymer coating is essentially uniform, and also possesses a uniform thickness for a specific thickness level, the diffusion rate of the active agent can be kept fairly stable (zero order kinetics) throughout the lifetime of the delivery system. This system is described in Equation 12:

$$F = \frac{DKC_s}{L} t \quad \text{Eqn. 12}$$

where F is the flux, D is the diffusivity constant of the drug in the coating membrane, K the partition coefficient between the coating membrane and the medium, C_s is the drug solubility, t is the time taken to diffuse through the surface area and L is the membrane thickness through which the drug must diffuse. This equation is used in mathematical modeling of drug release from controlled drug release formulations where F represents the cumulative amount of drug released per unit surface area at time, t (188). A plot of F vs. t yields a regression equation with the slope of DKC_s/L , a zero order constant (k_0). In addition to the mathematical modeling of dissolution profiles, some comparison factors

have been officially stipulated to control changes that could occur between the different drug release profiles.

ii. Comparison of dissolution profiles

In various guidance documents, the Food and Drug administration (FDA) has proposed a comparison of dissolution profiles for similarity when data are available for at least three dissolution time profiles (189-192). The recommendations guiding this comparison include number of units (12), limit of variability mean dissolution values at different time points (10 - 20%), dissolution test conditions for different dosage forms (immediate and modified release), etc. The comparison is achieved either by model dependent (curve-fitting) or model-independent (statistical) methods. The former involves linear regression of the percentage dissolved at specific time points while the model independent analysis involves statistical moment based comparison, repeated measure split-plot, two way ANOVA, etc. (190), most of which could be very complicated. The method mostly adopted by the FDA is a simpler model independent mathematical approach proposed by Moore and Flanner (189) using two factors, f_1 and f_2 shown in the following equations:

$$f_1 = \frac{\{[\sum_{t=1}^n |R_t - T_t|]\}}{[\sum_{t=1}^n R_t]} * 100 \quad \text{Eq.13}$$

$$f_2 = 50 \text{LOG}\{[1 + (\frac{1}{n}) \sum_{t=1} (R_t - T_t)^2]^{-0.5} * 100\} \quad \text{Eq.14}$$

where Rt and Tt are the cumulative percentage dissolved at each n time point for the reference and test formulations respectively, Σ is the summation over all time points and LOG is logarithm to base 10.

The factor f_1 is directly proportional to the average difference between the two profiles, while f_2 is inversely proportional to the average squared difference between the two profiles, and emphasizes the larger difference among all the time-points. The f_1 factor measures the difference, while the f_2 factor measures the closeness, between the two profiles. Because of the nature of measurement, f_1 has been described as difference factor, whereas f_2 is the similarity factor (191).

Similarity in product performance is a major factor in dissolution studies and comparisons. Thus, regulatory interest lies in knowing the extent of similarity between two curves, and in measuring which curve is more sensitive to large differences at any particular time point. Consequently, the f_2 comparison has been the focus in Agency guidance documents. When the two profiles are identical, $f_2 = 50 \times \log(100) = 100$ and approaches 0 ($50 \times \log \{ [1 + 1/n \Sigma (100)^2]^{-0.5} \times 100$) as the dissimilarity increases. An average difference of 10% at all measured time points results in an f_2 value of 50. FDA has therefore set a public standard of f_2 value between 50-100 to indicate similarity between two dissolution profiles and a point-to-point difference of not more than 10%. Although this range is considered wide by some authors, from a public health point of view, and as a regulatory consideration, f_2 comparison metric with a value of 50 or greater is a conservative but reliable estimate to assure product equivalence. Generally, f_1 values up to 15 (0 – 15) ensure similarity of the two curves being compared.

As already discussed, controlled drug release is mostly achieved using the polymeric reservoir and matrix devices. Cellulose derivatives are commonly used as polymeric films in the reservoir systems, while the polymeric matrix material may be plastics, e.g. methylacrylate-methyl methacrylate, polyvinyl chloride, cellulose derivatives (hydrophilic polymers) or fatty compounds including carnauba wax (a natural wax product extracted from the leaves of a Brazilian palm tree, *Copernicia cerifera* (192)).

6. Polymeric Membranes and Sustained Drug Release

The use of polymeric film membranes has attracted considerable attention in the development of controlled release drug delivery systems in recent years. There has been a drastic shift from the originally used solutions of polymeric materials in organic solvents to the use of aqueous polymeric dispersions with different commercial names and potential applications in sustained release preparations (23). There is also considerable shift from the originally coated tablets to the use of sustained release multiparticulate/pellet delivery systems (193) using fluid-bed film coating and drying equipment.

Film coatings are applied to pellet and tablet formulations for several reasons including controlled release, taste masking, and improved stability (194). Pellet qualities, especially the shape of pellets, have been shown to influence the deposition of film coatings in a fluid-bed process. In a previous report, eight pellet batches were used to monitor the pellet shape as a function of the film thickness formed (194). Four of these were spherical visually, and the other four batches can be described as ovoids, dumbbells,

long dumbbells, and cylinders respectively. The average coat thickness of the pellets assessed by cross-sectional measurements did not appear to be influenced by the initial shape of the pellets.

Among the aqueous polymeric films used in the manufacturing industries, the ethylcellulose and polymethacrylic acid based films have been widely employed. This is due to their inertness, solubility in relatively non-toxic solvents and availability in resins with different properties (195). Surelease[®] and Eudragit[®] NE 30D are typical examples of this class of coating materials.

a. Surelease[®]

Surelease[®] is an aqueous polymeric dispersion of ethylcellulose. It is a latex coating system of fully plasticized ethylcellulose dispersions with 25% weight/weight (w/w) solids content (23). The dispersion contains dibutyl sebacate and oleic acids as plasticizers and fumed silica as an anti-adherent, in ammoniated water. Plasticizers reduce the minimum film forming temperatures as well as the glass transition temperatures, and consequently, increase the flexibility of the film coatings. Surelease[®] has been shown to be superior to several other polymers when sustained release (pellet and tablet) delivery is required, as well as with the use of the rotor-disk module (175).

Although some studies have been reported on controlled release forms of ibuprofen tablets (22-25,196) only one such formulation, namely, Brufen Retard[®], is available in the market (26). A study using ibuprofen tablets compressed from ibuprofen granulated with different concentrations of Surelease[®] showed that the tablets made from polymer-containing granules demonstrated more prolonged release profiles than control

tablets that contained no polymer (23). It was also observed that increasing the amount of Surelease[®] in the tablets resulted in a reduction in ibuprofen release rate and a linearization of the drug release curves. This was reported to be due to the higher degree of imperfection in the formation of the film membrane around ibuprofen by these low polymer levels, which might have caused increased diffusion of the drug from the dosage forms. In addition, at lower polymer concentrations (1.2 - 3.5%), the release of this acidic drug (pKa 4.8) was affected by the pH of the dissolution medium, hence, the release was considerably lower at pH 1.2 than at pH 7.5 (Figure 11). The latter results resembled

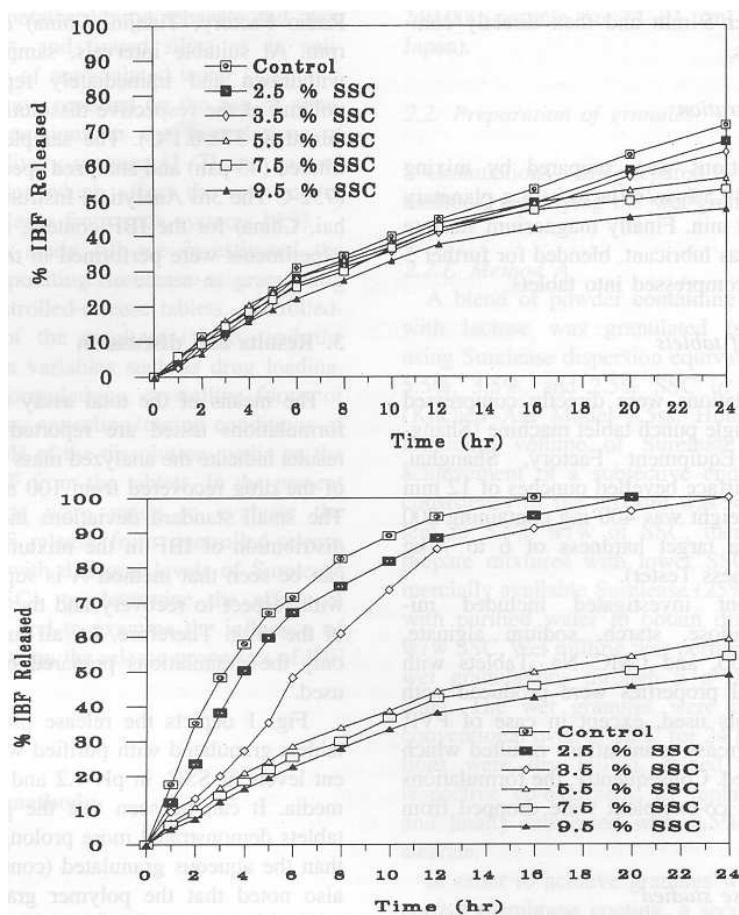


Figure 11. Release profiles of ibuprofen from tablets granulated with water (control) and different levels of Surelease[®] in pH 1.2 (Upper) and 7.5 (Lower) dissolution media (23).

those obtained with both unprocessed pure ibuprofen and processed uncoated drug at both pH values used in the study. These studies indicate that drug release rate from Surelease[®] is dependent on the thickness of the coating material, and the equilibrium solubility of the drug, which in turn is dependent on the pH of its solution (23).

From these and other studies, drug release mechanisms at both pH values were reported to be both diffusion and dissolution controlled. However, at the high pH (≥ 7.5), the release rates of pellets and tablets coated with higher Surelease[®] levels depended not only on the solubility of the drug, but also on the polymer/dissolution medium partition coefficient.

b. Poly(ethylacrylate-methylmethacrylate (Eudragit[®] NE 30D)

In processing sustained release preparations, usually additional excipients like plasticizers and glidants may be required. Modern sustained release dosage forms require reliable and minimized number of excipients to ensure a release rate of the active drug that is reproducible within a narrow range. Eudragit[®] polymers fulfill these requirements to a very high extent (197), thereby enabling research and development to create tailor-made solutions. These products are used in the pharmaceutical industry for the development of formulations for enteric and controlled-release oral products, as well as for providing protective coatings and taste masking for bitter oral dosage forms (194).

The Eudragit[®] RL- and RS-types are based on copolymers of acrylate and methacrylates with quaternary ammonium groups as functional groups. The latter determine the permeability and swellability of the films in water. The Eudragit[®] RL-types contain higher amount of the quaternary ammonium groups and therefore form

highly permeable films with little delaying action. The RS-types that contain lesser amount of the quaternary ammonium functional groups are poorly permeable, swell less easily but slow down drug diffusion very noticeably. The Eudragit[®] NE-types that include the NE 30 grade contain no functional groups but are ethylacrylate methylmethacrylate copolymers with a neutral ester group. They are both permeable and swellable in water, and are used for granulation processes and sustained release coatings (198). For the sustained release applications, their usual formulation amounts are 5 - 20% calculated on the drug weight, although sufficient release is usually obtained at 14% polymer addition (Figure 12).

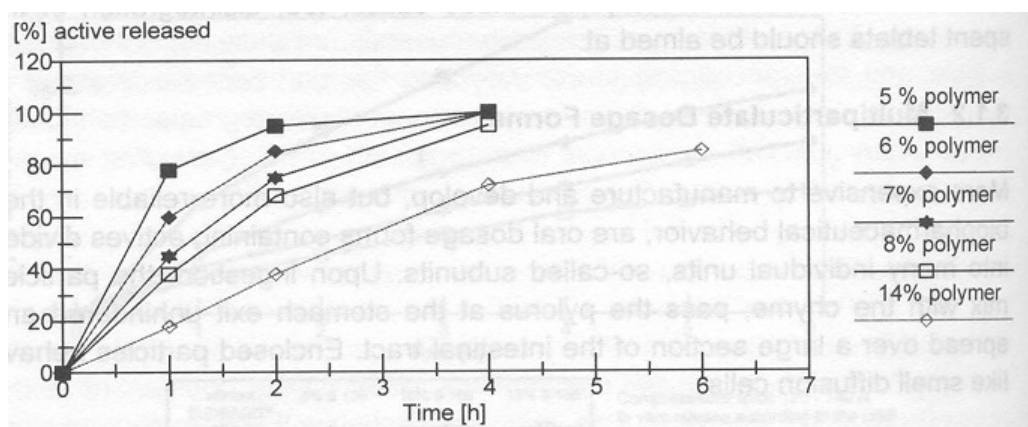


Figure 12. Coating of potassium chloride crystals with aqueous dispersion of Eudragit[®] NE 30 D (199).

Eudragit[®] NE 30D [poly(ethylacrylat-methylmethacrylat)] is an aqueous dispersion of a neutral copolymer based on ethyl acrylate and methyl methacrylate polymers, and containing 30% w/w dry polymer substance. Eudragit[®] NE 30D polymer film is water insoluble, permeable, swellable and pH independent (200,201). The water

permeability of the polymer film is critical to drug dissolution profiles; it determines both the onset of drug release and the release rates of the drug products. The release profiles can be determined by varying mixing ratios and/or film thickness of the product. As shown in Figure 12, increasing amounts of polymer has been shown to decrease release rate *in vitro*.

Besides ethyl acrylate and methyl methacrylate, the only component in the polymer latex dispersion is about 1.5% (on the dry polymer basis) surfactant, nonoxynol 100 (202). At higher concentrations, this surfactant has been shown to crystallize out from polymer films during storage, and to decrease drug release during aging. Therefore, drying of the moistened drug/polymer mixture to a residual water content of <2% is necessary to avoid changes on the release profile during storage.

For the coating process, Eudragit[®] NE 30D neither contains nor needs any plasticizer, however, stickiness shown by this product can be improved by using glidants such as talc or glyceryl monostearate. It is used in the coating of small particles for directly compressed and wet granulated products. If the coating with this polymer is complete, the model represented in Equation 12 (reservoir delivery system) is expected. If the coating is not complete (i.e. a more porous membrane exists), a mixed release mechanism with both square root of time (Equation 7) and zero order (Equation 12) release components, which has recently been proposed (177) could be operating. This is represented in Equation 15:

$$Q = Kt^{\frac{1}{2}} + \frac{DKCs}{L}t \quad \text{Eqn.15}$$

The pellet dosage forms of diffusion- or dissolution-controlled products can be encapsulated using hard gelatin capsules, or prepared as a tablet. In most cases where gelatin encapsulation were used, the physical characteristics evaluated included bulk and tapped densities, Carr's compressibility index, and drug release properties (203,204). The release profiles can be assessed as a mean dissolution time (MDT) and its variance (VDT) or by comparison using the similarity factor. The mechanism of dissolution could be assessed from the value of the relative dispersion (RD) of the mean dissolution time. In some cases where the pellets are tableted, the possible relationship between the properties of the pellets and those of the tablets is evaluated by canonical analysis followed by multiple regression analysis (205). In the latter studies, it was found that only about 51% of the tablet properties could be predicted from the properties of the pellets.

One of the advantages of encapsulated pelleted products is that the onset of absorption is less sensitive to stomach emptying (206). Additionally, because of their small size the entrance of the pellets into the small intestine (where the majority of drug absorption occurs) is expected to be more uniform than with non-disintegrating extended-release tablet formulations.

7. Hard Gelatin Encapsulation and Technology

a. Hard Gelatin Encapsulation

Most capsules are made from gelatin that is also widely used in many food products. Gelatin is a mixture of water-soluble proteins derived primarily from collagen, the main naturally-occurring protein constituent of connective tissue (207). Gelatin is

defined as a versatile container that can encapsulate powders, pellets, liquids, semi-solid formulations, caplets, tablets and even combinations of these (Figure 13).



Figure 13: Capsules as versatile container for different pharmaceutical dosage forms (208).

Capsules are made from pharmaceutical grade gelatin that has met the stringent requirements of the United States Pharmacopoeia and other international organizations that set standards for products used in medicines. In the body, the water-soluble gelatin shell dissolves in the stomach, releasing its contents within the first few minutes of swallowing.

Both tablets and capsules are well-proven and well-accepted dosage forms. However, capsules have the added advantages of masking the taste and/or odor of specific medicinal compounds, are easy to swallow, have attractive appearance, color, and can also be easily filled and processed (209). The capsule provides a simple way for the patient to take medications or supplements, and many pharmaceutical companies use capsule-filling machines as a convenient way to package a pharmaceutical product for single or multiple doses. Additionally, capsules require fewer excipients and have been

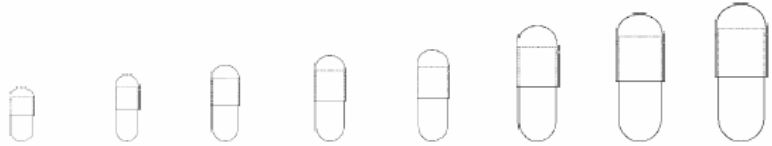
shown to be more suitable for sustained release dosage forms. Therefore, capsules can promote patient compliance (210).

b. Hard Gelatin Capsule Technology

A detailed step-by-step description of hard gelatin capsule production has been given (211). These are manufactured from melted gelatin in demineralized water with the addition of any needed additives like dyes and opacifants, in feed tanks that gravity-feed the mixture into a dipper section. Herein, the capsule cap and body are molded onto their respective stainless steel pin bars dipped into the gelatin solution. Once dipped, the pin bars rise to the upper deck allowing the cap and body to set. Then, gently moving air that is precisely controlled for volume, temperature, and humidity, dries the capsule halves up to a stipulated amount of moisture, while precision controls constantly monitor humidity, temperature, and gelatin viscosity throughout the production process. Once drying is complete, the pin bars are moved to an automatic table section where the capsule halves are stripped from the pins. The cap and body lengths are then precisely trimmed to an acceptable tolerance, and joined automatically in joiner blocks. The finished capsules are pushed onto a conveyer belt, which empties them into a container.

Throughout the production process, capsule qualities, size, moisture content, wall thickness, and color, are monitored. Capsules are sorted and often visually inspected on specially designed inspection stations. Perfect capsules are imprinted with a particular logo on high-speed capsule printing machines, and thereafter sterilized and packaged as required.

The most commonly used capsule sizes range from 000 to 5, largest to smallest size respectively, and have corresponding fill powder volumes and weights (Figure 14). If a greater extent of compression is required in order to fill large dose drugs or to use a smaller capsule size, the dosator nozzle principle discussed in a later section usually works more successfully for granules, but not necessarily for pellets that do not require the formation of firm plugs for filling.



Size	5	4	3	2	1	0	00	000
Volume (ml)	0.13	0.21	0.30	0.37	0.50	0.68	0.95	1.37
Typical Fill Wt. (mg) Depends on Powder Density	60-130	95-210	135-300	165-370	225-500	305-680	430-950	615-1370

Figure 14. Capsules showing approximate sizes and typical fill weight (212).

c. Capsule Filling Machine Instrumentation

Capsule-filling machines generally consist of a through-hole for accommodating the cap of a capsule and a body transport member having a body pocket for accommodating a body of the capsule (213). It also comprises of a filling system for filling the capsule contents. The contents are typically pharmaceutical products (powders, pellets, oils) and foods. The filling system includes a force-feeding screw disposed in a chamber, and has a lower end opening above the body transport member. Thus, powders/pellets supplied into the chamber are compulsorily force-fed into the capsule body by the force-feeding screw. Consequently, even if the substances to be filled into a

capsule have low bulk density and inferior formability and fluidity, they can be compulsorily force-fed into the capsule body by the screw system. By so doing, filled capsule in which a predetermined amount of the contents is filled can be produced with certainty. The cap transport part includes a plurality of segments that includes the cap pocket. These segments are individually vertically movable with respect to one another and also in a vertical direction away from the body transport member.

A modern and ideal capsule-filling machine is designed to fill the material which could be very low in bulk density and very inferior in fluidity or formability. These could include crushed substance of weeds, grass or tea leaves or silicon dioxide. Most of these are difficult for a conventional filling machine because of the uncertainty of the expected fill amount. The machines typically form the capsule contents (plugs, pellet dose, etc.) once and charge them as such into the capsule body. Alternatively, vibrations are applied to the substances that facilitate their flowing into the capsule body. It is expected that for every capsule filling machine, various products of different qualities could be filled well into a capsule reproducibly.

There are basically two types of automatic capsule filling machines that are commonly used in the pharmaceutical field, based on their mechanisms of filling. These are the dosator and the tamping and dosing disk (tamp filling) machines.

d. Types of Automatic Capsule Filling Machines

1. Tamp filling machine

The dosing disk consists of a rotating steel plate with precisely bored holes that form the dosing chamber. This machine depends on pushing pins through a powder bed

so that a unit dose is transferred into a dosing disk cavity. This dose is then ejected into the capsule body. The important process variables of the tamping capsule filling machine include the fill weight, the tamping force, the number of tamps, the operational speed, powder bed height, and formulation variables such as the presence or absence of lubricants and disintegrants. These variables have been widely studied and their requirements at various filling conditions validated (214,215). It has also been reported that substance flowability affects the filling weight adversely.

The operational speed is the operating rate of the machine that has been shown to relate strongly with the filled capsule characteristics, especially, the average capsule fill weight (216). Variability in the latter is expressed as standard deviation and coefficient of fill weight variation.

Recent adaptations of the tamp-filling machine for pellet filling include gravity-feeding of the pellets from a hopper into main pellet housing. A male and a female gates control the amount of pellet that could be filled into the capsules (Figure 21). In this case, the shuttle speed, which regulates the length of time the gates could remain open, is an important variable that affects the capsule fill weight (217).

The instrumentation of tamp-filling capsule machine is normally described in different ways. In some studies, it was described using strain gauges, by moving an instrumented piston from one compression station to the next (218). These revealed important relationships between compression force, piston setting, and final fill weight, with the latter being a complex interaction of all compression stations. In another report, the instrumentation of a Bosch GKF 400S tamp-filling machine was described using a

prototype of a pneumatic tamping head equipped with a piezoelectric force transducer (219).

During continuous capsule filling, feedback control of capsule fill weight can be achieved. Podczeck (219) established this mechanism by replacing the springs of a conventional tamping machine situated between tamping pins and the upper part of the tamping head with a pneumatic system. He reported that the air pressure inside the pneumatic chamber can be regulated through a feedback switch valve, and that the use of the pneumatic tamping head is limited to the control of fill weight during tamping. Therefore, major adjustments of fill weight at the set-up stage of the machine should be made by alteration of the tamping pin and powder bed height settings. Although the principles of capsule fill weight control by continuous monitoring of tamping forces have been established, the transfer of the system to full industrial use requires further development by every machine manufacturer.

A trend has been observed toward slower dissolution rate with increasing number of tamps due to increased compactedness, and also depending on the type of filler used (220). The inclusion of a disintegrant tends to nullify the effects of number of tamps or tamping force and enhances drug dissolution markedly. Insoluble fillers appear to cause some drugs to follow a diffusion mechanism from insoluble matrix model regardless of the number of tamps or their intensity. Using drug plugs, mercury intrusion pore size distribution data and other studies suggest that for tamp forces 100 or 200 N, only two tamps are sufficient for a good powder consolidation. However, the tamp filling machine has also been reported to be very suitable for pellets that do not require plug formation in order to be properly filled (215).

2. Dosator filling machine

The dosator principle is used by numerous intermittent-motion and continuous-motion capsule-filling machines. Its instrumentation has been likened to that of tablet machines because they both rely on compression process (215). The compressibility is related to the tapped density of the materials, thus, it is suitable for powders that require high compressibility for encapsulation. Very flowable powders and consequently pellets have been found difficult to densify and fill using this machine leading to greater variation in fill weight.

The important variables for this system include the type and level of lubricant and the ejection force, powder bed height, piston height, and compression force on the ejection forces generated during the filling process. It has been observed that the ejection force increased with increasing the powder bed height, piston height and compression force (219). In a study using a Zanasi LZ 64 machine with intermittent operation, the effect of the excipient- and machine parameters on the filling of the capsule and the dissolution rate using caffeine as model substance was determined (221). Sufficient lubrication of the capsule powder mixture measurable by low ejection forces is critical for a uniform fill weight. However, addition of too much lubricant prevented the compact from forming and increased the standard deviation of the fill weight (222). Another report also showed that for an effectively lubricated formulation, a lubricant film is formed and maintained on the inside of the dosator nozzle during a run, which maintains the ejection force of the process (223). However, for a less effectively lubricated film, where the lubricant film is not formed and maintained, the ejection force increases slightly as each slug is ejected.

3. Comparison of the tamp and dosator capsule filling machines

A comparison of the effectiveness of the above two commonly used capsule-filling mechanisms have been made by several authors (204,224). In one of the studies, four different granule size fractions of Sorbitol instant[®] were filled into hard gelatin capsules on a tamp filling (Bosch) and a dosator nozzle machine (Zanasi). An acceptable filling performance was always observed and was independent of the machine type employed. A direct relationship between the angle of internal flow and the coefficient of fill weight variation has also been recorded for both systems (224). However the tamp filling machine was found to be slightly better for the coarser granule size fractions, because it does not require the formation of a firm plug.

It has therefore been concluded that in situations where a low plug density is an essential prerequisite for product qualities including drug dissolution and bioavailability, the tamp-filling machine is more suitable. The dosator machine is preferred when higher compressibility is required as to fit large drug doses into small capsule sizes. The compressibility issue is however not applicable to the filling of pharmaceutical pellets that are normally $\geq 400 \mu\text{m}$, especially as it has been shown that particles larger than $40 \mu\text{m}$ do not efficiently form a plug (215). Additionally, the dosator machine is not suitable for the filling of pellets since their inability to form plugs will lead to loss of metered doses from the nozzle during its passage from the hopper to the capsule body.

In a previous report, a dosator and a tamping capsule filling machines were used to study the relation between variation of filling weight and powder flowability in connection with filling mechanism (225). The angle of repose, the minimum orifice diameter and the discharge rate through orifices were measured. The orifice diameter is

the length of a straight line which passes through the center of the orifice, and terminates at the circumference. The minimum orifice diameter was closely related to the discharge rate through orifices. The angle of repose was used as an index of flowability representing the mobility of the particles on the surface of a powder bed, while the minimum orifice diameter was used as one representing the mobility of the particles in a powder bed under dynamic conditions. In both systems, no good correlations were found between the angle of repose and the minimum orifices. However, a good correlation was found between the variation of filling-weight and the minimum orifice diameter in a dosator system. In tamping system, the variation of filling-weight was closely related to the angle of repose. In this system, a minimum point appeared in the plots of the angle of repose *versus* the coefficient of variation of filling-weight. This indicated that as the angle of repose increases, the variation of filling-weight is governed by both the variation of the powder-bed-height (an increasing factor) and the amount that escapes the filled capsule (a decreasing factor).

Consequently, the tamp filling machine (Figure 15), which has been shown to



Figure 15: Tamp capsule filling machine with color touch-screen control (left; 226).

posses the ability of handling a wider range of products than a dosator machine, including medicinal herbs, will be used in our study.

e. Stages of Hard Gelatin Encapsulation Process

All capsule-filling machines rectify, separate, fill and join empty capsules that are thereafter ejected from the system (227). Modern capsule fillers are designed to offer precise dosing, high speed, and easy changeover and cleanup.

1. Rectification

In order to obtain a capsule product as described above, the cap transport portion is placed on the body transport member such that the cap and body pockets are aligned with each other. This arrangement can accommodate an empty capsule in which the cap and the body are temporarily coupled to each other.

2. Separation

The empty capsule is transported in the formed capsule pocket in an erected position, with the cap directed upward. During transportation of the empty capsule, the cap and the body are separated from each other inside the capsule pocket, the cap is held in the cap pocket while the body is held in the body pocket. Thereafter, the cap and body transport members are separated from each other.

3. Filling

The material or medicament is directly force-fed and filled into the body by the force-feeding screw.

4. Joining and ejection

Finally, the cap transport member is placed onto the body transport member such that they are once more aligned with each other, and then coupled to each other within the capsule pocket, to produce a filled capsule product.

f. Comparison of Hard Gelatin Encapsulation of Various Dosage Forms

1. Powder

The filling of powders in capsules demands a powder with good pharmacotechnological properties for samples to be constant, and to facilitate its transfer into the capsule (228). Thus the powder bulk and tapped densities, its various flow angles: repose, internal flow, and friction, as well as some machine variables are of great importance (229). The range of powder combinations that can be filled on the tamp filling machine exceeds that applicable to a dosator nozzle system. However, the latter is used very extensively because large doses of highly compressible drugs can be filled into smaller capsule sizes. Microcrystalline cellulose (MCC) and silicified microcrystalline cellulose (SMCC) powdered formulations are mostly used as fillers in powder capsule technology (230), while lactose, Mg stearate, and sodium lauryl sulfate are mostly used as lubricants (231,232).

The problems encountered with powder filling are numerous and depend on the type of material. Filling problems due to powder flooding could be solved by increasing the powder bed height in the powder bowl. Inappropriate powder bed height adversely affects the capsule fill weight, an effect which increases with decreasing powder flow. Tamping pin setting and powder bed height influence capsule fill weight of powders and even granulated products having poor flowability. However, for moderate flowing powders and granules, the coefficient of fill weight variation, an attribute of the powder distribution into the capsules, appeared to be nearly independent of powder bed height or tamping pin setting. The filling performance of powders with poor flow properties could therefore be adjusted by optimizing both machine settings.

2. Liquids and semi-liquids

Liquid and semi-solid formulations in hard gelatin capsules provide alternate choice over soft gelatin capsules for improving bioavailability and stabilizing moisture- or oxygen-sensitive drugs, processing for low melting point drugs and achieving good content uniformity for low-dose drugs. They are also convenient delivery route for administering high potency compounds. In addition to high patient acceptability, they can also improve product stability (233). Other advantages of this technology over soft gelatin capsules have been demonstrated, especially the flexibility of developing solid dispersion and controlled-release formulations. These products include oils, waxes, polyethylene glycols, pluronics, surfactants, self-emulsifying system and polyglycolized glycerides (Gelucire[®]) with a range of melting point and hydrophilic-lipophilic balance

(HLB) values and. Important processing variables include filling temperature, cooling rate, and shear rate and should be carefully evaluated (234).

3. Tablets

Tablets are encapsulated for various purposes, including improved stability and taste. A fiber-optic probe or an electrochemical device is usually incorporated in the system to verify the dosing (226,235). This is coupled with a reject mechanism that rejects capsules with missing tablets. It is recommended that tablet dimensions and hardness specifications be maintained within strict tolerance, to assure proper tablet feed. Spherical tablets are most suitable for this technology.

It has however been shown that in comparison with tablets, pellet encapsulation is the technology of choice both for immediate and sustained release formulations. Moreover, it is not plausible to compress coated pellets into tablets due to cracking of the protective and sustained release coatings. In order to maintain the geometry of pellets, coated and uncoated, encapsulation is therefore the preferred method.

4. Pellets

Pellets are very suitable for hard gelatin encapsulation because of their regularity of shape, good flowability and other physiological and mechanical qualities. Pellets can be filled into hard gelatin capsules using different methods that include feed-frame, dosing chamber and vacuum dosator methods. In the feed frame method, most pellet formulations are designed with a bulk density to fill the capsule body completely. The

vacuum dosator method maintains strictly the dosator mechanism already discussed. The dosing chamber method (Figure 16) is widely utilized by many machine types including the tamp filling machines, because it allows for partial dosing of the capsule, as well as for dosing capsules with two types of pellets or beads. These pellet formulations must be free flowing and free from agglomerations or electrostatic charge that interfere with pellet discharge into the capsule body from the dosing chamber. Narrow to uniform particle sizes also facilitate accurate dosing.

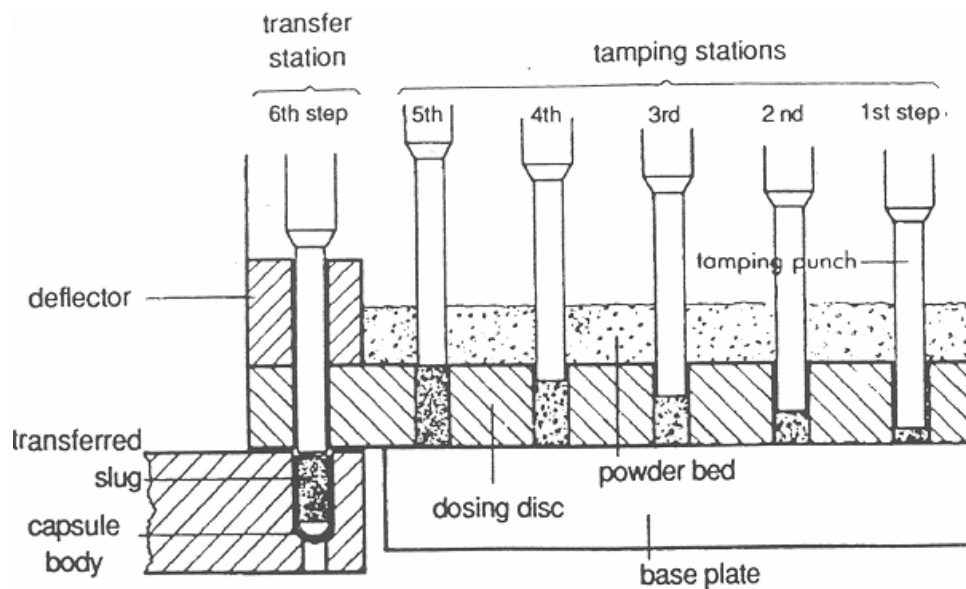


Figure 16: Tamping pellet filling system (227).

A new automatic ultrasonic control system has been developed for the determination of the filling height in pellet encapsulation, and integrated into an intermittently operating high output capsule filling machine (236). Measurement of the time required for transmission of several ultrasonic impulses determines the height to which each capsule has been filled. Utilizing this in-line measuring system, it is possible

to monitor the fill mass of all capsules without a reduction in throughput. Furthermore, the sporadic occurrence of overfilled or under filled capsules can be detected with a high probability and such capsules rejected, contrary to manual in process control methods. This new filling monitoring system has been successfully validated and also used successfully in routine operation.

In a previous study (209), film coated and uncoated pellets of different shapes, varying from spherical to cylindrical, were filled into hard shell capsules. It was observed that when no film coat was applied, the pellets needed not be perfectly spherical in order to be filled reproducibly. Thus, an aspect ratio (i.e. the ratio of the maximum and minimum dimensions of a particle) of ≤ 1.2 was suitable for encapsulating the pellets into hard gelatin capsules, and only very pronounced surface roughness hindered the filling process. After coating of the pellets with an ethylcellulose film, none of the batches could be filled to an acceptable standard, because electrostatic loading led to a blockage of the filling mechanism. The addition of 1% talcum powder was sufficient to remove all charges. It is therefore necessary to monitor the surface roughness and pellet shape/aspect ratio for efficient encapsulation of coated and uncoated pellets respectively.

Pellet encapsulation also leads to reproducible gastrointestinal transit times that result in increased efficacy and safety of these dosage forms compared to single unit dosage forms or tablets (70). Furthermore, predictable concentration/time profiles can be achieved and local mucosa irritations reduced. Using traditional extrusion/spheronization process for theophylline, it has been shown that several process steps are necessary to obtain the finished encapsulated dosage form. However, the pharmacokinetic and clinical

advantages already mentioned compensated the increased investment necessary for this pellet development (70). The use of the rotor-disk module in both spheronization and coating processes will eliminate the several steps involved in the traditional spheronization process, thereby leading to a reduction in processing time and cost.

To confirm these advantages, two sustained-release (pellets in hard gelatin capsules) forms of propranolol have been compared with ordinary sustained release propranolol tablets (237). The bioavailability of the capsules was more acceptable than that of the tablets due to improved absorption and efficacy.

Despite the several advantages of microparticulate dosage forms and capsules over tablets, there are no ibuprofen pellet formulations in the market in both immediate and sustained release forms. Additionally, elaborate studies have not been done to elucidate the advantages and drawbacks of the fluid-bed rotor-disk machine. Therefore, the specific aims of this research are as follows:

- 1) Development of ibuprofen spheroids from different drug particle sizes and different drug loads using the rotor-disk fluid-bed technology and Avicel[®] as the major excipient and spheronization enhancer, sodium lauryl sulfate as lubricant and water as the granulating liquid.
- 2) Optimization of the developed process and product variables using statistically designed factorial experiment.
- 3) Scale-up of process and batch size from development to pilot and eventually to semi-production sizes.

4) Polymer coating and encapsulation of coated and uncoated microparticulates using hard gelatin capsules for comparative evaluation of controlled and immediate release delivery systems.

II. EXPERIMENTAL

A. Materials and Equipment

The materials and equipment used in the study are shown in Tables II and III respectively.

Table II: List of Materials

Material	Lot/Batch Number	Manufacturer/Supplier
Ibuprofen (20 μ)	LPL-4814	Albemarle Corp., Baton Rouge, LA
Ibuprofen (40 μ)	LPL-5810	Albemarle Corp., Baton Rouge, LA
Avicel [®] RC-581	B106C	FMC Biopolymer, Princeton, NJ
Avicel [®] CL-611	A178N	FMC Biopolymer, Princeton, NJ
Sodium lauryl sulfate	S0180	Spectrum Chemicals, Gardena, CA
HPMC (Methocel [®])	E5LV	Dow Chemical Co., Midland, MI
Talc	W47835P09	Spectrum Chemicals, Gardena, CA
Surelease [®]	E-7-19010	Colorcon, West Point, PA
Eudragit [®] NE 30D	1290112016	ROHM Technical Inc., Malden, MA
Hard gelatin capsules	619067	Capsugel, Greenwood, SC
Sodium hydroxide	S3183	Fisher Scientific, Pittsburgh, PA
Acetonitrile (HPLC grade)	943286	Fisher Scientific, Pittsburgh, PA
Glacial acetic acid	903092	Fisher Scientific, Pittsburgh, PA
Potassium phosphate monobasic	966500	Fisher Scientific, Pittsburgh, PA
Methanol (HPLC grade)	970703	Fisher Scientific, Pittsburgh, PA
Triethylamine	920412	Fisher Scientific, Pittsburgh, PA
Polysorbate 80	A38-500	Fisher Scientific, Pittsburgh, PA

Table III: List of Equipment

Equipment	Model Number	Manufacturer/supplier
Fluid-bed Granulator	FL-MULTI-1	Vector Corporation, Cranbury, NJ
Fluid-bed Granulator	FL-MULTI-15	Vector Corporation, Cranbury, NJ
Fluid-bed Granulator	FLN-120	Vector Corporation, Cranbury, NJ
Glatt Fluid-bed	WSC-5	Glatt, Binzen, Germany
Capsule filling machine	K150i	Romaco/Index, Pompton Plains, NJ
Liquid Chromatography system	LC-10AS	Shimadzu Scientific Instruments, Columbia, MD
Auto Injector	SIL-10A	Shimadzu Scientific Instruments, Columbia, MD
UV-VIS Detector	SPD-10A	Shimadzu Scientific Instruments, Columbia, MD
System Controller	SCL-10A	Shimadzu Scientific Instruments, Columbia, MD
Precolumn	LUNA 5 C18	Phenomenex, Torrance, CA
Column	IB-SIL 5 C18	Phenomenex, Torrance, CA
Ezchrom [®] Software	Version 3	Shimadzu Scientific Instruments, Columbia, MA
Vander Kamp Tap Density tester	10705	Van-Kel Industries, Edison, NJ
Computrac [®] Moisture Analyzer	Max 200	Arizona Instrument, Las Vegas, NV
Image analyzer	Quantimet 500	Leica Cambridge LTD., Cambridge, UK
Image analysis software	QWIN	Leica Cambridge LTD., Cambridge, UK
Microscope	Microstar IV	Bordersen Instrument Co., Valencia, PA
Sieve Shaker	18480	CSC Scientific Co., Inc., Fairfax, VA
Mettler moisture analyzer	Mettler Pm 100	Mettler Toledo Inc., Columbus, OH
Denver Instruments balance	B077193	Denver Instruments Company, Arvado, CO
Dissolution Apparatus	VK-600	VanKel Industries, Inc., Edison, NJ
JMP [®] software	Versions 3.0 & 4.0	SAS Institute, New York, NY
Scanning electron microscope	Hitachi S510	Hitachi, Tokyo, Japan
Scanning electron microscope	Philips XL 30 FEG	Holland, Netherlands
Cressington Sputter Coater	108	Franklin Electric, Bluffton, IN
Hummer Sputtering System	LO.2	ANATECH Ltd., Alexandria, VA

B. Methodology

The methodology is divided into four phases:

1. Feasibility studies in the spheronization and scale-up of ibuprofen microparticulates using the fluid-bed rotor-disk technology and also using only Avicel[®] as spheronization enhancer, sodium lauryl sulfate as lubricant and water as binder.
2. Optimization of the developed process and product variables using statistically designed factorial experiment.
3. Evaluation of the effects of drug loading, particle size and intermediate size scale-up using the fluid-bed rotor-disk technology.
4. Coating of spheronized ibuprofen microparticulates and encapsulation of coated and uncoated formulations using hard gelatin capsules for sustained and immediate release delivery systems.

Phase 1

Feasibility Studies To Evaluate the Spheronization and Scale-up of Ibuprofen

Microparticulates

a. Blending and spheronization

1. Spheronization of 0.75 kg trial batch

Preliminary spheronization was performed in FLM-1 fluid-bed granulator, VPS Corporation, Cranbury, NJ (Figure 17) using a teflon plate (9") and 0.75 kg batch of

ibuprofen and Avicel[®] RC-581 (1:1), with 1% SLS. Spheroids were successfully made. The moisture content of the powder bed was checked at regular intervals using a Mettler moisture balance (Mettler Pm100 and LP16, Mettler Toledo Inc., Columbus, OH).

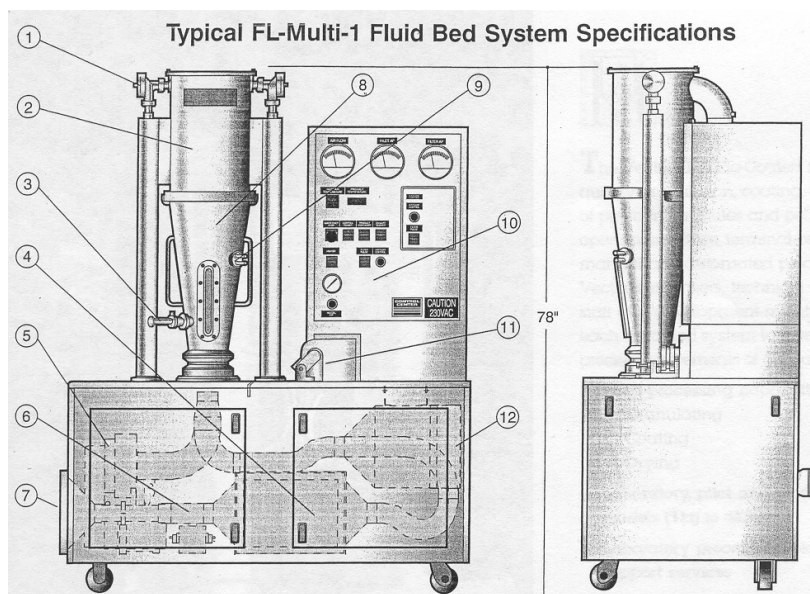


Figure 17. Components of Vector FL-Multi 1 fluid-bed granulator. (1) Pulse valve, (2) Cartridge filters, (3) Sample port, (4) Process air heater, (5) Exhaust blower, (6) Air flow station, (7) Inlet air filter, (8) Interchangeable processing inserts, (9) Spray gun, (10) Control panel, (11) Solution pump, (12) High Efficiency Particle Arresting (HEPA) filters (97).

It was observed that, the amount of water needed to provide appropriate consistency was between 50 and 52% of the dry powder blend. Based on this observation, FLM-15 (Figures 4 and 18; 12" plates), together with the conditions stated on Table IV were used for initial batches of 1 kg, which were later scaled up to 5 kg and 10 kg pilot batches using 19" plate.

Table IV. Spheronization Conditions and Process Parameters

	Equipment	FLM-15		
	Parameters			
Batch size		1 kg	5 kg	10 kg
Plate size		12"	19"	19"
Centrifugal force (N)		41,667	41,667	41,667
Plate material type/contour		SS/smooth	SS/smooth	SS/smooth
		Tef./waffle	Tef./waffle	Tef./waffle
Spraying				
	Air volume (cfm) A ₁ and A ₂ values	50	90	140
	Plate gap (mm)	0.8	3.5	6
	Spray rate (g/min) B ₁ and B ₂ values	50	90	140
	Rotor speed (rpm)	500	300	200
	Inlet air temperature (°C)	25-30	25-30	25-30
	Product temperature (°C)	18-22	18-22	18-22
	Atomization air pressure (psi)	45	45	45
Drying				
	Air volume (cfm)	85	145	220
	Plate gap (mm)	1.3	5.0	8
	Rotor speed (rpm)	150	124	124

SS/smooth: Stainless steel smooth; Tef./waffle: Teflon waffle

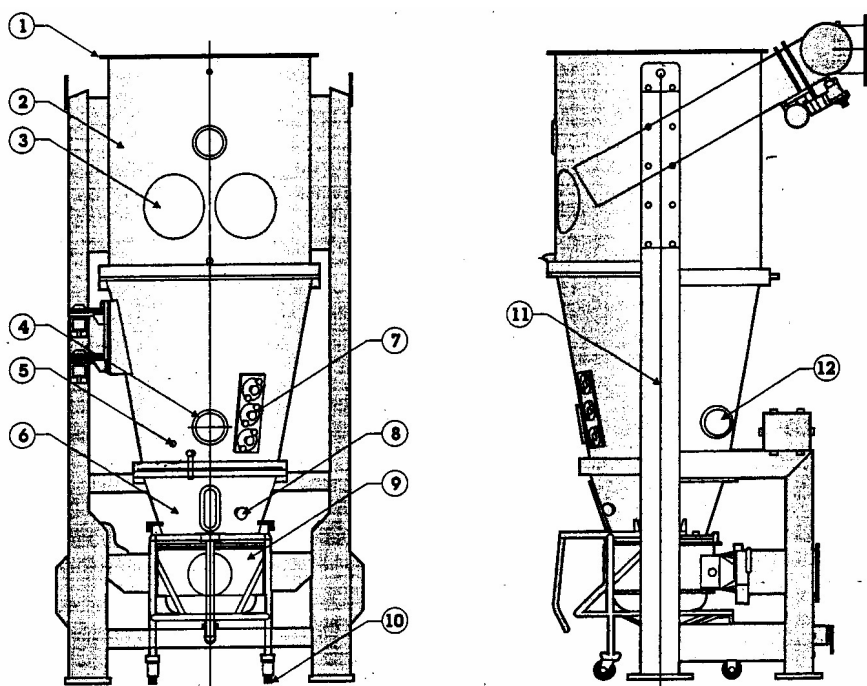


Figure 18. Components of the Vector FLM-15 equipment. (1) Top exhaust vent (2) Filter chamber (3) Filter access doors (4) View windows (5) Temperature probe (6) Product container (7) Spray gun ports (8) Sample port (9) Inlet air plenum (10) product container cart (11) Support frame (12) Inspection light windows (97).

2. Spheronization of 1 kg batches

Several formulation (Table VA) and process (Table VB) variables resulting in the development of eleven different batches were used to determine those parameters that will yield spheroids with acceptable characteristics. These preliminary parameters are shown in Table VI.

Ibuprofen (20 μm) and Avicel[®] RC-581 or CL-611 were sieved through a size 16 (1,180 μm) mesh sieve. Weighed amounts (1:1) of the sieved ibuprofen and Avicel[®]

Table VA. Formulation Variables

Variables	Batch size		
	1 kg	5 kg	10 kg
Avicel [®] type	RC-581	RC-581	RC-581
	CL-611		
Binder	Water	Water	Water
	HPMC		
SLS (1%)	Present	Present	Present
	Absent		
Talc (3%)	Present	Absent	Absent
	Absent		
PEG (25%)	Present	Absent	Absent
	Absent		

Table VB. Process Variables

Variables	Batch size		
	1 kg	5 kg	10 kg
Stainless steel/Waffle plate	Used	Not used	Not used
	Not used		
Stainless steel/Smooth plate	Used	Used	Used
	Not used		
Teflon/Waffle plate	Used	Used	Used
	Not used		
500 rpm	Used	Used	Used
	Not used		
650 rpm	Used	Not used	Not used
	Not used		

RC-581 or CL-611 were blended with and without 1% SLS, and spheronized in FLM-15 using water or HPMC solution as binders. The other formulation and process variables are shown in Tables VA and VB. The inlet and exhaust flaps were kept open and a frequency drive device was used to adjust the control of the air-flow. Fluidization of powder blend was achieved by centrifugal, vertical and gravitational forces, as well as heated air drawn through a gap around the rotor-disk and also by the nozzle pressure (47,95).

The air volume and velocity of air can be adjusted with the gap-adjustment ring below the disk. This aids in air distribution while the rotor-disk is spinning in a clockwise direction. The fine powders lifted up by the fluidization air are restricted by polyester air filters (in the upper part of the equipment chamber) that are intermittently cleaned or cleared by a pulsating jet of air, enabling them to be returned to the batch (98). Spheronization end point was visually assessed, based on experience and the fluidization pattern that has been observed to correspond to moisture content of 50 - 52%.

Drying was performed at gradual inlet temperature increases of 10 °C every 5 min up to 60 °C. This staged drying was done to prevent case hardening of the spheroids. The end point for drying was achieved when the product temperature reached 50 °C. The moisture content at the end of spheronization and drying periods were measured to determine loss on drying (LOD; 139) using the moisture balance at 85 °C and the result was recorded when the value became constant. The 85 °C was chosen to achieve optimal moisture loss with the product remaining intact.

Table VI. Variables Involved in the Preliminary Trial Batches

Trials	1	2	3	4	5	6	7	8	9	10	11
Variables	Standard	No SLS	Avicel [®] CL-611	Smooth disk	650/SS Smooth disk	HPMC (5%)	500/tef Waffle disk	650/tef Waffle disk	650/SS Waffle disk	PEG (25%)	Talc (3%)

*Standard formulation

1 % SLS: surfactant and wetting agent

Avicel[®] RC-581: filler, binder

Plate material type: stainless steel

Plate contour: waffle

500/SS: rotational speed/stainless steel

Water: granulating liquid

PEG: Polyethylene glycol.

Consequent to data analyses of the eleven spheronized batches and the resultant product characteristics (yield, particle size, size distribution, sphericity, etc.), eight of these 1 kg batches were replicated twice and analyzed further (Table VI, trials 1-8). Two of the replicated formulations (trials 4 and 7) were used to make two batches each of 5 kg, 10 kg pilot scale-up trials (trials 12 - 15).

3. Spheronization of Pilot scale batches (5 kg and 10 kg batches)

Scale-up was based on geometric similarity using the plate radius (R) and centrifugal force (Fc) as similarity factors, as shown in equations 5 and 6 for rotational speed (V) and centrifugal force (Fc) respectively. These equations are modifications of the Froude's number equation as reported by Horsthuis, *et al.* (137).

$$V = \sqrt{\frac{Fc * R}{W}} \quad \text{Eqn.5}$$

$$Fc = \frac{W * V^2}{R} \quad \text{Eqn. 6}$$

Using known values of weight (1 kg), rotational speed (500 rpm) and plate radius (6"), the centrifugal force was calculated to be 41,667 Newtons. Using this value, the rotational (rotor) speeds during spheronization phase for 5 kg and 10 kg batches were calculated from equation 6 to be 300 and 200 rpm respectively (Table IV). The Froude's numbers for 1 kg, 5 kg and 10 kg batches were of 72.00, 41.04 and 18.24 respectively.

For drying of the scale-up batches, a reduced rotor speed was used. The two plate types and contours used for these two batches are shown in Figure 19. The principle of geometric similarity was also applied to other process variables using the results of the

1 kg batches as well, and also using the air volume indicator present on the equipment (101). The air volume that gave the desirable fluidization for the scale-up batches was obtained visually by tuning the frequency drive of the exhaust blower in order to balance the air volume and velocity. This correlated with an increased air volume of 10 cfm for each additional kilogram powder (Table IV). The spray rate multiplier for the scale-up batches was determined as the ratio of the two air volumes needed for fluidization of both batches, and was calculated from known values using Equation 4.

$$B_2 = \frac{A_2 * B_1}{A_1} \quad \text{Eqn. 4}$$

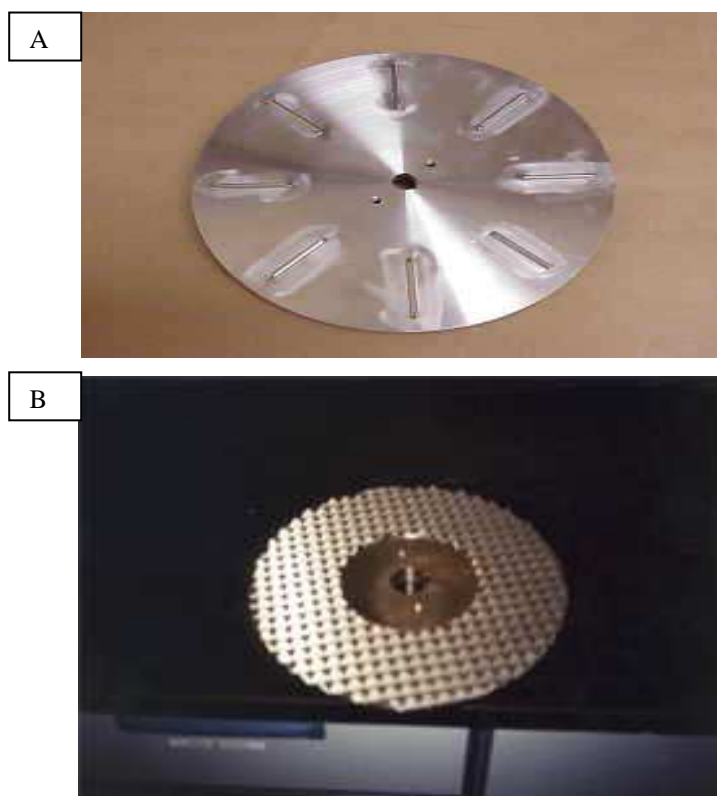


Figure 19. Rotor-disk plates for fluid-bed machines, stainless steel/smooth (A);
teflon/waffle (B) (97).

b. Physical Characteristics of Developed Microparticulates

Acceptance criteria were set for the physical qualities of the spheroids based on literature (6,9) and FDA guidance for immediate release dosage forms (147). These included high product yield: $\geq 85\%$, adequate sphericity: ≥ 0.85 , high drug content: $\geq 90\%$, good dissolution profile: $Q_{20} \geq 80\%$, good flowability: $\theta \leq 30^\circ$, granule size distribution in the range between 250 and 850 μm [(20/60 mesh) chosen as our usable fraction]: $\geq 85\%$ of the total product. This tight fraction was chosen to achieve homogenous surface area, in order to account better for any differences in drug dissolution profiles.

1. Yield of microparticulates

The yield of the granules was taken as a percentage of the ratio of the total output obtained from batch processing and the initial weight of the powder blend (1 kg).

2. Particle size distribution

The particle size of ibuprofen was determined using an image analyzer (Quantimet 500, Leica, USA) interfaced with a microscope (Reichert, Bordenen Instrument Co., Inc., Valenca). This is based on transfer of a two-dimensional image of the representative pellet sample to a video screen and computation of the area and equivalent circle diameter (μm) of the individual particles (78). The ibuprofen powder was dispersed in water by gentle vortexing for adequate dispersion and accurate analysis. The computed equivalent circle diameter represents the particle size of the mounted sample. An average of 30 particles was taken.

Microparticulate size distribution was determined using conventional sieve analysis performed once per replicate batches of each formulation. Spheroids weighing 100 g were placed on the uppermost of nested sieve with mesh sizes 16, 20, 40, 60, 80, and corresponding to mean pore sizes of 1,180, 850, 425, 250, 180 μm , respectively. The sieve-nest was vibrated in a shaker for 5 min and the weight of each sieve was measured before and after, to calculate the weight of granules retained on each sieve. The frequency is the percentage of granules obtained in the different sieves to the total weight (100 g) of the particles used for the analysis. Using the frequency data, the log-normal distribution on a probability scale was plotted and the geometric mean diameter d_g , and the geometric standard deviation δ_g were calculated. The results reported are the means of two replicate batches and their corresponding geometric standard deviations (Tables XXA and B).

The usable fraction (UF) is the percentage of the total fraction of spheroids obtained from the 20 - 60 (granules with size ranges between 250 and 850 μm) mesh sizes and the initial weight used for particle size analysis (100 g).

3. Density of the granules

True density (ρ) was determined from the sample mass and volume using a Quantachrome multipychnometer[®] (Vincentown, NJ). The system and samples of known weight were purged of contaminated gas, moisture and vapor for a minimum of 20 min by placing the latter in the instrument using helium gas. Sample volume (V_s) was calculated from cell and reference volumes (V_c and V_r respectively) obtained by calibration of a reference spherical material, using the manufacturer's protocols which includes

Equation 16:

$$V_s = V_c - V_r \left[\left(\frac{P_1}{P_2} \right) - 1 \right] \quad \text{Eqn.16}$$

where P_1 and P_2 are the pressures obtained from the reference and cell volumes respectively.

4. Drug content and HPLC assays

i. Sample preparation

Standards were prepared in triplicates using a concentration range between 2.5 and 300 $\mu\text{g/ml}$ of methanol. The determination of ibuprofen in the granules was conducted by extracting the drug twice from known sample weight of the product using 3 ml methanol.

ii. HPLC assay

Fifty microlitre of standards was directly injected into the HPLC (Shimadzu Scientific Instruments, Inc., Columbia, MD), consisting of C_{18} reverse phase column (100 x 4.6 mm, 5 μm , Phenomenex, MD). The HPLC method (238) is a modification of Tsao and Savage (239), in which the mobile phase consisted of acetonitrile:water:glacial acetic acid:triethylamine (600:400:1:0.2). The mobile phase was vacuum filtered and degassed simultaneously using a Branson 3200 ultrasonicator (Branson cleaning equipment, CT). Ibuprofen was monitored by UV detector at 265 nm wavelength, and the results were reported as the means of data from nine replicates of standards analyzed on three different days. A calibration curve was set up and the method was validated for both accuracy and

inter-day reproducibility, namely, coefficient of variation, using Equations 17 and 18. The regression equation was linear with a correlation coefficient (R^2) of 0.9996.

$$\% \text{ Accuracy} = \frac{\text{Measured concentration}}{\text{Expected concentration}} \times 100 \quad \text{Eqn. 17}$$

$$\% \text{ Interdaycoefficient of variation(CV)} = \frac{\text{Standard deviation}}{\text{Mean concentration}} \times 100 \quad \text{Eqn. 18}$$

The samples were also analyzed as stated for the standards, however, known concentrations of ibuprofen standard were injected separately and analyzed simultaneously with them. The results were reported as the means of data from six replicates obtained from two different batches.

5. Dissolution

The dissolution of the produced microparticulates was carried out using the USP apparatus I at a rotation speed of 100 rpm. Known amount of sample was weighed into 3x2-cm diameter stainless steel minibaskets with 40-mesh screens that held each sample in the six flasks. Simulated intestinal fluid (USP) containing 0.02% Tween 80 (enzyme grade) at pH 7.4 ± 0.05 was used as the dissolution medium with a temperature of 37 ± 0.1 °C. One milliliter sample was collected at specific intervals and filtered immediately using a 5 micron hydrophilic nylon filter membrane (B. Braun Medical Inc., PA, USA). The removed volume was not replaced in the dissolution vessel, but was factored into the calculation during the data analysis. Fifty microlitres of the samples and known standard concentrations were analyzed by HPLC with ibuprofen concentration monitored by UV

detector at 265 nm, as already stated. The results were reported as the means of data of 9 - 12 dissolution vessels from replicate batches.

6. Flowability

The angle of repose (θ) and Carr's compressibility index (240) were used to determine the flowability of the spheroids. Values of θ less than 30° as well as values of Carr's index below 15% were considered good product flowability.

i. Angle of repose

Weighed amount of granules was gently poured into an 8 oz funnel that was mounted on a stand and with the orifice covered. The covered end was gently opened so that the granules flowed freely on a dark surface. The diameter and height of the granules were measured and the angle of repose calculated using the following Equation:

$$\theta = \left(\frac{H}{R}\right) \tan^{-1} \quad \text{Eqn.19}$$

where H and R are the height and radius respectively formed by the granules. The results reported are the means of six replicates of two batches.

ii. Carr's index determination

The bulk and tap densities of the pellets were determined with Vanderkamp[®] Tap density tester (Van-Kel Industries Inc., NJ). The Carr's compressibility index was calculated using the following Equation:

$$\% C = \frac{D_T - D_B}{D_T} * 100 \quad \text{Eqn. 20}$$

where C is the compressibility index while D_T and D_B are tap and bulk densities respectively.

7. Granule friability test

The friability tester of tablets was used to test the resistance of the pellets to abrasion. Size fraction of 250-850 μm placed in the Roche friabilator was subjected to a falling shock for 15 min at 30 rpm, sieved for 10 min and the weight loss was recorded.

8. Sphericity and roundness of granules

Sphericity and roundness were determined using a Quantimet image analyzer 500 interfaced with a microscope in which the roundness, perimeter (P_m) and the particle projected area (A) were measured (78). These were used to calculate sphericity (S), a reciprocal of the roundness factor, as shown in the equation 21 below (241):

$$S = \frac{4A*3.142}{P_m^2} \quad \text{Eqn. 21}$$

A perfectly spherical particle will have a value of 1.0 while non-spherical particle will have a value of 0.1.

9. Scanning electron microscopy (SEM)

The samples were placed on a sample stub containing double-sided transparent adhesive tapes. They were then coated under reduced pressure (~0.8 mbar) with gold for 2 min using a Cressington Sputter Coater 108 (Franklin Electric, Bluffton, IN) and observed under a scanning electron microscope (Hitachi S510, Tokyo, Japan) at 10 kV.

c. Statistical analysis

The influence of the independent variables on the pellet characteristics was analyzed by standard deviation and relative standard deviation, while the yield variable was also analyzed by one-way ANOVA and student's *t-test* techniques using the JMP IN[®] version 3.2 statistical software.

Phase 2

Optimization of the Developed Process and Product Variables Using Statistically Designed Factorial Experiment.

a. Experimental Design

The results of the feasibility studies showed that two formulation (binder and surfactant levels) and one process (plate type-contour) variables were critical to the quality of the spheroids prepared in the rotor-disk fluid-bed equipment (47). Based on these results, a 2x2x3 full factorial design was generated using a JMP IN[®] based software and consisting of two binder levels (X1), two surfactant levels (X2), and a three level plate type (X3) in which two-two level factors were collapsed into a single three level

factor. An additional blocking effect was studied in which every experiment in each block was randomly replicated, to assess the effect of batch replication on the chosen product qualities and on the main factors. This increased the statistical power of our design in that the experimental runs were increased from twelve to 24 and the randomization ensured that each of the experiments had one over twelve (within each block) chances of being run at any given time. This design allows the estimation of statistical significance of the effect and interactions of the three product and process variables (X1 - X3) on several spheroid qualities in the generated experimental runs. The experimental design matrix is shown in Table VII, and the different levels of the three factors shown in Table VIII. In Table VII, the levels for each of the formulation parameters are represented by a (-) sign for the low and a (+) sign for the high levels.

In the matrix of the factorial design shown in Table VII, each line identifies the experimental condition for each batch (X1 - X3), and each experiment gives a result (Y). From these, and applying factorial design mathematical model, one obtains a general linear analysis (242,243):

$$Y_{ijkl} = \mu + a_i + b_j + ab_{ij} + c_k + ac_{ik} + bc_{jk} + d_l + ad_{il} + bd_{jl} + cd_{kl} + e_{ijkl} \quad \text{Eqn. 22}$$

where Y_{ijkl} is the response variable, μ is the mean value, a_i , b_j , c_k and d_l are the main effect coefficients (binder level, surfactant level, plate type and block respectively), while ab_{ij} , ac_{ik} , bc_{jk} , ad_{il} , bd_{jl} , and cd_{kl} are the second level coefficient of interactions, and e_{ijkl} the error value.

Previous studies have shown that higher order interactions are generally not likely to exist, and also are uninterpretable even when they are significant (112,244).

Table VII: Experimental Design Matrix for Optimization Studies

B l o c k 1		
X 1	X 2	X 3
- 1	1	- 1
- 1	- 1	0
1	1	0
1	- 1	1
- 1	1	0
1	1	- 1
- 1	- 1	1
1	- 1	- 1
- 1	1	1
1	1	1
1	- 1	0
- 1	- 1	- 1
B l o c k 2		
X 1	X 2	X 3
- 1	- 1	0
- 1	1	- 1
1	1	- 1
- 1	- 1	1
1	- 1	0
1	- 1	1
- 1	1	0
- 1	1	1
- 1	- 1	- 1
1	- 1	- 1
1	1	0
1	1	1

X1: Binder level; High (1), Low (-1)

X2: Surfactant level; High (1), Low (-1)

X3: Plate type; Stainless steel waffle (-1), Stainless steel smooth (0), Teflon waffle (1)

Consequently, interactions of three or more factors were confounded with two-factor interactions and were assumed to be insignificant for the purposes of this design. Moreover, because blocking (d_i) had no statistically significant effect on eleven out of the twelve response variables (Y), and consequently yielded statistically insignificant interactions with the main effects [(a_i, b_j, c_k) results not shown] their

Table VIII: Experimental Design for Optimization Studies

Runs	Batch name*	Binder level	Surfactant level	Plate type
1	Formulation 1a	1200	20	SS-Waf
2	Formulation 2a	1200	10	SS-Sm
3	Formulation 3a	1350	20	SS-Sm
4	Formulation 4a	1350	10	Tef-Waf
5	Formulation 5a	1200	20	SS-Sm
6	Formulation 6a	1350	20	SS-Waf
7	Formulation 7a	1200	10	Tef-Waf
8	Formulation 8a	1350	10	SS-Waf
9	Formulation 9a	1200	20	Tef-Waf
10	Formulation 10a	1350	20	Tef-Waf
11	Formulation 11a	1350	10	SS-Sm
12	Formulation 12a	1200	10	SS-Waf
13	Formulation 2b	1200	10	SS-Sm
14	Formulation 1b	1200	20	SS-Waf
15	Formulation 6b	1350	20	SS-Waf
16	Formulation 7b	1200	10	Tef-Waf
17	Formulation 11b	1350	10	SS-Sm
18	Formulation 4b	1350	10	Tef-Waf
19	Formulation 5b	1200	20	SS-Sm
20	Formulation 9b	1200	20	Tef-Waf
21	Formulation 12b	1200	10	SS-Waf
22	Formulation 8b	1350	10	SS-Waf
23	Formulation 3b	1350	20	SS-Sm
24	Formulation 10b	1350	20	Tef-Waf

*: The "a" and corresponding "b" of each number are random replicates of the same

formulation and give the mean of the dependent variables presented in Table XX below.

interaction factors (ad_{il} , bd_{jl} , and cd_{kl}) were eliminated while their degrees of freedom were added to that of the error factor, thereby increasing the statistical power of the design. The new linear equation is represented in Equation 23:

$$Y_{ijkl} = \mu + a_i + b_j + ab_{ij} + c_k + ac_{ik} + bc_{jk} + d_l + e_{ijkl} \quad \text{Eqn. 23}$$

b. Blending and spheronization

This was performed as already described above (pp 88 - 92) and also in our published report (47), except that both 1 and 2% SLS were used, and spheronization was performed using fixed amount (120 or 135% of the starting material) of water as binder solution (Table VIII). Drying was performed till 50 °C product temperature was reached and moisture content was used as a measure for loss on drying (LOD). The granulation end-point was obtained at the set binder content values (Table VIII).

c. Physical characterization of spheroids

These were performed as already described in the feasibility studies. The yield of the granules was taken as a percentage of the ratio of the final weight obtained after the production processes and the initial weight of the powder blend. Microparticulate size distribution was determined using conventional sieve analysis and the geometric mean diameter and geometric standard deviations calculated. Usable products were considered as granules with size ranges between 250 and 850 μm (20/60 mesh size), and were used in the different analyses to obtain the response variables (Y). The drug content and the dissolution assays were analyzed using the HPLC reversed phase column and ibuprofen was monitored by UV detector at 265 nm wavelength. However, the samples were

filtered using 0.45 micron hydrophilic wovlen nylon filter membrane (B. Braun Medical Inc., PA, USA). The sphericity and roundness of the spheroids were determined using an image analyzer (Quantimet 500, Leica[®], USA) interfaced with a microscope (Reichert, Bordersen Instrument Co., Inc., Valenca). Spheroid friability, flowability, Carr's index, tap and bulk densities were performed exactly as described earlier.

Scanning electron microscopy (SEM)

The samples were placed on a sample stub with double-sided carbon tapes, evacuated, back-filled with argon under reduced pressure (0.1 torr). They were then coated with palladium using a Hummer Sputtering System LO.2, (ANATECH Ltd., Alexandria, VA), and observed under a scanning electron microscope (Philips XL 30 FEG CDU[™] LEAP[™], Holland, Netherlands) at 1 kV.

d. Statistical analysis

The influence of the independent variables on the characteristics of microparticulates was analyzed by the ANOVA method using the JMP[®] software. Pareto charts were used to show the scaled estimates of the effects of the studied product and process variables on the physical characteristics of spheroids (245). The effect of a factor or an interaction is considered significant as long as it is superior to the experimental error (246,247).

Phase 3

Drug Loading, Particle Size Effects. Scale-up to Intermediate Scale Using the Fluid-bed Rotor-disk Technology

The results from the optimization studies indicated that higher binder content caused higher yield of the spheroids while stainless steel smooth plate gave more consistent product quality especially with respect to yield, drug content, sphericity and usable fraction. Additionally, higher binder content in combination with the lower surfactant level yielded more acceptable spheroid characteristics as specified in the set acceptance criteria (page 94). The formulation consisting of high binder level, low surfactant level (1%), and made with stainless steel smooth plate was therefore chosen for the studies in this section.

a. Effects of drug particle size and drug loading on the characteristics of ibuprofen microparticulates

1. Experimental design

Drug particle size and drug load have been shown as among the limitations of the rotor-disk fluid-bed technology (15,154). In order to investigate these observations, a 2x3 full factorial design was generated using a JMP IN[®] based software and consisting of two drug particle sizes (X1) and three drug loads (X2). The experimental runs were replicated to assess the effect of batch replication on the chosen product qualities and on the main factors. The replication also increased the statistical power of our design by increasing the

experimental runs from six to twelve. Additionally, this design allows the estimation of statistical significance of the effect and interactions of the two product variables (X1 and X2) on several spheroid qualities in the generated experimental runs. The experimental design matrix is shown in Table IX, and the different levels of the two factors shown in Table X. In Table IX, the levels for each of the formulation parameters are represented by a (-) sign for the low, and a (+) sign for the high levels.

**Table IX: Experimental Design Matrix for Drug Particle Size and Drug Load
Effects on Spheroid Characteristics**

Number of runs	Replication	X1	X2
1	-1	-1	-1
2	1	-1	-1
3	-1	-1	0
4	1	-1	0
5	-1	-1	1
6	1	-1	1
7	-1	1	-1
8	1	1	-1
9	-1	1	0
10	1	1	0
11	-1	1	1
12	1	1	1

X1: Drug particle size (μm); 20 (-1), 40 (1)

X2: % drug load; 50 (-1), 65 (0), 80 (1)

In the matrix of the factorial plan represented in Table IX, each line identifies the experimental condition for each batch of the factors (X1 and X2), and each experiment gives a result (Y) that will be applied to a general linear model based on the algorithm of Yates, as shown in equation 24:

$$Y_{ijk} = \mu + a_i + b_j + ab_{ij} + c_k + ac_{ik} + bc_{jk} + e_{ijk} \quad \text{Eqn. 24}$$

where Y_{ijk} is the response variable, μ is the mean value, a_i and b_j are the main effect coefficients (drug particle size and drug load) respectively, while c_k is the replication

Table X: Experimental Design for Drug Particle Size and Drug Load Effects on Spheroid Characteristics

Number of runs	Batch name	Drug Particle Size (μm)	% Drug Load
1	Ibu 20-50a	20	50
2	Ibu 20-50b	20	50
3	Ibu 20-65a	20	65
4	Ibu 20-65b	20	65
5	Ibu 20-80a	20	80
6	Ibu 20-80b	20	80
7	Ibu 40-50a	40	50
8	Ibu 40-50b	40	50
9	Ibu 40-65a	40	65
10	Ibu 40-65b	40	65
11	Ibu 40-80a	40	80
12	Ibu 40-80b	40	80

*: The "a" and corresponding "b" of each number are replicates of the same formulation and give the mean of the dependent variables presented in Table XXV below.

effect. The parameters ab_{ij} , ac_{ik} , and bc_{jk} are the second level coefficient of interactions, and e_{ijk} is the error value.

As already mentioned, previous studies have shown that higher order interactions are generally not likely to exist, and also are uninterpretable even when they are significant (93,244). Consequently, interactions of three or more factors were confounded with two-factor interactions and were assumed to be insignificant for the purposes of this design. Moreover, because replication (c_k) had no significant effect on ten out of the twelve response variables, and also yielded statistically insignificant interactions with the main effects (a_i , b_j), their interaction factors (ac_{ik} and bc_{jk}) were eliminated while their degrees of freedom were added to that of the error factor, thereby increasing the statistical power of the design. The new linear equation is represented in Equation 25:

$$Y_{ijk} = \mu + a_i + b_j + ab_{ij} + c_k + e_{ijk} \quad \text{Eqn. 25}$$

2. Blending and spheronization

This was performed as already described in the feasibility studies (pp 88 - 92) and also in our published report (47). Spheronization end point was visually assessed, based on experience and the fluidization pattern that gave the most acceptable product qualities.

This has been observed to correspond to moisture content of 50 - 55% for the drug:Avicel[®] 50:50 ratios, 45 – 48% for the 65:35 ratios, and 37 – 41% for the 80:20% ratios, for both drug particle sizes (Table XI). These amounts of water did not yield much oversized spheroids, and were recorded with regard to both the drug particle size and the drug load. Drying was performed as previously reported, with the end point achieved

Table XI. Binder and Time Conditions During Spheronization and Drying Processes

% ibuprofen	20 micron ibuprofen			40 micron ibuprofen		
	50	65	80	50	65	80
Binder added during spheronization (kg)	1.525 ± 0.04	1.265 ± 0.08	1.085 ± 0.16	1.394 ± 0.02	1.189 ± 0.02	0.910 ± 0.03
Total time [(spheronization and drying) mins]	67.5 ± 0.95	54.5 ± 2.12	46.5 ± 2.12	75.0 ± 1.14	66.0 ± 2.83	53.1 ± 0.41
Moisture content at end of spheronization	50.69 ± 0.27	45.21 ± 0.02	37.27 ± 1.05	55.81 ± 0.56	48.45 ± 0.47	41.44 ± 0.07

when the product temperature reached 50 °C. The plate gap was adjusted from 0.8 – 1.0 cm and the air volume from 85 - 90 cfm, to ensure proper fluidization of the pellets.

3. Physical characterization of spheroids

These were performed as already described in the feasibility studies (pp 94 - 99). The yield of the granules was taken as a percentage of the ratio of the final weight obtained after the production processes and the initial weight of the powder blend. The moisture content was measured as a function of time for all the batches, and the values at the end of spheronization process are shown in Table XI and Figure 36. Microparticulate size distribution was determined using conventional sieve analysis. Usable products were considered as granules with size ranges between 250 and 850 μm (20/60 mesh size), and were used in the different analyses to obtain the response variables. The drug content and the dissolution assays were analyzed using the HPLC reversed phase column with ibuprofen monitored by UV detector at 265 nm wavelength. The samples were filtered through 0.45 micron hydrophilic wovlen nylon filter membrane (B. Braun Medical Inc., PA, USA). The sphericity and roundness of the spheroids were determined using an image analyzer (Quantimet 500, Leica[®], USA) interfaced with a microscope (Reichert, Bordersen Instrument Co., Inc., Valenca). Spheroid friability, flowability, Carr's index, tapped and bulk densities were performed exactly as already described. The scanning electron microscope analysis for studying the morphology of the spheroids was performed exactly as described in phase 2 (page 105).

4. Statistical analysis

The influence of the independent variables on the characteristics of microparticulates was analyzed by the ANOVA method using the JMP[®] software. Pareto and interaction plots were also used as described earlier (245).

b. Effects of Intermediate Size Scale-up on the Characteristics of Ibuprofen Microparticulates

Results from the drug load and drug particle size effects showed that the three drug loads were spheronizable, however, drug loads of 50% and 65% had similar characteristics and significantly affected most of the physical characteristics studied. As was previously observed (157), the 80% drug load was more difficult to spheronize and also had high standard deviations between most of the obtained replicate values, and was therefore difficult to replicate. Additionally, drug particle size of 20 μm had the most significant effects on the spheroid qualities studied. Therefore, 50% and 65% drug loads as well as 20 μm sized ibuprofen were used for further studies.

1. Experimental design

In order to study the scalability of the optimized product and process variables to semi-production size, a 2x2 full factorial design was generated using a JMP IN[®] based software and consisting of two batch sizes (X1) and two drug loads (X2). The experimental runs were replicated for the reasons already mentioned in the previous experiments. The experimental design matrix is shown in Table XII and the different levels of the two factors are shown in Table XIII. The general linear model and the

model deduced to increase the statistical power of the experiments are as shown in Equations 26 and 27 respectively. However, a_i and b_j are the main effect coefficients (batch size and drug load) respectively.

$$Y_{ijk} = \mu + a_i + b_j + ab_{ij} + c_k + ac_{ik} + bc_{jk} + e_{ijk} \quad \text{Eqn. 26}$$

$$Y_{ijk} = \mu + a_i + b_j + ab_{ij} + c_k + e_{ijk} \quad \text{Eqn. 27}$$

Table XII: Experimental Design Matrix for Intermediate Size Scale-up Effect on the Characteristics of Ibuprofen Microparticulates

Number of runs	Replication	X1	X2
1	-1	-1	-1
2	1	-1	-1
3	-1	-1	1
4	1	-1	1
5	-1	1	-1
6	1	1	-1
7	-1	1	1
8	1	1	1

X1: Batch size (kg); 1 (-1), 50 (1)

X2: Drug load (%); 50 (-1), 65 (1)

Table XIII: Experimental Design for Intermediate Size Scale-up Effect on the Characteristics of Ibuprofen Microparticulates

Number of runs	Formulation name	Batch Size	% Drug Load
1	1kg-50%-a	1	50
2	1kg-50%-b	1	50
3	1kg-65%-a	1	65
4	1kg-65%-b	1	65
5	50kg-50%-a	50	50
6	50kg-50%-b	50	50
7	50kg-65%-a	50	65
8	50kg-65%-b	50	65

*: The "a" and corresponding "b" of each number are replicates of the same formulation and give the means of the dependent variables presented in Table XXVII below.

2. Blending and spheronization

This was performed as already described in the feasibility studies (pp 92 and 93) and also in our published report (47). The FLM-15 was used for the 1 kg batches, while a FLN-120 having the same geometric similarities was used for the 50 kg batches. The specifications of both equipment are shown in Figures 18 and 20 respectively. For the large-scale equipment and process, the principles of dynamic geometric similarity as well as trial and error (137,138) were applied to obtain fluidization air volume that efficiently fluidized the powder bed throughout the wetting and drying periods (Equations 4 – 6; 102). The obtained spheronization conditions, compared to those used for the pilot

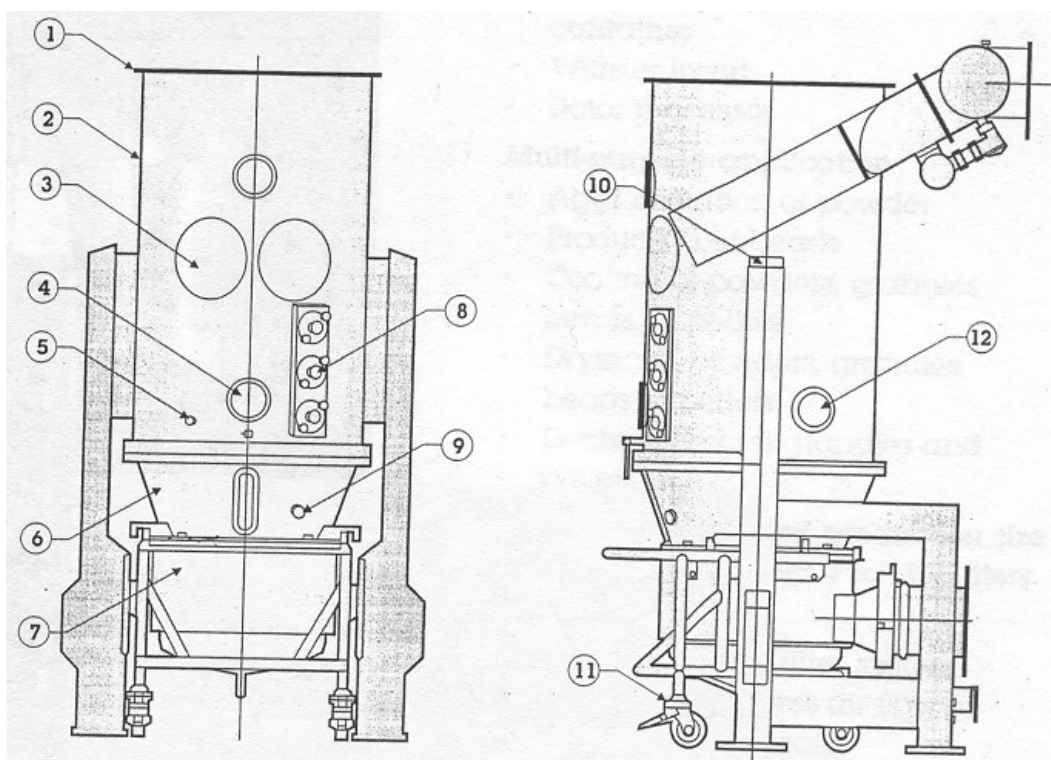


Figure 20. Components of the Vector FLN-120 fluid-bed machine with the numbers corresponding with the same equipment parts as were specified in Figure 18 (97).

scale batches are shown in Table XIV. The range of the rotor speed used during the spheronization period corresponded to Froude's numbers of 6.02 -17.28. Spheronization end point was also determined as previously reported, based on experience and acceptable fluidization pattern, and the results are shown in Table XV. Drying was performed as previously reported, with the end point achieved when the product temperature reached 50 °C.

Table XIV: Spheronization Conditions of Scale-up Batches

	Parameters				
Batch size		1 kg	5 kg	10 kg	50 kg
Plate size		12"	19"	19"	39.5"
Centrifugal force (N)		41,667	41,667	41,667	41,667
Plate material type/contour		SS/smooth	SS/smooth	SS/smooth	SS/smooth
		Teflon/waf.	Teflon/waf.	Teflon/waf.	NA
Spraying					
	Air volume (cfm) A1 and A2	50	90	140	500-1500
	Plate gap (mm)	0.8	3.5	6	NA
	Spray rate (g/min) B1 and B2	50	90	140	470 - 500
	Rotor speed (rpm)	500	300	200	130 - 135
	Inlet air temperature (°C)	25 - 30	25 - 30	25 - 30	25 - 30
	Product temperature (°C)	18 - 22	18 - 22	18 - 22	18 - 22
	Atomization air pressure (psi)	45	45	45	45
Drying					
	Air volume (cfm)	85	145	220	1100 - 1300
	Plate gap (mm)	1.3	5	8	NA
	Rotor speed (rpm)	150	124	124	75

Table XV. Binder and Time Conditions for Spheronization and Drying Processes of Intermediate Size Scale-up Ibuprofen Microparticulates

Batch sizes	1 kg		50 kg	
	50	65	50	65
% ibuprofen				
Binder added during spheronization (kg)	1.525 ± 0.04	1.265 ± 0.08	55.22 ± 1.11	53.00 ± 1.41
Total time [(spheronization and drying) mins]	67.50 ± 0.95	54.50 ± 2.12	246.50 ± 5.66	198.00 ± 2.83
Moisture content at end of spheronization	50.69 ± .0.27	45.21 ± 0.02	47.55 ± 1.74	40.59 ± 0.01

3. Physical characterization of spheroids

These were performed as already described in the feasibility studies (pp 94 - 99). The yield of the granules was taken as a percentage of the ratio of the final weight obtained after the production processes and the initial weight of the powder blend. Microparticulate size distribution was determined using conventional sieve analysis. Usable products were considered as granules with size ranges between 250 and 850 μm (20/60 mesh size), and were used in the different analyses to obtain the response variables (Y). The drug content and the dissolution assays were analyzed using the HPLC reversed phase column with ibuprofen monitored by UV detector at 265 nm wavelength. The samples were filtered using 0.45 micron hydrophilic wolvern nylon filter membrane (B. Braun Medical Inc., PA, USA). The sphericity and roundness of the spheroids were determined using an image analyzer (Quantimet 500, Leica[®], USA) interfaced with a microscope (Reichert, Bordersen Instrument Co., Inc., Valenca). Spheroid friability,

flowability, Carr's index, tapped and bulk densities were performed exactly as already described. The scanning electron microscope analysis for studying the morphology of the spheroids was also performed exactly as described in phase 2 (page 105).

4. Statistical analysis

The influence of the independent variables on the characteristics of microparticulates was analyzed by the ANOVA method using the JMP[®] software. Pareto and interaction plots were also used as described earlier (245).

Phase 4

Coating and Encapsulation of Spheronized Ibuprofen Microparticulates Using Hard Gelatin Capsules

The results of the scale-up experiments showed that replication did not affect the physical characteristics of both spheroid batch sizes and that both the drug loads used and the rotor-disk spheronization process are scalable. Therefore, 1 kg batch size with 65% drug load (Table XIII, Runs #7 and 8) were pulled and used to study the effect of polymer film coating and hard gelatin encapsulation on the qualities of the spheroids.

a. Polymer Film Coating of Spheroids

1. Preliminary studies using Glatt fluid-bed

To investigate the feasibility of coating the spheroids, the Glatt fluid-bed (Glatt WSG-5 Wurster column/Fluid-bed) was first used to coat 6 x 1 kg batches using three

coating levels each of Surelease[®] (5, 10 and 15%) and Eudragit[®] (8, 14 and 20%) polymers. The fluid-bed conditions used were almost the same for both polymers and are as follows: inlet air temperature (26 °C), outlet air temperature (24 - 28 °C), air of operation (2 mbar), air of atomization (2 - 4 mbar), flow rate (40 g/min). The batches were pre-warmed for 10 min before applying the film coats. Moisture content was analyzed before and after the pre-warming, after the polymer application and at the end of the process. The products were analyzed for yield, usable fraction and drug release. Based on the obtained results (not shown), the coating conditions and the rotor-disk conditions from previous studies (47,199), the levels and conditions for our rotor-disk fluid-bed coating were selected. These are shown in Tables IX (page 107) and XVI.

2. Experimental design for rotor-disk fluid-bed coating

A 2x3 full factorial experimental design was generated using the JMP software, consisting of 2 levels of polymer film type (X1) and three coating levels (X2). The polymer levels were chosen based on manufacturer's technical literature (of the polymers). Consideration of the coating levels that would allow for rotor-disk processing in the equipment was also made. The generated design was replicated to study the reproducibility of the rotor-disk coating process and also to increase the statistical power of the design. The experimental design matrix and the different levels of the two factors are shown in Tables IX (where, in this case, X1 is the polymer type and X2 the coating level; page 107) and XVI respectively. A stainless steel plate (12") was used with a batch size of 700 g.

**Table XVI: Experimental Design for the Coating of Spheronized Ibuprofen
Microparticulates**

Number of runs	Batch name	Polymer type	Polymer level (%)
1	SR-7.5a	Surelease [®]	Low (7.5)
2	SR-7.5b	Surelease [®]	Low (7.5)
3	SR-10a	Surelease [®]	Medium(10)
4	SR-10b	Surelease [®]	Medium(10)
5	SR-12.5a	Surelease [®]	High (12.5)
6	SR-12.5b	Surelease [®]	High (12.5)
7	EUD-12.5a	Eudragit [®] NE 30D	Low (12.5)
8	EUD-12.5b	Eudragit [®] NE 30D	Low (12.5)
9	EUD-14a	Eudragit [®] NE 30D	Medium(14)
10	EUD-14b	Eudragit [®] NE 30D	Medium(14)
11	EUD-15.5a	Eudragit [®] NE 30D	High (15.5)
12	EUD-15.5b	Eudragit [®] NE 30D	High (15.5)

*: The "a" and corresponding "b" of each number are replicates of the same formulation and give the mean of the dependent variables presented in Table XXIX below.

3. Rotor-disk fluid-bed coating

i. Coating of spheroids with Surelease[®] polymer

The Surelease[®] product containing 25% dry polymer weight was mixed with appropriate amount of distilled water to bring it to 15% total solids content (174). The spheroids (700 g) were pre-warmed to ~ 30 °C product temperature. The coating conditions and formulations are shown in Tables XVII and XVIII respectively. The

Table XVII. Conditions and Process Parameters Used for the Coating of 700 g Ibuprofen Spheroids

		Surelease [®]			Eudragit [®] NE 30D		
	<i>Coating level (%)</i>	<i>7.5</i>	<i>10</i>	<i>12.5</i>	<i>12.5</i>	<i>14</i>	<i>15.5</i>
Coating							
	Air volume (cfm)	60 - 85					
	Plate gap (mm)	1.0 – 1.5					
	Rotor speed (rpm)	200 -250					
	Inlet air temperature (°C)	40 - 50					
	Spray rate (g/min)	5.5 -7.5	5.5 -10.0	5.5 – 10.0	5.5 -7.5	5.5 -10.0	5.5 – 10.0
Drying							
	Air volume (cfm)	80 - 90	80 - 100	80 - 150	80 - 90	80 - 100	80 - 150
	Plate gap (mm)	1.5					
	Rotor speed (rpm)	250					

Table XVIII. Formulation of the Aqueous Dispersions Used for the Coating of 700 g Ibuprofen Spheroids

Polymer type	Surelease[®]			Eudragit[®] NE 30D		
<i>Coating level (%)</i>	<i>7.5</i>	<i>10</i>	<i>12.5</i>	<i>12.5</i>	<i>14</i>	<i>15.5</i>
Formulation						
Surelease polymeric solution (g)	210	280	350	NA		
Surelease polymer (solids; g)	52.5	70	87.5			
Water ad (to dilute to 15% solids; g)	350	466.67	583.33			
Eudragit polymeric solution	NA			291.67	326.67	361.67
Eudragit polymer (solids; g)				87.5	98	108.5
Talc (20% of dry polymer; g)				17.5	19.6	21.7
Water ad (to dilute to 25% solids; g)				420	470.4	520.8
Solid content (% w/w) of the dispersion	15			25		

coating conditions were adjusted to ensure that spraying was performed continuously during a greater period of the process. The product temperature was maintained between 35 and 40 °C. Spraying was intermittently interrupted to ensure proper fluidization of the spheroids, avoid agglomeration and minimize attrition problems. The total amount of the polymer shown in Table XVIII was used to obtain the theoretical percentage weight gain required for each of the batches.

ii. Coating of spheroids with Eudragit[®] NE 30 D polymer

A known weight of talc (20% w/w of the total dry polymer weight) was dissolved in an appropriate amount of distilled water with constant stirring. The talc solution was passed through a 60 mesh sieve (250 µm) to remove any undissolved particles. Eudragit[®] (30% w/w) was diluted in the talc solution to obtain 25% total solid content (Table XVIII), which was constantly stirred. The spheroids (700 g) were pre-warmed to ~ 30 °C product temperature in the rotor-disk fluid-bed. The coating conditions are as shown in Table XVII, and were adjusted to ensure that spraying was performed continuously during a considerable period of the process. The product temperature was maintained at 30 °C. Although talc was added in the spraying solution to prevent agglomeration, spraying was intermittently interrupted to ensure proper fluidization of the spheroids. The formulation contents are as shown in Table XVIII.

4. Physical characterization of the coated spheroids

Particle size analysis was performed by the traditional sieve analysis method and the usable fraction was calculated as has been previously described. The geometric mean

and standard deviations were also calculated. The yield of the coated products was calculated as a percentage of the product output and the total weight of the solid content of the starting material [spheroids (700 g), talc, Surelease[®] and Eudragit[®]] as applied to specific batches (Table XVIII). The true and bulk densities, flowability, friability, scanning electron microscope were performed as already explained in the previous sections. The compressibility index was also calculated. However, there was little to no volume change after several taps of the spheroids. This conforms with the reports that the bulk and not the tapped densities is used as a measure for calculating capsule fill weight and size for pellets (227). It also supports the results that compressibility is not required for pellet filling, thus the preference for tamp filling machine for these products over the dosator machines. Drug content testing was performed as already described and the weight of the polymer was accounted for in the calculations. Drug release studies were also performed as already reported, however, the time taken for 50% (T_{50}) of the drug to be released was used to measure the coating efficiency and duration of release instead of the Q_{20} used for the immediate release preparations (160,248).

i. Comparison of dissolution profiles

Model-independent methods (Equations 13 and 14 previously shown), difference and similarity (f_1 & f_2) factors respectively, were used to compare dissolution profiles for

$$f_1 = \frac{\{[\sum_{t=1}^n |R_t - T_t|]\}}{[\sum_{t=1}^n R_t]} * 100 \quad \text{Eq.13}$$

$$f_2 = 50 \log \{ [1 + (\frac{1}{n}) \sum_{t=1}^n n(R_t - T_t)^2]^{-0.5} * 100 \} \quad \text{Eqn.14}$$

similarity. An f_1 value up to 15 (0 – 15) and an f_2 value between 50 and 100 showed that the two dissolution profiles were similar.

ii. Mathematical modeling of drug release

The drug release data from uncoated and coated pellets were analyzed with square-root of time equation (Higuchi equation, Equation 7), Peppas equation (Equation 9), zero-order kinetic (Equation 12), and first-order kinetic (Equation 28). The data were also fitted to a recently developed combined mechanistic release kinetics (zero-order and square root of time Equation 15; 177). It was assumed that that release occurred as soon as the matrix is placed in contact with fluid and thus predicts an intercept at the origin.

$$Q = kt^{\frac{1}{2}} \quad \text{Eqn. 7}$$

$$\log (Mt / M) = \log k + n \log t \quad \text{Eqn. 9}$$

$$Q = \frac{DKCs}{L} t \quad \text{Eqn.12}$$

$$Q = Kt^{\frac{1}{2}} + \frac{DKCs}{L} t \quad \text{Eqn.15}$$

$$\ln (100 - Q) = \ln Q_0 - k_1 t \quad \text{Eqn. 28}$$

Where k_1 is the first order release equation coefficient.

5. Statistical analysis

The influence of the independent variables on the characteristics of microparticulates was analyzed by the ANOVA method using the JMP[®] software. Pareto and interaction plots were also used as described earlier (245).

b. Hard Gelatin Encapsulation of Spheroids

1. Experimental design

From our statistical analyses and the physical characteristics (bulk density, friability, flow properties and T_{50}) of the coated spheroids, the two replicate batches coated with 12.5% Surelease[®] level were pulled for hard gelatin encapsulation. A 2x2x3 full factorial experiment was designed consisting of two spheroid preparations, uncoated and coated (X1), and using two machine variables, (namely, two levels of machine operational speeds (X2) each operated at three different shuttle speeds (X3). Size 0 hard gelatin capsules were used. A cross section of the pellet feeder assembly of the *Index K150i* series (Figure 15) used for the pellet encapsulation is shown in Figure 21A, while Table XIX shows the experimental matrix /design.

The shuttle gate controls the length of time the male and female gates could remain open (Figures 21A & B). These gates regulate the amount of pellets that could be filled into pellet feeder, which feeds the empty capsules. It is therefore expected that the capsules filled at longer shuttle speed will contain higher amount of pellets since the gates will be left open long enough for enough pellets to be collected into the feeder.

In the matrix of the factorial plan represented in Table XIX, each line identifies the experimental condition for each batch of the factors (X1 – X3), and each experiment

gives a result (Y) that will be applied to a general linear model based on the algorithm of Yates, as shown in equation 29:

$$Y_{ijk} = \mu + a_i + b_j + ab_{ij} + c_k + ac_{ik} + bc_{jk} + e_{ijk} \quad \text{Eqn. 29}$$

where Y_{ijk} is the response variable, μ is the mean value, while a_i , b_j and c_k are the main effect coefficients, type of formulation, operational speed and shuttle speed respectively.

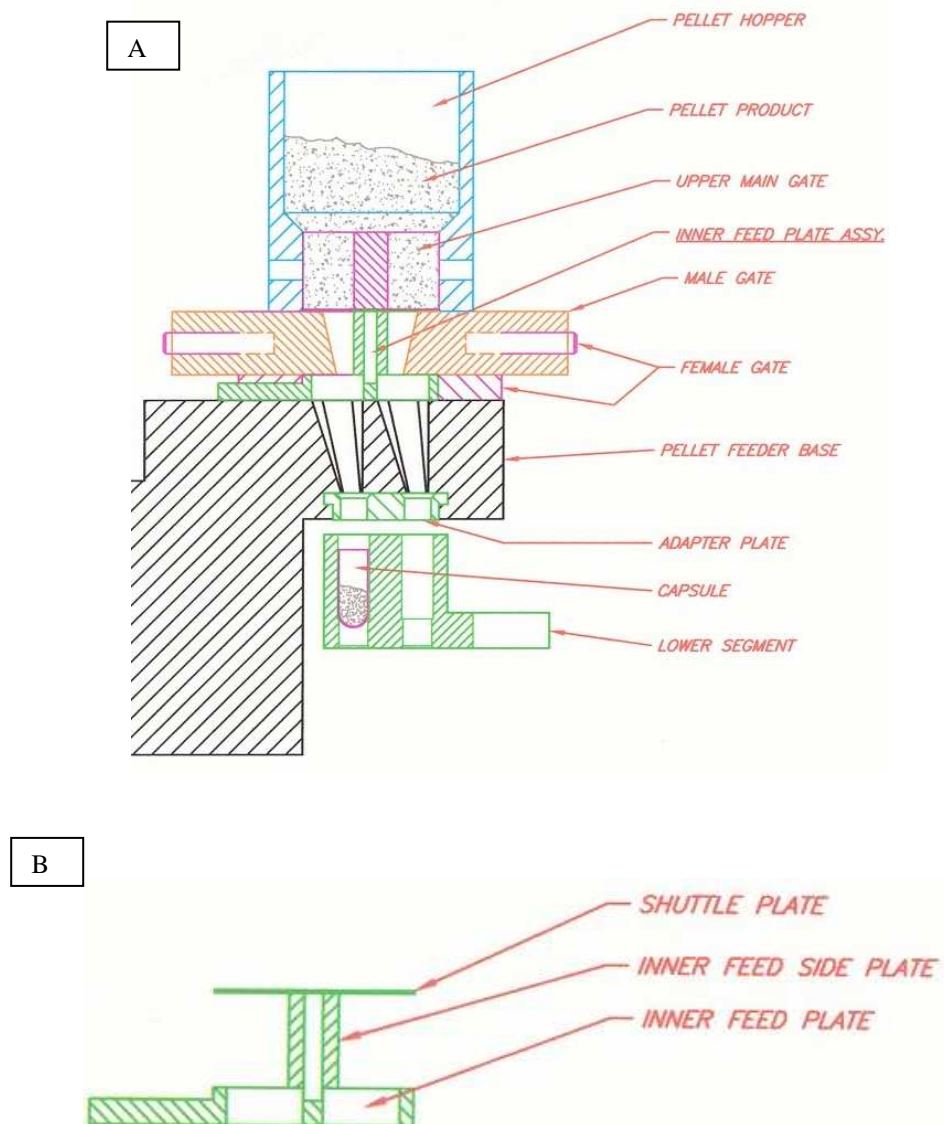


Figure 21. Cross-section of pellet feeder assembly (A)

Inner feed plate assembly (B) (217)

Table XIX Experimental Design Matrix for Encapsulation of Coated and Uncoated Ibuprofen Microparticulates

Number of runs	X1	X2	X3
1	1	1	1
2	1	1	0
3	1	1	-1
4	1	-1	1
5	1	-1	0
6	1	-1	-1
7	-1	1	1
8	-1	1	0
9	-1	1	-1
10	-1	-1	1
11	-1	-1	0
12	-1	-1	-1

X1: Type of formulation; coated or uncoated; X2: Operational speeds; 1, 2;

X3: Shuttle speeds; 1 – 3

The parameters ab_{ij} , ac_{ik} , and bc_{jk} are the second level coefficient of interactions, and e_{ijk} is the error value. The experiments were not replicated due to limitations of materials. Consequently, the interaction factors were eliminated from the analyses to increase the statistical power of the error. The equation involving only the main effects therefore becomes:

$$Y_{ijk} = \mu + a_i + b_j + c_k + e_{ijk} \quad \text{Eqn. 30}$$

2. Pellet encapsulation

The theoretical pellet fill weight was calculated based on the drug content and release, and also in Equation 31.

$$\text{Density} = \frac{\text{Weight}}{\text{Volume}} \quad \text{Eqn. 31}$$

The “0” or “00” capsule sizes will be required to fill 430 or 600 mg respectively of our coated pellets that will contain 300 - 400 mg ibuprofen drug/capsule. As stated on page 51, the equivalent total daily dose should generally be the same in switching a patient from immediate release to prolonged release product, although in most cases, an effective response has been achieved with a lower dose of the sustained release product (168). By filling 300 - 400 mg/capsule, it would be easy to study the efficacy of the drug at different doses. However, the available encapsulation machine did not have the capabilities required for filling size 00 capsules. Consequently, the highest amount of the pellets that could fill the “0” capsule size was used as our target weight. This enabled extrapolation of results obtained to calculate the amount of pellets required to fill the “00” capsule size, using the information provided in Figure 14.

The pellets were filled into size 0 hard gelatin capsules on a Romaco K-series (Figure 15) automatic tamp filling (gravity filled) machine with a 15 mm dosing disk. The operational speeds used were 75 and 85 rpm and the shuttle speeds were 260, 280 and 300 milliseconds. These variables were chosen based on the flowability of the pellets, as well as conditions that will prevent pellet losses, considering the small batch size of the

coated pellets (~ 1 kg). Approximately 200 capsules were collected from each run and were stored in tight polyethylene bags for further studies.

3. Physical characterization

The determination of the geometric mean diameter, friability, flowability, bulk and true densities of the pellets have been previously reported (pp 123 and 124).

i. Fill weight and coefficient of fill variation

The capsule fill weight and the coefficient of fill variation (CV) of 20 individual capsules were determined. Filled capsules were weighed on Denver Instruments balance and a set of 20 readings was used for calculating the average, standard deviation and percentage of fill weight variation (%CV). The average weight of 20 empty gelatin capsules was used as the blank weight.

ii. Dissolution test

Based on the results of the average fill weight, SD and %CV, the dissolution studies of the formulations encapsulated at 75 rpm and 280, 300 msec were performed accordingly. Six randomly selected capsules were used to investigate the ability of the capsule contents to be released. The drug release profiles were compared using difference and similarity factors. The data were also fitted to Higuchi, Peppas, zero-order, first-order, as well as the combined kinetics equations, as already described, in order to determine the mechanisms of drug release from the formulations.

4. Statistical analysis

The mathematical and statistical analyses were performed with Microsoft Excel and JMP software packages, as already described. *Studentized* residuals test statistic was used to check for patterns and outliers while Dubin-Watson test statistic was used to test for possible correlations between the pairs of observations. The statistical significance was set at $p < 0.05$.

III. RESULTS AND DISCUSSIONS

Phase 1

Feasibility Studies in the Spheronization and Scale-up of Ibuprofen

Microparticulates

a. Drying time

The time it took for the product made with similar plates to reach 50°C increased as percentage yield and batch size increased. For the batches made with stainless steel smooth plates, the times were 29 – 40 minutes for the 1 kg batches and 36 – 79 minutes for the scale-up batches. For teflon waffle plate batches, the drying times were 47 – 64 minutes for the 1 kg batches and 47 – 90 minutes for the scale-up batches. Not only are these results in agreement with previous reports that drying efficiency decreases with increased batch size (142,251), but, as mentioned earlier, the data also confirm that the heat conductivity of the stainless steel disk added to the overall drying efficiency of the process (125) while teflon had insulating effect (47). Moreover, it has been shown that at any given time, the moisture content of the granules depends on wettability and evaporation, which in turn are controlled by liquid flow rate and inlet temperatures respectively (252). Equilibrium liquid flow rate has been defined as one at which liquid supply is balanced by evaporation, and a critical liquid flow rate as one above which fluidization is impossible due to cohesion in the bed (253). Though the liquid flow rate is the same in both plate types used, the insulating nature of the teflon material could hinder the attainment of equilibrium during processing, thereby affecting the balance between

liquid supply and evaporation, which in turn might have adversely affected the drying efficiency of these batches.

b. Physical Characteristics of Developed Microparticulates

The following physical characteristics apply to all the batch sizes, i.e., 1 kg, 5 kg and 10 kg, unless stated otherwise.

1. Yield of spheroids

i. Yield of one kilogram batches

The replicated eight 1 kg batches produced using FLM-1 had yield values ranging from 58.0% - 91.2%, however, most of the batches yielded granules varying from 74% - 85% (Table XXA). This could be considered satisfactory since even with starting materials that are “ideal” in formulating spheres e.g. 100% Avicel[®], the process output was approximately 80% (249). As already stated, the spheroid batches having 50 - 52% binder content at the end of the spheronization process had better product characteristics. Trials 4 and 7 had desirable qualities that met our set acceptance criteria ($\geq 85\%$), and were selected for further studies.

Effect of SLS and Talc: The batches spheronized without SLS (trial 2) as well as that containing SLS and talc (results not shown) had lower yield. The lower yield from trial 2 could be due to the lack of SLS that affected wetting of the powders thereby enhancing losses to the fluid-bed walls and filters. The low yield obtained from the batch containing SLS and talc could be caused by a possible interaction between the SLS and

Table XXA. Physical Characteristics of 1 kg Batches (Means of replicated batches)

Parameters	Trials							
	1	2	3	4	5	6	7	8
	*Standard	No SLS	Avicel®CL-611	Smooth disk	650/SS	HPMC	500/tef	650/tef
% Yield	73.75 ± 2.33	58.0 ± 4.24	71.45 ± 3.89	85.40 ± 6.65	70.10 ± 2.55	80.0 ± 10.32	91.2 ± 32.24	79.05 ± 1.34
% Moisture content	1.75 ± 0.35	6.56 ± 2.34	1.66 ± 0.91	2.71 ± 1.70	2.96 ± 2.20	2.1 ± 0.43	6.85 ± 2.34	8.1 ± 4.10
% Drug content	93.46 ± 1.17	73.77 ± 3.32	91.69 ± 2.09	94.47 ± 0.65	94.30 ± 3.88	94.3 ± 8.48	91.44 ± 1.64	99.95 ± 4.08
Geometric mean diameter (µm)	438 ± 1.57	577 ± 1.43	445 ± 1.59	455 ± 1.57	363 ± 1.95	403 ± 1.63	417 ± 1.80	415 ± 1.78
Sphericity	0.90 ± 0.00	0.92 ± 0.01	0.89 ± 0.01	0.88 ± 0.09	0.87 ± 0.04	0.84 ± 0.01	0.91 ± 0.00	0.90 ± 0.01
Flowability (deg)	21.45 ± 1.05	23.07 ± 0.14	22.09 ± 1.88	23.36 ± 0.75	25.31 ± 1.06	24.84 ± 0.00	22.49 ± 0.83	24.37 ± 0.40
Carr's index (%)	8.56 ± 0.76	6.61 ± 0.40	9.85 ± 0.21	8.92 ± 3.97	9.34 ± 0.05	11.82 ± 1.19	8.92 ± 0.53	10.14 ± 0.25
True density (g/cm ³)	1.29 ± 0.00	1.30 ± 0.00	1.29 ± 0.00	1.30 ± 0.00	1.29 ± 0.01	1.28 ± 0.01	1.31 ± 0.01	1.28 ± 0.00
Bulk density (g/cm ³)	0.67 ± 0.00	0.77 ± 0.02	0.69 ± 0.02	0.64 ± 0.08	0.67 ± 0.05	0.58 ± 0.01	0.66 ± 0.01	0.67 ± 0.00
Tap density (g/cm ³)	0.73 ± 0.00	0.82 ± 0.01	0.76 ± 0.02	0.69 ± 0.06	0.74 ± 0.05	0.65 ± 0.00	0.73 ± 0.02	0.75 ± 0.00
Q ₂₀ (%)	86.74 ± 2.39	74.66 ± 2.92	87.47 ± 4.12	83.27 ± 5.02	90.42 ± 7.64	75.14 ± 1.85	91.75 ± 2.07	85.09 ± 1.71
Friability (%)	0.34 ± 0.47	0.67 ± 0.48	0.17 ± 0.24	1.5 ± 1.66	1.67 ± 1.41	1.17 ± 0.71	0.33 ± 0.71	1.84 ± 0.71

LOD: % loss on drying.

Highlighted batches were used for further studies

Table XXB. Physical Characteristics of Scale-up Batches (Means of replicated batches)

Plate material/contour	Stainless steel/smooth plate			Teflon/Waffle plate		
Batch size	1 kg	5 kg	10 kg	1 kg	5 kg	10 kg
Trials	4	12	13	7	14	15
Plate size	12"	19"	19"	12"	19"	19"
% Yield	85.40 ± 6.65	87.16 ± 7.13	83.97 ± 2.33	91.2 ± 32.24	96.35 ± 5.5	87.84 ± 11.7
% LOD	2.71 ± 1.70	1.85 ± 0.35	2.46 ± 0.64	6.85 ± 2.34	11.21 ± 7.62	10.65 ± 11.10
% Drug content	94.47 ± 0.65	99.2 ± 4.90	90.52 ± 4.71	91.44 ± 1.64	98.23 ± 1.89	98.65 ± 4.37
Geometric mean diameter (µm)	455 ± 1.57	483 ± 1.61	545 ± 1.67	417 ± 1.80	553 ± 1.54	603 ± 1.79
Sphericity	0.88 ± 0.09	0.90 ± 0.01	0.90 ± 0.01	0.91 ± 0.00	0.89 ± 0.01	0.88 ± 0.02
Flowability (deg)	23.36 ± 0.75	19.54 ± 1.08	24.11 ± 5.39	22.49 ± 0.83	19.29 ± 0.73	25.17 ± 7.59
Carr's index. (%)	8.92 ± 3.97	6.71 ± 1.23	6.21 ± 4.3	8.92 ± 0.53	5.33 ± 0.19	7.84 ± 2.75
True density (g/cm ³)	1.30 ± 0.00	1.28 ± 0.01	1.28 ± 0.02	1.31 ± 0.01	1.28 ± 0.01	1.27 ± 0.01
Bulk density (g/cm ³)	0.64 ± 0.08	0.65 ± 0.03	0.64 ± 0.04	0.66 ± 0.01	0.67 ± 0.01	0.63 ± 0.00
Tap density (g/cm ³)	0.69 ± 0.06	0.70 ± 0.03	0.68 ± 0.00	0.73 ± 0.02	0.71 ± 0.04	0.69 ± 0.00
Q ₂₀ (%)	83.27 ± 5.02	82.95 ± 12.66	85.53 ± 5.08	91.75 ± 2.10	79.47 ± 12.88	86.76 ± 13.00
Friability (%)	1.50 ± 1.66	1.50 ± 1.65	1.50 ± 1.17	0.33 ± 0.71	1.00 ± 0.00	4.00 ± 4.71

talc, that also led to delayed wetting of the granules during processing, and consequently resulted in the powder blend losses.

Binder effect: Use of HPMC as binder improved the yield compared to the standard formulation (Table XXA, trial 6 vs.1), although it had higher standard deviation.

Rotor speed effect: Lower disk speed (500 rpm) produced higher yields than higher disk speed (650 rpm, Table XXA, trials 1 and 7 vs. 5 and 8 respectively). This could be due to reduced centrifugal forces that minimized the collision of the spheres with the walls of the rotor container as well as losses into the cartridges. This resulted in more efficiently fluidization of the spheroids, as has been reported with the traditional extrusion/spheronization method (250).

Rotor-disk plate material effect: Higher yield was obtained from the teflon waffle plate batches in comparison to those made with stainless steel waffle plate (trials 7 and 8 vs. 1 and 5 respectively). The yield was measured immediately after the process, thus, any free or residual moisture that was not dried by the drying process formed part of the product yield. As can be seen from Table XXA, the moisture content for the formulations produced with the teflon plate ranged between 6.85 to 8.10% as compared to 1.75 to 2.96% of the stainless steel plate batches. The higher moisture content for the teflon plate could have contributed to increase in the yield value. The teflon disk tends to insulate the bed from some of the drying medium thus retaining a higher moisture level, and also resulting in higher yield. In contrast, the stainless steel disk allows for better

conduction of heat and consequently better heat transfer and drying, resulting to reduced moisture content that consequently led to reduced product yield, compared to the output from batches made with the teflon plate.

ii. Yield of pilot scale-up batches

The two batches selected for scale-up (smooth stainless steel 500 rpm and waffle teflon 500 rpm) are highlighted in Table XXA. The yield values were similar for 1, 5 and 10 kg for the batches made with stainless steel smooth plate 84% - 87% (Table XXB). For the teflon plate, the values increased (88% -96%) compared to those of the stainless steel plate, though with higher LOD values as mentioned earlier. However, student's *t-test* and one way ANOVA of the teflon plate data did not give any statistical difference between the yield results presented in Table XX ($p < 0.05$). Nevertheless, increased fluidization air was used during the drying period to ensure that the LOD values of all future batches would be $\leq 5\%$ at the drying end point. There was statistically no difference in the LOD values of 10 kg and 5 kg or 1 kg batches made with the teflon plate.

Generally, the batch size did not affect the characteristics of 5 kg and 10 kg batches using 19" plate, which was desirable. In a previous report involving traditional extrusion/spheronization (142), it was shown that undesirable product qualities could result if inappropriate plate size was used relative to batch size. This is because at very low load, there are relatively insufficient granules to interact with each other, thereby leading to poor particle/particle interaction, while the opposite is true at high loads.

2. Density, Carr's index and Flowability

These qualities were used as indices for the flow properties of the spheroids. The low values of Carr's index (less than 15%) signify good flowability of the granules. This was confirmed with the angle of repose of all the formulations being less than or equal to 30 degrees ($\pm 0.13^\circ$ to 7.59° SD; 240), as also shown in Tables XXA and B above. As shown in Table XXA, the flowability was decreased by the use of HPMC (trial 6) and high rotor speed (trials 5 and 8) that could have resulted in higher level of non-spherical and smaller geometric mean size of granules respectively. Use of HPMC (trial 6) and high speed (trials 5 and 8) also produced granules with increased tap density and percent compressibility and thus bad flow characteristics.

The results of the true densities before and after purging were practically similar, and almost similar results were obtained from all the batches (Tables XXA and B). From these results, it could be inferred that the samples have similar moisture content, indicating that the LOD (apart from influencing the yield that was measured immediately after production), might not have affected other product characteristics determined during storage at ambient conditions.

3. Drug content and Dissolution analyses

Calibration curve

Good linearity ($r^2 = 0.9996$) was obtained from the calibration curve (Figure 22). The percent accuracy ranged between 75 and 101% and the percent interday coefficient of variation (CV) ranged between 0.10 and 11% (Table XXI), with the lowest concentration

observed as an outlier. These results indicate acceptable accuracy and reproducibility for the assay method, respectively.

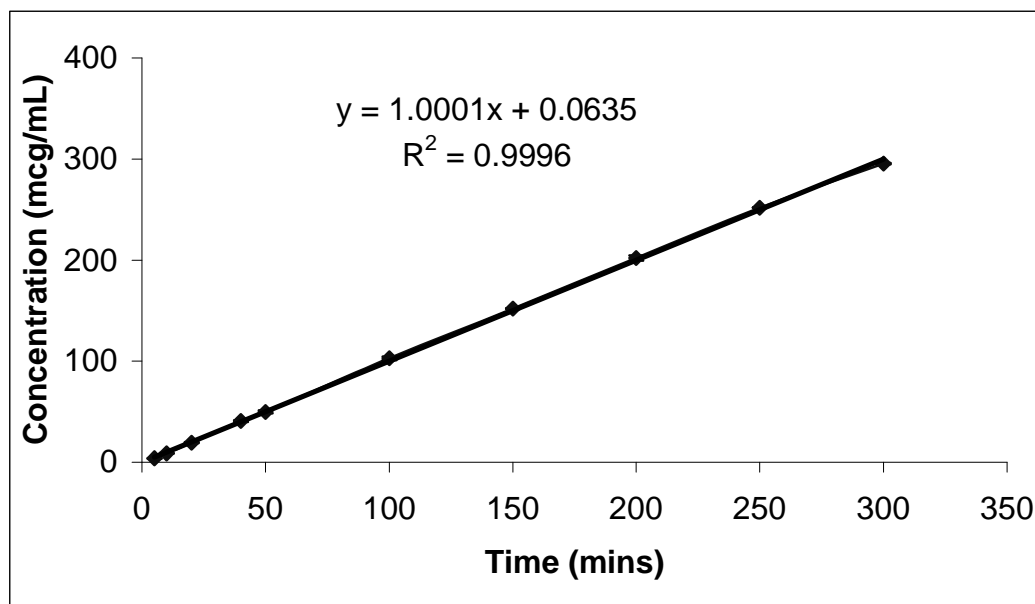


Figure 22: Calibration curve for HPLC analyses

Drug Content Analysis: With the exception of the batch without sodium lauryl sulfate (SLS; Tables XXA and XXB), the mean percentages of drug content obtained from six replicate samples ranged between $90.52\% \pm 4.71\%$ and $98.65\% \pm 4.37\%$ ibuprofen, calculated on the content of theoretical formulation. This indicated that the fluid-bed processes (blending, spheronization, drying) did not affect the ratio of the ibuprofen drug to the Avicel[®] RC-581 in the powder blend. It has been shown that by adding surfactant to a spheronization system, the interaction between the liquid and the powder changes (56), as a result of greater accessibility of the pore structure by the liquid

within the powder bed. It is therefore possible that the absence of SLS delayed the wettability of the powder blend, leading to the loss of the lighter-weighted ibuprofen drug.

Table XXI: Accuracy and precision of HPLC Assay

Concentration ($\mu\text{g/mL}$)			
Expected	Obtained	% Accuracy	Interday CV (%)
5	3.77	75.4	11.64
10	8.68	86.8	3.44
20	19.14	95.68	2.69
40	40.45	101.12	2.14
50	49.55	99.11	3.02
100	102.63	102.63	1.72
150	151.88	101.25	0.23
200	202.12	101.06	1.3
250	251.97	100.79	0.11
300	295.61	98.54	0.25

Dissolution studies: The Q_{20} for all the formulations calculated using the obtained drug content was $\geq 80\%$, except the batch containing HPMC and that without SLS that released 75% and 74% respectively of ibuprofen at the same time (Tables XXA and B, and Figures 23A and B). The variability between the replicate batches was generally around 5%. The slower release from granules made with HPMC as binder or in the absence of SLS could be attributed to densification, retardation of diffusion from the

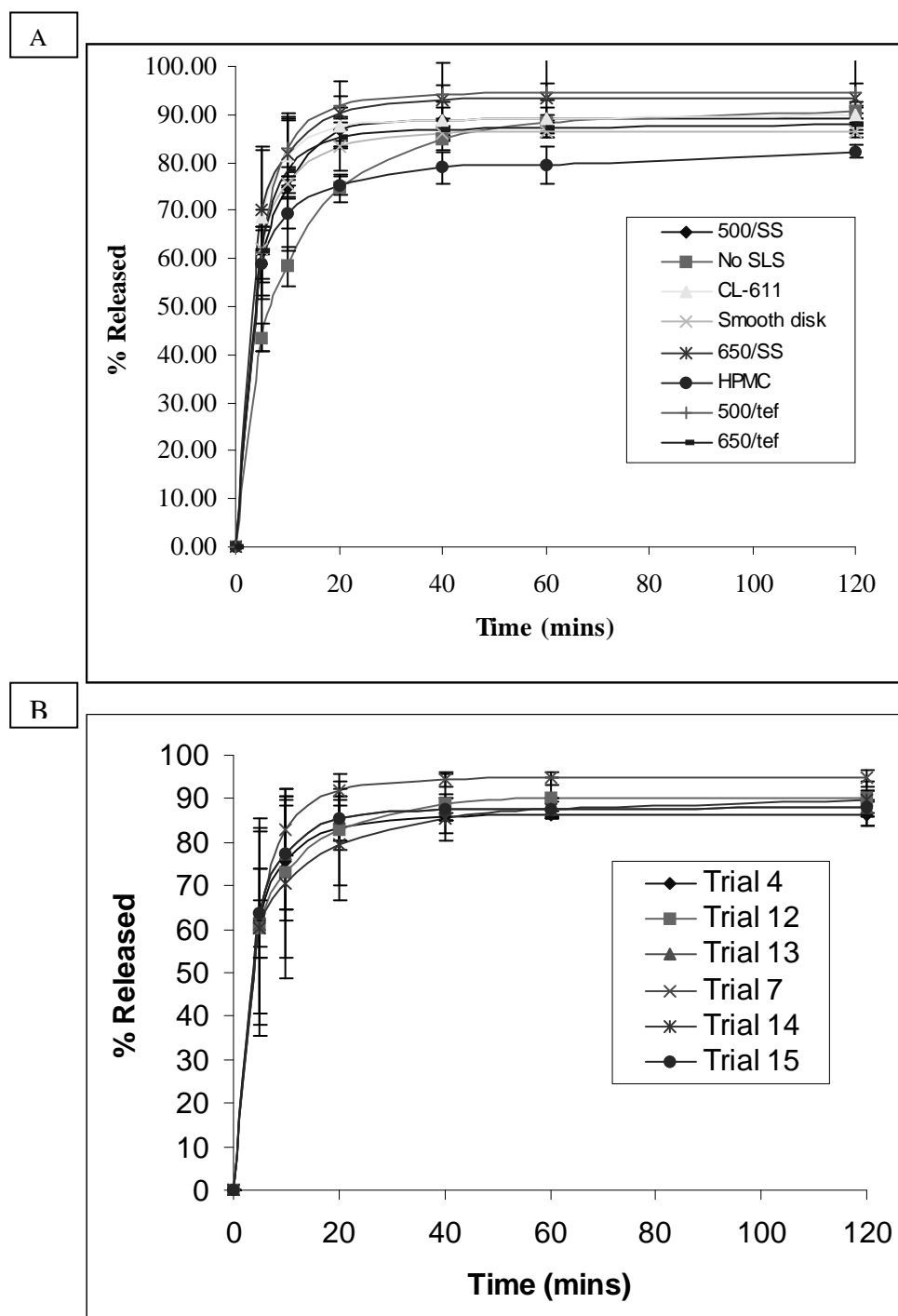


Figure 23. Panel A: Profiles of 1 kg replicated batches. Panel B: Profiles of pilot scale-up batches. Trial 4: SS/Sm/1 kg; Trial 12: SS/Sm/5 kg; Trial 13: SS/Sm/10 kg; Trial 7: Tef/Waf/1 kg; Trial 14: Tef/Waf/5 kg; Trial 15: Tef/Waf/10 kg. SS/Sm: stainless steel/smooth; Tef/Waf: Teflon/waffle.

granules and larger particle size (Figure 23A) that then reduced the surface area of the granules respectively. There was no difference in drug release in batches made with Avicel[®] RC and CL cellulose types contrary to previous reports in which extrusion spherization technique was used (254,255).

4. Friability

As shown in Table XXA, the percentage weight loss from the batches was generally less than 5% (± 0.00 to 4.71 SD). However, increased rotor speed (trials 5 vs. 1 and 8 vs. 7), use of HPMC (trial 6 vs. 1), and use of different plate contours (trial 4 vs. 1) increased the friability due to attrition and weakly agglomerated particles.

5. Sphericity and morphology of the granules

The sphericity of the microparticulates was in the range of 0.84 ± 0.01 to 0.92 ± 0.01 , which is close to 1.0, the optimal value for sphericity (Table XXA). The sphericity was reduced by the use of HPMC as binder (Figure 24G). HPMC increases the viscosity of the binder, which could influence the resistance of liquid to flow. This has been shown to affect the consistency of the wet powder mass, which in turn would influence the process ability to produce spherical pellets (56). Moreover, a 5% HPMC solution was used as the binder. It could be that a lower percentage with a lesser effect on binder viscosity would have resulted in a more spherical product.

Sphericity was not affected by the use of SLS although the SLS is supposed to enhance the wetting, which could enhance formation of spherical particles (54). Moreover, neither batch nor process scale-up seemed to affect the sphericity of the

granules (Table XXB). The results represented in Tables XXA and XXB are the sphericity means of 30 - 60 pellets from replicate batches. Figures 24A-C show the morphology of 1 kg, 5 kg and 10 kg batches of both plate material types (teflon and

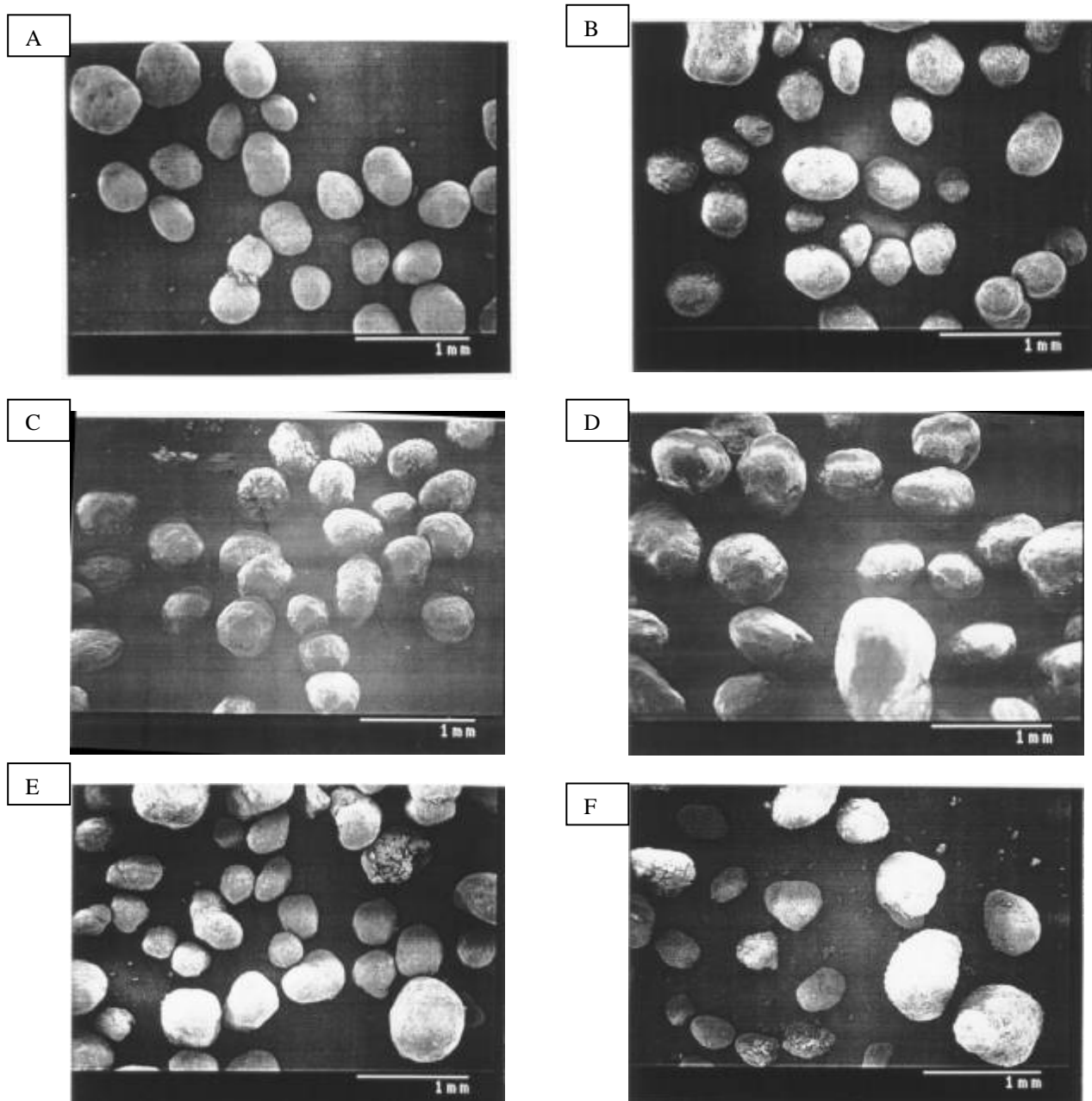


Figure 24. Scanning electron micrographs (x30) of ibuprofen granules made with stainless steel and with Teflon/waffle plates (see below).

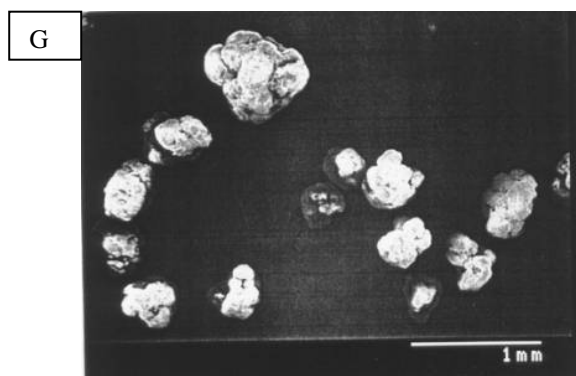


Figure 24 (Contd). Scanning electron micrographs (x30) of ibuprofen granules made with stainless steel plate, 1 kg (Panel A); 5 kg (Panel B); 10 kg (Panel C); and with Teflon/waffle plate 1 kg (Panel D); 5 kg (Panel E); 10 kg (Panel F). 1 kg batch made with HPMC as binder on a stainless steel plate (Panel G).

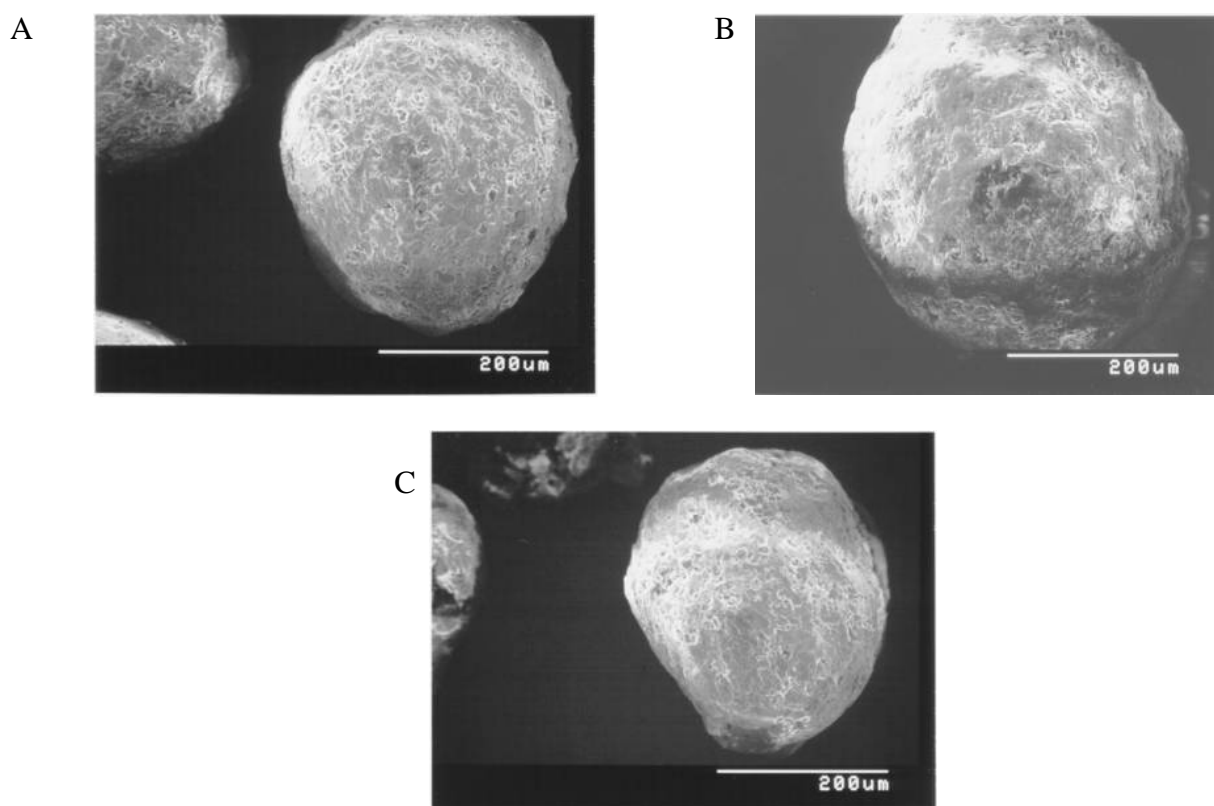


Figure 25. Scanning electron micrographs (x200) of ibuprofen granules made with stainless steel plate, 1 kg (Panel A); 5 kg (Panel B); 10 kg (Panel C).

stainless steel), and the 1 kg produced with HPMC as binder using the stainless steel plate. Figures 25A-C show typical morphology of the microparticulates at higher magnification.

6. Size distribution of granules

Size distributions for most of the batches depicted log normal distribution (results not shown), with the values of the 20/60 mesh products ranging between 88 - 96%, except for the 1 kg batch made with stainless steel waffle plate at 650 rpm (trial 5) and that containing HPMC as binder (trial 6).

For the laboratory scale batches, the presence of surfactant (SLS; trial 1 vs. 2) and use of water (in the standard) as binder (trial 6 vs. 1) decreased particle size (Figure 26A). Mean particle size increased in the absence of SLS, probably because in this situation, the surface energy required to reduce the particle size to what would be obtainable under similar conditions in the presence of the surfactant increases. It could also be due to decreased wettability that made these spheroids less vulnerable to attrition during drying. Type of Avicel[®] hydrocolloid (trial 1 vs. 3), and disk contour type (trial 4 vs. 1) did not affect the distribution. Rotor speed (650 rpm) decreased the particle size of the products made with stainless steel plate compared to the 500 rpm used in the standard (trial 5 vs. 1), while plate type slightly increased the particle size at higher speed (formulations 8 vs. 5; Figure 26A). The geometric mean diameters of the granules together with the geometric standard deviations are shown in Table XXA and Figure 26A.

The difference in size distribution between the batches could be attributed mainly to the formulation components and process variables, because the size distribution of the

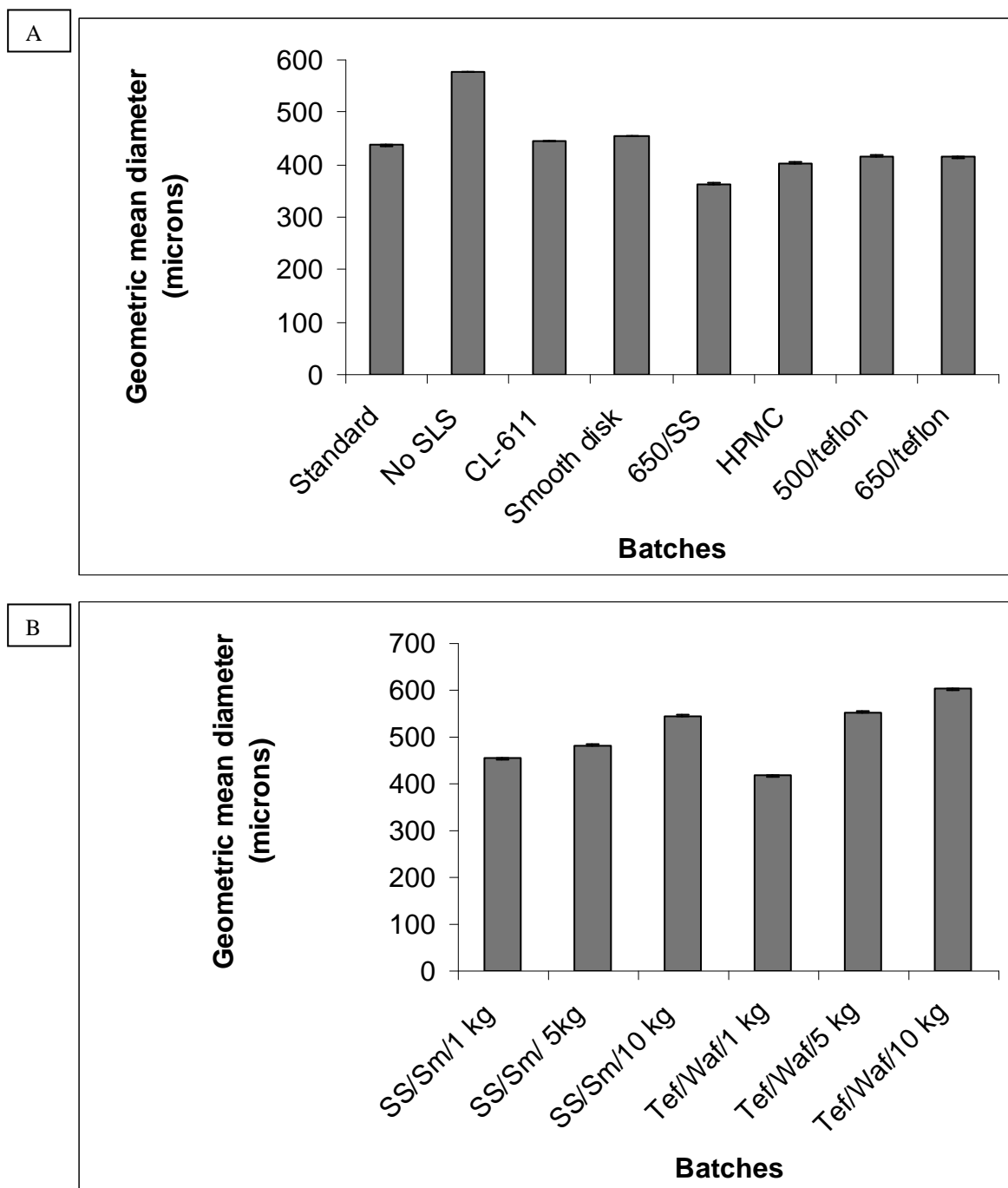


Figure 26. Panel A: Geometric mean diameter of 1 kg replicated batches.

Panel B: Geometric mean diameter of scale-up batches. The error bars did not show because of the very low geometric standard deviation (1.43 -1.95 μm).

starting raw materials were kept uniform by sieving the powders through a 16 mesh size prior to blending and spheronization. The decrease in the mean diameter with increased rotor speed (trial 1 vs. 5), could be due to surface defects on the pellets by the high speed, thereby producing more fines (7,256).

In the scale-up batches, the particle size, especially that of the teflon plate batches, appeared to increase with larger batch size (Figure 26B). This is due to greater attrition by the smaller sized batches that are lighter, more readily fluidized, falling from higher heights during drying. It could also be due to increased tendency of the particles to bind together due to the increased surface area of the larger batch sizes. The stainless steel batches had less attrition presumably because the spheroids dry up more easily than the products of equivalent batch sizes made with the teflon plate. Despite the increased particle size, the 20/60 mesh sizes yield in each of the scale-up batches was up to 85% thereby meeting the set acceptance criteria (page 94). These observations however did not correlate with the report that the granule size is inversely related with the batch size (142), and will therefore be further investigated.

In summary, trials 4 and 7 (Table XXA & B) were chosen as desirable preparations based on the acceptance criteria such as yield, drug content, dissolution and sphericity studies for rational screening and statistical design, as will be shown in the next phase.

Phase 2

**Optimization of the Developed Process and product Variables Using Statistically
Designed Factorial Experiment**

a. Experimental Design

Tables XXII and XXIII show the respective results of the means of replicate batches and *p-values* of the independent variables (block and main effects) obtained from the statistically analyzed full factorial blocked randomized design. Table XXIV summarizes the qualities of the pellets by grouping them according to the used plate types and contours. The effect of the main factors on spheroid qualities will be discussed in the sections addressing affected physical characteristics.

Binder level: The importance of water, used as binder or granulating liquid in the spheronization process, and the moisture content in the product, with respect to the physical performance of the end product have been reported in various studies (78,257). We have also shown that good spheroid qualities were obtained when the moisture content in the bed at the end of spheronization process was 50 – 52% (47), at defined parameters. It is therefore evident that variation in the amount of water used for the production of formulations of similar composition and batch size will affect most of the spheroid qualities, as will be discussed in the respective sections. Higher binder content implied higher yield of the spheroids and *vice versa*. These results are shown in Tables XXII and XXIII and also in the Pareto charts (Figure 27).

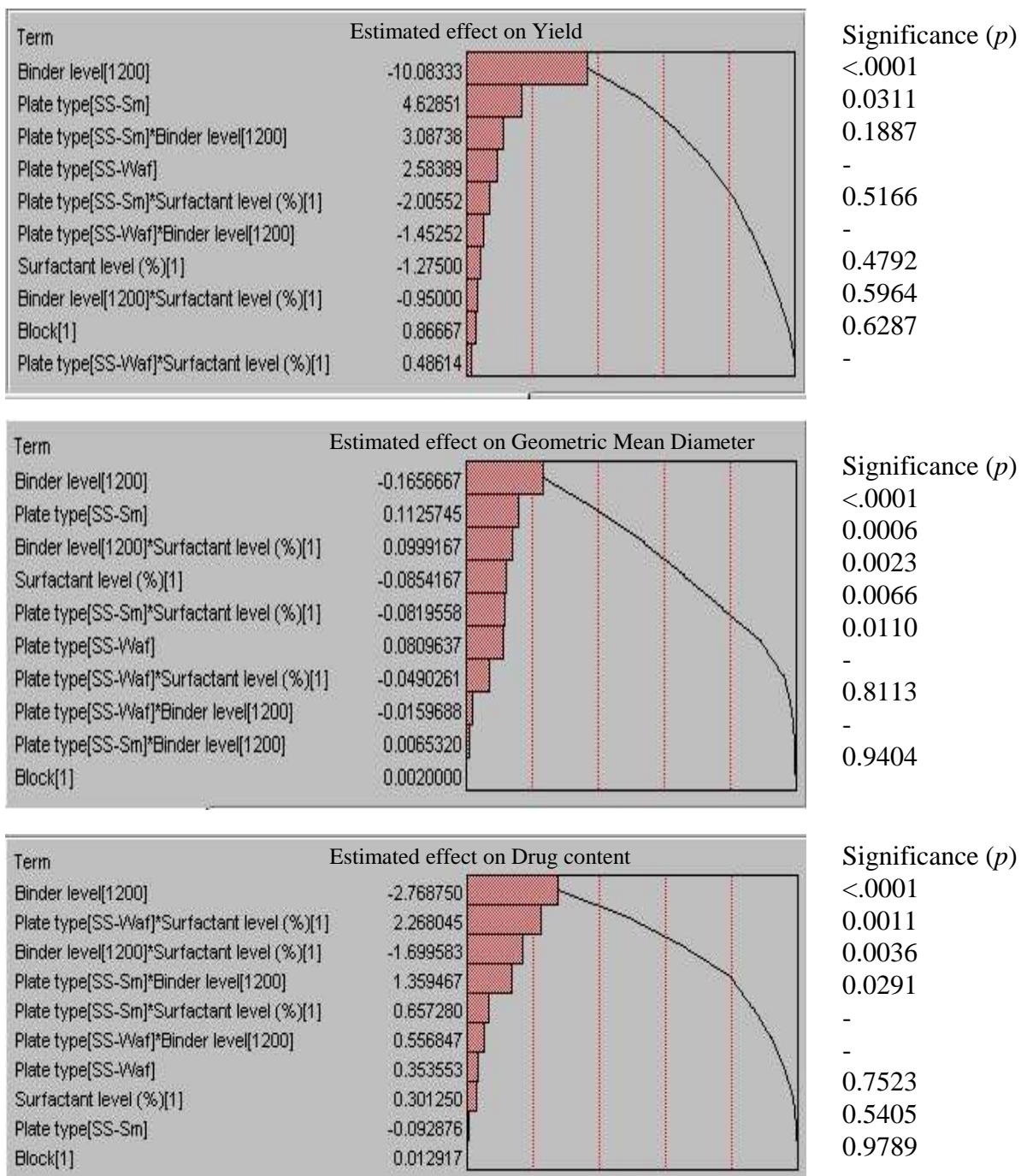
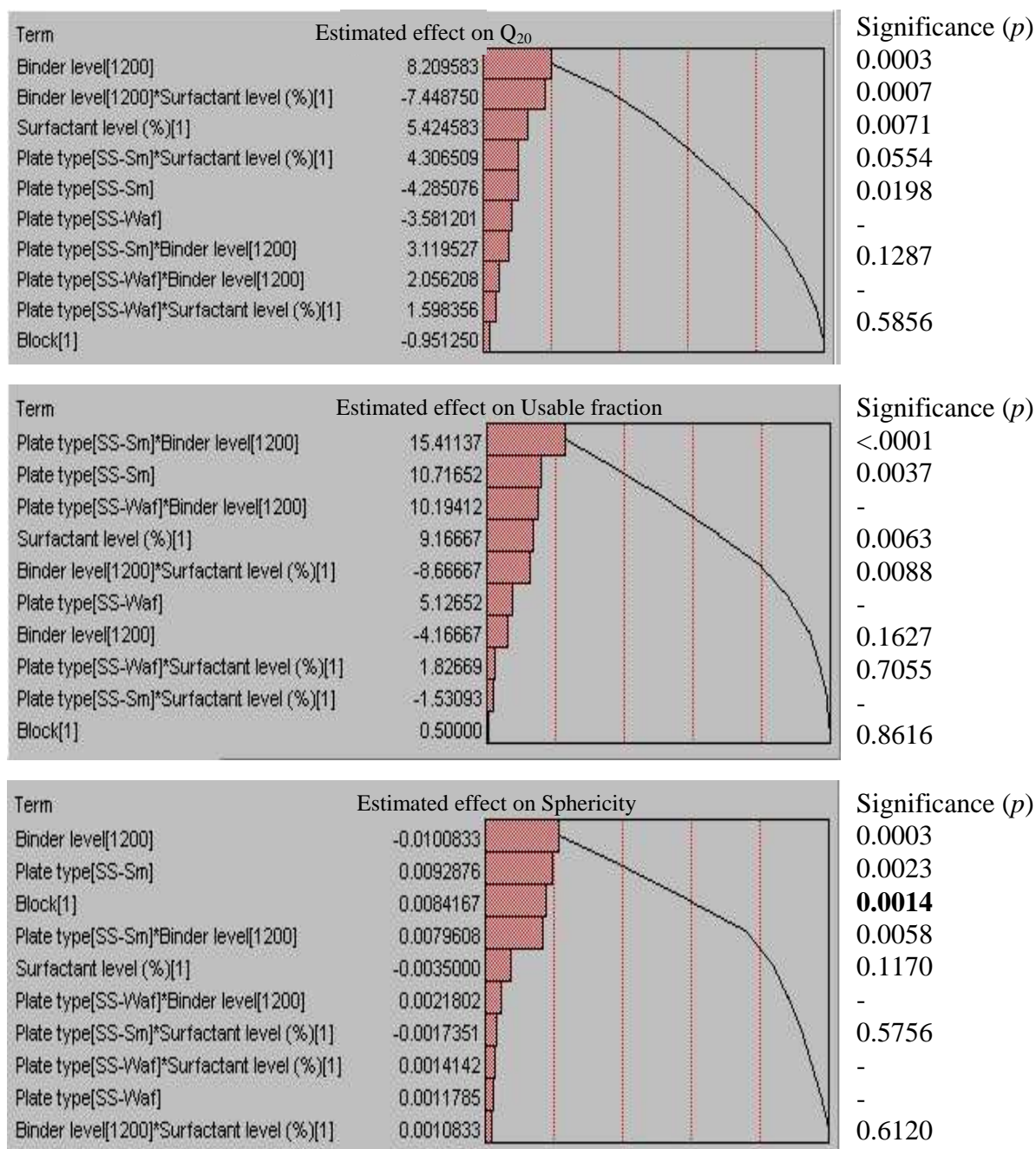


Figure 27. Pareto plots of effects of main factors on the specified product qualities



Pareto plots of effects of main factors on the specified product qualities (Contd.).

Surfactant level: Surfactant level significantly affected the Q_{20} , the geometric mean diameter, the LOD and the usable fraction ($p < 0.05$). In the presence of high binder and high surfactant levels, increase in geometric mean diameter, which consequently

decreased the Q_{20} of the spheroids was observed (Table XXII). Thus, in the presence of high amount of water as the granulating liquid, SLS appears to lose some of its surface-active property that should reduce the particle size of the spheroids. This result was confirmed by the highly statistical significance observed in the interaction between the high binder and surfactant levels.

Plate type: As seen in Table XXIII, plate type significantly influenced the yield, sphericity, friability; bulk density, geometric mean diameter, the Q_{20} and usable fraction ($p < 0.05$). Stainless steel smooth plate gave more consistent product quality especially with respect to yield, drug content, usable fraction. The effects of plate type on product yield, geometric mean diameter, drug content, Q_{20} , usable fraction and sphericity are also represented with the Pareto plots of some of the response variables (Figure 27).

Blocking effect: Blocking had no significant effect on eleven of the twelve product characteristics studied (Table XXIII), and also had no significant interactions with the main factors [(X1 - X3), indicating batch-to-batch reproducibility. A significant blocking effect ($p = 0.0014$) was observed with the sphericity response variable, which could actually be considered insignificant. This is because the data showed that the difference between the sphericity values [that should range between 0.1 (non spherical) – 1 (most spherical)] of the two blocks was very minute such that any slight change appeared statistically significant. However, although the observed difference would not be clinically important, this effect was tested further.

To test the significance of the blocking effect, statistical analysis was performed on the formulations within the individual blocks. Significant effect ($p = 0.02$) was observed only with the binder level in block 1 of Table VII, which was found to be insignificant for the whole model test ($p > 0.05$). In block 2, significant effects were observed with two of the main factors, namely, binder level ($p = 0.0008$) and plate type ($p = 0.0033$), and there was also significant interaction between binder level and plate type ($p = 0.013$). This blocking effect could be attributed to extraneous factors like humidity and temperature changes which have been shown to have possible effects on spheroid preparation (9), since the formulations in each of the blocks were produced at two different periods. However, the results from both blocks were generally within our set acceptance criteria and the variability between blocks was very minute.

Interaction: Some of interaction results are shown in Figure 28. There was significant interaction ($p < 0.05$) between binder level and plate type on the drug content, sphericity, friability and LOD response variables. Low binder yielded lower and less spherical spheroids as well as reduced usable fraction with teflon plate (Formulations 7 and 9). There were also significant interactions between the binder and the surfactant levels on the drug content, true density, LOD, the Q_{20} , usable fraction and geometric mean diameter response variable. High binder-High surfactant levels resulted in bigger spheroids for the batches made with the stainless steel plates. Significant ($p < 0.05$) interactions were also observed between the plate type and surfactant level on the drug content, bulk density and geometric mean diameter response variables.

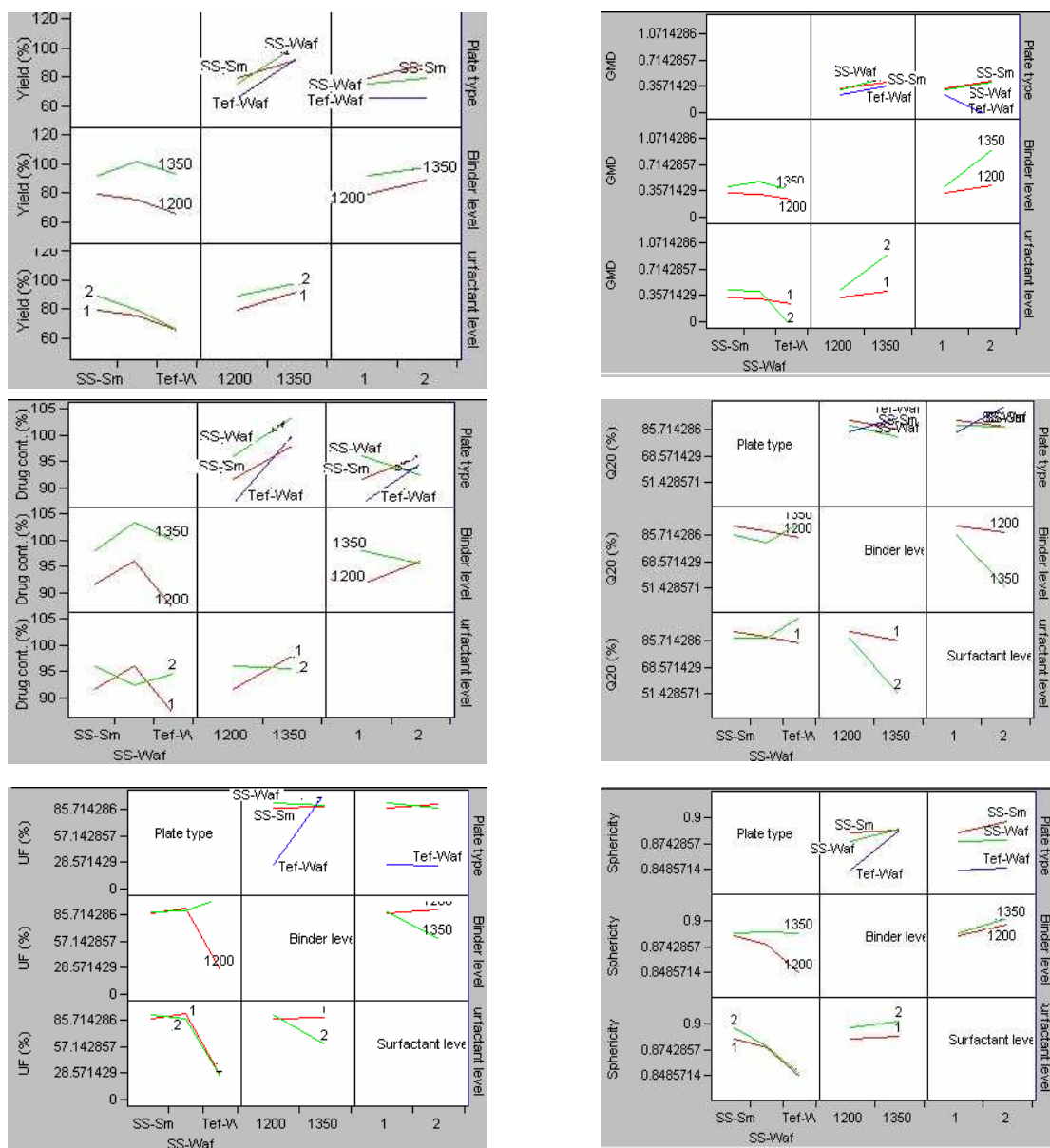


Figure 28. Interaction plots of the effects of main factors on specified qualities.

b. Physical Characteristics of the Spheroids

1. Scanning electron microscopy

As shown in Tables XXII & XXIV and Figures 29 and 30, and also as already explained in the interaction studies, high binder/high surfactant (HbHs) levels with stainless steel smooth or waffle plates (Formulations 3 and 6 respectively) produced spherical but very big spheroids (~1 mm). In contrast, low binder/high surfactant (LbHs) and high binder/low surfactant (HbLs) levels with stainless steel smooth plate (Formulations 5 and 11 respectively) resulted in spherical and smaller microparticulates within the acceptable criterion range of 0.35 –0. 5 mm. However, batches made with low binder/low surfactant (LbLs) or low binder/high surfactant (LbHs) levels and with teflon waffle plate (Formulations 7 and 9) produced very small spheroids (0.036 and 0.130 mm) with low sphericity. These results correlated with other observations and statistical analysis with regard to significance of binder level in the formation of well granulated spheroids (93,122). Typical morphology of the three different spheroid groups is shown in Figures 29 and 30.

2. Moisture content determination (Loss on drying)

Following our observations from previous studies, the moisture content at the end of drying of the products was generally $\leq 5\%$ (Table XXII). The highest values were obtained with the batches (Formulations 3 and 6) made with high binder-high surfactant (HbHs) levels and using the stainless steel plates. This could be due to the large sizes (949 and 1070 μm) of these pellets that could reduce the efficient drying of the stainless

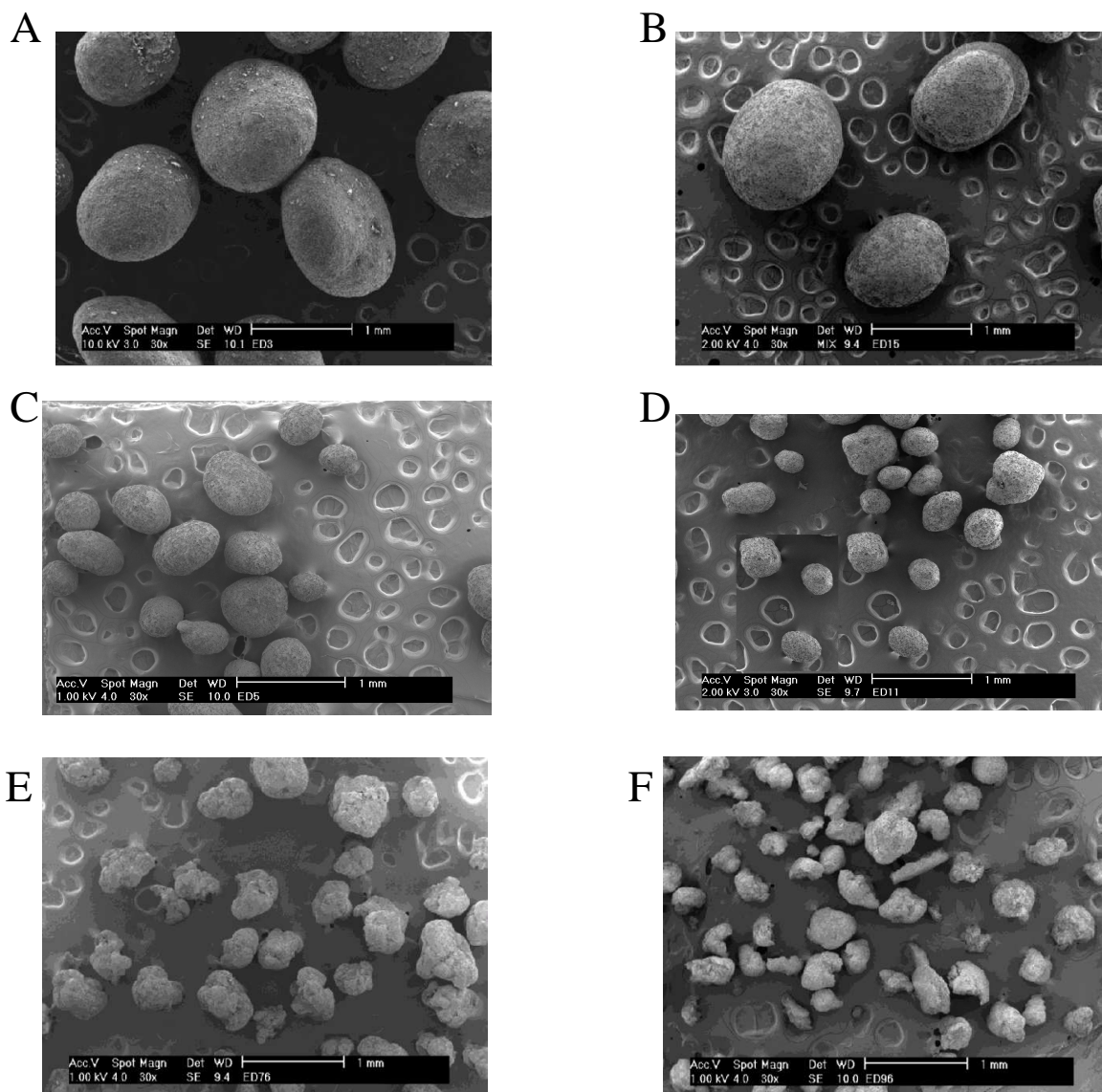


Figure 29: Scanning electron micrographs (30x) of ibuprofen granules. Formulations 3 and 6 (Panels A & B); Formulations 5 and 11 (Panels C & D); Formulations 7 and 9 (Panels E & F).

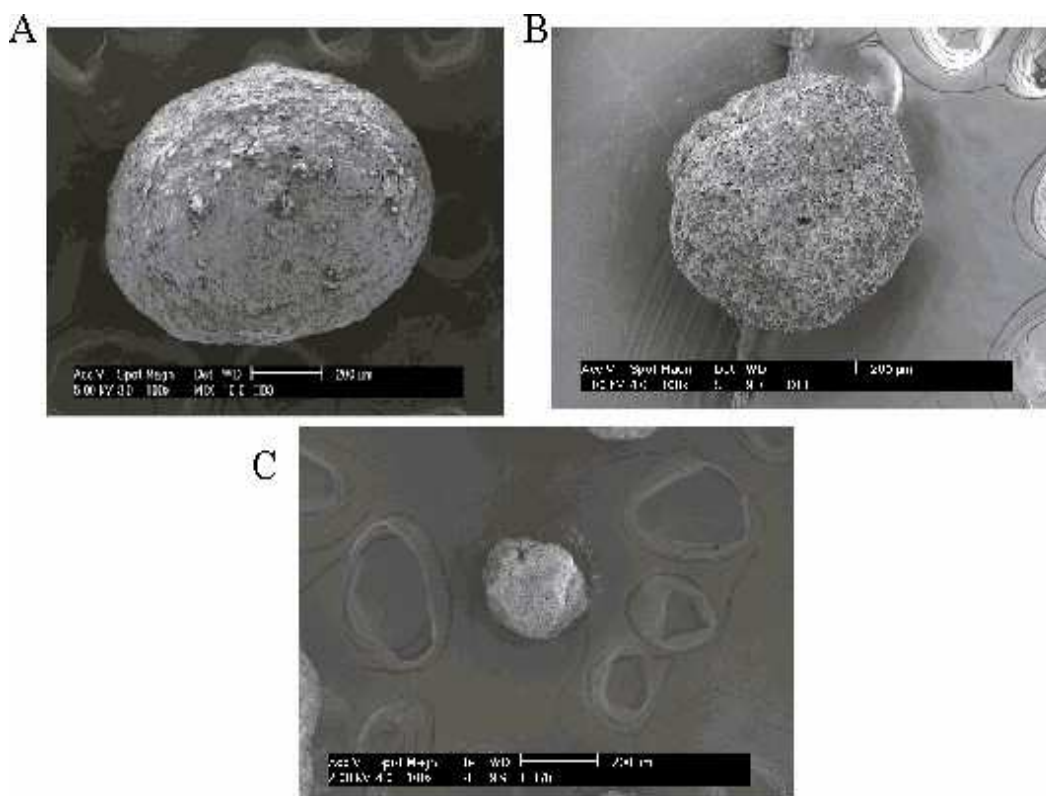


Figure 30: Scanning electron micrographs (100x) of ibuprofen granules.

Formulations 3 (A); 11 (B); 7 (C).

steel plate material. In contrast, the formulation (#10) made with the teflon plate using HbHs levels at a fixed binder level had smaller sized pellets (356 μm). This observation indicated that the teflon plate required higher amount of binder to yield products of similar sizes as those made with the stainless steel plate. The results were also supported by previous report that was obtained with the teflon plate. The smaller sized pellets obtained with this plate must have contributed to the effects of plate type on most of the spheroid qualities. In addition, these smaller sized pellets were easier to dry than the larger sized pellets obtained with the stainless steel plates, despite the insulating nature (lower drying efficiency) of the teflon material.

TABLE XXII. Physical Characteristics of Optimized Ibuprofen Spheroids.

	Form. 1	Form. 2	Form. 3	Form. 4	**Form. 5	Form. 6
Physical characteristics	Experimental variables					
	LbHsSS-waf	LbLsSS-sm	HbHsSS-sm	HbLsTef-waf	LbHsSS-sm	HbHsSS-waf
% Yield	80.85 ± 3.04	77.15 ± 9.83	95.85 ± 6.86	87.75 ± 7.57	89.7 ± 3.54	97.3 ± 1.56
% Moisture content	2.10 ± 0.13	2.00 ± 0.01	5.15 ± 0.23	1.52 ± 0.56	1.55 ± 0.23	4.22 ± 0.01
% Drug content	93.43 ± 2.17	92.57 ± 3.91	93.06 ± 1.40	96.67 ± 3.38	98.74 ± 0.81	92.76 ± 3.47
Geometric mean diameter (µm)	350 ± 1.55	354 ± 1.42	949 ± 1.40	460 ± 1.41	396 ± 1.35	1070 ± 1.40
Sphericity	0.87 ± 0.01	0.87 ± 0.00	0.89 ± 0.02	0.88 ± 0.00	0.89 ± 0.03	0.89 ± 0.02
Flowability (deg)	18.76 ± 0.54	20.38 ± 0.33	17.85 ± 0.00	17.92 ± 1.94	17.60 ± 1.95	19.14 ± 0.65
Carr's index. (%)	7.43 ± 1.55	9.12 ± 2.35	3.00 ± 0.59	7.48 ± 1.86	8.11 ± 0.24	3.78 ± 0.09
True density (g/cm ³)	1.30 ± 0.00	1.25 ± 0.01	1.22 ± 0.02	1.29 ± 0.01	1.29 ± 0.01	1.23 ± 0.00
Bulk density (g/cm ³)	0.63 ± 0.01	0.61 ± 0.09	0.78 ± 0.01	0.65 ± 0.07	0.64 ± 0.01	0.77 ± 0.00
Q ₂₀ (%)	89.85 ± 1.48	91.00 ± 1.13	47.55 ± 7.14	84.35 ± 5.02	89.90 ± 0.28	47.25 ± 0.49
Friability (%)	0.67 ± 0.00	0.67 ± 0.94	0.33 ± 0.00	0.67 ± 0.47	0.67 ± 0.47	0.5 ± 0.24
Usable fraction (%)	92.00 ± 2.83	81.00 ± 7.07	54.00 ± 14.14	93.00 ± 1.41	97.00 ± 1.41	43.00 ± 1.41

Low binder (Lb), High binder (Hb)

Low surfactant (Ls), High surfactant (Hs)

Stainless steel smooth (SS-sm), Stainless steelwaffle (SS-waf), Teflon waffle (Tef-waf)

Form.: Formulation

**The highlighted formulations showed the most acceptable spheroid qualities

TABLE XXII. Physical Characteristics of Optimized Ibuprofen Spheroids (Contd.).

	Form. 7	Form. 8	Form. 9	Form. 10	**Form. 11	Form. 12
Physical characteristics	Experimental variables					
	LbLsTef-waf	HbLsSS-waf	LbHsTef-waf	HbHsTef-waf	HbLsSS-sm	LbLsSS-waf
% Yield	68.65 ± 6.29	104.00 ± 9.9	60.4 ± 2.26	92.65 ± 18.87	92.10 ± 0.99	71.85 ± 4.6
% Moisture content	0.37 ± 0.13	0.44 ± 0.13	2.60 ± 0.30	1.69 ± 0.13	1.80 ± 0.43	2.50 ± 0.28
% Drug content	89.24 ± 2.18	99.96 ± 6.75	92.66 ± 0.94	99.79 ± 3.20	96.80 ± 0.47	93.96 ± 5.20
Geometric mean diameter (µm)	130 ± 2.54	417 ± 1.47	36 ± 5.93	356 ± 1.74	386 ± 1.48	384 ± 1.61
Sphericity	0.84 ± 0.01	0.88 ± 0.02	0.84 ± 0.00	0.89 ± 0.02	0.88 ± 0.01	0.88 ± 0.01
Flowability (deg)	24.36 ± 1.41	18.42 ± 0.44	26.47 ± 3.57	20.52 ± 1.88	20.93 ± 1.8	18.95 ± 1.85
Carr's index. (%)	10.85 ± 0.48	7.42 ± 1.39	18.61 ± 13.95	9.24 ± 0.86	8.07 ± 2.44	7.63 ± 1.41
True density (g/cm ³)	1.31 ± 0.00	1.28 ± 0.00	1.27 ± 0.04	1.28 ± 0.02	1.29 ± 0.00	1.29 ± 0.00
Bulk density (g/cm ³)	0.56 ± 0.02	0.65 ± 0.02	0.54 ± 0.05	0.60 ± 0.02	0.62 ± 0.03	0.65 ± 0.06
Q ₂₀ (%)	88.90 ± 5.23	88.95 ± 6.01	89.25 ± 1.48	91.80 ± 2.12	92.45 ± 3.61	87.35 ± 3.61
Friability (%)	0.37 ± 0.24	0.44 ± 0.24	7.62 ± 2.76	0.50 ± 0.71	1.00 ± 0.00	0.67 ± 0.94
Usable fraction (%)	37.00 ± 15.56	95.00 ± 1.41	13.00 ± 7.07	78.00 ± 19.80	94.00 ± 0.00	87.00 ± 9.90

Low binder (Lb), High binder (Hb)

Low surfactant (Ls), High surfactant (Hs)

Stainless steel smooth (SS-sm), Stainless steelwaffle (SS-waf), Teflon waffle (Tef-waf)

Form.: Formulation

**The highlighted formulations showed the most acceptable spheroid qualities

TABLE XXIII: *P*-values of Independent Variables for the Optimized Ibuprofen Spheroids

<i>Dependent variables</i>	Independent variables				Interactions		
	Blocking	Plate type	Binder level	Surf. level			
	1	2	3	4	2*3	2*4	3*4
Yield	NS	S (0.03)	S (<.0001)	NS	NS	NS	NS
Drug cont.	NS	NS	S (<.0001)	NS	S (0.0291)	S (0.0011)	S (0.0036)
Q ₂₀	NS	S (0.0198)	S (0.0003)	S (0.0071)	NS	NS (0.055)	S (0.0007)
Carr's Index	NS	NS (0.06)	S (0.03)	NS	NS	NS	NS
Flowability	NS	NS (0.067)	NS	NS	NS	NS	NS
Friability	NS	S (0.0001)	S (0.0001)	NS	S (0.0001)	NS	NS
Bulk density	NS	S (0.0046)	S (0.0017)	NS (0.08)	NS	S (0.0522)	S (0.0572)
True density	NS	NS	NS	NS (0.06)	NS	NS	S (0.0468)
Geom. m. diam.	NS	S. (0.0006)	S (<.0001)	S (0.0066)	NS	S (0.011)	S (0.0023)
Moisture content	NS	NS	NS (0.0857)	S (0.0026)	S (0.0049)	NS	S (0.0007)
Usable fraction	NS	S (0.0037)	NS	S (0.0063)	S (<.0001)	NS	S (0.0088)
Sphericity	S (0.0014)	S (0.0023)	S (0.0003)	NS	S (0.0058)	NS	NS

S: Significant

NS: Non-significant

Bold: indicates the few NS results obtained with the binder level factor in comparison to those obtained with the plate type and surfactant level factors.

TABLE XXIV: Summary of the Optimized Ibuprofen Spheroid Qualities

Plate type	Form. number	Form. vars	Physical Characteristics			
			Yield (%)	Q20 (%)	Geom. Mean	Usable
					diam. (mm)	fraction (%)
	12	Lb-Ls	71.85 ± 4.6	87.35 ± 3.61	384 ± 1.61	87.00 ± 9.90
SS-Waf	1	Lb-Hs	80.85 ± 3.04	89.85 ± 1.48	350 ± 1.55	92.00 ± 2.83
	8	Hb-Ls	104.00 ± 9.9	88.95 ± 6.01	417 ± 1.47	95.00 ± 1.41
	6	Hb-Hs	97.3 ± 1.56	47.25 ± 0.49	1070 ± 1.40	43.00 ± 1.41
	2	Lb-Ls	77.15 ± 9.83	91.00 ± 1.13	354 ± 1.42	81.00 ± 7.07
	5	Lb-Hs	89.7 ± 3.54	89.90 ± 0.28	396 ± 1.35	97.00 ± 1.41
SS-Sm	11	Hb-Ls	92.1 ± 0.99	92.45 ± 3.61	386 ± 1.48	94.00 ± 0.00
	3	Hb-Hs	95.85 ± 6.86	47.55 ± 7.14	949 ± 1.40	54.00 ± 14.14
	7	Lb-Ls	68.65 ± 6.29	88.90 ± 5.23	130 ± 2.54	37.00 ± 15.56
	9	Lb-Hs	60.4 ± 2.26	89.25 ± 1.48	36 ± 5.93	13.00 ± 7.07
Tef-Waf	4	Hb-Ls	87.75 ± 7.57	84.35 ± 5.02	460 ± 1.41	93.00 ± 1.41
	10	Hb-Hs	92.65 ± 18.87	91.80 ± 2.12	356 ± 1.74	78.00 ± 19.80

TABLE XXIV: Summary of the Optimized Ibuprofen Spheroid Qualities (Contd.)

Plate type	Form. number	Form. vars	Physical characteristics		
			Drug cont. (%)	Carr's index (%)	Sphericity
	12	Lb-Ls	93.96 ± 5.20	7.63 ± 1.41	0.88 ± 0.01
SS-Waf	1	Lb-Hs	97.3 ± 1.56	7.43 ± 1.55	0.87 ± 0.01
	8	Hb-Ls	99.96 ± 6.75	7.42 ± 1.39	0.88 ± 0.02
	6	Hb-Hs	92.76 ± 3.47	3.78 ± 0.09	0.89 ± 0.02
	2	Lb-Ls	92.57 ± 3.91	9.12 ± 2.35	0.87 ± 0.00
	5	Lb-Hs	98.74 ± 0.81	8.11 ± 0.24	0.89 ± 0.03
SS-Sm	11	Hb-Ls	96.80 ± 0.47	8.07 ± 2.44	0.88 ± 0.01
	3	Hb-Hs	93.06 ± 1.40	3.00 ± 0.59	0.89 ± 0.02
	7	Lb-Ls	89.24 ± 2.18	10.85 ± 0.48	0.84 ± 0.01
	9	Lb-Hs	92.66 ± 0.94	18.61 ± 13.95	0.84 ± 0.00
Tef-Waf	4	Hb-Ls	96.67 ± 3.38	7.48 ± 1.86	0.88 ± 0.00
	10	Hb-Hs	99.79 ± 3.20	9.24 ± 0.86	0.89 ± 0.02

The statistical analyses also showed that surfactant level significantly affected the moisture content of the products ($p = 0.0026$). This might have led to the significant interaction ($p = 0.0007$) between these two factors that resulted in the yield of oversized granules. The same reasons already given for the stainless steel and teflon plates might have led to the significant interaction ($p = 0.0049$) observed between plate type and binder level.

3. Yield and usable fractions of spheroids

The yield of the formulations ranged from $60.4 \pm 2.26\%$ - $104 \pm 9.9\%$ with the usable fractions (250 - 850 μm) ranging between $37 \pm 15.56\%$ - $97 \pm 1.41\%$ respectively (Table XXII).

Comparing batches made with similar plates, the formulations with low binder level gave lower yield values (1 and 12 vs. 6 and 8 respectively; 2 and 5 vs. 11 and 3 respectively; 7 and 9 vs. 4 and 10 respectively). The lower yield obtained from the low binder batches could be attributed to insufficient amount of binder being added to the powder blend leading to the production of more fines that were lifted up by the fluidization air into the filters, and also coated the walls of the fluid-bed. These observations were made more apparent from the results obtained with the geometric mean diameter (see below).

By comparing different batches made with plate material types of similar contours [Teflon waffle (TW) and stainless steel waffle (SSW)], it was observed that the latter yielded more products than the former (Formulations 4 vs. 8; 10 vs. 6; 9 vs. 1; 7 vs. 12).

This could be attributed to the production of more fines by the teflon material than the stainless steel material that could also lead to more losses, as already explained.

Plate contour was affected by the binder and (more or less) by the surfactant levels. At low binder level, the stainless steel smooth contour yielded higher microparticulates and more usable fractions than the SSW plate irrespective of the surfactant levels (Formulations 5 vs. 1 and 2 vs. 12). This could be due to the loss of products in the waffle contour, as previously explained (47). However, at higher binder levels, the SSW plate yielded more products and more or less equal usable fractions (Formulations 6 vs. 3 and 8 vs. 11) than the SS-smooth plate. The latter observation could be due to the formation of large sized spheroids that were neither lost in the filters nor in the waffle contours. The high binder-high surfactant batches are however practically unusable within our set acceptance criteria.

The results from Tables XXII & XXIV are supported by those of the *p-values* obtained using the JMP[®] software analyses (Table XXIII). These show that binder level and plate type significantly affected the product yield ($p < 0.0001$ and $p = 0.0311$ respectively). However, there was no significant interaction observed between any of the main factors ($p > 0.05$) on the yield product variable.

4. Drug content

Binder level significantly affected this response variable ($p < 0.0001$). Low binder levels generally resulted in reduced drug content, probably due to some losses that could occur from insufficient wetting of the product at any stage of its development. As already explained, there was also significant interaction between plate type and binder

level ($p = 0.0291$), plate type and surfactant level ($p = 0.0011$) and also binder and surfactant levels ($p = 0.0036$) on this spheroid quality. However, the results obtained from all the formulations are within our set acceptance criteria ($\geq 85\%$), as shown in Table XXII.

5. Friability

As shown in Table XXII, the percentage weight loss from all the formulations was generally $< 1\%$, except that of the batch made with teflon plate and low binder (formulation 9) that also produced the smallest sized spheroids (geometric mean diameter 36 ± 5.93) and the lowest usable fraction ($13 \pm 6.7\%$). It was observed that both binder level and plate type significantly affected this response variable ($p < 0.0001$), and there was also significant interaction observed between these two factors ($p < 0.0001$).

Generally, low binder content produced more friable spheres. These results could be related to the explanations given under the LOD section. At low binder levels there will not be enough binder for particle-particle contact and adhesion that will lead to the formation of primary and strong secondary nuclei (76), thereby forming friable spheroids.

6. True density and compressibility

The statistical analyses showed that none of the main factors significantly affected the true density of the microparticulates. The closest was the effect of the surfactant level ($p = 0.06$) and its interaction with binder level ($p = 0.048$). Different binder and surfactant levels might have led to different pellet sizes, which might have affected the true density of the pellets. Bulk density was significantly affected by plate type

($p = 0.0046$) and binder level ($p = 0.0017$), however, no significant interaction was observed between these factors ($p > 0.05$). Our results correspond with previous reports (using the traditional extrusion-spheronization process) that bulk density which greatly influences the packing properties of spheres is greatly dependent on the diameter of the pellets (134,258). Thus, there would be no change in the volume occupied by pellets of high geometric mean diameter leading to high bulk density of the microparticulates (Formulations 3 and 6). For true density that directly affects the compactness of substances, high geometric mean diameter is indicative of larger air pockets, and consequently, lower true density. However, we observed the lowest true density values for the spheroids with the highest geometric mean diameter (Table XXII), as was also observed by other authors (259). This is probably due to larger air pockets entrapped by these bigger microparticulates that are practically open porous structures, as shown in Figure 30 above, and therefore would result in low true density (low compactedness) spheroids.

The percent compressibility (Carr's index) was significantly affected by binder level ($p = 0.032$). It has been shown that during spheronization, agglomerates grow by coalescence (44), which depends on plastic deformability of the wet material mass. Sufficient binder is therefore required for the powder materials to achieve plastic deformation, which is related to the compressibility of the product, Hence the observed statistically significant effect at two binder levels. The p -value for plate type was 0.0642 but there was no significant interaction observed. The results of the Carr's index (generally $< 15\%$) indicate that the granules have acceptable bulk and true densities for

the production of unit dosage forms except for formulation 9, which also has the lowest usable fraction, smallest geometric mean diameter and the poorest flowability (Table XXII).

Flowability was slightly affected by plate type ($p = 0.067$), though not statistically significant ($p > 0.05$), which could be attributed to the higher fines produced by the teflon plate material as already discussed.

7. Sphericity of the granules

The sphericity values of most of the microparticulates were within our set acceptance criterion (≥ 0.85), which is close to 1.0, the optimal value for sphericity (Table XXII). The sphericity was reduced by the use of teflon waffle plate except in the presence of high binder levels (Formulations 7 and 9 vs. 4 and 10). This could be due to the production of more fines in the presence of low binder levels by this plate type, thus producing less spheronized microparticulates, and also indicating the need for higher binder level by this plate type. Statistically, it was observed that binder level and plate type significantly affected this response variable ($p = 0.003$ and 0.023 respectively), and there was also significant interaction between these factors ($p = 0.0058$). Batch replication (blocking) was also observed to affect the sphericity of the batches ($p = 0.0014$). This effect has been elaborated on page 152.

8. Size distribution of granules

The geometric mean diameter of the microparticulates ranges from $36 \pm 5.93 \mu\text{m}$ - $1070 \pm 1.14 \mu\text{m}$ (Table XXII; Figure 31) respectively. Three groups can be distinguished from the observed experimental results. The first group comprised of formulations 3 and 6 that present very large spheroid sizes caused probably by the simultaneous use of high binder and high surfactant levels, which could lead to excessive agglomeration (260). The second group included formulations 7 and 9 with very small spheroid sizes due to low binder level with the teflon plate material which tends to produce more fines than similar batches made with the stainless steel plates. The results from both groups are in

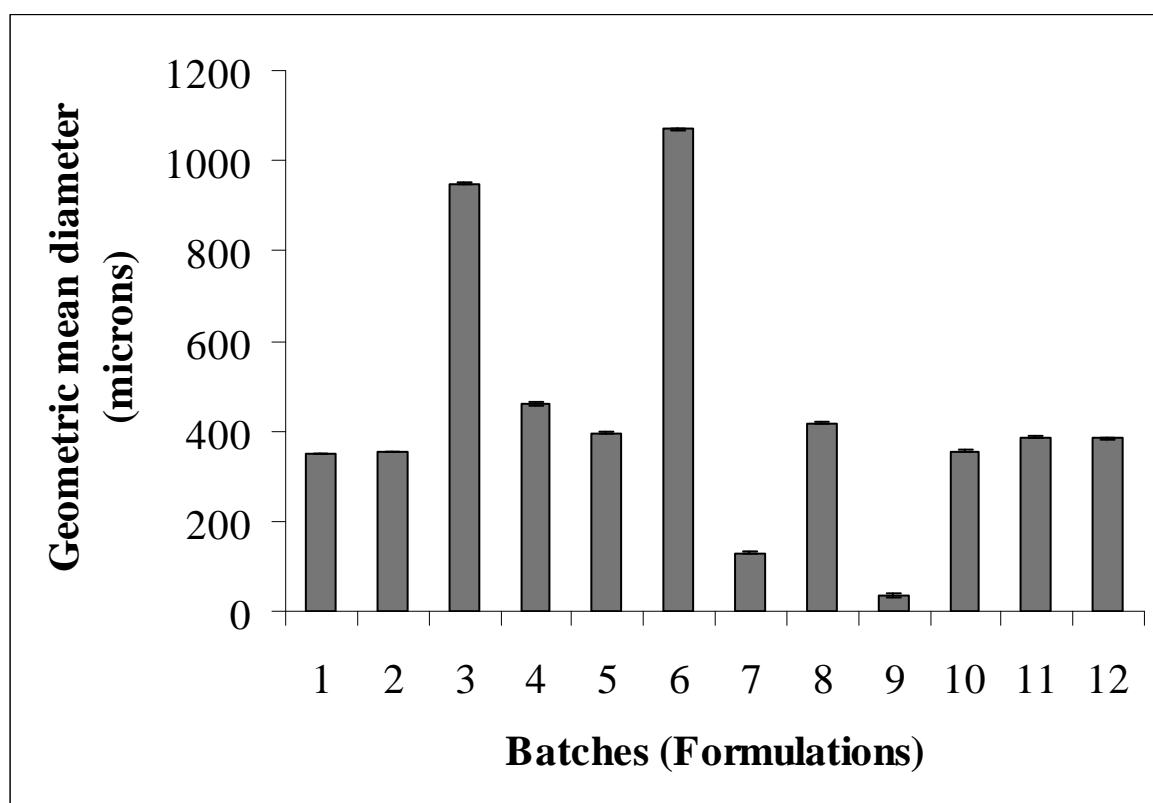


Figure 31: Geometric mean diameters of experimentally designed replicated batches.

accordance with previous experiments that showed that the higher the amount of binder, the more spherical the particles and the larger their sizes, and *vice versa* (261).

The last group consisting of intermediate sizes (e.g. Formulations 5 and 11) with geometric mean diameter ranging from $350 \pm 1.55 \mu\text{m}$ - $460 \pm 1.41 \mu\text{m}$ respectively are mostly results of low levels of either the binder or the surfactant. This group, with usable fractions mostly $> 85\%$ fell within our set acceptance criteria and comprised our most acceptable formulations.

As explained in various sections, the statistical data show that the three main factors significantly affected this response variable (Table XXIII), namely, binder level ($p < 0.0001$), plate type ($p = 0.0006$) and surfactant level ($p = 0.0066$). There was significant interaction between plate type and surfactant level ($p = 0.011$) and also binder and surfactant levels ($p = 0.0023$). Both effects could be related to our observation of the smaller pellets obtained with the different binder and surfactant levels when used with the different plate types. Thus, the simultaneous presence of high binder and surfactant levels in the formulation made with teflon plate material (Formulation 4) did not lead to the production of big sized spheres (Table XXII; Figure 31), as seen with formulations 3 and 6. This could be attributed to the hydrophobic nature of the teflon material that prevented fast spreading of the hydrophilic binder. Consequently higher amount of binder was required for miscibility with the powder and formation of good spheroids.

9. *Ibuprofen release from granules*

All the formulations released > 80% of the drug within 20 minutes (Q_{20}), except the batches with large sizes (Formulations 3 and 6) that consequently reduced the surface area of the granules (Table XXII; Figures 32A & B). These formulations consisted of HbHs levels and made with stainless steel smooth and waffle plates respectively. Statistically, it was observed that plate type ($p = 0.0198$), binder level ($p = 0.0003$) and

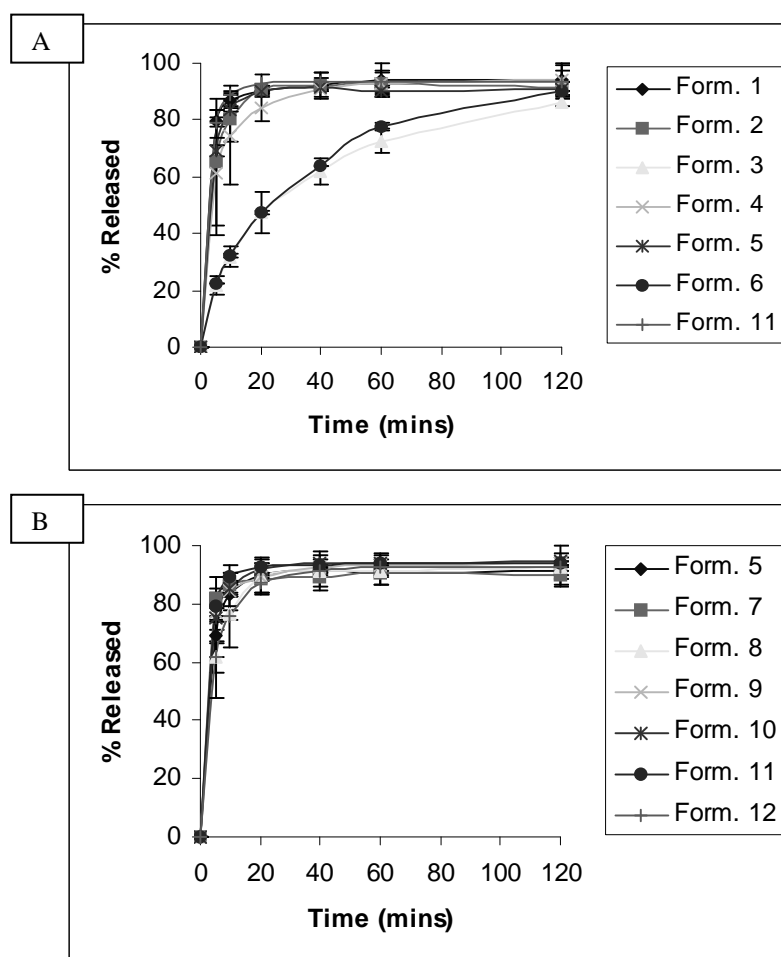


Figure 32: Dissolution profiles of experimentally designed replicated batches.

Formulations 1-6, 11 (Panel A); Formulations 5, 7-12 (Panel B).

surfactant level ($p = 0.0071$) significantly affected this response variable (Table XXIII), which could be related to their effects on the spheroid sizes. As already explained, there was significant interaction between binder and surfactant levels ($p = 0.0007$). High binder level might have resulted in reduced surface active properties of SLS that ordinarily would result in smaller particle sizes. Consequently, larger spheroids were produced. The interaction between plate type and surfactant level ($p = 0.0554$) should also be noted though not statistically significant ($p > 0.05$).

Based on the results of the statistical analyses (effects of binder, SLS and plate type) and our set acceptance criteria such as yield, drug content, dissolution and sphericity studies, Formulation 11 (Tables XXII and XXIV) was chosen as the optimized preparation and was subsequently used to study the effects of particle size and drug load on spheroid qualities.

Phase 3

The Effects of Drug particle Size, Drug Loading and Intermediate Size Scale-up on the Characteristics of Ibuprofen Microparticulates

a. Effects of drug particle size and drug loading

1. Experimental design

Drug micron size: Drug particle size significantly ($p < 0.05$) affected some of the physical characteristics studied, namely, moisture content ($p = 0.0203$), bulk density ($p = 0.0088$), flowability ($p = 0.0028$), sphericity ($p = 0.0034$) and usable fractions

($p = 0.0214$). These results are as expected as similar observations have been previously reported necessary for most of these variables (52,153). The bigger micron sized ibuprofen (40 μm) resulted in higher LOD, lower sphericity and lower bulk density. The latter two observations could be a result of the bigger sizes breaking up during drying, leading to lower bulk density of the spheres. These outcomes would affect the sphericity and bulk density of the pellets. These results are shown in Tables XXV and XXVI and in Figure 33.

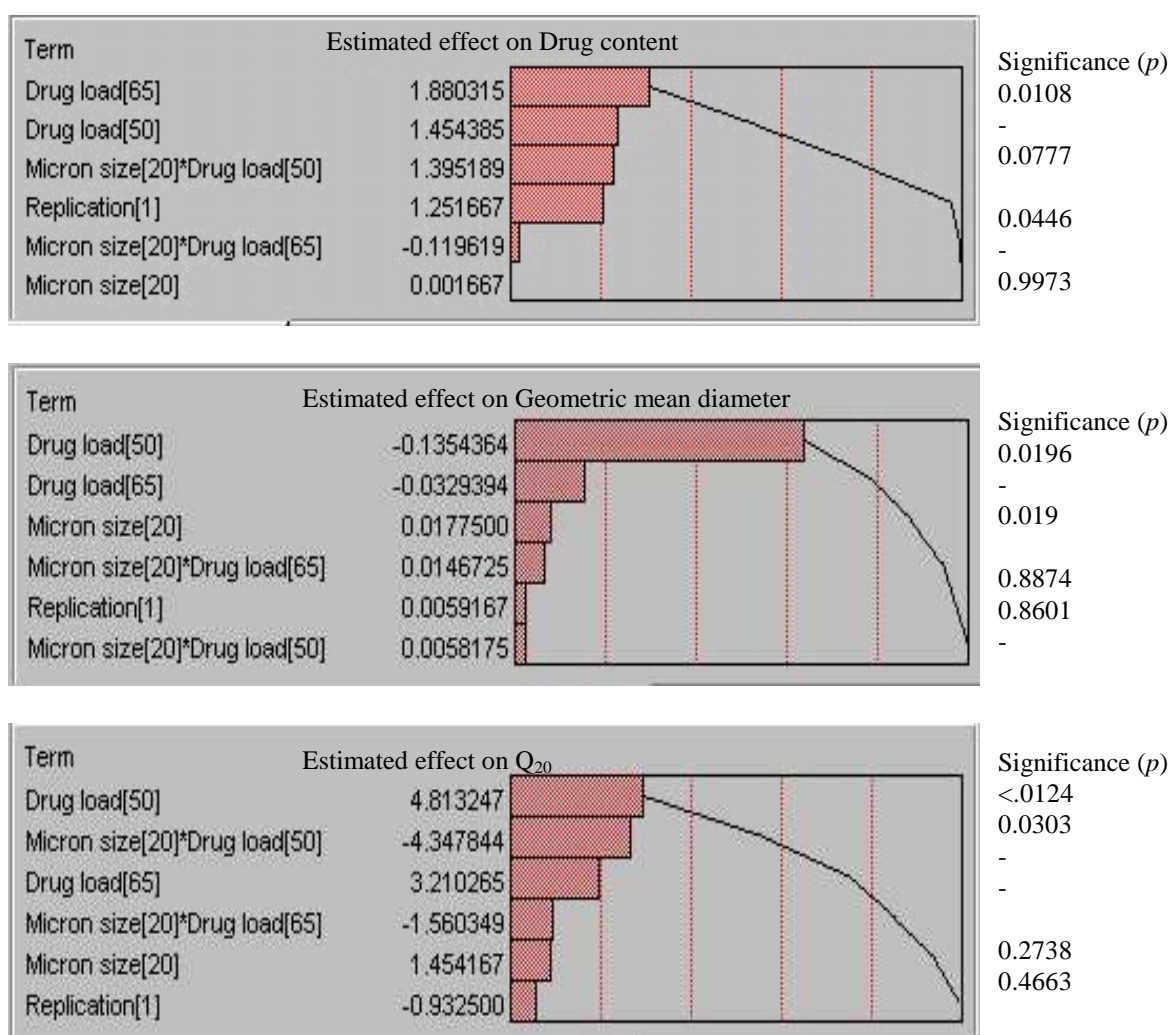


Figure 33. Pareto plots of effects of main factors on the specified product qualities.

Drug load: Drug load significantly affected most of the qualities of the spheroids, except the yield, flowability and Carr's index. The insignificant effect on Carr's index was not expected since the bulk and tapped densities ($p < 0.001$) from which it was calculated were significantly affected by drug load (Tables XXV and XXVI). However, these observations conform with the reports that there may be other factors such as GMD and LOD contributing to the qualities of the finished product. The observed increase in GMD with increased drug load could be due to the reduced amount of Avicel[®] RC-581 (a spheronization enhancer) in the system, which might have exposed the products to be easily over granulated.

Replication: Replication had no significant effect on ten of the twelve product characteristics studied (Table XXVI), as well as no significant interactions with the main effects [(drug load & drug micron size); results not shown], indicating batch-to-batch reproducibility. The result obtained with the drug content response variable could be considered statistically significant ($p = 0.0446$). However, this result falls on the borderline of our set level of significance ($p = 0.05$). In addition, the drug contents of all the response variables were $> 90\%$ (above our set acceptance criteria). Although statistical significance ($p = 0.0069$) was observed with friability, the friability values of all the response variables could be considered negligible ($< 2\%$).

Interaction: There was significant interaction ($p < 0.05$) between drug micron size and drug load on the flowability ($p = 0.0371$) and Q_{20} ($p = 0.0303$) variables (Table XXVI). These results are also shown in interaction plots (Figure 34).

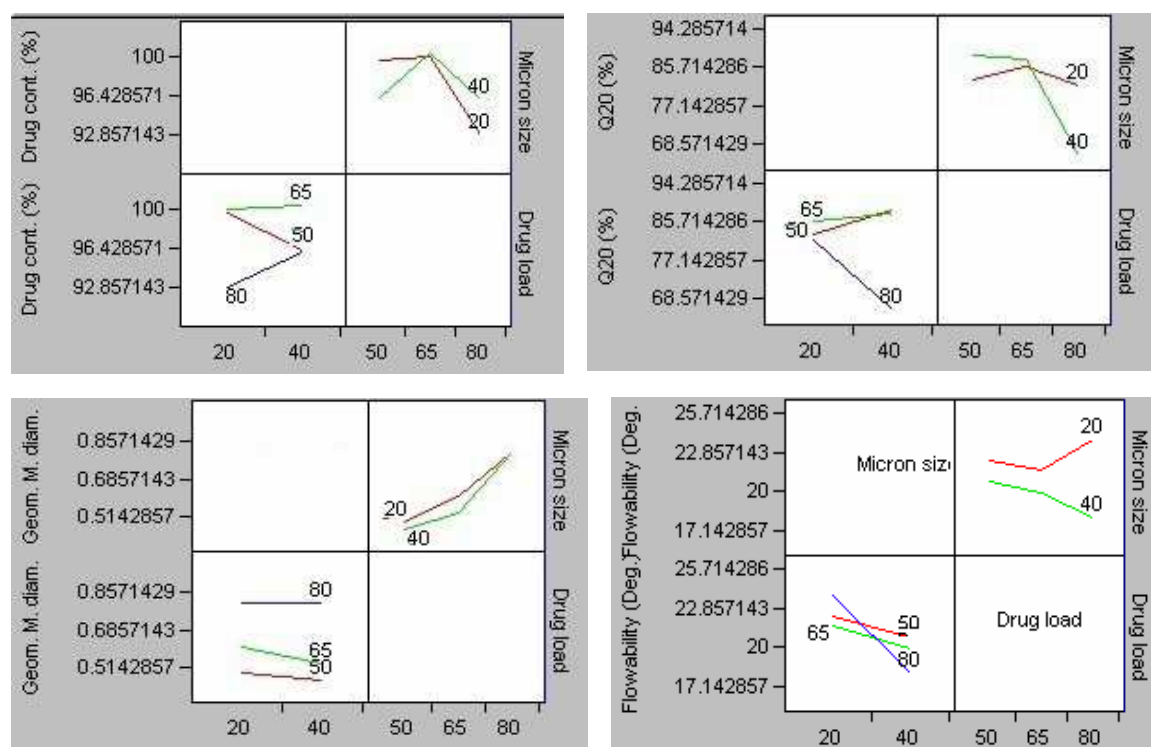


Figure 34. Interaction plots of the effects of main factors on specified qualities.

2. Physical characterization of granules

i. Scanning electron microscopy

Figure 35 shows typical morphology of the spheroids obtained from the three drug loads. As shown in Table XXV and Figure 35, the size of the microparticulates increased with increased drug load. This could be due to the reduced amount of Avicel[®], the water absorber in the system that increased the chances of over granulation of the spheroids.

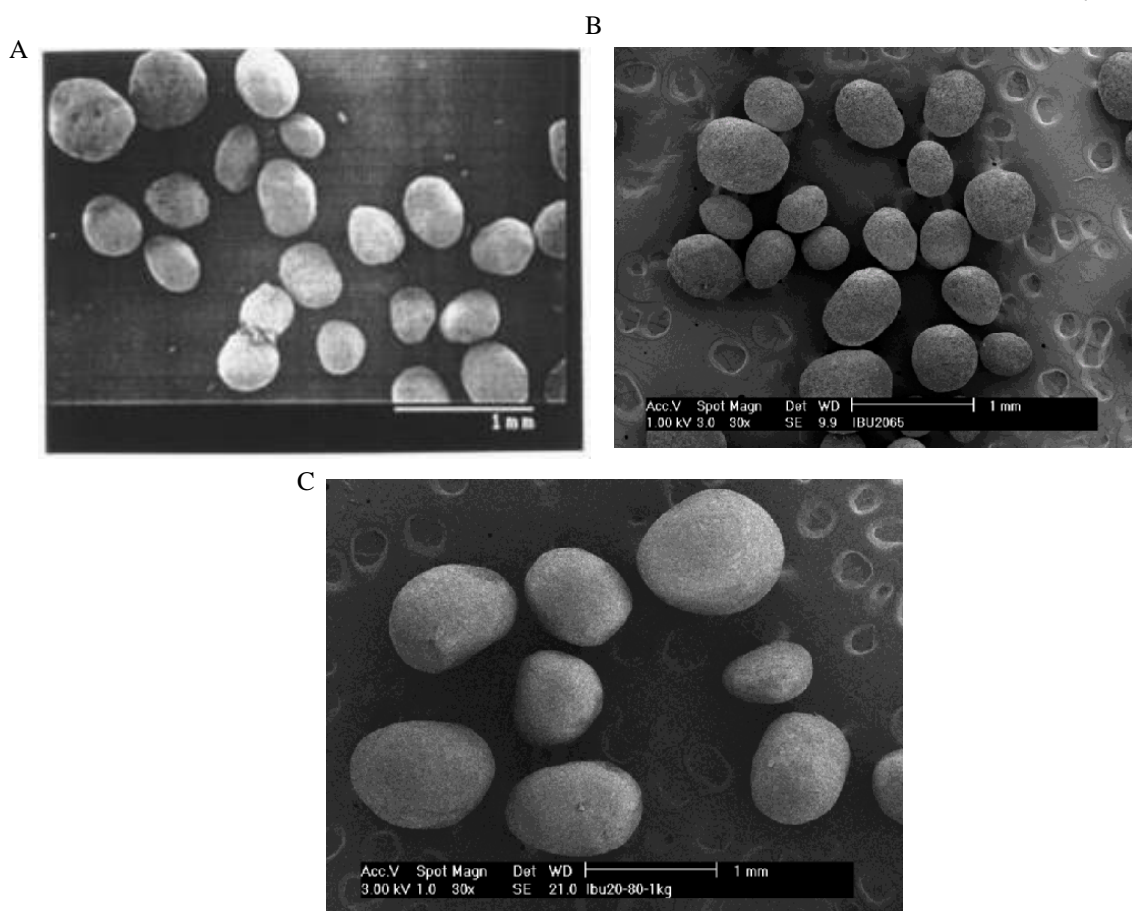


Figure 35: Scanning electron micrographs (30x) of ibuprofen formulations (20 μm drug size and 1 kg batch) for the different drug loads, A (50%); B (65%); and C (80%).

ii. Moisture content/Loss on drying analyses

Binder amount: As expected, the amount of binder needed for spheronization of the different drug levels was inversely related to drug load (Table XI). This indicates that, as previously reported (44,49), Avicel[®] acted as molecular sponge that absorbed water, thus the requirement for higher amount of binder as Avicel[®] level increased. It was also observed that at each drug level, less binder was required to spheronize the 40 micron sized ibuprofen, however, these batches took longer processing time.

Table XXV. Physical Characteristics of Drug Micron Size/Drug Load Batches (Means of replicated batches)

	20 micron size ibuprofen			40 micron size ibuprofen		
% ibuprofen	50	65	80	50	65	80
Physical characteristics						
% Yield	90.85 ± 7.99	87.7 ± 1.56	76.35 ± 10.11	85.60 ± 0.00	94.27 ± 0.07	93.6 ± 2.83
% Moisture content	1.7 ± .14	0.89 ± 0.01	0.71 ± 0.28	1.72 ± 0.14	1.69 ± 0.15	0.94 ± 0.20
% Drug content	98.55 ± 5.08	98.79 ± 0.95	91.57 ± 1.27	94.96 ± 1.10	99.13 ± 1.11	94.81 ± 1.12
Geometric mean diameter (µm)	485 ± 1.52	605 ± 1.45	697 ± 1.98	456 ± 1.37	528 ± 1.42	802 ± 1.35
Sphericity	0.91 ± 0.00	0.91 ± 0.01	0.88 ± 0.01	0.871 ± 0.017	0.882 ± 0.00	0.873 ± 0.00
Flowability (deg)	22.15 ± 0.00	21.43 ± 1.16	23.72 ± 1.73	20.63 ± 0.11	19.88 ± 0.11	17.95 ± 0.21
Carr's index. (%)	8.03 ± 1.67	6.02 ± 0.06	7.23 ± 1.38	6.79 ± .32	6.83 ± 0.92	8.43 ± 5.29
True density (g/cm ³)	1.29 ± 0.02	1.24 ± 0.00	1.18 ± 0.00	1.29 ± 0.00	1.21 ± 0.04	1.18 ± 0.01
Bulk density (g/cm ³)	0.69 ± 0.01	0.63 ± 0.01	0.58 ± 0.03	0.64 ± 0.02	0.57 ± 0.01	0.57 ± 0.00
Q ₂₀ (%)	83.94 ± 4.00	86.87 ± 1.34	82.80 ± 6.19	89.48 ± 4.93	88.38 ± 3.73	67.04 ± 0.26
Friability (%)	0.50 ± 0.24	0.50 ± 0.24	1.17 ± 0.71	0.84 ± 0.23	1.00 ± 0.47	1.17 ± 0.23
Usable fraction (%)	91.00 ± 1.41	85.00 ± 1.41	59.00 ± 7.07	97.00 ± 1.41	92.00 ± 0.00	70.00 ± 5.66

TABLE XXVI: P-values of Independent Variables of Drug Micron Size/Drug Load Batches

Dependent variables	Independent variables			
	Replication [1, 2]	Micron size (MS) [20 μ m, 40 μ m]	Drug load (DL) [50%, 65%, 80%]	Interactions (MS * DL)
Yield	NS	NS	NS	NS (0.0681)
Moisture content	S (0.0446)	NS	S (0.0108)	NS (0.0777)
LOD	NS	S (0.0203)	S (0.003)	NS (0.0689)
Q ₂₀	NS	NS	S (0.0124)	S (0.0303)
Geometric mean diameter	NS	NS	S (0.0196)	NS
True density	NS	NS	S (0.0003)	NS
Bulk density	NS	S (0.0088)	S (0.001)	NS
Carr's index	NS	NS	NS	NS
Flowability	NS	S (0.0028)	NS	S (0.0371)
Friability	S (0.0069)	NS (0.0584)	S (0.0315)	NS
Sphericity	NS	S (0.0034)	S (0.0282)	NS (0.0613)
Usable fraction	NS	S (0.0214)	S (0.0004)	NS

Moisture content in the fluid-bed: A plot of the moisture content for both drug particle sizes during spheronization and drying processes in function of time (Figure 36) showed that, as stated above, with the two drug micron sizes, the amount of the liquid binder needed for the spheronization of the powder blends decreased as the drug load increased. It was also observed that the products containing 20% Avicel® or 80% drug load were easily overspheronized, resulting in larger particle sizes. This is in accordance with the report that the lower the amount of Avicel® in the spheronization of most model drugs, the more difficult the spheronization process (49). The moisture content at the end of drying of the products was generally < 2% (Table XXV).

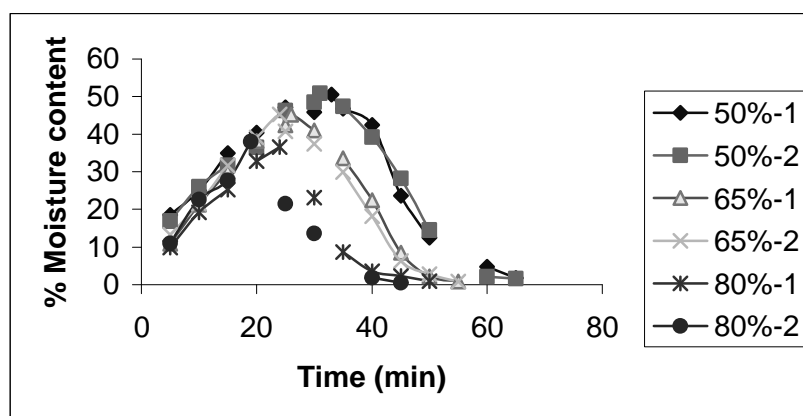


Figure 36: The moisture content profile of 20 micron ibuprofen as a function of time (1 & 2 represent replicate batches).

iii. Yield and usable fractions of spheroids

The yield of the formulations ranged from $76.35 \pm 10.11\%$ - $94 \pm 0.07\%$ with the usable fractions (250 - 850 μm) ranging between $59 \pm 7.07\%$ – $97 \pm 1.41\%$ respectively (Table XXV). Comparing batches made with 20 micron sized ibuprofen, the percent yield decreased as drug load increased. This could be attributed to the poor wettability of

the batch due to increased ibuprofen that led to more losses in the system. The 40 micron sized ibuprofen yielded slightly more products although this was not statistically significant (Table XXVI).

The usable fraction was significantly affected by both drug micron size ($p = 0.0004$) and drug load ($p = 0.0214$). As shown in Table XXV, the fraction decreased as drug load increased, possibly due to greater percentage of oversized fraction that increased with increased drug load.

iv. Drug content

Although drug content was significantly affected by replication ($p = 0.0446$) and drug load ($p = 0.0108$), all the formulations had drug contents $> 90\%$ thereby meeting our set acceptance criteria ($\geq 85\%$). The lower drug content obtained with the 80% drug loaded 20 micron sized batch supports the hypothesis that the poor wettability of this more micronized drug size led to more losses of the drug to the fluid-bed walls, and consequently to decreased drug content.

v. Friability

As shown in Table XXV, the percentage weight loss from all the formulations was generally less than 2%, indicating that all the formulations could withstand processing frictional forces. The statistical importance of these results has been discussed above.

vi. True density and compressibility

In both particle sizes, bulk and true densities decreased with increased drug loads. Considering the nature or composition of the blend, Avicel[®] is bulkier and has higher particle density than ibuprofen. Consequently, increasing the amount of ibuprofen, i.e. decreasing Avicel[®] content should lead to decreased bulk and true densities as observed. In addition, at each drug level, the densities of the 20 micron sized ibuprofen are higher than those of the 40 micron sizes. These could be explained by the higher geometric mean sizes obtained from the 20 micron sizes, as already explained on page 168. The 50% drug loads of both drug micron sizes have almost similar GMDs and consequently slightly similar densities. These results are supported by those of the statistical analyses shown in Table XXVI. It was observed that drug load ($p = 0.0003$) significantly affected the true density of the microparticulates.

Bulk density was also significantly affected by drug load ($p = 0.001$) as well as micron size ($p = 0.0088$), however, no significant interaction was observed between these factors ($p > 0.05$). The percent compressibility (Carr's index) was generally $< 15\%$, indicative of the acceptable flowability of the spheroids as well as good bulk and true densities for the production of both single unit- (tablets) and multi unit (capsules) dosage forms.

vii. Flowability

The finer sized ibuprofen resulted in lower flowability (Table XXV). These results were as previously reported (52,153).

viii. Sphericity of the granules

The sphericity of most of the microparticulates fell within our set acceptance criteria (≥ 0.85), which is close to 1.0, the optimal value for sphericity (Table XXV). The sphericity of the 20 micron sized ibuprofen batches were slightly higher than the 40 micron sized batches. This could be explained by the smaller size of the particles that could form less porous bond with Avicel[®], thereby leading to smoother surface texture. Statistically, sphericity was significantly affected by drug load ($p = 0.0282$) and micron size ($p = 0.0034$), but no significant interaction was observed between these factors.

ix. Size distribution of granules

The geometric mean diameter of the microparticulates ranged from $456 \pm 1.37 \mu\text{m}$ - $802 \pm 1.35 \mu\text{m}$ (Table XXV; Figure 37) respectively. Within the batches made of the two ibuprofen micron sizes, the GMD increased with increased drug load, which could be either due to overgranulation or improved bonding due to higher amount of ibuprofen. This observation was also found to be statistically significant ($p = 0.0196$), as already discussed on page 168.

x. Ibuprofen release from granules

All the formulations released more than 80% of the drug within 20 min, except the batch containing 80% ibuprofen spheronized using the 40 micron sized drug. This could be due to the bigger GMD that consequently reduced the surface area of the granules (Table XXV; Figure 38). For the same reason, the Q_{20} was lower with the 80% drug load.

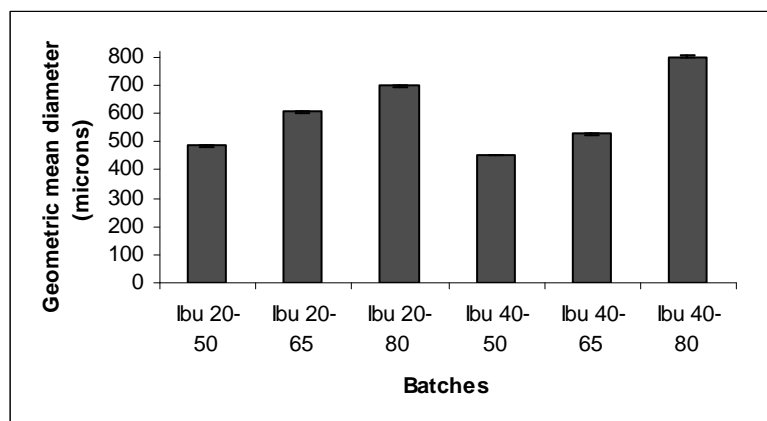


Figure 37: Geometric mean diameters of drug particle size/drug load batches.

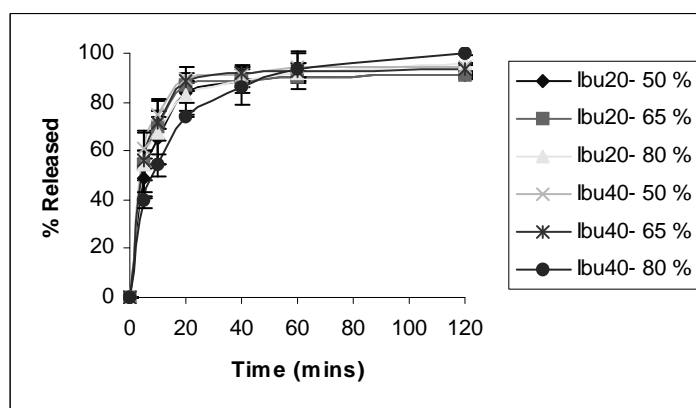


Figure 38. Dissolution profiles of drug particle size/drug load batches.

Statistically, it was observed that drug micron size ($p = 0.0034$) and drug load ($p = 0.0282$) significantly affected this response variable (Table XXVI). There was also interaction between these main factors, although this was not statistically significant ($p = 0.0613$) based on our set significant level ($p < 0.05$).

In addition, the 65% drug loaded formulation of the 20 μm ibuprofen had similar characteristics with the previously optimized 50% and had the most significant positive effects on the products. This was therefore chosen for intermediate batch size scale-up.

b. Effect of Intermediate Size Scale-up on the Characteristics of Ibuprofen

Microparticulates

1. Experimental design

Batch size: Batch size significantly ($p < 0.05$) affected some of the physical characteristics studied, namely, bulk density ($p = 0.0072$), tapped density ($p = 0.0124$), friability ($p = 0.0146$) and usable fractions ($p = 0.0009$). These results were as expected as similar observations have been reported for most of these variables (101,140).

Increased batch size led to higher densities, lower friability and lower usable fractions.

The latter could be due to increased spheroid size as it affected only the 1 kg batches that have considerably big differences in their particle sizes. These results are shown in Tables XXVII and XXVIII and in the Pareto plots (Figure 39).

Drug load: Drug load significantly ($p < 05$) affected the densities of the spheroids (Table XXVIII). This is due to the difference in the densities of the powder blends used in the formulations, which contained different percentages of Avicel[®] and the drug. As was previously obtained, higher drug loads resulted in lower bulk ($p = 0059$), tapped ($p = 0071$) and true ($p = 0022$) densities.

Replication: Replication had no significant effect ($p > 0.05$) on all twelve product characteristics studied (Table XXVIII), as well as no significant interactions with the main effects [(batch size and drug load); results not shown], indicating batch-to-batch reproducibility.

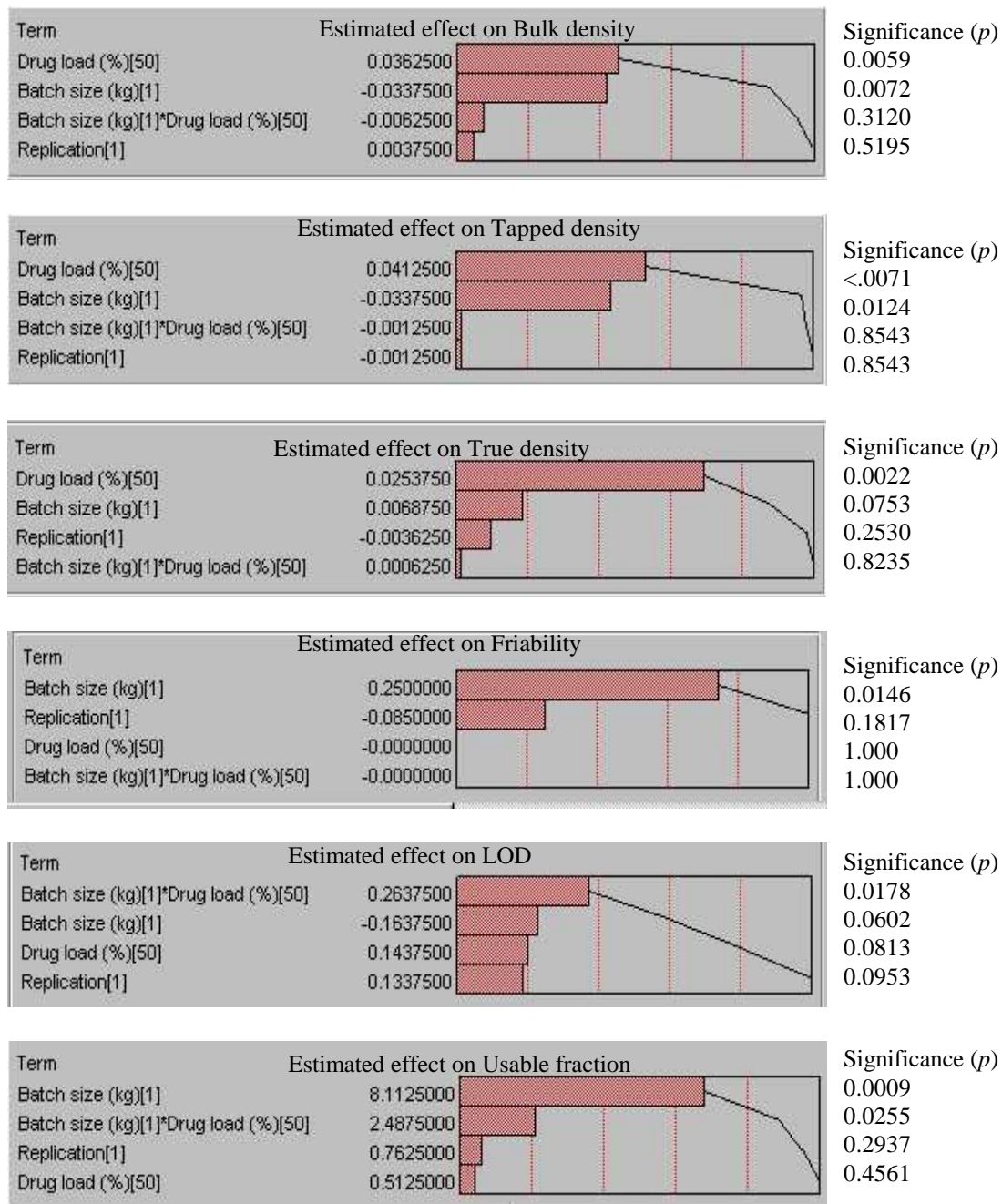


Figure 39. Pareto plots of effects of main factors on the specified product qualities.

Interaction: The interaction results are shown in Figure 40. There was significant interaction ($p < 0.05$) between batch size and drug load on the LOD ($p = 0.0178$) and usable fraction ($p = 0.0255$) variables (Table XXVIII; Figure 40).

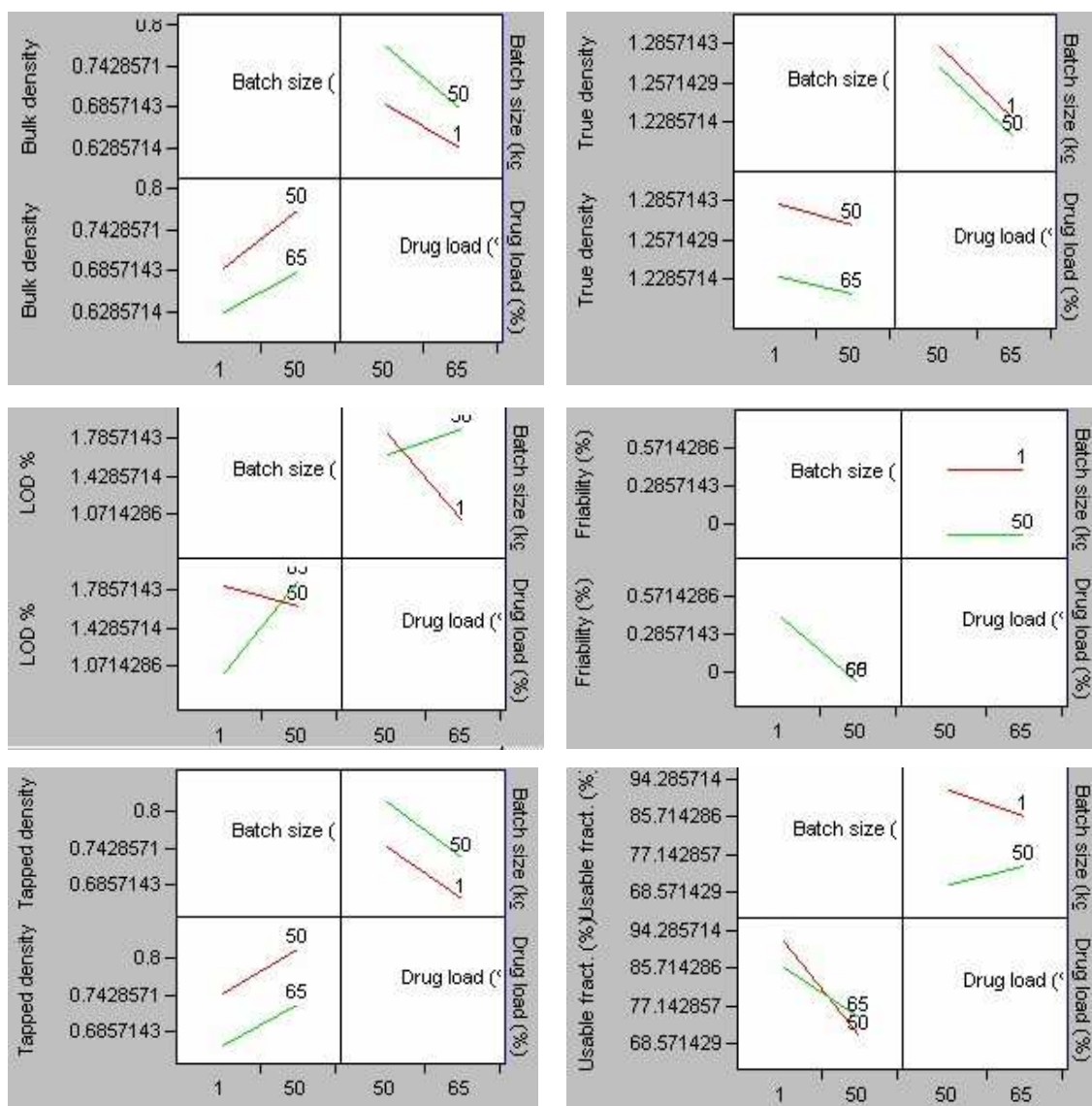


Figure 40. Interaction plots of the effects of main factors on specified qualities.

Considering the significant interaction obtained with the usable fraction, and the fact that significant effect was obtained from batch size alone, it can be inferred that increased batch size resulted in decreased usable fraction.

However, the results obtained are within our set acceptance criteria that were based on published results from other reporters (6,9).

2. Physical characteristics of pellets

i. Scanning electron microscopy

Figure 41 shows typical morphology of the spheroids obtained from the two drug loads (Figures 41A & B) and the two batch sizes (Figures 41B & C). As shown in Table XXVII and Figure 41, the size of the microparticulates increased with increased drug load at the 1 kg level. This effect was not pronounced at the scale-up level. This could be due to the fact that although the percentage of Avicel[®] present in the fluid-bed is the same in both batch sizes, the increased batch size of Avicel[®] might have enhanced its water-absorbing properties in the system and therefore reduced the chance of over granulation.

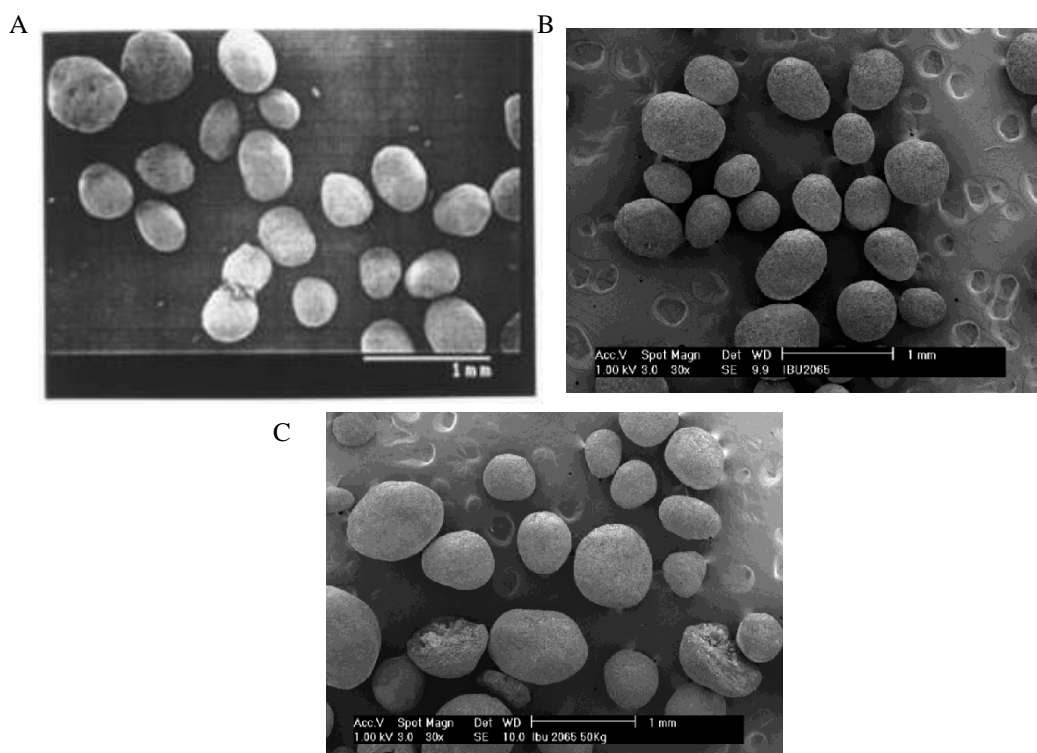


Figure 41: Scanning electron micrographs (30x) of ibuprofen formulations (20 μ m drug particle size) containing different drug loads, A (1 kg, 50%); B (1 kg, 65%), and C (50 kg, 65%).

Table XXVII. Physical Characteristics of Batch Size/Drug Load Batches (Means of replicated batches)

Batch size	1 kg		50 kg	
% ibuprofen	50	65	50	65
Physical characteristics				
% Yield	90.85 ± 7.99	87.7 ± 1.56	95.70 ± 0.18	91.38 ± 0.76
% Moisture content	1.7 ± .14	0.89 ± 0.01	1.50 ± 0.27	1.74 ± 0.35
% Drug content	98.55 ± 5.08	98.79 ± 0.95	101.5 ± 2.16	102.09 ± 0.06
Geometric mean diameter (µm)	485 ± 1.52	605 ± 1.45	522.00 ± 2.04	538.00 ± 1.95
Sphericity	0.91 ± 0.00	0.91 ± 0.01	0.91 ± 0.00	0.91 ± 0.01
Flowability (deg)	22.15 ± 0.00	21.43 ± 1.16	22.99 ± 0.47	20.84 ± 0.46
Carr's index. (%)	8.03 ± 1.67	6.02 ± 0.06	6.14 ± 0.16	6.85 ± 1.94
True density (g/cm ³)	1.287 ± 0.02	1.235 ± 0.00	1.27 ± 0.01	1.22 ± 0.00
Bulk density (g/cm ³)	0.69 ± 0.01	0.63 ± 0.01	0.77 ± 0.02	0.68 ± 0.01
Tapped density	0.75 ± 0.02	0.67 ± 0.01	0.82 ± 0.02	0.73 ± 0.00
Q ₂₀ (%)	83.1 ± 1.68	83.1 ± 1.68	83.1 ± 1.68	87.45 ± 1.05
Friability (%)	0.50 ± 0.24	0.50 ± 0.24	0.00 ± 0.00	0.00 ± 0.00
Usable fraction (%)	91.0 ± 1.41	85.0 ± 1.41	69.8 ± 2.12	73.75 ± 2.19

TABLE XXVIII: P-values of Independent Variables of Batch Size/Drug Load Batches

Dependent variables	Independent variables			Interactions
Physical characteristics	Replication	Batch size	Drug load	Interactions
	1	2	3	2 * 3
Yield	NS	NS	NS	NS
Drug content	NS	NS	NS	NS
LOD	NS	NS (0.0602)	NS (0.0813)	S (0.0178)
Q ₂₀	NS	NS	NS	NS
Geometric mean diameter	NS	NS	NS	NS
True density	NS	NS (0.0753)	S (0.0022)	NS
Bulk density	NS	S (0.0072)	S (0.0059)	NS
Tapped density	NS	S (0.0124)	S (0.0071)	NS
Carr's index	NS	NS	NS	NS
Flowability	NS	NS	NS (0.0774)	NS
Friability	NS	S (0.0146)	NS	NS
Sphericity	NS	NS	NS	NS
Usable fraction	NS	S (0.0009)	NS	S (0.0255)

ii. Moisture content/Loss on drying analyses

Binder amount: As expected and also as was previously observed, the amount of binder needed for spheronization of the different drug levels was inversely related to drug load (Table XV), although the amount used for the 50 kg-65% drug load appeared to be high. This could be due to some human error as both the total time used for spheronization and the percent moisture at the end of the spheronization process reflect an inverse relationship to the drug load. These results indicated that, as previously stated, Avicel[®] acts as molecular sponge that absorbed water. Additionally, the amount of binder needed for the process also decreased as the batch size increased. From Table XV, it is apparent that a processing time was reduced by 13x for intermediate batch compared to the small scale batch irrespective of the drug load used (Equations 32 and 33). This confirmed the reproducibility of the process.

For the 50% drug load:

$$\frac{67 \text{ min (Average value for two batches of the 1 kg batches)} * 50}{246 \text{ min (Average value for two batches of the 50 kg batches)}} = 13 \quad \text{Eqn. 32}$$

For the 65% drug load:

$$\frac{54.5 \text{ min (Average value for two batches of the 1 kg batches)} * 50}{198 \text{ min (Average value for two batches of the 50 kg batches)}} = 13 \quad \text{Eqn. 33}$$

Moisture content in the fluid-bed: A plot of the moisture content for both batch sizes during spheronization and drying processes in function of time (Figure 42) showed that with the two sizes, the amount of the liquid binder needed for the spheronization of

the powder blends decreased as the drug load increased. These correlated with previous reports and our earlier explanations about the function of microcrystalline cellulose as a molecular sponge for water absorption. The moisture content at the end of drying of the products was generally < 2% (Table XXVII).

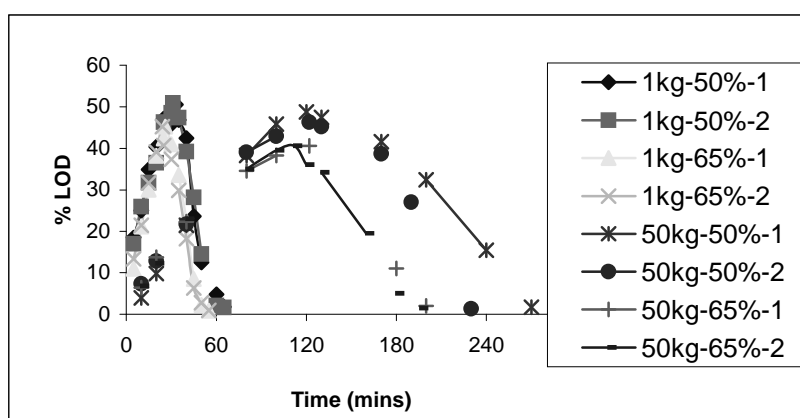


Figure 42: The moisture content profile of scale-up batches as a function of time.

(1 & 2 represent replicate batches).

iii. Yield and usable fractions of spheroids

The yield of the formulations ranged from $87.7 \pm 1.56\%$ - $95.7 \pm 0.18\%$ with the usable fractions (250 - 850 μm) ranging between $69.8 \pm 2.12\%$ - $91 \pm 1.41\%$ respectively (Table XXVII). Comparing the two batch sizes, increased batch resulted in increased product output, which could be attributed to decreased amount lost as a percentage of the initial powder blend input. Comparing the two drug loads within each of the batch sizes, increased load resulted in decreased product output, as was observed in the previous section, which could be attributed to higher amount of the lower weighted ibuprofen in

the larger drug load formulation. However, the analysis showed that these observations were not statistically significant (Table XXVIII).

The usable fraction was influenced by both batch size and drug load (Table XXVII). The fraction decreased as drug load increased, however, increased batch size appeared to have positively affected the usable fraction since the 50 kg-65% batch yielded slightly higher amount than the 50 kg-50% formulation. These results were supported by the statistical results that showed a significant effect ($p = 0.0009$) of the batch size on this variable, as well as a significant interaction effect ($p = 0.0255$).

iv. Drug content

All the formulations had drug contents $> 90\%$ thereby meeting our set acceptance criteria ($\geq 85\%$).

v. Friability

As shown in Table XXVII, the percentage weight loss from all the formulations was generally less than 1. Thus, although the statistical results show a significant effect of batch size on friability ($p = 0.0146$), this effect was obtained between 0 and 0.5% values and could be considered clinically unimportant.

vi. True density and compressibility

In both batch sizes, bulk, tapped and true densities decreased with increased drug loads, which could be due to the reasons explained in the previous section. In addition, at each drug level, the true densities were similar as could be expected, being the same

formulation and moreover, true density is indicative of the importance of compactness of substances. However, the bulk and tapped densities, which reflect the packing properties of spheres, increased with increased batch size. These could be as a result of other product qualities including pellet sizes. The percent compressibility (Carr's index) was generally $< 15\%$, indicative of the acceptable flowability of the spheroids as well as good bulk and true densities for the production of both single unit- and multi unit dosage forms.

vii. Flowability

The flowability of the products fall within our set acceptance criteria ($\theta < 30^\circ$). In addition, no significant effect was observed on this variable by the main factors.

viii. Sphericity of the granules

The sphericity of all the microparticulates fall within our set acceptance criteria (≥ 0.85), which is close to 1.0, the optimal value for sphericity (Table XXVII).

ix. Size distribution of granules

The geometric mean diameters of the microparticulates range from $485 \pm 1.52 \mu\text{m}$ - $605 \pm 1.45 \mu\text{m}$ (Table XXVII; Figure 43). Within the 1 kg batches, the GMD increased with increased drug load, which could either be due to over granulation or improved bonding due to higher amount of ibuprofen. For the 50 kg batches, the effect of drug load on GMD appeared to be improved with the increased batch size, although these results were statistically insignificant ($p > 0.05$).

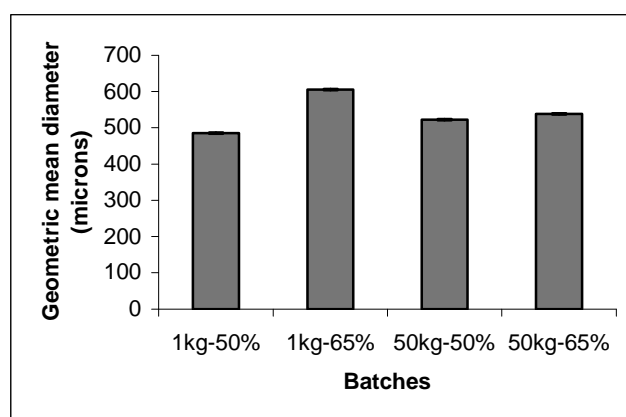


Figure 43: Geometric mean diameters of batch size/drug load batches.

x. Ibuprofen release from granules

All the formulations released more than 80% of the drug within 20 min. As observed by other reporters, the Q_{20} was higher for the higher drug loaded batches at each batch size, despite the larger GMD of the 1 kg batch containing 65% drug load (Table XXVII; Figures 43 & 44).

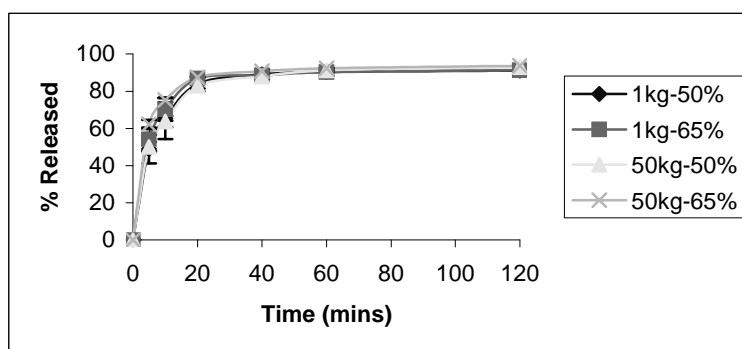


Figure 44. Dissolution profiles of batch size/drug load batches.

In summary, increased batch size reduced the processing time at both drug loads and also improved some spheroid qualities such as geometric mean diameter (Table XVII and Figure 43). The dissolution of the 65% drug load 50 kg batch size was the most acceptable (highest Q_{20}). This formulation was therefore chosen for coating.

Phase 4

Coating and Encapsulation of Spheronized Ibuprofen Microparticulates Using Hard Gelatin Capsules

a. Effects of coating

1. Experimental design

Polymer type: Polymer type significantly ($p < 0.05$) affected most of the qualities of the spheroids, except the T_{50} , geometric mean diameter (GMD), the friability and the sphericity. The core pellets used in this experiment were similar for both Eudragit[®] and Surelease[®]. The levels were chosen such that the medium level in each case represented the company recommended level to obtain satisfactory coating. It is therefore evident from our results that these recommended levels are somehow equivalent in the coating capacities of the two polymers. However, the polymer level necessary to achieve the objective (prolonged drug release) is formulation-dependent. These results are shown in Tables XXIX and XXX and also in the Pareto plots in Figure 45.

Polymer level: Polymer level significantly ($p < 0.05$) affected some of the physical characteristics studied, namely, yield ($p = 0.0370$), T_{50} ($p = 0.0165$), bulk density ($p = 0.0462$), true density ($p = 0.0072$), flowability ($p < 0.0001$), and usable fractions ($p = 0.0071$). Most of these results were as expected. Drug release has been variously reported to decrease with increased polymer level (175,176). Increased polymer level was also expected to increase particle size/geometric mean diameter, which will affect the flowability and densities of the formulations, as already explained in previous

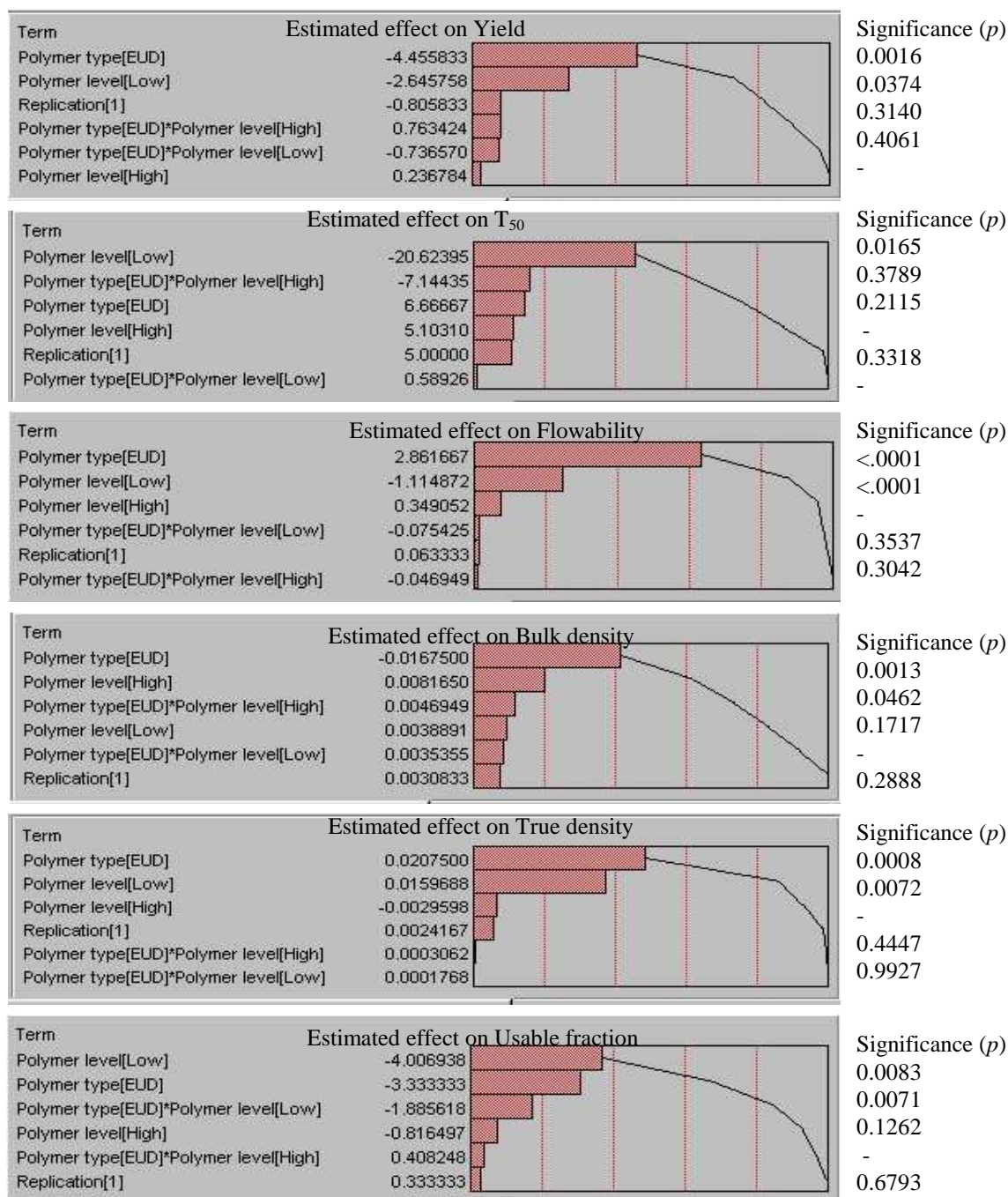


Figure 45. Pareto plots of effects of main factors on the specified product qualities.

sections. The discrepancy observed within the batches coated with the Eudragit[®] polymer could be due to an uncontrollable sedimentation of talc present in the coating solution

tubing that might have altered most of the results expected from this polymer type and levels. Possible explanations with regard to this observation will be discussed at the various sections of the product quality variables. The statistical results obtained with this variable are shown in Tables XXIX and XXX and also in the Pareto plots in Figure 45.

Replication: Replication had no significant ($p > 0.05$) effect on all the product characteristics studied (Table XXIX), as well as no significant interactions with the main effects [(polymer type and level); results not shown]. Although these results support batch-to-batch reproducibility of the process, some effort and experience with the fluid-bed are required in order to achieve this goal.

Interaction: There was no significant interaction ($p > 0.05$) between polymer type and

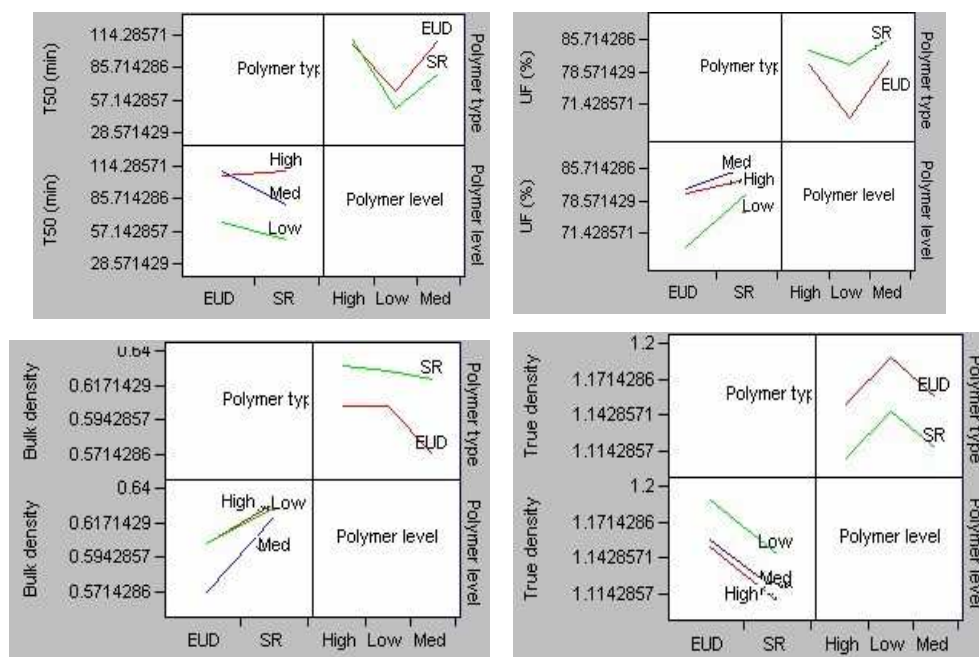


Figure 46. Interaction plots of the effects of main factors on specified qualities.

polymer level. There were also no significant interactions between these main factors and replication. These results, some of which are presented in Figure 46 support the feasibility of the process.

2. Physical characterization of granules

i. Scanning electron microscopy

The size of the microparticulates increased directly with coating Table XXIX and Figures 47 & 48. The pore size decreased, suggestive by the smoother surface of the coated pellets. Thus, the particle size distribution and drug release were subsequently affected, as will be discussed further in the respective sections.

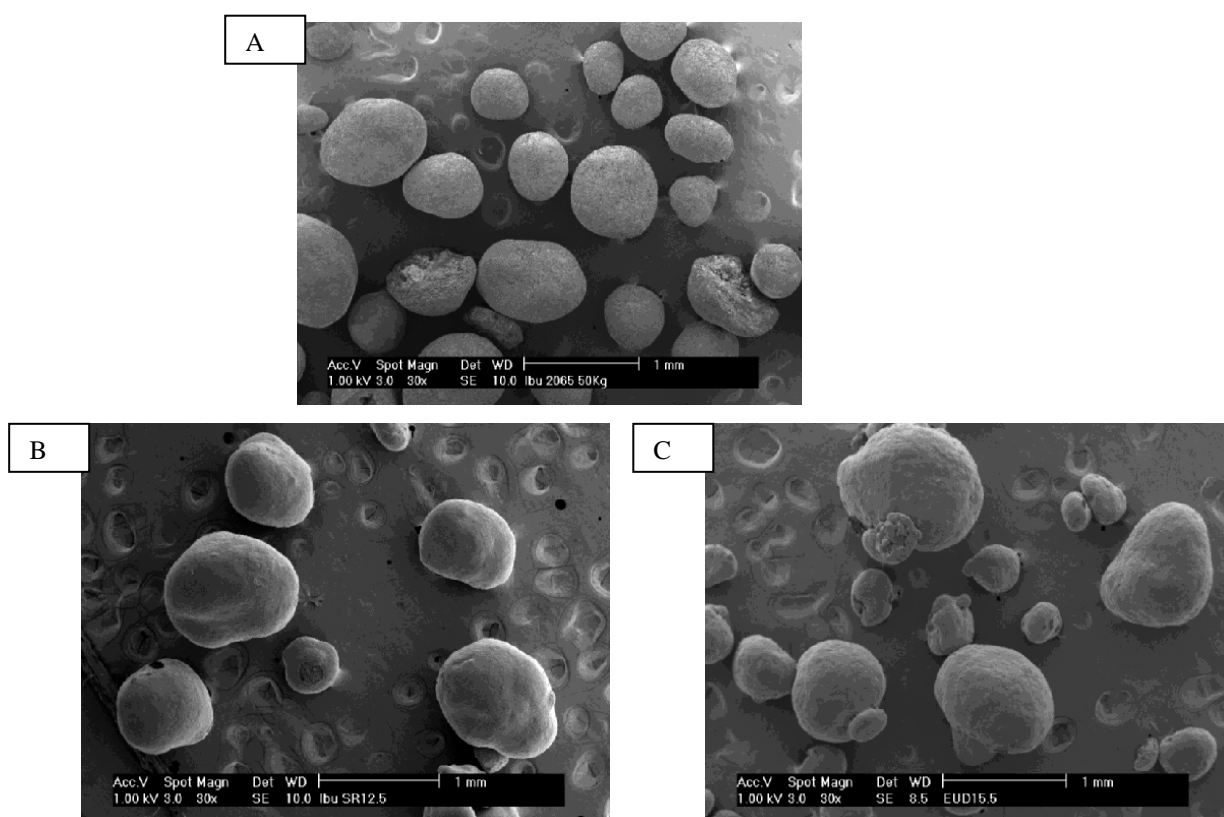


Figure 47: Scanning electron micrographs (30x) of ibuprofen granules (65 % drug load).

Uncoated ibuprofen (A); Surelease® 12.5% (B); Eudragit® NE 30D 15.5% (C).

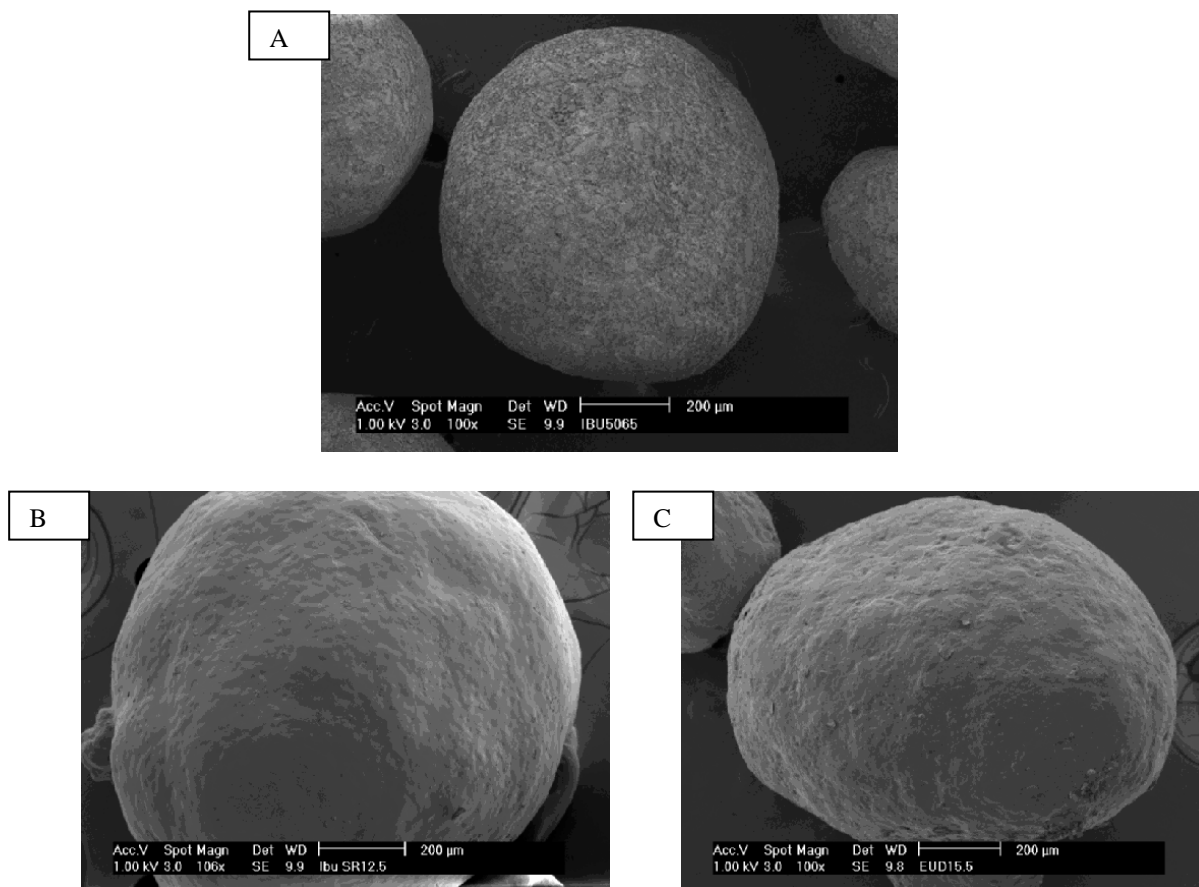


Figure 48: Scanning electron micrographs (100x) of ibuprofen granules (65 % drug load).

Uncoated ibuprofen (A); Surelease® 12.5% (B); Eudragit® NE 30D 15.5% (C).

ii. Yield and usable fractions of spheroids

The yield of the formulations ranged from $82.36 \pm 0.53\%$ – $98.05 \pm 1.47\%$ with the usable fractions (250 - 850 µm) ranging between $68 \pm 2.83\%$ – $83 \pm 2.82\%$ respectively (Table XXIX). The percent yield of the batches coated with Surelease® was greater than that of the Eudragit® batches. The percent yield was calculated based on the ratio of the product output to the total weight of solids present in the fluid-bed. This, as referred to earlier could be due to talc sedimentation in the tubing. This observation was

TABLE XXIX. Physical Characteristics of Coated Ibuprofen Spheroids (Means of replicated batches)

Polymer type		Surelease			Eudragit		
% Coating level	0 (Uncoated)	7.5	10	12.5	12.5	14	15.5
Physical characteristics							
% Yield	91.38 ± 0.76	93.35 ± 2.35	98.05 ± 1.47	96.76 ± 0.54	82.36 ± 0.53	88.31 ± 4.76	90.76 ± 2.81
% LOD	1.74 ± 0.35	0.66 ± .21	0.76 ± 0.21	0.81 ± 0.14	0.87 ± 0.007	1.25 ± 0.19	1.29 ± 0.28
% Drug content	102.09 ± 0.06	108.22 ± 0.25	107.57 ± 0.55	109.02 ± 1.34	106.41 ± 1.28	105.95 ± 1.13	105.43 ± 2.47
Geometric mean diameter (µm)	538.00 ± 1.95	643 ± 0.04	680 ± 0.06	685 ± 0.05	725 ± 0.00	670 ± 0.01	669 ± 0.02
Sphericity	0.91 ± 0.01	0.85 ± 0.026	0.86 ± 0.05	0.87 ± 0.01	0.86 ± 0.01	0.88 ± 0.01	0.88 ± 0.01
Flowability (deg)	20.84 ± 0.46	21.06 ± 0.35	22.78 ± 0.00	23.75 ± 0.00	26.57 ± 0.00	28.73 ± 0.12	29.47 ± 0.30
True density g/cm ³)	1.22 ± 0.00	1.14 ± 0.01	1.12 ± 0.02	1.11 ± 0.01	1.19 ± 0.00	1.12 ± 0.01	1.15 ± 0.01
Bulk density g/cm ³)	0.68 ± 0.01	0.63 ± 0.01	0.62 ± 0.02	0.63 ± 0.01	0.60 ± 0.00	0.57 ± 0.00	0.60 ± 0.00
T50 (min)	< 15	45 ± 7.07	75 ± 21.21	105 ± 21.21	60 ± 0	105 ± 21.21	100 ± 14.14
Friability (%)	0.00 ± 0.00	0.33 ± 0.00	0.34 ± 0.47	0.17 ± 0.23	0.17 ± 0.23	0.33 ± 0.00	0.33 ± 0.00
Usable fraction (%)	73.75 ± 2.19	80.00 ± 0.00	86.00 ± 2.82	83.00 ± 4.24	68.00 ± 2.83	81.00 ± 1.41	80.00 ± 0.00

TABLE XXX: P-values of Independent Variables of Coated Ibuprofen Spheroids

Dependent variables	Independent variables			Interactions (PT*PL)
Physical characteristics	Replication (2x)	Polymer type (PT) [Surelease [®] , Eudragit [®]]	Polymer level (PL) [Low, Medium, High]	
	1	2	3	2 * 3
Yield	NS	S (0.0016)	S (0.0370)	NS
Drug content	NS	S (0.0269)	NS	NS
LOD	NS	S (0.0248)	NS	NS
t ₅₀	NS	NS	S (0.0165)	NS
Geometric mean diameter	NS	NS	NS	NS
True density	NS	S (0.0008)	S (0.0072)	NS
Bulk density	NS	S (0.0013)	S (0.0462)	NS
Carr's index	NS	NS	NS	NS
Flowability	NS	S (<.0001)	S (<.0001)	NS
Friability	NS	NS	NS	NS
Sphericity	NS	NS	NS	NS
Usable fraction	NS	S (0.0083)	S (0.0071)	NS

confirmed with the fact that within the batches coated with Eudragit[®], the percent yield increased with the theoretical coating level and increased solid content. The talc effect would be more pronounced on the batches coated with the lower polymer level as any effect on the ratios (used for yield calculation) would have greater effect on the lower polymer level.

The usable fractions were mostly < 85% of the product output. This could be attributed to some amount of agglomeration that led to increased particle size. However, values as lower than this have been reported acceptable usable fraction in literature (9).

iii. Drug content

The drug content ranged between $105 \pm 1.13\%$ – $109 \pm 1.34\%$. Although these are greater than 100%, they fell within the USP recommended range for drug content. Additionally, standard solution analyzed with these samples (without the extraction process) also gave a drug content greater than 100%. The results could be due to some random analytical errors.

iv. Friability

During coating, pellets are subjected to appreciable frictional forces, thus friable pellets generate significant amount of fines, which can mix with the coating solution and affect the topography of the coated pellets. The pellets to be coated must therefore withstand the vigorous agitation that occurs in the coating chamber. As shown in Table XXIX, the percentage weight loss from the uncoated ibuprofen formulation used for coating was zero, indicating its suitability for the coating processes. The percentage

weight losses from all the coated formulations were also less than 2%. These formulations are therefore suitable for the hard gelatin encapsulation process that will be subsequently performed.

v. Densities

Coating with both polymers decreased both the bulk and true densities (Table XXIX). This could be attributed to increased pellet sizes due to coating. There were generally no significant difference between the densities of pellets coated with the same polymer, except with the batch coated with 14% Eudragit[®]. The inconsistencies observed with this polymer could be due to the presence of talc as has already been explained, that made it difficult to calculate the actual amount of polymer in the batches. This inconsistency was also made obvious with the release pattern observed with these Eudragit[®] batches, as will be shown below.

It was not possible to calculate the tapped density of the batches because the volume of most of the formulations increased with successive taps, thus making the tapped density higher than the bulk density. This phenomenon was not problematic for future (encapsulation) study as it has been reported that the bulk and not the tapped density is used to calculate the fill weight for pellets. Consequently, the compressibility index could also not be calculated.

vi. Flowability

The flowability of the products fell within the generally acceptable flowability criterion ($\theta < 30^\circ$). However, flowability decreased with increased polymer level.

Considering the batches coated with Surelease[®], the flowability trend could be due to increased diameter of the pellets that retarded flow properties, while the reduced flow within the Eudragit[®] batches could be due to increased tackiness with increased polymer caused by the absence of the sedimented talc in the products. This tackiness must have led to the difference in the flowability between the two polymer types that resulted in high significant level observed from this variable with both polymer type ($p < 0.0001$) and level ($p < 0.0001$). It could therefore be better to add the talc directly to the fluid-bed instead of dissolving it in the coating solution.

vii. Sphericity of the granules

The sphericity of both the coated and uncoated spheroids fell within our set acceptance criteria (≥ 0.85 ; Table XXIX). No significant difference was observed between the results obtained from these analyses. However, the pellets coated with Surelease[®] appeared to be better spheres visually.

viii. Size distribution of granules

The geometric mean diameters of the microparticulates ranged from $643 \pm 0.04 \mu\text{m}$ - $725 \pm 0.00 \mu\text{m}$ (Table XXIX; Figure 49). As expected, all the coated batches were larger than the uncoated formulation, confirming an increased diameter of the pellets due to the coating levels. Within the batches coated with Surelease[®], there was slight but statistically insignificant increase in diameter as the coating level increased. This indicated the consistency of this coating material. With the batches coated using Eudragit[®] polymer, a discrepancy in the geometric diameter was observed. The batch

with the theoretical lowest polymer level was larger than the batches coated with higher polymer levels. Most of these pellets appeared to be agglomerated.

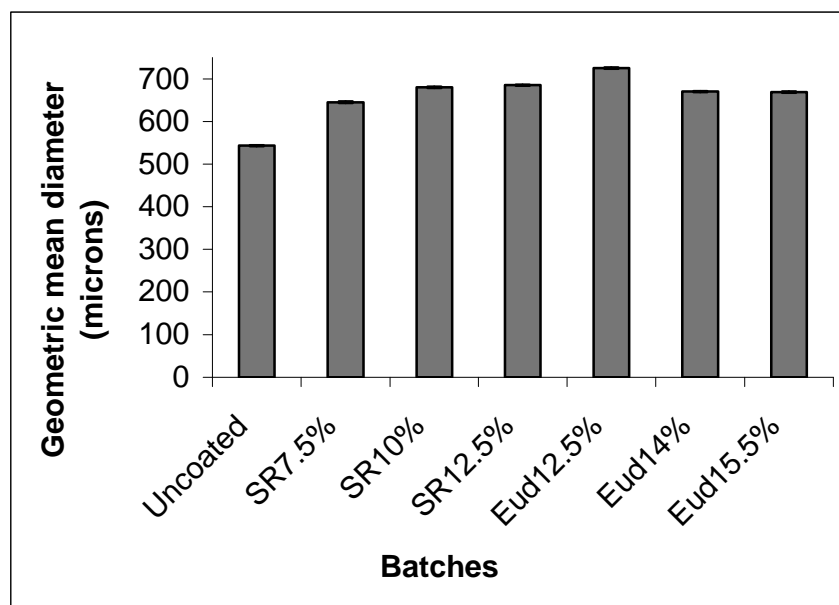


Figure 49: Geometric mean diameters of uncoated and coated ibuprofen pellets.

ix. Ibuprofen release from pellets

The uncoated formulation released 50% (T_{50}) of its drug content within 15 min. On the contrary, the release rates of the coated formulations were retarded (Table XXIX and Figure 50). The T_{50} of the replicate batches of these coated formulations ranged between 45 ± 7.07 min - 105 ± 21.21 min, depending on the coating level.

Several factors affected the release rate of modified release formulations (175,176,262). These include the type of equipment used for coating, the porosity of the products, surface area, type of dissolution medium, coating level, physical characteristics of the model drug, etc. In the case of pellets, type of spheronization technique and pellet

sizes have been reported as among the major factors affecting their release characteristics. Potter *et al.* (263), showed that at the same coating level using Surelease[®], the T_{50} of chlorpheniramine pellets was 40 min (500 – 600 μm), 3 hrs (850 – 1000 μm) and 5 hrs (1000 – 1400 μm). The mean diameter of our pellets was between 642 – 725 μm (Figure 49), with the mode value lying generally at 425 μm . Pellet size could therefore explain the results obtained from our dissolution analysis.

As shown in Figure 50, the release rates of the formulations decreased as the coating levels increased. This observation was more consistent with the batches coated

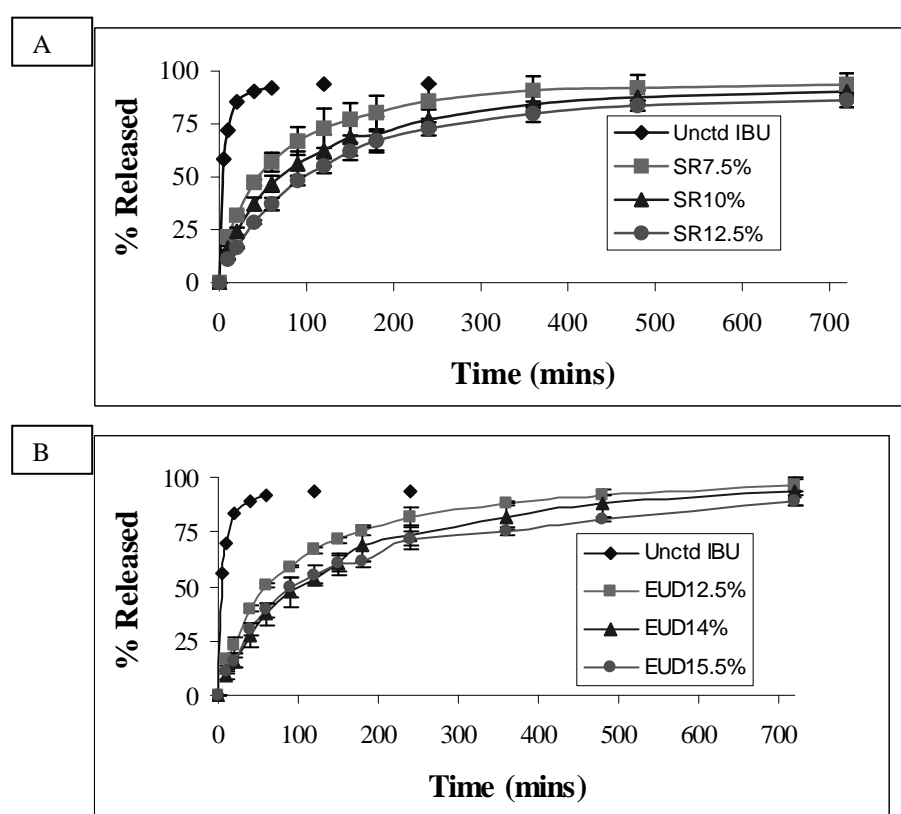


Figure 50. Dissolution profiles of ibuprofen pellets. Uncoated pellet and pellets coated with Surelease[®] polymer (Panel A), Uncoated pellet and pellets coated with Eudragit[®] polymer (Panel B).

with Surelease[®] polymer. The batches coated with 14% and 15.5% Eudragit[®] released equivalent amount of drugs till 60% of their contents were released, consistent with the discrepancy that has been observed in the product qualities of these batches. However, at the highest polymer coating level for both polymers, a prolonged release was observed generally.

x. Kinetics of drug release

Kinetically, the decreased drug release observed with increased polymer levels is due to simultaneous increase in coating thickness and length of diffusion pathway (175,188). These confirmed that the coating process was successfully achieved. With uncoated pellets as well as at low coating levels, pores exist at the pellet surface or at pellet-coating interface of the latter due to the coating imperfections achieved at these levels. Drugs readily diffuse through these pores, thus the cumulative drug release in this case is linear with the square root of time (Equation 7). The pores are sealed as coating levels increase so that drug is released through an intact membrane and consequently follow the zero order release kinetics (Equation 12). The transition point where drug release is defined by the zero order kinetics is called the critical coating level. Drug release has also been shown to follow first order kinetics (Equation 28). Our data were therefore fitted to these equations, to Peppas empirical equation (Equation 9) and to a recently proposed combined mechanistic kinetics (Equation 15; 177). The Peppas equation constant incorporates the structural and geometric characteristics of the release device (264). The combined mechanistic equation constants incorporate the Higuchi and

zero-order release kinetics. The results of these studies are shown in Figures 51, 52 and Table XXXI.

$$Q = kt^{\frac{1}{2}} \quad \text{Eqn. 7}$$

$$\log (Mt / M) = \log k + n \log t \quad \text{Eqn. 9}$$

$$F = \frac{DKCsA}{L} \quad \text{Eqn. 12}$$

$$Q = Kt^{\frac{1}{2}} + \frac{DKCs}{L}t \quad \text{Eqn. 15}$$

$$\ln (100 - Q) = \ln Q_0 - k_1 t \quad \text{Eqn. 28}$$

Uncoated pellets: Drug release from uncoated beads can be described by the pore controlled release model, and mathematically by the square root equation (Equation 7). Figure 51 shows plots of cumulative percent drug release vs. square root of time of all the formulations. Table XXXI shows the results of the parameters of the drug release equations. The best correlation coefficients were achieved with the combined mechanistic and Higuchi equations. However, the release rate of uncoated formulation depicted by the Higuchi constant (k_H) shows a high linear release constant compared to the coated pellets. These indicate that the uncoated pellets follow an inner matrix (Higuchi) release model.

Coated pellets: As previously discussed, Surelease[®] and Eudragit[®] polymers form water permeable but insoluble polymeric membranes that allow controlled

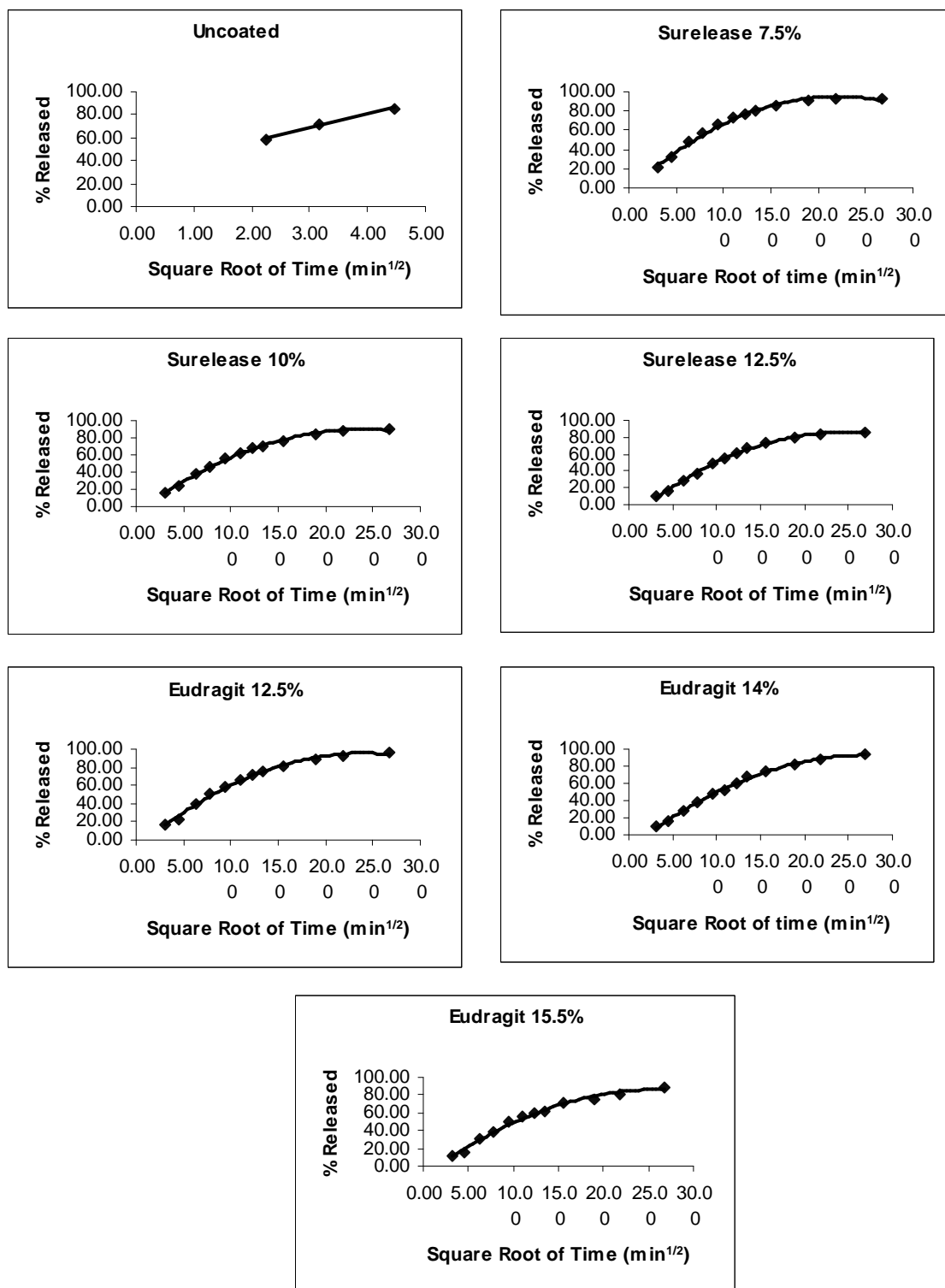


Figure 51. Mathematically modeled drug release of uncoated and coated ibuprofen pellets

Table XXXI. Results of Regression Equations for Drug Release from Uncoated and Coated Pellets According to Equations 7, 12, 28, 15, and 9 Respectively.

Formulations	Kinetic models					
	Higuchi equation		Zero order		First order	
	R ²	k _H	R ²	k ₀	R ²	k ₁
Uncoated	0.9543	19.491	0.7445	3.7974	0.9358	0.0395
SR 7.5%	0.9639	5.6918	0.7977	0.3163	0.9545	0.0034
SR 10%	0.9815	5.2065	0.8473	0.2955	0.9553	0.0026
SR 12.5%	0.9899	5.1117	0.908	0.2991	0.9794	0.0024
EUD 12.5%	0.9796	5.6065	0.8494	0.319	0.9698	0.003
EUD 14%	0.9892	5.1572	0.9183	0.3036	0.9833	0.0024
EUD 15.5%	0.9821	4.9152	0.8811	0.2844	0.9609	0.0022

Formulations	Kinetic models					
	Combined mechanistic equation			Peppas equation		
	R ²	k ₀	k _H	R ²	k _p	n
Uncoated	0.9997	3.03	32.55	0.8594	0.2303	1.5443
SR 7.5%	0.9959	0.23	9.27	0.9041	0.304	0.7648
SR 10%	0.9938	0.13	7.22	0.935	0.2428	0.7578
SR 12.5%	0.99	0.01	5.28	0.9758	0.1431	0.7722
EUD 12.5%	0.9904	0.13	7.63	0.9414	0.2313	0.7746
EUD 14%	0.9893	0.01	4.96	0.9828	0.1153	0.7812
EUD 15.5%	0.9843	0.05	5.72	0.9708	0.1477	0.7677

release of the model drug. Drug release from such systems can either be dissolution-controlled (Equation 7), membrane-controlled (Equation 12) or a combination of both processes (Equation 15), depending on the coating levels (265,266). As shown in the scanning electron micrographs in Figures 47 & 48, the uncoated pellets used for coating have pores. If all the pores of the core ibuprofen pellets are blocked by permeable coating membranes of the polymers, the coating is complete, and the drug release is controlled by

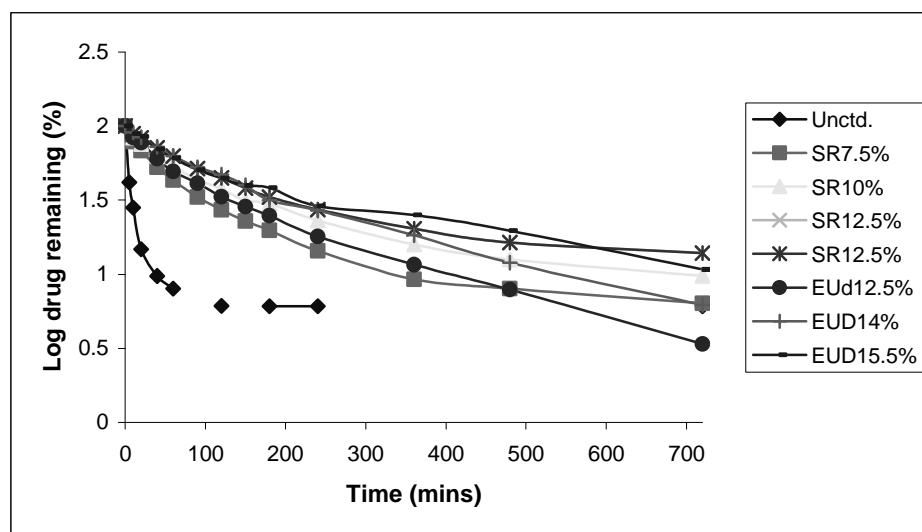


Figure 52: First order release profiles from uncoated (Unctd) and coated ibuprofen pellets

the coating film. The release rate will depend on the polymer film/dissolution medium partition coefficient and zero order kinetics will be followed. Table XXXI shows that the highest correlation coefficient was achieved with the combined mechanistic and Higuchi equations. The correlation coefficients obtained with the first order kinetics appeared to be better than those of the zero order kinetics. However, the n values from the Peppas equation were > 0.75 for all the coated formulations, an inclination towards the zero order release mechanism. These results, together with the first order plot shown in Figure 52 exclude first order kinetics from the release mechanism of the coated pellets.

Figure 51 also shows that although good correlation was obtained with the coated pellets for the Higuchi model, the coated pellets did not follow pure Higuchi mechanism. Therefore, the kinetics of drug release from these coated pellets follows either a complex system or a combination of square root of time and zero-order kinetics (Equation 15). Thus, a non-Fickian diffusion through the polymer films ($0.5 < n < 1$) was followed.

xi. Comparison of in vitro dissolution profiles using difference and similarity factors

Drug release decreased as polymer levels increased. Table XXXII lists some time points and (their respective) percentage dissolution of both the uncoated and coated pellet formulations. Table XXX shows the *p-values* of some of the product qualities. The time taken for both 50% ($p = 0.0165$) and 80% dissolutions (T_{50} and T_{80} respectively) varied for the different formulations, and were significantly affected by the coating levels. Results from difference and similarity factors calculations (Table XXXIII) showed that the profile of the uncoated pellets was different from those of all the coated pellets ($f_1 > 15$ and $f_2 < 50$). These indicated that the release was dependent on the coating level.

TABLE XXXII: Mean Percent Dissolution of Ibuprofen Spheroids at the Specified Time Points

	Time (min)	10	20	60	120	240	480
Batches		Mean percent dissolution \pm SD					
Uncoated		75.32 \pm 1.22	87.43 \pm 0.03	92.36 \pm 0.28	93.63 \pm 0.52	93.90 \pm 0.46	93.90 \pm 0.20
Surelease [®] 7.5%		21.55 \pm 0.66	31.8 \pm 0.35	56.94 \pm 4.43	72.91 \pm 9.25	85.61 \pm 8.3	92 \pm 6.16
Surelease [®] 10%		16.36 \pm 0.94	24.19 \pm 1.78	46.82 \pm 3.76	62.41 \pm 7.56	76.98 \pm 4.72	87.47 \pm 3.38
Surelease [®] 12.5%		11.00 \pm 0.35	16.56 \pm 0.4	37.23 \pm 2.96	55.24 \pm 3.44	72.66 \pm 3.09	83.63 \pm 2.41
Eudragit [®] 12.5%		16.26 \pm 2.37	22.91 \pm 4.07	50.62 \pm 0.98	66.69 \pm 1.25	82.06 \pm 4.21	92.09 \pm 0.01
Eudragit [®] 14%		9.42 \pm 1.80	15.76 \pm 3.11	37.3 \pm 5.16	53.00 \pm 2.77	73.13 \pm 4.10	88.04 \pm 6.14
Eudragit [®] 15.5%		11.18 \pm 0.93	15.28 \pm 2.35	39.05 \pm 3.35	55.44 \pm 3.97	71.12 \pm 4.26	80.39 \pm 0.90

TABLE XXXIII: Values of Difference and Similarity Factors (f_1 and f_2 respectively) for Uncoated and Coated Pellets

Reference formulation	Test formulation	F_1 value	F_2 value
Uncoated	Surelease [®] 7.5%	32.04	23.10
Uncoated	Surelease [®] 10%	40.81	19.25
Uncoated	Surelease [®] 12.5%	47.95	16.2
Surelease [®] 7.5%	Surelease [®] 10%	12.91	54.44
Surelease [®] 7.5%	Surelease [®] 12.5%	23.42	41.71
Surelease [®] 10%	Surelease [®] 12.5%	12.06	58.68
Uncoated	Eudragit [®] 12.5%	37.72	19.9
Uncoated	Eudragit [®] 14%	47.89	15.89
Uncoated	Eudragit [®] 15.5%	48.68	16.13
Eudragit [®] 12.5%	Eudragit [®] 14%	16.33	50.65
Eudragit [®] 12.5%	Eudragit [®] 15.5%	17.59	49.87
Eudragit [®] 14%	Eudragit [®] 15.5%	1.51	71.75

For the pellets coated with Surelease[®], the f_2 values indicate that the batch coated with 7.5% was similar ($f_2 > 50$) to the profile of 10% coating level batch, but was significantly different ($f_2 < 50$) from the pellets coated with 12.5% polymer. The same trend of f_2 values was obtained from the batches coated with Eudragit[®], although to a very limited level. The f_2 values indicated that the batch coated with 12.5% polymer level was not significantly different from those coated with 14% ($f_2 = 50.65$) and was slightly different ($f_2 = 49.87$) from the batch coated with 15.5% polymer. However, the results of the 15.5% coating level showed some discrepancies, as already observed from other product variables.

Generally, f_1 values confirmed the results of the f_2 factor. However, the results of comparisons between Eudragit[®] 12.5% and 14% and Eudragit[®] 12.5% and 15% appeared

to be on a borderline. Thus, the more generally accepted results from f_2 factor were considered more conclusive in these cases. The batch coated with 12.5% Surelease[®] was therefore chosen to study the effects of encapsulation on the uncoated and coated spheroids.

b. Effect of Encapsulation on the Characteristics of Ibuprofen Microparticulates

1. Experimental design and Physical characteristics of pellets

A major objective of encapsulated formulations is to ensure that each capsule provides the expected dose of drug and that the drug should be released from the capsule to ascertain its bioavailability. Tables XXXIV and XXXV show the respective results of the effects of encapsulation on pellet qualities and the *p-values* of the independent variables obtained from the statistically analyzed factorial design.

i. Formulation type

Fill weight: Formulation type significantly ($p < 0.05$) affected the average fill weight of the pellets (Figure 53). As has been previously reported by other authors, this could be due to the effects of factors, e.g. flowability of the pellets (224,225,228). Based on the results of the angle of repose of the pellets before encapsulation, (Table XXIX), the uncoated pellets ($\theta = 19.29^\circ$) were more flowable than the coated pellets ($\theta = 23.75^\circ$), and consequently resulted in higher fill weights within the experimentally specified time (Table XXXIV). Studentized residuals test statistic showed some likely pattern, however, based on Dubin-Watson there was no correlation between the observations ($p < 0.05$). The result causing the observed pattern could therefore be an outlier.

TABLE XXXIV: Effects of Encapsulation Variables on Uncoated and Coated Ibuprofen Spheroids

Operational speed (rpm)	Shuttle speed (msecs)	Uncoated					Coated				
		Average fill weight (mg)	SD	%CV	Drug content (mg)	~ T ₅₀ (mins)	Average fill weight (mg)	SD	%CV	Drug content (mg)	~ T ₅₀ (mins)
	260	517.03	16.95	3.28	-	-	467.8	14.97	3.2	-	-
75	280	528.2	8.87	1.68	358.47	7	463.15	12.92	2.79	292.25	90
	300	528.35	7.24	1.37	363.24	6	483.2	10.78	2.23	302.65	120
	260	511.51	10.22	2	-	-	460.7	18.48	4.01	-	-
85	280	503.91	16.58	3.29	-	-	470.33	18.32	3.89	-	-
	300	487.24	26.8	5.51	-	-	471.58	11.63	2.47	-	-
Unencapsulated		528.35			352.23	5	483.2			300.68	120

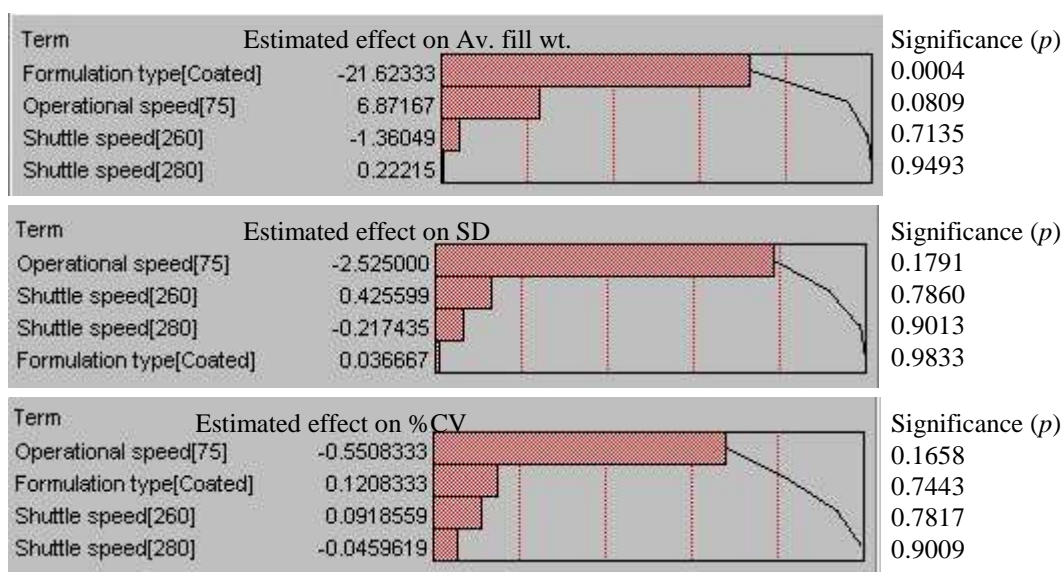


Figure 53. Pareto plots of effects of main factors on the specified product qualities

TABLE XXXV: *P*-values of Independent Variables of Encapsulated and Unencapsulated (Uncoated and Coated) Ibuprofen Spheroids

Dependent variables	Independent variables		
<i>Physical characteristics</i>	<i>Formulation type</i>	<i>Operational speed</i>	<i>Shuttle speed</i>
Average Fill weight	S (0.0004)	NS	NS
SD	NS	NS	NS
%CV	NS	NS	NS

Standard deviation and coefficient of fill weight variation: The more flowable uncoated pellets resulted in lower standard deviations and consequently in lower fill weight variations. The bar diagram presented in Figure 54 shows that with the two formulation types (uncoated and coated), the SD and %CV were generally lower for the uncoated than with the coated pellets. The highest variability was however observed with the uncoated pellets encapsulated at the highest operational and shuttle speeds. This result

could be due to some interactions between the flowability of the pellets and these different factors. There was no pattern observed with this variable and autocorrelation result was also not significant ($p > 0.05$).

ii. Operational speed

Although the operational speed was observed to be statistically insignificant ($p > 0.05$), Table XXXIV shows that within each formulation type at different operational speeds, the average fill weight was slightly higher for the lower speed than the higher speed. Figure 53 also shows that the lower speed (75 rpm) contributed more to the operational speed effect than the higher speed (85 rpm). This implied that for formulations of similar flowability, a certain amount of speed is required for machine operation as to achieve a desirable fill weight for the capsules.

As can be seen from the Pareto plots (Figure 53) and Table XXXIV, the operational speed had more effect on the standard deviation and consequently on the coefficient of fill variation than the other factors. Although these results were observed to be statistically insignificant ($p > 0.05$), they were similar to those obtained previously in literature with tamp filling machines using powders (216). Higher speeds generally led to higher SD and %CV. This could be because with high operational speed, there was insufficient time to achieve consistent fill weight and reproducibility, thereby introducing more filling errors. There was no pattern observed with this variable and autocorrelation result was also not significant ($p > 0.05$).

iii. Shuttle speed

The results obtained with the shuttle speed (which regulates how long the feeder assembly stays open to fill the capsules) varied for each formulation type. For the uncoated pellets with very good flow properties, there was no difference between fill weight at the medium and highest shuttle speeds. This indicated that 280 msec was sufficient for maximum fill weight of this formulation (Figure 5). For the coated batches, the highest fill weight was also obtained at the lowest operational speed. However, higher shuttle speed (300 msec) was required to achieve higher fill weights compared to those obtained with the lower shuttle speeds (260 and 280 msec). These results were as expected because higher shuttle speed allows more time for the capsule feeder to obtain

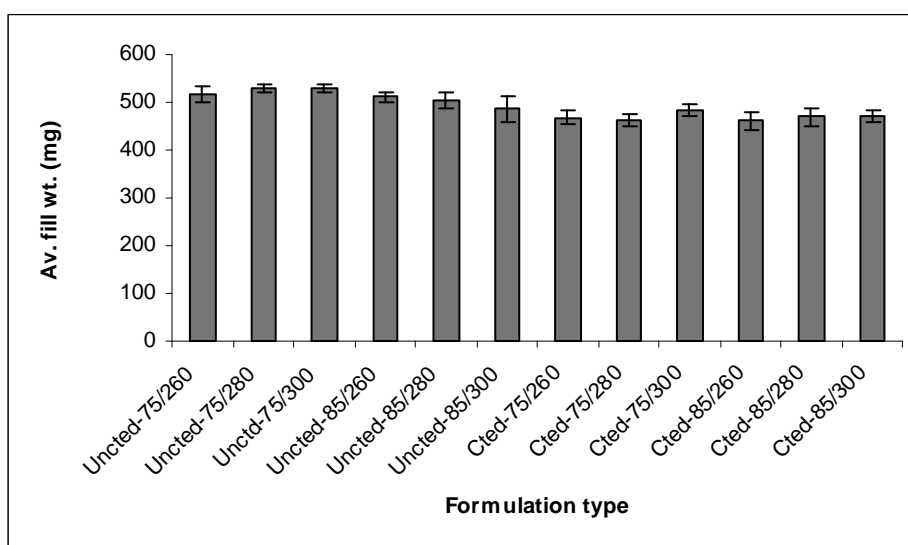


Figure 54. Average fill weight (\pm SD) of ibuprofen pellets at different shuttle sizes and operational speeds.

Uncted: Uncoated pellets; Cted: Coated pellets

75, 85: Operational speeds, 75 rpm and 85 rpm

260, 280, 300: Shuttle speeds, 260 msec, 280 msec, 300 msec.

more pellets that will be fed into the capsules. The results obtained with the high shuttle speed at high operational speed might therefore be due to possible interactions between the product qualities, e.g. flowability, and these different factors.

Apart from the uncoated formulation filled at high operational (85 rpm) and shuttle (300 msec) speeds, the SD and %CV decreased as shuttle speed increased (Table XXXIV). A possible explanation to this has been given above, i.e. there was enough time for sufficient pellets to fill the gelatin capsules, leading to filling consistency and reproducibility. This could lead to reduced variability in the capsule fill weight. These observations shown in Figures 54 and 55, were however statistically insignificant ($p > 0.05$).

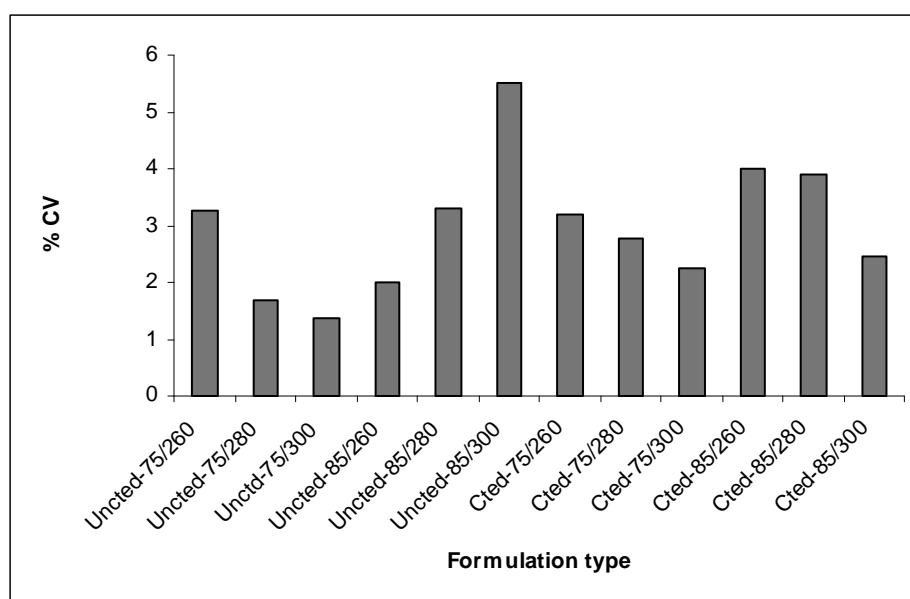


Figure 55. %CVs of the fill weight of ibuprofen pellets at different shuttle sizes and operational speeds.

Uncted: Uncoated pellets; Cted: Coated pellets

75, 85: Operational speeds, 75 rpm and 85 rpm

260, 280, 300: Shuttle speeds, 260 msec, 280 msec, 300 msec.

In summary, formulation type had significant effect on the average capsule fill weight. Within similar formulation types, high operational speed generally led to increased SD and CV. Additionally, with the two formulation types and using the lower speed (75 rpm), high shuttle speed resulted in higher fill weight, lower SD and consequently to reduced %CV. The formulations encapsulated at low operational speed (75 rpm) and at the medium (280 msec) and high (300 msec) shuttle speeds were therefore selected to study the content uniformity and release profiles of the encapsulated pellets.

iv. Drug content

The drug content was calculated as the amount of drug / capsule content used for the dissolution experiments. Table XXXIV shows that the drug content was directly related to the fill weight of the capsules, with the drug content of the uncoated pellets being higher than that of the coated pellets per capsule. These results confirm the reproducibility of the processes involved in the spheronization and encapsulation steps.

v. Ibuprofen release from granules

The percent drug release was normalized for drug content. The uncoated formulations (encapsulated and unencapsulated) consistently released more than 80% of the drug within 20 min. As was observed before encapsulation, the T_{50} of the coated formulation was ~ 120 min. The T_{50} of the pellets encapsulated at 300 msec was higher than that encapsulated at 280 msec, although the former had more ibuprofen content. Although the gelatin capsules dissolved within 5 min of the dissolution analysis, the

pellets remained undispersed throughout the analytical period. Thus, the release of the capsules containing higher amount of pellets might have been retarded by the higher packing of the content (Table XXIV and Figure 56).

Figure 56 also show that while the uncoated pellets released almost all their drug contents within 40 min, the coated pellets sustained ibuprofen release up to 12 hr. This confirmed that encapsulation had no undesirable effect on the formulated ibuprofen microparticulates.

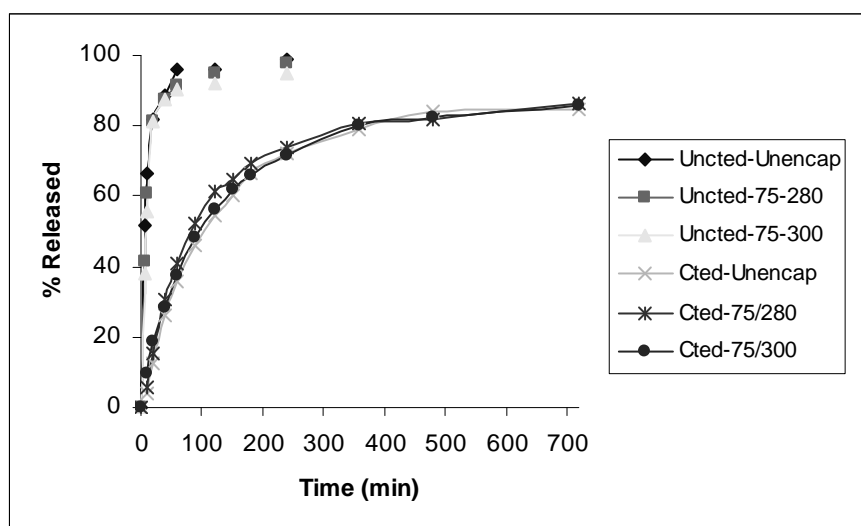


Figure 56. Dissolution profiles of encapsulated and unencapsulated (uncoated and coated) ibuprofen spheroids.

Uncted: Uncoated pellets;

Cted: Coated pellets;

Unencap: Unencapsulated pellets

75, 85: Operational speeds; 75 rpm and 85 rpm;

280, 300: Shuttle speeds; 280 msecs, 300 msecs.

vi. Drug release kinetics

The release mechanism also showed similar results with the unencapsulated pellets (Table XXXVI). However, encapsulation of the uncoated pellets, especially at 75 rpm and 300 msec yielded higher correlation coefficients. The Higuchi release constant was however comparatively unaffected. It is possible that smoother release profile was achieved by adding the encapsulated pellets in the dissolution baskets, than by pouring

Table XXXVI. Results of Regression Equations for Drug Release from Encapsulated and Unencapsulated (Uncoated and Coated) Pellets According to Equations Equations 7, 12, 28, 15, and 9 Respectively.

Formulations	Kinetic models					
	Higuchi equation		Zero order		First order	
	R ²	k _H	R ²	k _o	R ²	k ₁
Uncted-Unencap	0.9543	19.491	0.7445	3.7974	0.9358	0.0395
Uncted-75/280	0.9981	18.402	0.8848	3.82	0.9925	0.0359
Uncted-75/300	0.9985	18.149	0.9255	3.85	0.0361	0.9975
Cted-Unencap	0.9899	5.1117	0.908	0.2991	0.9794	0.0024
Cted-75/280	0.9698	5.4677	0.8712	0.3166	0.9563	0.0026
Cted-75/300	0.9873	5.0532	0.8954	0.294	0.9697	0.0023

Formulations	Kinetic models					
	Combined mechanistic equation			Peppas equation		
	R ²	k _o	k _H	R ²	k _p	n
Uncted-Unencap	0.9997	3.03	32.55	0.8594	0.2303	1.5443
Uncted-75/280	0.999	0.3924	20.09	0.899	0.1878	1.5209
Uncted-75/300	1	0.4966	16.01	0.9103	0.1751	1.5128
Cted-Unencap	0.99	0.01	5.28	0.9758	0.1431	0.7722
Cted-75/280	0.9717	0.05	6.3212	0.9792	0.0451	0.8242
Cted-75/300	0.9882	0.03	5.5603	0.9755	0.1368	0.7753

them in the basket. For the coated pellets, encapsulation, especially at the same conditions (75 rpm, 300 msec) yielded results that were very similar to the unencapsulated spheroids. The n values of Peppas equation were also > 0.75 , thereby depicting a non-Fickian diffusion through the polymer film membrane.

vii. Comparison of in vitro dissolution profiles using difference and similarity factors

Table XXXVII shows some time points and (their respective) percentage dissolution of both the uncoated and coated, unencapsulated and encapsulated pellet formulations.

Results from difference and similarity factors calculations (Table XXXVIII) showed that the profiles of all the batches of each formulation type (uncoated and coated) were similar ($f_1 < 15$ and $f_2 > 50$). However, the profiles of all the uncoated pellets were different from those of all the coated pellets ($f_1 > 15$ and $f_2 < 50$). These show that the ibuprofen release profile depended on the formulation type (coated vs. uncoated). These results also confirmed that encapsulation did not alter the release properties of the pellets. Consequently, the encapsulated pellets could be used for immediate (uncoated) and controlled (coated) delivery of ibuprofen.

Using capsule size 0, the results showed that the highest fill weight and least variabilities were obtained in both coated and uncoated ibuprofen pellets with operational speed 75 rpm and shuttle speed 300 msec on the *K150i* (tamp filling) encapsulation machine. The encapsulation process did not affect the drug content and release profiles of the pellets (Table XXXIV and Figure 56). Under these conditions, about 530 mg of

TABLE XXXVII: Mean Percent Dissolution of Encapsulated and Unencapsulated (Uncoated and Coated) Ibuprofen Spheroids at the Specified Time Points

	Time (min)	10	20	60	120	240	480
Formulation type		Mean percent dissolution					
Uncoated-Unencapsulated		66.55	81.95	96.16	96.00	-	-
*Uncoated-75/280		60.89	81.41	91.49	94.72	-	-
*Uncoated-75/300		55.68	81.48	90.09	91.97	-	-
Coated-Unencapsulated		4.19	12.27	36.00	54.76	72.13	83.84
*Coated-75/280		5.92	15.11	40.97	61.11	73.93	81.61
*Coated-75/300		9.6	18.60	37.52	56.26	71.36	82.29

*: Encapsulated batches

75, 85: Operational speeds; 75 rpm and 85 rpm

280, 300: Shuttle speeds; 280 msec, 300 msec.

TABLE XXXVIII: Values of Difference and Similarity Factor (f_1 and f_2) for Encapsulated and Unencapsulated (Uncoated and Coated) Pellets

REFERENCE FORMULATION	TEST FORMULATION	F_1 VALUE	F_2 VALUE
1	2	3.57	74.68
1	3	6.29	63.22
1	4	68.53	15.75
1	5	63.86	17.11
2	3	2.83	78.7
2	5	62.52	18.32
2	6	64.85	17.80
3	5	61.43	19.18
3	6	61.79	19.32
4	5	5.87	70.56
4	6	4.73	71.49
5	6	1.08	72.69

Bold: The release profiles of reference and test formulations were different.

1. Uncoated and unencapsulated; 2. Uncoated and encapsulated at 75 rpm and 280 msecs
3. Uncoated and encapsulated at 75 rpm and 300 msecs; 4. Coated and unencapsulated
5. Coated and encapsulated at 85 rpm and 280 msecs
6. Coated and encapsulated at 85 rpm and 300 msecs

uncoated ibuprofen spheroids could be filled into this capsule size while about 485 mg coated pellets could be filled into the same capsule size (Table XXXIV). Based on the

results of the drug content, these pellet weights contained 365 and 302 mg ibuprofen respectively.

Thus, the following information could be deduced using the information in Figure 14: Uncoated pellets; capsule size “0”, 0.68 mL contained 365 mg ibuprofen/capsule, therefore, capsule size “00”, 0.95 mL could hold 510 mg ibuprofen/capsule theoretically. Coated pellets; capsule size “0” contained 302 mg ibuprofen/capsule, therefore, 420 mg ibuprofen could be encapsulated into the “00” size capsule.

It is expected that $\geq 25\%$ of the content of the coated pellets will be released within 15 min of delivery to achieve a therapeutic level for the drug. The use of microparticulate system would also facilitate dose adjustment by varying capsule sizes and fill weights without reformulating the product (9). It is also possible to mix coated and uncoated pellets at different levels. The initial burst effect will be achieved with drug release from the uncoated pellets, while sustained delivery will be maintained with the coated pellets (177).

IV. CONCLUSIONS

Phase 1

Ibuprofen spheres with good physical characteristics were developed using the rotor-disk fluid-bed technology, a one-step closed process that did not require additional unit processes. Based on plate radius and centrifugal force used as similarity factors for scale-up, the batch size and process could be scaled up to 5x and 10x. An attempt to simultaneously characterize spheronized ibuprofen granules, as well as process and batch scale-up was made. Consequently, further efforts were centered on experimental design for critical study of important process variables and formulation, on scale-up and coating for slow release properties.

Phase 2

Experimentally designed studies on different process and product variables, and based on our set acceptance criteria showed that the formulations spheronized using low binder level, high surfactant level, stainless steel smooth plate (Formulation 5) and also that produced with high binder level, low surfactant level, stainless steel smooth plate (Formulation 11) were most acceptable. The statistical design or approach also highlighted complexity and interplay of various variables in the outcome or predicted characteristics. It also showed the importance of rational approach in product development especially in multivariable unit process, as the case of rotor-disk fluid-bed operated. In consideration of the obtained data as well as previous reports (134,249,252,257) in which binder level had significant effect on most of the desirable

spheroid characteristics, with low binder level forming spheroids with low product quality, the conditions set in formulation 11 were used for further studies.

Phase 3

Using the optimized formulation to study some of the major formulation variables in rotor-disk fluid-bed technology, such as drug load, drug particle size and scale-up, our results showed that both particle sizes of ibuprofen are spheronizable at the different drug levels studied. Although the time and amount of binder required for the formulations decreased with increased drug concentration while spheroid size increased, there were generally no differences observed in the physical characteristics of equivalent load of both ibuprofen particles. The reduced surface area due to increased size slowed the rate of drug release with the highest drug load, while the low and medium sized drug loads showed very similar characteristics.

Intermediate size (50 kg) scale-up of the 65% drug load showed that, in contrast to the 1 kg batches, increased batch size reduced the effects of drug load on spheroid size and drug release, possibly due to an observed interaction between these two factors (batch size and drug load). Statistical analysis showed that true and bulk densities were significantly affected by both ibuprofen drug load and batch size, while replication did not alter the physical characteristics of both spheroid batch sizes, showing batch-to-batch reproducibility.

However, in future work, process parameters, e.g. rate of binder addition and end point for the binder addition will need to be optimized. These might solve the problem

encountered with spheronization processes using increased drug loads. From the results, it can be inferred that the rotor-disk spheronization process is scalable.

Phase 4

Coating of 0.7 kg batches of the scaled-up formulation showed that ibuprofen product characteristics, e.g. pellet size, drug release, bulk density, etc. depended on the coating levels. As previously reported, we observed slower release with increased coating level. This confirmed the successfulness of the coating process. The average fill weight of the encapsulated spheroids was mostly affected by the formulation types. Encapsulation of the microparticulates had no undesirable effect on the qualities of both formulation types. Therefore, the formulation has a lot of pharmaceutical market potentials (70).

We have statistically studied the effects of various formulation and product variables on the development of spheronized microparticulates using the rotor-disk fluid-bed technology. Our experience showed that a tighter spheroid fraction would be obtained if an in-process means of monitoring moisture content in the fluid-bed is introduced. This is because the moisture content is closely associated with the spheroid size and size distribution (44).

Although ibuprofen was used as the model drug, the process could be extended to other poorly water soluble drugs. Additionally, with careful manipulation of the variables and parameters studied in this work, the process could be applied to water soluble drugs as well. These will aid in the production of several pharmaceutical products with reduced cost e.g. amount of excipients and production time.

IV. APPENDIX

**This appendix consists of typical examples of raw data generated during
the study**

Figure 57. Log-Probability Profiles for Sieve Analysis of 1 kg Replicated Batches from Feasibility Studies

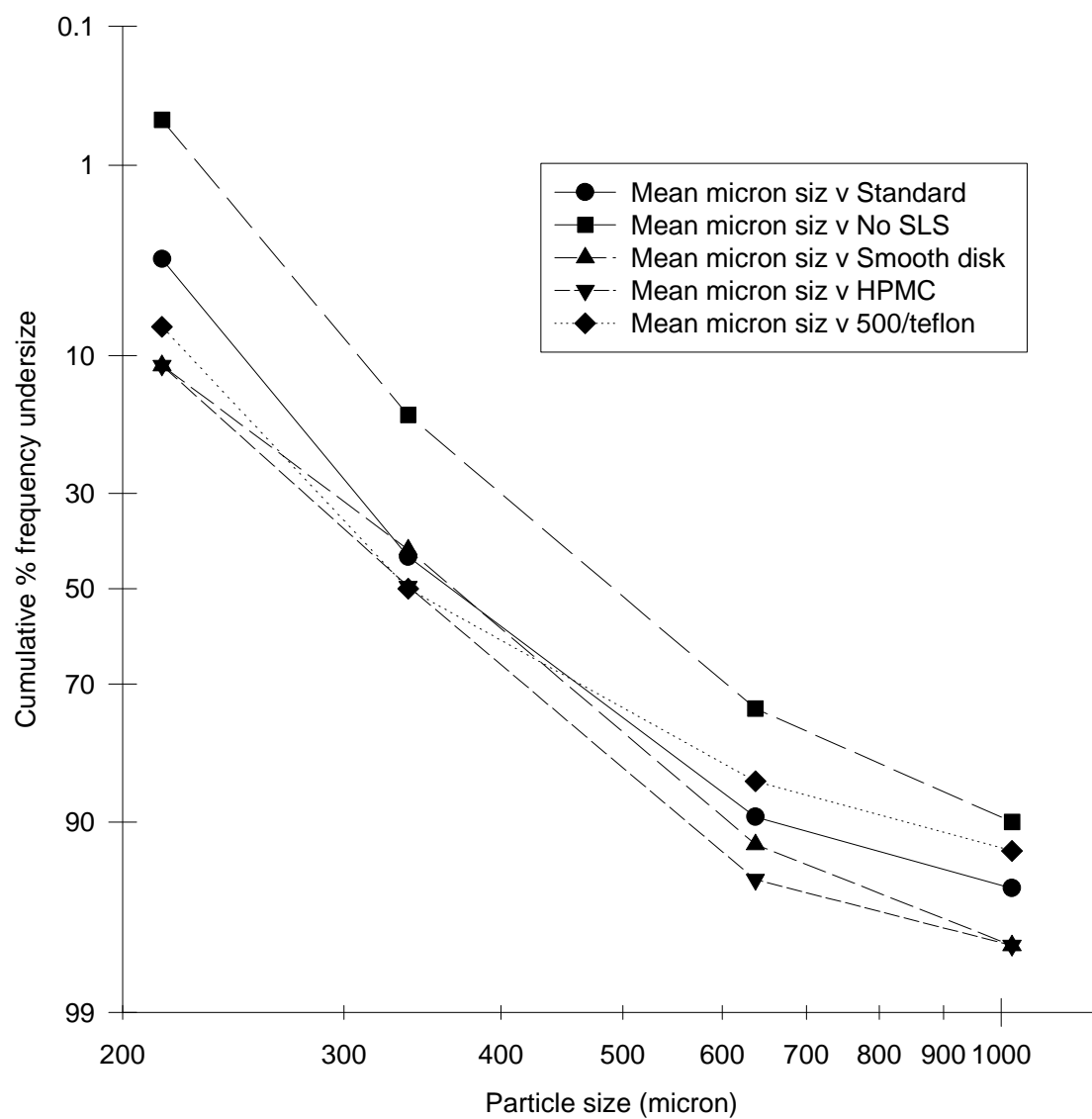


Figure 58. Log-Probability Profiles for Sieve Analysis of Pilot Size Scale-up

(1 kg, 5kg and 10 kg) Replicated Batches from Feasibility Studies

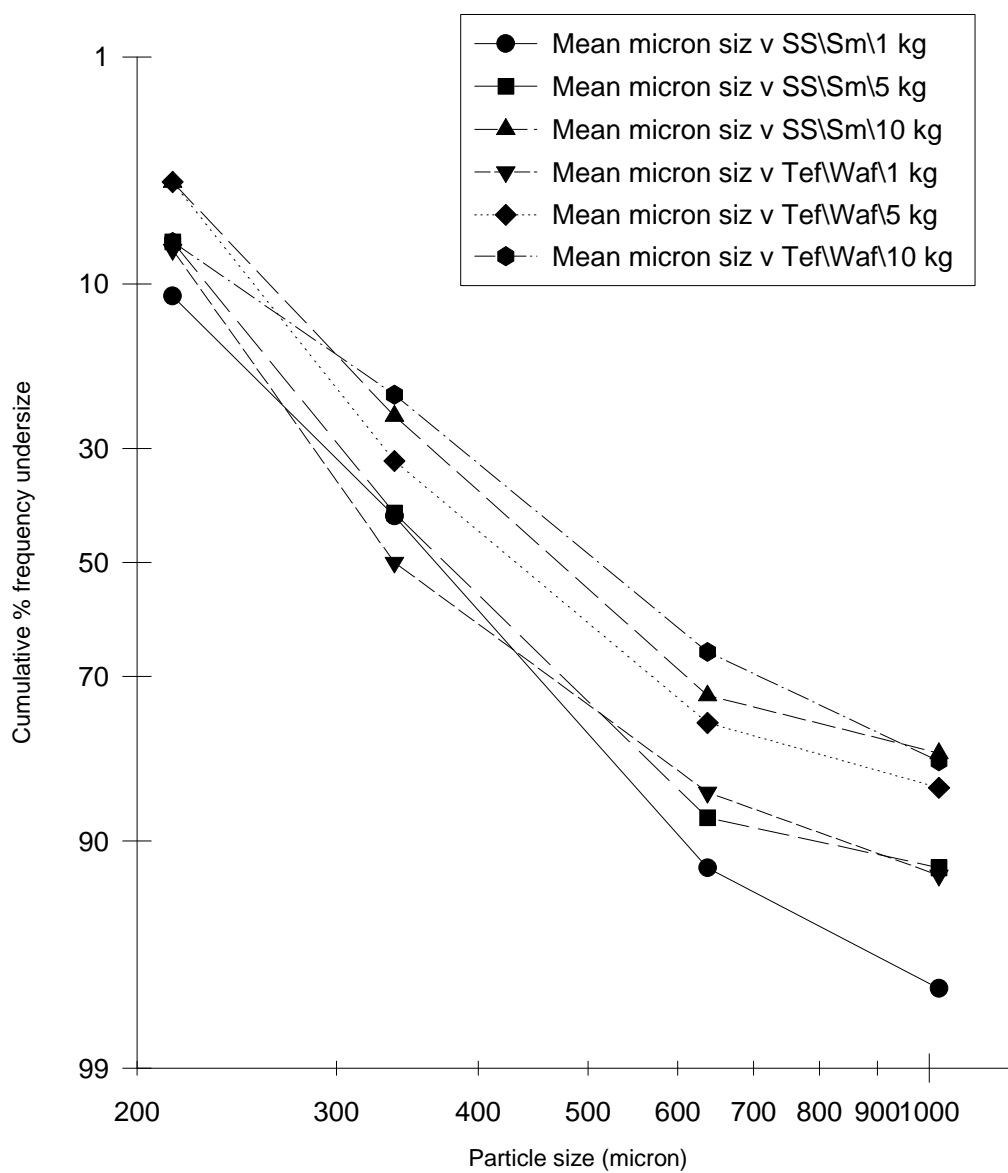


Table XXXIX. Sphericity Analysis of SS/Sm/1 kg (Trial 4) Batch from Feasibility Studies

Sample #	Area	Perimeter	Roundness	Sphericity
1	172440.77	1596.66	1.11	0.85
2	85836.72	1095.65	1.05	0.90
3	140054.00	1397.66	1.04	0.90
4	145441.75	1425.75	1.05	0.90
5	117719.24	1278.26	1.04	0.91
6	129925.26	1362.54	1.07	0.88
7	171147.28	1545.15	1.04	0.90
8	135543.20	1369.57	1.03	0.91
9	161336.42	1495.99	1.04	0.91
10	88412.76	1102.68	1.03	0.91
11	91745.16	1135.45	1.05	0.89
12	159993.59	1505.35	1.06	0.89
13	138333.00	1378.93	1.03	0.91
14	145737.72	1421.07	1.04	0.91
15	118678.41	1287.63	1.04	0.90
16	144636.05	1460.87	1.10	0.85
17	125809.09	1374.25	1.12	0.84
18	114332.04	1292.31	1.09	0.86
19	110314.52	1259.53	1.08	0.87
20	95691.42	1208.03	1.14	0.82
21	171695.36	1627.09	1.15	0.82
22	87930.44	1133.11	1.09	0.86
23	97401.47	1177.59	1.06	0.88
24	113997.70	1322.74	1.15	0.82
25	106412.10	1261.87	1.12	0.84
26	115866.70	1294.65	1.08	0.87
27	101599.85	1238.46	1.13	0.83
28	122586.31	1474.92	1.33	0.71
29	129963.63	1385.95	1.11	0.85
30	95691.42	1208.03	1.14	0.82
Average	124542.45	1337.26	1.09	0.87

**Table XL. Sphericity Analysis of SS/Sm/5 kg (Trial 12) Batch from
Feasibility Studies**

Sample #	Area	Perimeter	Roundness	Sphericity
1	99462.30	1186.96	1.06	0.89
2	335744.80	2172.58	1.05	0.89
3	121013.30	1311.04	1.06	0.88
4	181539.10	1601.34	1.06	0.89
5	121375.00	1311.04	1.06	0.89
6	115614.60	1275.92	1.05	0.89
7	137582.10	1409.36	1.08	0.87
8	162777.90	1526.42	1.07	0.88
9	100925.70	1179.93	1.03	0.91
10	151536.50	1449.16	1.04	0.91
11	139423.70	1388.29	1.03	0.91
12	99462.30	1186.96	1.06	0.89
13	388208.20	2380.94	1.09	0.86
14	162777.90	1526.42	1.07	0.88
15	100925.70	1179.93	1.03	0.91
16	141687.31	1404.68	1.04	0.90
17	178617.77	1582.61	1.05	0.90
18	277367.50	1947.83	1.02	0.92
19	281505.70	1964.21	1.03	0.92
20	185627.88	1638.80	1.08	0.87
21	187502.34	1603.68	1.03	0.92
22	172588.80	1540.47	1.03	0.91
23	124493.66	1325.08	1.05	0.89
24	158585.00	1479.60	1.03	0.91
25	218655.91	1734.78	1.03	0.91
26	288532.20	1996.99	1.03	0.91
27	172210.58	1545.15	1.04	0.91
28	180048.30	1570.90	1.03	0.92
29	166417.20	1512.38	1.03	0.91
30	148330.20	1449.16	1.06	0.89
Average	176684.65	1546.09	1.05	0.90

Table XLI. Sphericity Analysis of SS/Sm/10 kg (Trial 13) Batch from Feasibility Studies

Sample #	Area	Perimeter	Roundness	Sphericity
1	233279.02	1805.02	1.04	0.90
2	258869.44	1898.66	1.04	0.90
3	312812.66	2128.09	1.08	0.87
4	349101.84	2217.06	1.05	0.89
5	212555.64	1734.78	1.06	0.89
6	350811.91	2221.74	1.05	0.89
7	199445.28	1666.89	1.04	0.90
8	183276.56	1603.68	1.05	0.90
9	183276.56	1603.68	1.05	0.90
10	332516.59	2151.51	1.04	0.90
11	211388.20	1709.03	1.03	0.91
12	211892.45	1711.37	1.03	0.91
13	269036.53	1938.46	1.04	0.90
14	191865.16	1652.84	1.06	0.88
15	291963.25	2032.11	1.06	0.89
16	153180.81	1467.89	1.05	0.89
17	114600.60	1261.87	1.04	0.90
18	143265.83	1442.14	1.09	0.87
19	121281.84	1292.31	1.03	0.91
20	93252.41	1151.84	1.06	0.88
21	110166.53	1245.49	1.05	0.89
22	104943.22	1210.37	1.04	0.90
23	104406.09	1224.42	1.07	0.88
24	156935.25	1533.45	1.12	0.84
25	87376.86	1130.77	1.09	0.86
26	109262.18	1238.46	1.05	0.90
27	158848.08	1488.96	1.04	0.90
28	135252.72	1367.22	1.03	0.91
29	101621.77	1205.69	1.07	0.88
30	102005.45	1222.07	1.10	0.86
Average	186283.02	1585.26	1.06	0.89

Table XLII. Sphericity Analysis of Tef/Waf/1 kg (Trial 7) Batch from Feasibility Studies

Sample #	Area	Perimeter	Roundness	Sphericity
1	186444.53	1624.75	1.06	0.89
2	128922.25	1332.11	1.03	0.91
3	154353.73	1479.60	1.06	0.89
4	91410.82	1144.82	1.07	0.88
5	149968.98	1442.14	1.04	0.91
6	89010.17	1116.72	1.05	0.90
7	117576.74	1282.94	1.05	0.90
8	92523.45	1142.48	1.06	0.89
9	100350.20	1186.96	1.05	0.90
10	132906.88	1367.22	1.05	0.89
11	144986.83	1423.41	1.05	0.90
12	107053.38	1238.46	1.07	0.88
13	128418.01	1343.81	1.05	0.89
14	106116.13	1238.46	1.08	0.87
15	124970.51	1350.84	1.09	0.86
16	122476.69	1313.38	1.05	0.89
17	220431.72	1805.02	1.11	0.85
18	112090.34	1238.46	1.02	0.92
19	133619.41	1376.59	1.06	0.89
20	118267.34	1289.97	1.05	0.89
21	136255.72	1390.64	1.06	0.89
22	169672.91	1540.47	1.05	0.90
23	157368.23	1479.60	1.04	0.90
24	93756.66	1156.52	1.07	0.88
25	147201.13	1449.16	1.07	0.88
26	102789.21	1184.62	1.02	0.92
27	137543.73	1428.09	1.11	0.85
28	158530.19	1481.94	1.04	0.91
29	94140.32	1144.82	1.04	0.90
30	109547.19	1254.85	1.08	0.87
Average	128956.78	1341.63	1.06	0.89

Table XLIII. Sphericity Analysis of Tef/Waf/5 kg (Trial 14) Batch from Feasibility Studies

Sample #	Area	Perimeter	Roundness	Sphericity
1	79599.43	1058.19	1.05	0.89
2	104449.93	1229.10	1.08	0.87
3	88133.23	1121.41	1.07	0.88
4	123797.59	1315.72	1.05	0.90
5	120646.06	1318.06	1.08	0.87
6	223632.58	1797.99	1.08	0.87
7	233322.86	1826.09	1.07	0.88
8	78300.45	1048.83	1.05	0.89
9	123797.59	1315.72	1.05	0.90
10	139051.00	1418.73	1.08	0.87
11	85102.28	1121.41	1.11	0.85
12	103989.54	1219.73	1.07	0.88
13	108933.33	1250.17	1.07	0.88
14	137335.47	1400.00	1.07	0.88
15	141479.05	1402.34	1.04	0.90
16	365150.00	2277.93	1.06	0.88
17	234342.31	1797.99	1.03	0.91
18	211985.63	1706.69	1.03	0.91
19	287041.38	2067.22	1.11	0.84
20	295553.25	2039.13	1.05	0.89
21	335103.59	2160.87	1.04	0.90
22	205118.03	1716.05	1.07	0.88
23	206789.72	1697.32	1.04	0.90
24	361494.22	2289.63	1.08	0.87
25	210999.06	1725.42	1.06	0.89
26	307726.38	2076.59	1.05	0.90
27	214605.50	1760.54	1.08	0.87
28	226740.27	1788.63	1.06	0.89
29	282135.94	2013.38	1.07	0.87
30	334314.31	2214.72	1.10	0.86
Average	199022.33	1639.19	1.06	0.88

**Table XLIV. Sphericity Analysis of Tef/Waf/10 kg (Trial 15) Batch from
Feasibility Studies**

Sample #	Area	Perimeter	Roundness	Sphericity
1	259647.72	1926.76	1.07	0.88
2	247162.19	1879.93	1.07	0.88
3	181413.05	1580.27	1.03	0.91
4	277932.09	2008.70	1.09	0.87
5	215515.34	1758.19	1.07	0.88
6	233465.36	1816.72	1.06	0.89
7	276194.63	1999.33	1.08	0.87
8	192506.42	1631.77	1.03	0.91
9	368345.38	2259.20	1.04	0.91
10	230390.56	1774.58	1.02	0.92
11	244279.22	1849.50	1.05	0.90
12	243468.05	1863.55	1.07	0.88
13	270680.81	1957.19	1.06	0.89
14	242169.06	1837.79	1.04	0.90
15	186296.55	1624.75	1.06	0.89
16	153202.73	1491.30	1.09	0.87
17	109240.26	1252.51	1.07	0.88
18	105579.00	1231.44	1.07	0.88
19	87338.49	1121.41	1.08	0.87
20	94743.22	1172.91	1.09	0.87
21	80569.56	1062.88	1.05	0.90
22	122997.38	1376.59	1.15	0.82
23	148702.91	1474.92	1.09	0.86
24	114496.46	1292.31	1.09	0.86
25	105688.63	1273.58	1.15	0.82
26	119275.83	1322.74	1.10	0.86
27	94798.03	1172.91	1.09	0.87
28	159730.52	1514.72	1.07	0.87
29	115921.50	1285.28	1.07	0.88
30	129936.22	1374.25	1.09	0.86
Average	180389.57	1572.93	1.07	0.88

Table XLV. Dissolution Data for Ibuprofen Release of Pilot Size Scale-up Replicated Batches from Feasibility Studies

Time (mins)	% Ibuprofen Released (S.D.)		
	SS/Sm/1 kg	SS/Sm/5 kg	SS/Sm/10 kg
5	62.02 (21.29)	60.35 (22.25)	63.64 (10.37)
10	75.73 (13.92)	72.89 (19.62)	77.53 (12.88)
20	83.27 (5.02)	82.95 (12.66)	85.53 (5.08)
40	85.86 (1.03)	88.97 (6.74)	87.61 (2.45)
60	86.27 (0.92)	90.18 (4.79)	87.79 (2.38)
120	86.41 (0.54)	90.06 (4.15)	87.96 (4.1)

Time (mins)	% Ibuprofen Released (S.D.)		
	Tef/Waf/1 kg	Tef/Waf/5 kg	Tef/Waf/10 kg
5	61.28 (5.42)	60.43 (24.86)	63.64 (10.37)
10	82.82 (5.83)	70.56 (21.64)	77.53 (12.88)
20	91.75 (2.07)	79.47 (12.88)	85.53 (5.08)
40	94.30 (1.64)	85.64 (5.30)	87.61 (2.45)
60	94.68 (1.66)	87.75 (1.65)	87.79 (2.38)
120	94.69 (2.01)	89.55 (0.07)	87.96 (4.10)

Figure 59. Log-Probability Profiles for Sieve Analysis of Experimentally Designed Replicated Batches

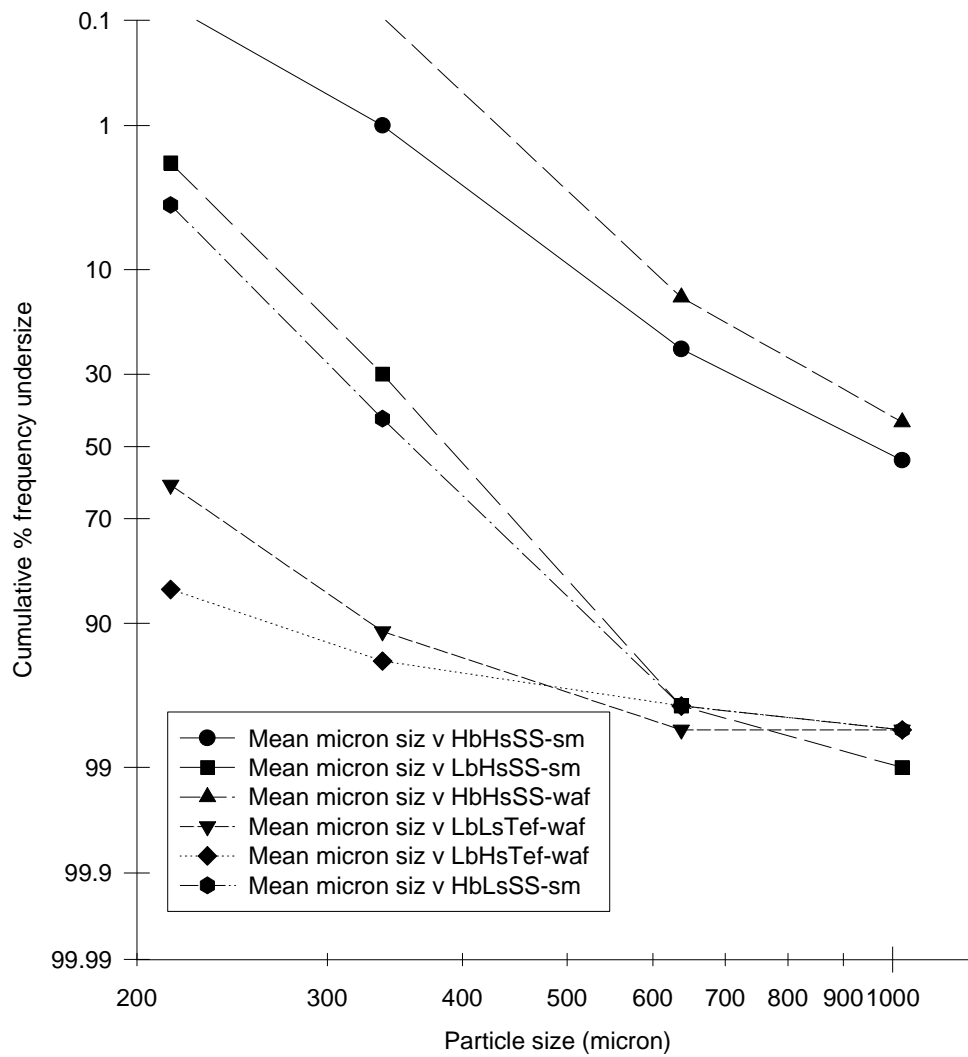


Table XLVI. Sphericity Analysis of LbHSSS-sm (Formulation 5) Spheroids from Experimentally Designed Batches

Sample #	Area	Perimeter	Roundness	Sphericity
1	224969.938	1751.17	1.019	0.92
2	191974.781	1620.067	1.022	0.92
3	164076.891	1510.033	1.039	0.90
4	99791.148	1172.91	1.031	0.91
5	86921.945	1102.676	1.046	0.90
6	251371.531	1865.886	1.035	0.91
7	124669.055	1315.719	1.038	0.91
8	179505.688	1566.221	1.022	0.92
9	124669.055	1315.719	1.038	0.91
10	179505.688	1566.221	1.022	0.92
11	176228.094	1549.833	1.019	0.92
12	83973.211	1081.605	1.041	0.90
13	170566.297	1533.445	1.031	0.91
14	118683.891	1271.237	1.018	0.92
15	116913.547	1266.555	1.026	0.92
16	207814.641	1723.077	1.068	0.88
17	190445.594	1662.207	1.085	0.87
18	174304.281	1580.267	1.071	0.88
19	253969.484	1908.027	1.072	0.88
20	219083.422	1765.217	1.063	0.88
21	289814.719	2022.742	1.055	0.89
22	241209.906	1847.157	1.057	0.89
23	130884.422	1353.177	1.046	0.90
24	84373.313	1095.652	1.064	0.88
25	184137.063	1631.772	1.081	0.87
26	104707.539	1236.12	1.091	0.86
27	189130.188	1659.866	1.089	0.86
28	226405.938	1828.428	1.104	0.85
29	259472.328	1959.532	1.106	0.85
30	293201.938	2081.271	1.104	0.85
Average	178092.52	1561.46	1.05	0.89

**Table XLVII. Sphericity Analysis of HbLsSS-sm (Formulation 11)
Spheroids from Experimentally Designed Batches**

Sample #	Area	Perimeter	Roundness	Sphericity
1	83627.906	1069.9	1.023	0.92
2	137658.844	1390.635	1.05	0.89
3	123797.586	1339.13	1.083	0.87
4	73005.883	1004.348	1.033	0.91
5	68259.406	962.207	1.014	0.93
6	62997.719	952.843	1.077	0.87
7	76069.719	1046.488	1.076	0.87
8	125474.75	1325.083	1.046	0.90
9	77160.422	1041.806	1.052	0.89
10	110078.844	1240.803	1.046	0.90
11	110034.992	1243.144	1.05	0.89
12	72337.211	994.983	1.023	0.92
13	152857.438	1456.187	1.037	0.91
14	110150.094	1247.826	1.057	0.89
15	251678.469	1931.438	1.108	0.85
16	207814.641	1723.077	1.068	0.88
17	190445.594	1662.207	1.085	0.87
18	174304.281	1580.267	1.071	0.88
19	253969.484	1908.027	1.072	0.88
20	219083.422	1765.217	1.063	0.88
21	219083.422	1765.217	1.063	0.88
22	241209.906	1847.157	1.057	0.89
23	130884.422	1353.177	1.046	0.90
24	84373.313	1095.652	1.064	0.88
25	259472.328	1959.532	1.106	0.85
26	184137.063	1631.772	1.081	0.87
27	104707.539	1236.12	1.091	0.86
28	149108.484	1470.234	1.084	0.87
29	189130.188	1659.866	1.089	0.86
30	226405.938	1828.428	1.104	0.85
Average	148977.31	1424.43	1.06	0.88

Table XLVIII. Dissolution Data for Ibuprofen Release of Experimentally Designed Replicated Batches

Time (mins)	% Ibuprofen Released (S.D.)		
	LbHsSS-waf	LbHsSS-sm	HbHsSSwaf
	(Formulation 3)	(Formulation 5)	(Formulation 6)
5	21.93 (3.20)	69.20 (2.06)	22.48 (0.19)
10	31.76 (3.66)	83.52 (0.59)	32.29 (0.64)
20	47.56 (7.17)	89.87 (0.30)	47.23 (0.47)
40	61.62 (4.58)	91.19 (0.68)	63.98 (0.06)
60	72.66 (3.20)	90.325 (1.20)	77.86 (1.19)
120	86.12 (1.57)	91.11 (2.48)	90.15 (0.04)

Time (mins)	% Ibuprofen Released (S.D.)		
	LbsTef-waf	LbHsTef-waf	HbLsSS-sm
	(Formulation 7)	(Formulation 9)	(Formulation 11)
5	82.08 (3.26)	77.04 (2.75)	78.89 (4.95)
10	86.62 (4.27)	84.46 (2.09)	89.02 (1.37)
20	88.90 (5.25)	89.23 (1.45)	92.47 (3.61)
40	89.53 (3.91)	92.44 (1.03)	93.23 (3.30)
60	90.30 (3.54)	93.51 (0.15)	93.63 (3.87)
120	90.08 (3.17)	93.83 (0.83)	93.67 (3.56)

Figure 60. Log-Probability Profiles for Sieve Analysis of Drug Load/Drug Particle Size Replicated Batches

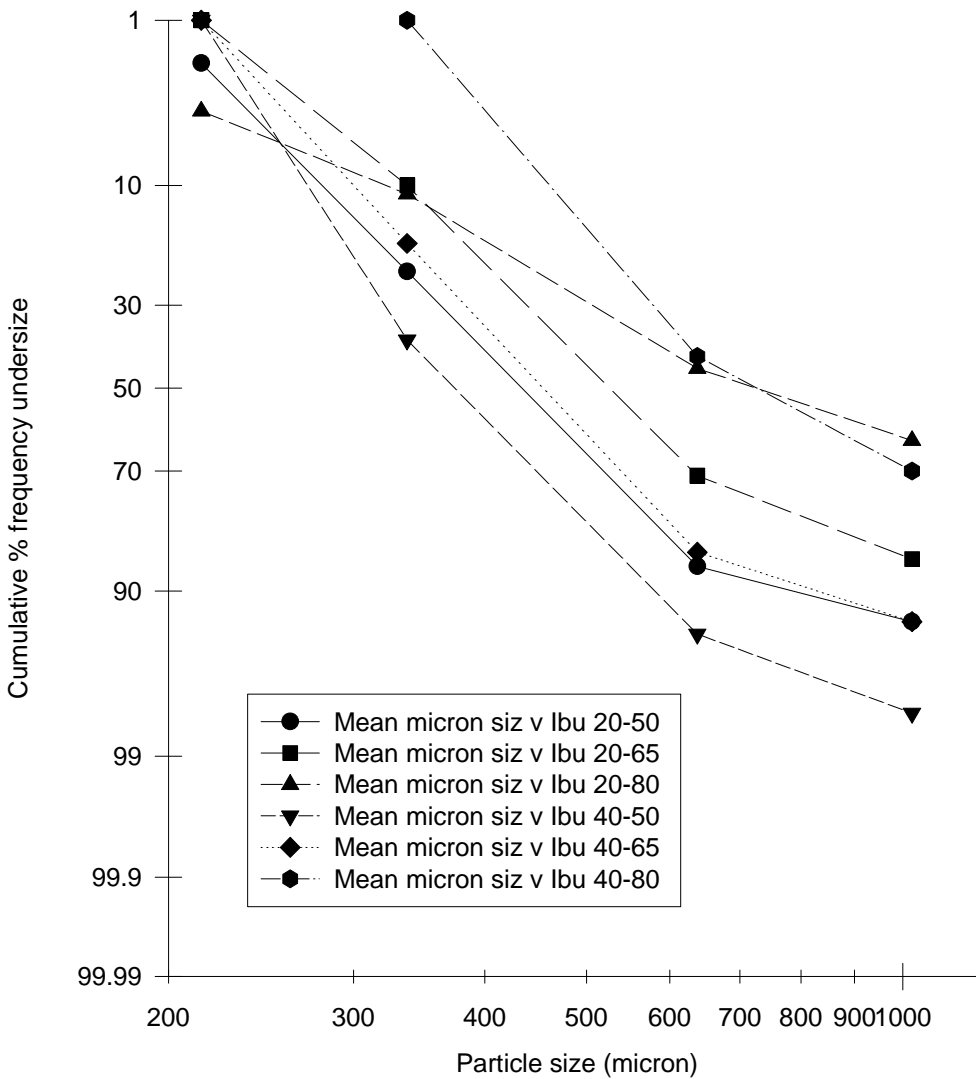


Table XLIX. Sphericity Analysis of Ibuprofen Spheroids from Drug Load/Drug Particle Size Replicated Batches (1kg, 20 Micron Size, 65% Drug Load)

Sample #	Area	Perimeter	Roundness	Sphericity
1	158058.83	1517.06	1.09	0.86
2	169914.06	1531.10	1.03	0.91
3	169914.06	1531.10	1.03	0.91
4	289491.34	2008.70	1.04	0.90
5	140152.66	1383.61	1.02	0.92
6	230428.92	1779.26	1.03	0.91
7	281631.69	2004.01	1.07	0.88
8	301708.31	2076.59	1.07	0.88
9	348685.31	2195.99	1.03	0.91
10	317049.44	2137.46	1.08	0.87
11	81495.83	1053.51	1.02	0.92
12	275821.94	2004.01	1.09	0.86
13	258737.89	1912.71	1.06	0.89
14	270735.63	1924.42	1.02	0.92
15	207376.17	1706.69	1.05	0.89
16	149810.05	1428.09	1.02	0.92
17	258710.48	1877.59	1.02	0.92
18	295262.75	2015.72	1.03	0.91
19	174254.95	1552.17	1.03	0.91
20	190966.30	1606.02	1.01	0.93
21	260650.73	1889.30	1.02	0.92
22	313782.78	2069.57	1.02	0.92
23	192122.77	1622.41	1.02	0.92
24	206559.52	1699.67	1.05	0.90
25	236112.64	1797.99	1.02	0.92
26	174814.02	1549.83	1.03	0.91
27	224536.94	1758.19	1.03	0.91
28	239203.89	1816.72	1.03	0.91
29	216945.86	1718.40	1.02	0.92
30	279384.53	1950.17	1.02	0.92
Average	230477.34	1770.60	1.04	0.91

Table L. Sphericity Analysis of Ibuprofen Spheroids from Drug Load/Drug Particle Size Replicated Batches (1kg, 40 Micron Size, 65% Drug Load)

Sample #	Area	Perimeter	Roundness	Sphericity
1	200963.48	1673.91	1.04	0.90
2	249179.16	1901.00	1.08	0.87
3	223007.77	1793.31	1.08	0.87
4	154370.17	1467.89	1.04	0.90
5	314402.13	2118.73	1.07	0.88
6	260267.06	1933.78	1.07	0.87
7	171350.06	1568.56	1.07	0.88
8	261467.39	1908.03	1.04	0.90
9	133838.64	1397.66	1.09	0.86
10	274462.66	1985.28	1.07	0.88
11	206882.89	1706.69	1.05	0.89
12	218940.92	1765.22	1.06	0.88
13	146461.20	1444.48	1.07	0.88
14	185342.86	1624.75	1.07	0.88
15	188143.61	1638.80	1.07	0.88
16	157439.48	1495.99	1.06	0.88
17	207469.34	1711.37	1.06	0.89
18	232955.64	1821.41	1.07	0.88
19	120207.59	1301.67	1.05	0.89
20	196173.17	1664.55	1.06	0.89
21	112950.84	1271.24	1.07	0.88
22	193257.31	1648.16	1.05	0.89
23	319822.78	2153.85	1.08	0.87
24	287644.28	2029.77	1.07	0.88
25	268543.25	1961.87	1.07	0.88
26	144334.61	1444.48	1.08	0.87
27	164712.67	1540.47	1.08	0.87
28	126686.03	1339.13	1.06	0.89
29	189530.28	1636.46	1.06	0.89
30	178075.16	1594.31	1.07	0.88
Average	202962.75	1684.76	1.07	0.88

**Table LI. Dissolution Data for Ibuprofen Release of Drug Load/Drug Particle Size
Replicated Batches**

Time (mins)	% Ibuprofen Released (S.D.)		
	Ibu 20-50	Ibu 20-65	Ibu 20-80
5	48.82 (7.73)	54.21 (6.32)	54.51 (14.00)
10	65.36 (10.95)	70.31 (6.17)	67.78 (12.92)
20	83.94 (4.00)	86.87 (1.34)	82.80 (6.19)
40	88.98 (2.67)	88.49 (0.69)	89.02 (5.04)
60	90.34 (2.13)	90.29 (0.12)	91.61 (3.95)
120	91.00 (0.90)	91.20 (0.11)	95.55 (0.78)

Time (mins)	% Ibuprofen Released (S.D.)		
	Ibu 40-50	Ibu 40-65	Ibu 40-80
5	61.21 (6.38)	56.25 (3.55)	39.92 (3.46)
10	75.10 (6.03)	71.78 (2.36)	54.14 (4.75)
20	89.48 (4.93)	88.38 (3.73)	74.34 (0.50)
40	91.35 (2.84)	92.13 (3.18)	86.07 (7.21)
60	94.04 (5.60)	93.09 (2.67)	93.33 (7.61)
120	94.01 (4.82)	93.22 (3.04)	99.65 (7.16)

**Figure 61. Log-Probability Profiles for Sieve Analysis of Intermediate Size Scale-up
Replicated Batches**

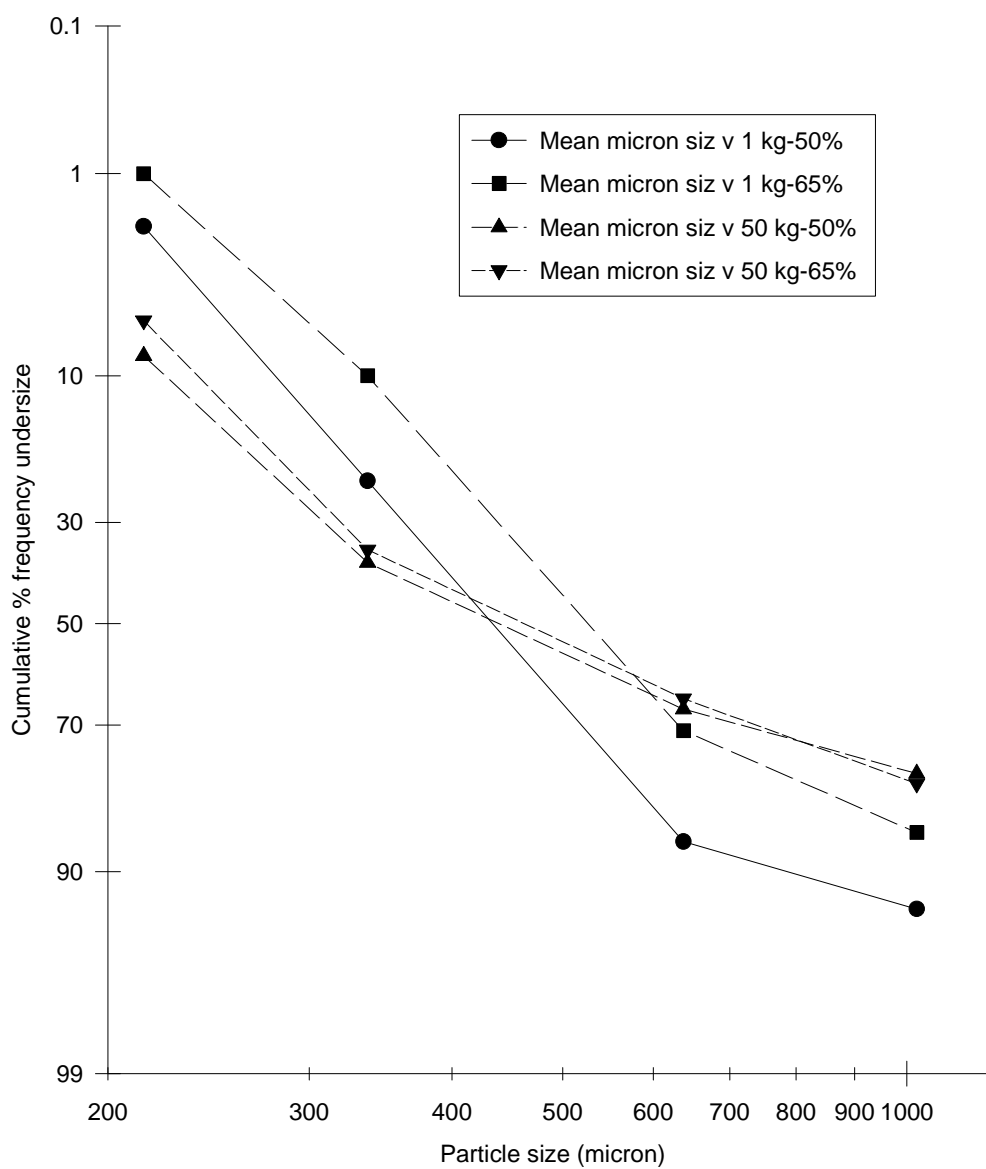


**Table LII. Sphericity Analysis of Intermediate Scale-up Ibuprofen Replicated
Batch (20 Micron, 50% Drug Load, 50kg Batch Size)**

Sample #	Area	Perimeter	Roundness	Sphericity
1.00	84844.67	1069.90	1.01	0.93
2.00	114019.63	1243.14	1.01	0.93
3.00	113783.95	1264.21	1.05	0.89
4.00	110330.96	1243.14	1.05	0.90
5.00	196485.58	1645.82	1.03	0.91
6.00	122125.91	1296.99	1.03	0.91
7.00	128538.59	1329.77	1.03	0.91
8.00	140432.19	1407.02	1.05	0.89
9.00	133444.02	1355.52	1.03	0.91
10.00	132287.53	1357.86	1.04	0.90
11.00	105030.91	1219.73	1.06	0.89
12.00	125524.08	1327.43	1.05	0.90
13.00	85677.77	1079.26	1.02	0.92
14.00	137757.50	1376.59	1.03	0.91
15.00	78053.81	1037.12	1.03	0.91
16.00	132638.31	1357.86	1.04	0.90
17.00	93652.52	1140.13	1.04	0.91
18.00	122800.06	1292.31	1.02	0.92
19.00	126883.34	1322.74	1.03	0.91
20.00	248844.83	1856.52	1.04	0.91
21.00	147168.23	1411.71	1.01	0.93
22.00	130418.54	1350.84	1.05	0.90
23.00	84948.81	1086.29	1.04	0.90
24.00	107332.90	1210.37	1.02	0.92
25.00	178338.25	1582.61	1.05	0.89
26.00	161254.20	1500.67	1.04	0.90
27.00	116546.33	1271.24	1.04	0.91
28.00	88801.90	1109.70	1.04	0.91
29.00	139873.14	1383.61	1.02	0.92
30.00	80673.70	1067.56	1.06	0.89
Average	125617.07	1306.59	1.03	0.91

**Table LIII. Sphericity Analysis of Intermediate Scale-up Ibuprofen Replicated
Batch (20 Micron, 65% Drug Load, 50 kg Batch Size)**

Sample #	Area	Perimeter	Roundness	Sphericity
1.00	83874.56	1079.26	1.04	0.90
2.00	86752.04	1095.65	1.03	0.91
3.00	211404.64	1702.01	1.02	0.92
4.00	183040.88	1599.00	1.04	0.90
5.00	83677.23	1067.56	1.02	0.92
6.00	218343.50	1727.76	1.02	0.92
7.00	150763.72	1432.78	1.02	0.92
8.00	132517.73	1348.50	1.03	0.92
9.00	177647.64	1563.88	1.03	0.91
10.00	130933.75	1339.13	1.02	0.92
11.00	126905.27	1334.45	1.05	0.90
12.00	213525.77	1704.35	1.02	0.92
13.00	178880.86	1587.29	1.05	0.89
14.00	209552.09	1690.30	1.02	0.92
15.00	102071.21	1182.27	1.02	0.92
16.00	158650.77	1486.62	1.04	0.90
17.00	113285.18	1259.53	1.05	0.90
18.00	283385.59	1973.58	1.03	0.91
19.00	83046.93	1076.92	1.04	0.90
20.00	170878.70	1554.52	1.06	0.89
21.00	108401.68	1236.12	1.05	0.89
22.00	114836.28	1275.92	1.06	0.89
23.00	129788.23	1336.79	1.03	0.91
24.00	348723.66	2205.35	1.04	0.90
25.00	150089.58	1446.82	1.04	0.90
26.00	137012.09	1378.93	1.04	0.91
27.00	117193.08	1282.94	1.05	0.89
28.00	231903.30	1788.63	1.03	0.91
29.00	120931.06	1304.01	1.05	0.89
30.00	129788.23	1336.79	1.03	0.91
Average	156260.18	1446.59	1.04	0.91

**Table LIV. Dissolution Data for Ibuprofen Release of Intermediate Batch size
(Replicated Batches)**

Time (mins)	% Ibuprofen Released (S.D.)			
	1 kg-50%	1 kg-65%	50 kg-50%	50 kg-65%
5	48.82 (7.73)	54.21 (6.32)	50.09 (2.7)	62.25 (2.44)
10	65.36 (10.95)	70.31 (6.17)	63.74 (2.94)	75.32 (1.22)
20	83.94 (4.00)	86.87 (1.34)	83.10 (1.68)	87.43 (0.03)
40	88.98 (2.67)	88.49 (0.69)	88.02 (1.13)	90.82 (0.75)
60	90.34 (2.13)	90.29 (0.12)	91.29 (0.02)	92.36 (0.28)
120	91.00 (0.90)	91.20 (0.11)	93.01 (0.67)	93.63 (0.52)

Figure 62. Log-Probability Profiles for Sieve Analysis of Uncoated and Coated Ibuprofen Spheroids (Replicated Batches)

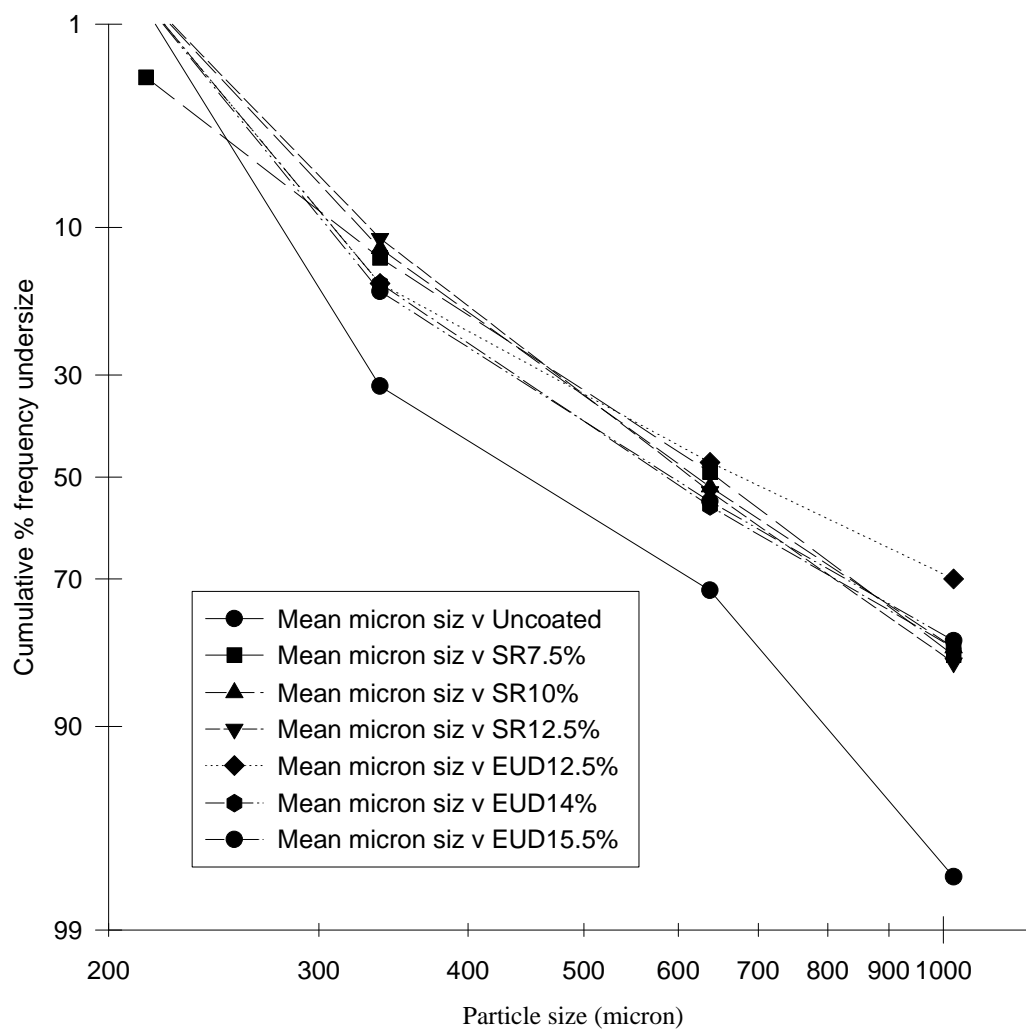


**Table LV. Sphericity Analysis of SR 12.5% Coated Ibuprofen Spheroids
(Replicated Batches)**

Sample #	Area	Perimeter	Roundness	Sphericity
1	157675.17	1493.65	1.06	0.89
2	128461.85	1348.50	1.06	0.89
3	170889.67	1554.52	1.06	0.89
4	337635.75	2205.35	1.08	0.87
5	167897.09	1545.15	1.06	0.88
6	116551.81	1275.92	1.04	0.90
7	212122.66	1734.78	1.06	0.89
8	170675.92	1563.88	1.07	0.88
9	96869.82	1165.89	1.05	0.90
10	122701.41	1299.33	1.03	0.91
11	117160.20	1287.63	1.06	0.89
12	99506.14	1170.57	1.03	0.91
13	196518.47	1669.23	1.06	0.89
14	208329.84	1727.76	1.07	0.88
15	123753.74	1296.99	1.02	0.92
16	257696.52	1903.34	1.05	0.89
17	106362.77	1212.71	1.03	0.91
18	220705.77	1748.83	1.04	0.91
19	106554.61	1217.39	1.04	0.90
20	181604.88	1573.24	1.02	0.92
21	192084.39	1634.11	1.04	0.90
22	114047.03	1257.19	1.04	0.91
23	78448.44	1037.12	1.03	0.92
24	157318.91	1463.21	1.02	0.92
25	233640.75	1814.38	1.05	0.89
26	135334.92	1374.25	1.04	0.90
27	72852.41	1018.40	1.06	0.88
28	185293.53	1634.11	1.08	0.87
29	171311.70	1547.49	1.05	0.90
30	227239.03	1781.61	1.04	0.90
Average	162241.51	1485.22	1.05	0.90

**Table LVI. Sphericity Analysis of EUD15.5% Coated Ibuprofen Spheroids
(Replicated Batches)**

Sample #	Area	Perimeter	Roundness	Sphericity
1	154222.19	1486.62	1.07	0.88
2	113175.56	1250.17	1.03	0.91
3	89514.42	1140.13	1.09	0.87
4	198398.42	1659.87	1.04	0.91
5	199023.25	1662.21	1.04	0.91
6	141895.59	1402.34	1.04	0.91
7	143622.08	1411.71	1.04	0.91
8	142427.25	1418.73	1.06	0.89
9	93318.18	1165.89	1.09	0.86
10	93531.94	1140.13	1.04	0.90
11	154863.45	1486.62	1.07	0.88
12	148034.22	1437.46	1.04	0.90
13	186488.38	1636.46	1.07	0.88
14	186581.55	1624.75	1.06	0.89
15	191624.00	1664.55	1.08	0.87
16	154249.59	1481.94	1.06	0.88
17	145228.00	1430.44	1.05	0.89
18	141199.52	1395.32	1.03	0.91
19	97823.50	1170.57	1.05	0.90
20	91202.55	1140.13	1.07	0.88
21	125255.52	1320.40	1.04	0.90
22	154249.59	1481.94	1.06	0.88
23	179127.50	1582.61	1.05	0.90
24	242728.13	1840.13	1.04	0.90
25	191624.00	1664.55	1.08	0.87
26	107376.74	1224.42	1.04	0.90
27	321406.75	2135.12	1.06	0.89
28	267617.00	1964.21	1.08	0.87
29	146159.75	1428.09	1.04	0.90
30	278809.03	1973.58	1.04	0.90
Average	162692.59	1494.04	1.05	0.89

Table LVII. Dissolution Data for Ibuprofen Release Coated Replicated Batches

Time (mins)	% Ibuprofen Released (S.D.)			
	Uncoated	SR 7.5%	SR 10%	SR 12.5%
5	62.25 (2.44)			
10	75.32 (1.22)	21.55 (0.67)	16.36 (0.93)	11 (0.35)
20	87.43 (0.03)	31.80 (0.37)	24.19 (1.78)	16.56 (0.40)
40	90.82 (0.75)	47.39 (1.46)	37.27 (3.05)	28.53 (0.98)
60	92.36 (0.28)	56.94 (4.43)	46.82 (3.76)	37.23 (2.96)
90		66.88 (6.58)	56.17 (5.78)	48.29 (2.28)
120	93.63 (0.52)	72.91 (9.25)	62.41 (7.56)	55.24 (3.44)
150		77.14 (7.59)	68.64 (8.63)	61.96 (4.06)
180		80.26 (7.91)	70.01 (8.44)	66.92 (4.52)
240	93.9 (0.46)	85.61 (8.30)	76.98 (4.72)	72.66 (3.09)
360		90.76 (6.89)	84.12 (1.46)	79.77 (3.95)
480		91.00 (6.16)	87.47 (3.38)	83.63 (2.41)
720	93.9 (0.20)	93.63 (5.39)	90.2 (4.01)	86.14 (3.27)

Time (mins)	% Ibuprofen Released (S.D.)			
	Uncoated	EUD 12.5%	EUD 14%	EUD 15.5%
5	62.25 (2.44)			
10	75.32 (1.22)	16.26 (2.37)	9.43 (1.80)	11.18 (0.93)
20	87.43 (0.03)	22.91 (4.07)	15.76 (3.11)	15.28 (2.35)
40	90.82 (0.75)	39.88 (1.34)	27.67 (5.78)	30.09 (2.49)
60	92.36 (0.28)	50.62 (0.98)	37.30 (5.16)	39.05 (3.35)
90		58.97 (0.21)	47.38 (6.80)	49.47 (4.75)
120	93.63 (0.52)	66.69 (1.25)	53 (2.77)	55.44 (3.97)
150		71.49 (1.44)	60.11 (4.75)	60.34 (3.69)
180		75.20 (2.07)	68.43 (9.38)	61.64 (0.16)
240	93.9 (0.46)	82.06 (4.21)	73.13 (4.10)	71.12 (4.26)
360		88.42 (0.55)	81.68 (5.30)	74.87 (1.74)
480		92.09 (0.01)	88.04 (6.14)	80.39 (0.90)
720	93.9 (0.20)	96.61 (2.58)	93.80 (6.65)	89.22 (2.28)

Table LVIII. Fill Weight and Statistical Parameters of Uncoated Ibuprofen Spheroids Encapsulated at 75 rpm and 280 msec

Sample #	Wt. capsule + spheroids (mg)	Av. wt. 20 empty capsules (mg)	Fill wt. spheroids (mg)
1	622.19	94.88	527.31
2	624.65	94.88	529.77
3	635.32	94.88	540.44
4	629.86	94.88	534.98
5	624.57	94.88	529.69
6	627.08	94.88	532.20
7	631.62	94.88	536.74
8	631.95	94.88	537.07
9	624.08	94.88	529.20
10	625.21	94.88	530.33
11	622.86	94.88	527.98
12	610.10	94.88	515.22
13	629.29	94.88	534.41
14	634.01	94.88	539.13
15	623.22	94.88	528.34
16	625.39	94.88	530.51
17	601.91	94.88	507.03
18	609.91	94.88	515.03
19	616.29	94.88	521.41
20	612.11	94.88	517.23
Average fill weight (mg)			528.20
Standard deviation			8.87
Coefficient of variation (%)			1.68

Table LVIX. Fill Weight and Statistical Parameters of Uncoated Ibuprofen Spheroids Encapsulated at 75 rpm and 300 msecs

Sample #	Wt. capsule + spheroids (mg)	Av. wt. 20 empty capsules (mg)	Fill wt. spheroids (mg)
1	617.23	94.88	522.35
2	608.26	94.88	513.38
3	611.68	94.88	516.80
4	617.65	94.88	522.77
5	625.15	94.88	530.27
6	626.09	94.88	531.21
7	630.84	94.88	535.96
8	629.47	94.88	534.59
9	621.19	94.88	526.31
10	627.60	94.88	532.72
11	629.39	94.88	534.51
12	616.45	94.88	521.57
13	620.57	94.88	525.69
14	628.66	94.88	533.78
15	624.45	94.88	529.57
16	613.77	94.88	518.89
17	632.14	94.88	537.26
18	625.23	94.88	530.35
19	635.21	94.88	540.33
20	623.54	94.88	528.66
Average fill weight (mg)			528.35
Standard deviation			7.24
Coefficient of variation (%)			1.37

**Table LX. Fill Weight and Statistical Parameters of Coated Ibuprofen Spheroids
Encapsulated at 75 rpm and 280 msec**

Sample #	Wt. capsule + spheroids (mg)	Av. Wt. 20 empty capsules (mg)	Fill wt. spheroids (mg)
1	552.89	94.88	458.01
2	547.78	94.88	452.90
3	569.09	94.88	474.21
4	554.30	94.88	459.42
5	536.72	94.88	441.84
6	536.67	94.88	441.79
7	573.11	94.88	478.23
8	581.93	94.88	487.05
9	566.62	94.88	471.74
10	554.00	94.88	459.12
11	537.81	94.88	442.93
12	551.14	94.88	456.26
13	552.14	94.88	457.26
14	557.43	94.88	462.55
15	560.84	94.88	465.96
16	574.71	94.88	479.83
17	556.03	94.88	461.15
18	574.26	94.88	479.38
19	565.69	94.88	470.81
20	557.52	94.88	462.64
Average fill weight (mg)			463.15
Standard deviation			12.92
Coefficient of variation (%)			2.79

Table LXI. Fill Weight and Statistical Parameters of Coated Ibuprofen Spheroids Encapsulated at 75 rpm and 300 msec

	Sample #	Wt. capsule + spheroids (mg)	Av. Wt. 20 empty capsules (mg)	Fill wt. spheroids (mg)
	1	587.86	94.88	492.98
	2	577.59	94.88	482.71
	3	589.83	94.88	494.95
	4	578.74	94.88	483.86
	5	583.14	94.88	488.26
	6	564.94	94.88	470.06
	7	569.66	94.88	474.78
	8	563.18	94.88	468.30
	9	585.63	94.88	490.75
	10	573.47	94.88	478.59
	11	591.24	94.88	496.36
	12	583.00	94.88	488.12
	13	558.88	94.88	464.00
	14	570.62	94.88	475.74
	15	596.40	94.88	501.52
	16	571.49	94.88	476.61
	17	571.94	94.88	477.06
	18	566.51	94.88	471.63
	19	587.53	94.88	492.65
	20	590.02	94.88	495.14
Average fill weight (mg)				483.20
Standard deviation				10.78
Coefficient of variation (%)				2.23

Table LXIIA. Dissolution Data for Ibuprofen Release of Encapsulated and Unencapsulated (Uncoated) Spheroids

Time (mins)	% Ibuprofen Released (S.D.)		
	Uncoated-Unencapd. (75/280)	Uncoated-Unencapd. (75/280)	Uncoated-Unencapd. (75/300)
5	51.71 (0.00)	41.59 (0.00)	38.18 (0.00)
10	66.55 (0.00)	60.89 (0.01)	55.68 (0.00)
20	81.95 (0.00)	81.41 (0.01)	81.48 (0.00)
40	88.69 (0.00)	87.34 (0.01)	87.24 (0.00)
60	96.16 (0.00)	91.49 (0.00)	90.09 (0.00)
90			
120	96 (0.00)	94.72 (0.00)	91.97 (0.00)
150			
180			
240			
360			
480			
720	99.03 (0.01)	97.9 (0.00)	95.06 (0.00)

Table LXIIB. Dissolution Data for Ibuprofen Release of Encapsulated and Unencapsulated (Coated) Spheroids

Time (mins)	% Ibuprofen Released (S.D.)		
	Coated-Uncapd.	Coated-Encapd. (75/280)	Coated-Encapd. (75/300)
10	4.19 (0.01)	5.92 (0.00)	9.6 (0.00)
20	12.27 (0.00)	15.11 (0.00)	18.6 (0.00)
40	25.87 (0.01)	30.44 (0.00)	28.62 (0.00)
60	36.00 (0.01)	40.97 (0.00)	37.52 (0.00)
90	45.83 (0.00)	52.36 (0.01)	48.1 (0.00)
120	54.76 (0.01)	61.11 (0.01)	56.26 (0.00)
150	60.12 (0.01)	64.63 (0.01)	62.18 (0.00)
180	66.48 (0.01)	69.16 (0.00)	65.8 (0.00)
240	72.13 (0.01)	73.93 (0.01)	71.36 (0.00)
360	79.19 (0.01)	80.93 (0.00)	80.29 (0.00)
480	83.84 (0.01)	81.61 (0.00)	82.29 (0.00)
720	84.77 (0.01)	86.18 (0.00)	85.53 (0.00)

VI. BIBLIOGRAPHY

1. B. Winther and N. Mygind . The therapeutic effectiveness of ibuprofen on the symptoms of naturally acquired common colds. *Am. J. Rhinol.* **15**:239-242 (2001).
2. T. Wyss-Coray and L. Mucke. Ibuprofen, inflammation and Alzheimer disease. *Nat. Med.* **6**:973-974 (2000).
3. P. L. McGeer and E. G. McGeer. The inflammatory response system of brain: implications for therapy of Alzheimer and other neurodegenerative diseases. *Brain Res. Rev.* **21**:195-218 (1995).
4. M. Jbilou, A. Etabia, A. M. Guyot-Hermann and J. C. Guyot. Ibuprofen agglomerates preparation by phase separation. *Drug. Dev. Ind. Pharm.* **25**:297-305 (1999).
5. N. Rasenack and B. W. Muller. Ibuprofen crystals with optimized properties. *Int. J. Pharm.* **245**:9-24 (2002).
6. E. Korakianiti, D. M. Rekkas, P. P. Dallas and N. H. Choulis. Development, production and *in-vitro* evaluation of enteric coated aspirin pellets. *The 18th Pharmaceutical Technology Conference and Exhibition Proceedings.* **2**:195-200 (1999).
7. C. Vervaet, L. Baert and J. P. Remon. Extrusion-spheronization. A literature review. *Int. J. Pharm.* **116**:131-146 (1995).
8. J. J. Sousa, A. Sousa, F. Podczek and J. M. Newton. Influence of process conditions on drug release from pellets. *Int. J. Pharm.* **144**:159-169 (1996).

9. R. L. Robinson and R. G. Hollenbeck. Manufacture of spherical acetaminophen pellets: comparison of rotary processing with multi-step extrusion and spheronization. *Pharm. Technol.* **15**:48-56 (1991).
10. G. Tomer, F. Podczek and J. M. Newton. The influence of type and quantity of model drug on the extrusion/spheronization of mixtures with microcrystalline cellulose. I. Extrusion parameters. *Int. J. Pharm.* **217**:237-248 (2001).
11. K. Olsen, A. Mehta. Fluid-bed agglomeration and coating technology - State of the art. *Int. J. Pharm.* **116**:131-146 (1995).
12. M. Friedman and M. Donbrow. Fluidized bed coating technique for production of sustained release granules. *Drug Dev. Ind. Pharm.* **4**:319-331 (1978).
13. B. Rambali, L. Baert and D. L. Massart. Scaling up of the fluidized bed granulation process. *Int. J. Pharm.* **252**:197-206 (2003).
14. C. Liew, L. Gu and P. Heng. The influence of operational variables on mean size and size distribution of spheroids produced by rotary spheronization using teardrop studs. *Int. J. Pharm.* **242**:345-348 (2002).
15. Gheber-Sellassie I. Pellets an Overview, In *Pharmaceutical Pelletization Technology*; Marcel Dekker, New York, Ch. 1, 1989.
16. G. Sienkiewicz, R. Pereira, E. M. Rudnic, J. M. Lausier and C. T. Rhodes. Spheronization of theophylline-Avicel[®] combinations using fluidized-bed roto granulation technique. *Drug Dev. Ind. Pharm.* **2**:173-182 (1997).
17. H. Cheng, J. D. Rogers, J. L. Demetriades, S. D. Holland, J. R. Seibold and E. Depuy. Pharmacokinetics and bioinversion of ibuprofen enantiomers in humans. *Pharm. Res.* **11**:824-830 (1994).

18. M. L. Chavez and C. J. DeKorte. Valdecoxib: a review. *Clin. Ther.* **25**:817-851 (2003).
19. P. McGettigan and D. Henry. Current problems with non-specific COX inhibitors. *Curr. Pharm. Des.* **6**:1693-1724 (2000).
20. C. M. Adeyeye J. D. Bricker V. D. Vilivalam and W. I. Smith. Acute gastrointestinal toxic effects of suspensions of unencapsulated and encapsulated ibuprofen in rats. *Pharm. Res.* **13**:784-93 (1996).
21. C. M. Adeyeye and J. C. Price. Development and evaluation of sustained-release ibuprofen-wax microspheres. II. In vitro dissolution studies. *Pharm. Res.* **11**:575-579 (1994).
22. C. De Brabander, C. Vervaet, L. Fiermans and J. P. Remon Matrix mini-tablets based on starch/microcrystalline wax mixtures. *Int. J. Pharm.* **199**:195-203 (2000).
23. G. M. Khan and J. B. Zhu. Ibuprofen release kinetics from controlled-release tablets granulated with aqueous polymeric dispersion of ethylcellulose II: Influence of several parameters and coexcipients, *J. Contr. Rel.* **56**:127-134 (1998).
24. E. S. Ghaly and S. P. R. Sepulveda. In-vitro evaluation of sustained release ibuprofen microspheres. *Health Sci. J.* **15**:97-100 (1996).
25. R. Ilango, S. Kavimani, B. Jaykar and G. Umamaheshwari. Dissolution studies on tablets of ibuprofen using chitosan. *Indian J. Exp. Biol.* **37**:505-508 (1999).
26. L. Fernandes and R. Jenkins. Investigation into the duration of action of sustained-release ibuprofen in osteoarthritis and rheumatoid arthritis. *Curr. Med. Res. Opin.* **13**:242-250 (1994).

27. <http://www.wcer.wisc.edu/step/ep301/Spr2000/esselman/IBUb.html>, with modifications.
28. M. Busson. Update on ibuprofen: review article. *J. Int. Med. Res.* **14**:53-62 (1986).
29. M. M. Wolfe. Risk factors associated with the development of gastroduodenal ulcers due to the use of NSAIDs. *Int. J. Clin. Pract. Suppl.* **135**:32-37 (2003).
30. Q. Xiaotao; Qian and S. D. Hall. Methods and compositions comprising R-ibuprofen. *US Patent # 6,255,347*.
31. http://www.pediatrics.wisc.edu/childrenshosp/parents_of_preemies/pda.html
32. J. Patel, I. Roberts, D. Azzopardi, P. Hamilton, and A. D. Edwards. Randomized double-blind controlled trial comparing the Effects of Ibuprofen with Indomethacin on Cerebral Hemodynamics in Preterm Infants with Patent Ductus Arteriosus. *Pediatr. Res.* **47**:36-36 (2000).
33. B. Van Overmeire, I. Follens, S. Hartmann, W. L. Creten and K. J. Van Acker. Treatment of patent ductus arteriosus with ibuprofen. *Arch. Dis. Child. Fetal Neonatal Ed.* **76**:179F-184 (1997).
34. J. S. Cohen. Why Aren't Lower, Effective, OTC Doses Available Earlier by Prescription? *Ann. Pharmacother.* **37**:136-142 (2003).
35. <http://web1.caryacademy.org/chemistry/rushin/StudentProjects/CompoundWebSites/1998/Ibuprofen/generic.htm>
36. L. E. Denton. Free-flowing ibuprofen granules. *PCT Int. Appl.* # **WO 8902266** (1989).

37. M. M. de Villiers, W. Liebenberg, S. F. Malan and J. J. Gerber. The dissolution and complexing properties of ibuprofen and ketoprofen when mixed with N-methylglucamine. *Drug Dev. Ind. Pharm.* **25**:967-972 (1999).
38. M. K. Ghorab and M. C. Adeyeye. Enhancement of ibuprofen dissolution via wet granulation with beta-cyclodextrin. *Pharm. Dev. Technol.* **6**:305-314 (2001).
39. Y. El-Said. Improvement of the dissolution rate of ibuprofen by spray-drying on microcrystalline cellulose. *J. Pharm. Sci.* **6**:87-107 (1989).
40. A. Debunne, C. Vervaet and J. P. Remon. Development and in vitro evaluation of an enteric-coated multiparticulate drug delivery system for the administration of piroxicam to dogs. *Eur. J. Pharm. Biopharm.* **54**:343-348 (2002).
41. K. E. Fielden, J. M. Newton and R. C. Rowe. Movement of liquids through powder beds. *Int. J. Pharm.* **79**:47-60 (1992).
42. K. E. Fielden, J. M. Newton P. O'Brien, and R. C. Rowe. Thermal studies on the interaction of water and microcrystalline cellulose. *J. Pharm. Pharmacol.* **40**:674-648 (1988).
43. <http://www.fmcbiopolymer.com/Biopolymer/>
44. J. Kristensen, T. Schaefer and P. Kleinebudde. Direct pelletization in a rotary processor controlled by torque measurements. II: Effects of changes in the content of microcrystalline cellulose. *Pharm. Dev. Tech.* **5**:247-256 (2000).
45. F. Nicklasson, B. Johansson and G. Alderborn. Occurrence of fragmentation during compression of pellets prepared from a 4 to 1 mixture of dicalcium phosphate dihydrate and microcrystalline cellulose. *Eur. J. Pharm. Sci.* **7**:221-229 (1999).

46. M. Dohi, Y. Uejima, T. Fujii. Powdery nasal compositions. *U. S. Patent # 6,428,805*, 2002.
47. B. N. Chukwumezie, M. Wojcik, P. Malak, M. C. Adeyeye. Feasibility studies in spheronization and scale-up of ibuprofen microparticulates using the fluid-bed technology. *AAPS PharmSciTech.* **3**:1-12 (2002).
48. J. Garcia and E. S. Ghaly. Evaluation of bioadhesive glipizide spheres and compacts from spheres prepared by extruder/marumerizer technique. *Pharm. Dev. Technol.* **6**:407-417 (2001).
49. P. W. S. Heng and O. M. Y. Koo. A study of the effects of the physical characteristics of microcrystalline cellulose on performance in extrusion spheronization. *Pharm. Res.* **18**:480-487 (2001).
50. J. M. Newton. The preparation of spherical granules by extrusion spheronization. *S.T.P. Pharma.* **6**:396-398 (1990).
51. J. A. C. Elbers, H. W. Bakkenes, J. G. Fokkens. Effect of amount and composition of granulation liquid on mixing, extrusion and spheronization. *Drug Dev. Ind. Pharm.* , **18**:501-517 (1992).
52. P. B. Deasy and M. P. Gouldson. In vitro evaluation of pellets containing enteric coprecipitates of nifedipine formed by non-aqueous spheronization. *Int. J. Pharm.* **132**:131-141 (1996).
53. S. R. Levis and P. B. Deasy. Pharmaceutical applications of size reduced grades of surfactant co-processed microcrystalline cellulose. *Int. J. Pharm.* **230**:25-33 (2001).

54. M. F. Law and P. B. Deasy. Effect of common classes of excipients on extrusion-spheronization. *Microencapsul.* **14**:647-57 (1997).
55. G. Dupont, M. P. Flament, P. Leterme, N. Farah and A. Gayot. Developing a study method for producing 400 microm spheroids. *Int. J. Pharm.* **247**:159-165 (2002).
56. S. Boutell, J. M. Newton, J. R. Bloor and G. Hayes. The influence of liquid binder on the liquid mobility and preparation of spherical granules by the process of extrusion/spheronisation. *Int. J. Pharm.* **238**:61-76 (2002).
57. R. Saowakontha, S. Jateleela, Somboon and P. Krisadaphong. Role of surfactants in fluidized bed granulation. II: Effects of various surfactants on the physical properties of sulfadimidine tablets. *Warasan Phesatchasat* **23**:13-21 (1996).
58. R. Junnila, J. Heinamaki and J. Yliruusi. Effects of surface-active agent on the size, shape and hardness of microcrystalline cellulose/maize starch pellets prepared by an extrusion-spheronization technique. *S.T.P. Pharma. Sci.* **8**:221-226 (1998).
59. M. T. Ercan. Radioactive microparticles: Part 2: medical applications. *Microspheres, Microcapsules & Liposomes* **2**:313-342 (1999).
60. A. J. Joshi. Microparticulates for ophthalmic drug delivery. *Ocul. Pharmacol.* **10**:29-45 (1994).
61. R. M. Palmer and H. E. Kaufman. Tear film, pharmacology of eye drops, and toxicity. *Curr. Opin. Ophthalmol.* **6**:11-16 (1995).
62. R. Herrero-Vanrell and M. F. Refojo. Biodegradable microspheres for vitreoretinal drug delivery. *Adv. Drug Deliv. Rev.* **52**:5-16 (2001).

63. V. P. Torchilin. Novel polymers in microparticulate diagnostic agents. *CHEMTECH* **29**:27-34 (1999).
64. V. P. Torchilin. Polychelating polymers as key components of microparticulate diagnostic agents. *Polymer Preprints* **39**:200-201 (1998).
65. M. J. Gamlen. Pellet manufacture for controlled release. *Manuf. Chem.* **56**:55-59, 1985.
66. K. W. Olsen. Fluid-bed equipment. *Pharm. Pelletization Tech.* Dekker, NY, pp. 39-70 1989.
67. I. Ghebre-Sellassie. Pellets: A general review. *Pharm. Pelletization Tech.* Dekker, NY, pp. 1-13 1989.
68. J. W. Conine and H. R. Hadley. Preparation of small solid pharmaceutical spheres. *Drug Cosmet. Ind.* **106**:38-41 (1970).
69. I. M. Jalal, H. J. Malinowski and W. E. Smith. Tablet granulation composed of spherical-shaped particles. *J. Pharm. Sci.* **61**:1466-1468 (1972).
70. A. Laicher and W. S. Fuchs. Pellet technology. Sustained-release pellets in hard gelatin capsules--a suitable dosage form for theophylline. *ARZNEIMITTEL-FORSCHUNG* **48**:540-547 (1998).
71. H. Lindner and P. Kleinebudde. Use of powdered cellulose for the production of pellets by extrusion/spheronization. *J. Pharm. Pharmacol.* **46**:2-7 (1994).
72. F. Podczeck and J. M. Newton. A shape factor to characterize the quality of spheroids. *J. Pharm. Pharmacol.* **46**:82-85 (1994).
73. M. Summers and M. Aulton. Granulation. *In Dosage form design and manufacture.* Ch. 25 pp 365 -378.

74. K. V. S. Sastry and D. W. Fuerstenau. Principles of agglomerating particulate materials by balling or granulation. *Proceedings - Institute for Briquetting and Agglomeration, Biennial Conference* **12**:113-124 (1971).
75. R. Thies and P. Kleinebudde. Melt pelletisation of a hygroscopic drug in a high shear mixer: Part 1. Influence of process variables. *Int. J. Pharm.* **188**:131-143 (1999).
76. P. Vonk, C. P. F. Guillaume, J. S. Ramaker, H. Vromans and N. W. F. Kossen. Growth mechanisms of high-shear pelletisation, *Int. J. Pharm.* **157**:93-102 (1997).
77. H. A. Rashid, J. Heinamaki and J. Yliruusi. Evaluation of four microcrystalline cellulose grades for preparing spherical beads in a centrifugal granulating process. *S.T.P. Pharma. Sci.* **8**:163-168 (1998).
78. S. H. Schaafsma, P. Vonk and N. W. Kossen. Fluid-bed agglomeration with a narrow droplet size distribution. *Int. J. Pharm.* **193**:75-187 (2000).
79. R. E. O'Connor and J. B. Schwartz. Extrusion and spheronization technology. *In Pharmaceutical Pelletisation technology*, Ghebre Selassie (Ed.), Ch. 7, Dekker, New York (1989).
80. R. D. Shah, M. Kabadi, D. G. Pope and L. L. Augsburger. Physicomechanical characterization of the extrusion-spheronization process. I. Instrumentation of the extruder. *Pharm. Res.* **11**:355-60 (1994).
81. J. F. Pinto, G. Buckton and J. M. Newton. The influence of four selected processing and formulation factors on the production of spheres by extrusion and spheronization. *Int. J. Pharm.* **83**:87-196 (1992).

82. L. Baert, D. Fanara, P. De Baets and J. P. Remon. Instrumentation of a gravity feed extruder and the influence of the composition of binary and ternary mixtures on the extrusion forces. *J. Pharm. Pharmacol.* **43**:745-749 (1991).
83. L. Baert, H. Vermeersch, J. P. Remon, J. Smeyers-Verbeke and D. L. Massart. Study of parameters important in the spheronization process. *Int. J. Pharm.* **96**:225-229 (1993).
84. L. Baert, D. Fanara, J. P. Remon and D. Massart. Correlation of extrusion forces, raw materials and sphere characteristics. *J. Pharm. Pharmacol.* **44**:676-678 (1992).
85. R. C. Rowe. Spheronization: a novel pill-making process. *Pharm. Int.* **6**:119-123 (1985).
86. K. Lovegreen and P. J. Lundberg. Determination of sphericity of pellets prepared by extrusion-spheronization and the impact of some process parameters. *Proceedings of the 18th Pharm. Tech. Conference.* Monte Cralo, 1989.
87. L. HellenY. Yliruusi and E. Kristofferson. Process variables of instant granulator and spheronizer: II. Size and size distributions of pellets. *Int. J. Pharm.* **96**:205-216 (1993).
88. L. Hasznos, I. Langer and M. Gyarmathy. Some factors influencing pellet characteristics made by an extrusion/spheronization process. Part I. Effects on size characteristics and moisture content decrease of pellets. *Drug Dev. Ind. Pharm.* **8**:409-437 (1992).
89. L. S. C. Wan, P. W. S. Heng and C. V. Liew. Spheronization conditions on spheroid shape and size. *Int. J. Pharm.* **96**:59-65 (1993)

90. B. Bataille, K. Ligarski, M. Jacob, C. Thomas and C. Duru. Study of the influence of spheronization and drying conditions on the physicommechanical properties of neutral spheroids containing Avicel PH 101 and lactose. *Drug Dev. Ind. Pharm.* **19**:653-671 (1993).
91. J. Perez and M. Rabiskova. Influence of the drying technique on theophylline pellets prepared by extrusion-spheronization. *Int. J. Pharm.* **242**:349-351 (2002).
92. R. M. Iyer, L. L. Ausburger, D. G. Pope and R. D. Shah. Extrusion/spheronization- effect of moisture content and spheronization time on pellet characteristics. *Pharm. Dev. Technol.* **1**:325-331 (1996).
93. J. Vertommen and R. Kinget. The influence of five selected processing and formulation variables on the particle size, particle size distribution and friability of pellets produced in a rotary processor. *Drug Dev. Ind. Pharm.* **23**:39-46 (1997).
94. A. D. Reynolds. A new technique for the production of spherical particles. *Mfg. Chem. Aerosol News* **41**:40-43 (1970).
95. D. M. Parikh. Fluid-bed processing in the 1990s. *Reprinted from Pharm. Technol. Suppl.* **October** (1996).
96. D. P. Rubino. Fluid-bed technology: Overview and criteria for process selection. *Pharm. Technol.* **June**:104-113 (1999).
97. VPS Corporation manual, with modifications.
98. T. Smith. Using cartridge filters for fluid-bed processes. *Powder and Bulk Engineering* **8**:19,21-4,26,28,30 (1994).

99. R. V. Nellore, G. S. Rekhi, A. S. Hussain, L. G. Tillman and L. L. Augsburger. Development of metoprolol tartrate extended-release matrix tablet formulations for regulatory policy consideration. *J. Contr. Rel.* **50**:247-56 (1998).
100. M. Hossain M and J. W. Ayres. Pharmacokinetics and pharmacodynamics in the design of controlled-release beads with acetaminophen as model drug. *J. Pharm. Sci.* **81**:444-448 (1992).
101. A. M. Mehta. Scale-up considerations in the fluid-bed processes for controlled release products. *Pharm. Tech.* **12**:46,47,50-52 (1988).
102. J. Z. Gao, A. Jain, R. Motheram, D. B. Gray and M. A. Hussain. Fluid-bed granulation of a poorly water soluble, low density, micronized drug: comparison with high shear granulation. *Int. J. Pharm.* **237**:1-14 (2002).
103. R. M. Iyer, L. L. Ausburger and D. M. Parikh. Evaluation of drug layering and coating: Effect of process mode and binder level. *Drug Dev. Ind. Pharm.* **19**:981-998 (1993).
104. C. Vecchio, F. Fabiani, M. E. Sangalli, L. Zema and A. Gazzaniga. Rotary tangential spray technique for aqueous film coating of indobufen pellets. *Drug Dev. Ind. Pharm.* **24**:269-274 (1998).
105. H. Kala, D. Hennig, H. Moldenhauer and G. Zessin. Construction, operation and initial experience with a laboratory apparatus for fluid-bed coating of particles. *Pharmazie* **38**:879-881 (1983).
106. A. Miwa, T. Yajima and S. Itai. Prediction of suitable amount of water addition for wet granulation. *Int. J. Pharm.* **195**:81-92 (2000).

107. J. Rantanen, E. Rasanen, J. Tenhunen, M. Kansakoski, J. Mannermaa and J. Yliruusi. In-line moisture measurement during granulation with a four-wavelength near infrared sensor: an evaluation of particle size and binder effects. *Eur. J. Pharm. Biopharm.* **50**:271-276 (2000).
108. G. I. Tardos, K. M. Irfan and P. R. Critical parameters and limiting conditions in binder granulation of fine powders. *Powder Technol.* **94**:245-258 (1997).
109. J. J. Sousa, A. Sousa, F. Podczeck and J. M. Newton. Factors influencing the physical characteristics of pellets obtained by extrusion-spheronisation. *Int. J. Pharm.* **232**:91-106 (2002).
110. H. J. Malinowski and W. E. Smith. Use of factorial design to evaluate granulations prepared by spheronization. *J. Pharm. Sci.* **64**:1688-1692 (1975).
111. S. Ogawa, T. Kamijima, Y. Miyamoto, M. Miyajima, H. Sato, K. Takayama, T. Nagai. A new attempt to solve the scale-up problem for granulation using response surface methodology. *J. Pharm. Sci.* **83**:439-443 (1994).
112. J. Vertommen, P. Rombaut, R. Kinget. Internal and external structure of pellets made in a rotary processor. *Int. J. Pharm.* **161**:225-236 (1998).
113. M. Kaji, H. Tomozawa, H. Miyanaga, T. Konuta, T. Toshinobu and H. Yazawa. Scale-up study for tumbling fluidized-bed granulation. *Pharm. Tech. Japan.* **11**:321-8 (1995).
114. J. F. Pinto, M. H. Lameiro and P. Martins. Investigation on the co-extrudability and spheronization properties of wet masses. *Int. J. Pharm.* **227**:71-80 (2001).

115. L. Alvarez, A. Concheiro, J. L. Gomez-Amoza, C. Souto and R. Martinez-Pacheco. Effect of microcrystalline cellulose grade and process variables on pellets prepared by extrusion-spheronization. *Drug Dev. Ind. Pharm.* **28**:51-456 (2002).
116. P. Kleinebudde, M. Schroder, P. Schultz, B. W. Muller, T. Waaler and L. Nymo. Importance of the fraction of microcrystalline cellulose and spheronization speed on the properties of extruded pellets made from binary mixtures. *Pharm. Dev. Tech.* **4**:397-404 (1999).
117. K. Umprayn, P. Chitropas and S. Amarekajorn. Influence of process variables on physical properties of the pellets using extruder and spheronizer. *Drug Dev. Ind. Pharm.* **25**:45-61 (1999).
118. C. V. Liew, L. S. Wan and P.W. Heng. Role of base plate rotational speed in controlling spheroid size distribution and minimizing oversize particle formation during spheroid production by rotary processing. *Drug Dev. Ind. Pharm.* **26**:953-963 (2000).
119. K. Knop and B. C. Lippold. Manufacture of granules and pellets in a pneumatically rotating fluidized bed. *Pharma. Acta Helv.* **67**:104-112 (1992).
120. J. K. Hughes and M. McNair. Process for preparing drug substances in beadlet form. *PCT Int. Appl.* # **WO 9300991** (1993).
121. R. Pisek, O. Planinsek, M. Odon, M. Tus and S. Srcic. Influence of rotational speed and surface of rotating disc on pellets produced by direct rotor pelletization. *Pharma. Ind.* **62**:312-319 (2000).

122. C. Schmidt and P. Kleinebudde. Comparison between a twin-screw extruder and a rotary ring die press. Part II: influence of process variables. *Eur. J. Pharm. Biopharm.* **45**:173-179 (1998).
123. D. Balakrishnan and M. R. Rao. Pressure drop and minimum fluidizing velocity in baffled fluidized beds. *Indian J. Tech.* **13**:199-204 (1975).
124. http://www.fluidairinc.com/magnaflo_2.htm
125. N. L. Franklin, P. H. Pinchbeck and F. Popper. A statistical approach to catalyst development. I. The effect of process variables on the vapor-phase oxidation of naphthalene. *Trans. Inst. Chem. Engrs.* **34**:280-293 (1956).
126. (<http://www.twequip.com/Equipment/k070100specs.htm>).
127. R. Pisek, J. Sirca, G. Svanjak and S. Srcic. Comparison of rotor direct pelletization (fluid-bed) and extrusion/spheronization method for pellet production. *Drugs Made in Germany* **45**:91-97 (2002).
128. M. Meshali, H. M. El-Banna and H. El-Sabbagh. Use of a fractional factorial design to evaluate granulations prepared in a fluidized bed. *Pharmazie* **38**:323-325 (1983).
129. H. A. Rashid, J. Heinamaki, O. Antikainen and J. Yliruusi. Influence of the centrifugal granulating process on the properties of layered pellets. *Eur. J. Pharm. Biopharm.* **51**:227-234 (2001).
130. M. C. Gohel, M. M. Patel, M. R. Patel and J. Gajjar. Studies in pellet preparation and development of modified release dosage forms of isosorbide dinitrate. *Eastern Pharmacist.* **39**:133-135 (1996).

131. H. A. Rashid, J. Heinamaki, O. Antikainen and J. Yliruusi. Effects of process variables on the size, shape, and surface characteristics of microcrystalline cellulose beads prepared in a centrifugal granulator. *Drug Dev. Ind. Pharm.* **25**:605-11 (1999).
132. B. Gajdos. Rotary granulators--evaluation of process technology for pellet production using a factorial experimental design. *Drugs Made in Germany.* **27**:30-34, 36 (1984).
133. I. Ghebre-Sellassie, R. H. Gordon, M. B. Fawzi and R. U. Nesbitt. Evaluation of a high speed pelletization process and equipment. *Drug Dev. Ind. Pharm.* **11**:523-1541 (1985).
134. T. Schaefer and O. Worst. Control of fluidized bed granulation. I. Effects of spray angle, nozzle height and starting materials on granule size and size distribution. *Arch. Pharm. Chem. Sci.* **5**:51-60 (1977).
135. B. Iskandarani, P. K. Shiroman and J. H. Clair. Scale-up feasibility in high-shear mixers: determination through statistical procedures. *Drug Dev. Ind. Pharm.* **27**:651-657 (2001).
136. S. Watano, Y. Sato, K. Miyanami, Y. Ito, T. Kamata and N. Oda. Scale-up of agitation fluidized bed granulation. III. Effects of powder feed weight and blade angle on granule size, shape and density. *Chem. Pharm. Bull.* **43**:1224-1226 (1995).
137. G. J. B. Horsthuis, J. A. H. Laarhoven, R. C. Rooij and H. Vroorans H. Studies on upscaling parameters of the Gral high shear granulation process. *Int. J. Pharm.* **92**:143-150 (1993).

138. L. H. Block. Scale-up of disperse systems: theoretical and practical aspects.
In: *Pharmaceutical dosage forms: Disperse systems*. Lieberman HA, Rieger MM, Banker GS, eds. New York: Marcel Dekker, pp 363-394 1998.
139. J. M. Matsen. Scale-up of fluidized bed processes: principle and practice.
Powder Technol. **88**:237-244 (1996).
140. A. Faure, P. York and R. C. Rowe. Process control and scale-up of pharmaceutical wet granulation processes: a review. *Eur. J. Pharm. Biopharm.* **52**:269-277 (2001).
141. L. H. Block. Process scale-up for pharmaceutical liquids and semisolids. *Am. Pharm. Rev.* **3**:12, 14-15 (2000).
142. J. M. Newton, S. R. Chapman and R. C. Rowe. The assessment of scale-up performance of the extrusion/spheronization process. *Int. J. Pharm.* **120**:95-99 (1995).
143. S. Watano, Y. Sato and K. Miyanami. Scale-up of agitation fluidized bed granulation. IV. Scale-up theory based on the kinetic energy similarity. *Chem. Pharm. Bull.* **43**:1227-1230 (1995).
144. L. L. Van Dierendonck, Scale up. Part 2. Similarity principles. Scale-up in bulk industry. *PT-Procestechniek* **45**:24-8 (1990).
145. R Edgeworth-Johnstone and M. W. Thring. Scaling-up of chemical plant and processes. *Joint Symposium Scaling-up Chem. Plant and Processes, London* (1957).
146. M. Zlokarnik. Scale-up of processes using material systems with variable physical properties. *Chem. Biochem. Eng. Quarterly* **15**: 43-47 (2001).

147. *FDA guidance for industry in <http://www.fda.gov/cder/guidance/cmc5.pdf>*
148. M. Landin, P. York, M. J. Cliff, R. C. Rowe and A. J. Wigmore. The effect of batch size on scale-up of a pharmaceutical granulation in a fixed bowl mixer granulator. *Int. J. Pharm.* **134**:243-246 (1996).
149. M. Landin, P. York, M. J. Cliff, R. C. Rowe and A. J. Wigmore. Scale-up of a pharmaceutical granulation in fixed bowl mixer-granulators. *Int. J. Pharm.* **133**:127-131 (1991).
150. T. Hlinak. Granulation and scale-up issues in solid dosage form development. *Am. Pharm. Rev.* **3**:33-36 (2000).
151. L. Mukadi, C. Guy and R. Legros. Parameter analysis and scale-up considerations for thermal treatment of industrial waste in an internally circulating fluidized bed reactor. *Chem. Eng. Sci.* **54**:3071-3078 (1999).
152. M. T. Hardin, D. A. Mitchell and T. Howes. Approach to designing rotating drum bioreactors for solid-state fermentation on the basis of dimensionless design factors. *Biotechnol. and Bioeng.* **67**:274-282 (2000).
153. A. Johansen and T. Schæfer. Effects of interactions between powder particle size and binder viscosity on agglomerate growth mechanisms in a high shear mixer,. *Eur. J. Pharm. Sci.* **12**:297-309 (2001).
154. G. A. Hileman, S. R. Goskonda, A. J. Spalitto and S. M. Upadrashta. Response surface optimization of high-dose pellets by extrusion and spheronization. *Int. J. Pharm.* **100**:71-79 (1993).

155. S. B. Bhardwaj, A. J. Shukla and C. C. Collins. Effect of varying drug loading on particle size distribution and drug release kinetics of verapamil hydrochloride microspheres prepared with cellulose esters. *J. Microencapsul.* **12**:71-81 (1995).
156. H. Atsumi, Y. Nozawa, Y. Sazuka, A. Miyagishima and T. Sonobe. Influence of load on particle size distribution of lactose fluidized powder. *Yakuzaigaku* **60**:88-100 (2000).
157. A. J. Shukla and J. C. Price. Effect of drug loading and molecular weight of cellulose acetate propionate on the release characteristics of theophylline microspheres. *Pharm. Res.* **8**:1396-1400 (1991).
158. J. S. Deng, L. Li, Y. Tian, E. Ginsburg, M. Widman and A. Myers. In vitro characterization of polyorthoester microparticles containing bupivacaine. *Pharm. Dev. Technol.* **8**:31-38 (2003).
159. Ibuprofen Official monograph. *United States Pharmacopoeia* **26/National Formulary** **21** p. 949 (2003).
160. S. Chen and R. Wetzel. Solubilization and disaggregation of polyglutamine peptides. *Protein. Sci.* **10**:887-91 (2001).
161. N. H. Gabboun, N. M. Najib, H. G. Ibrahim and S. Assaf. Release of salicylic acid, diclofenac acid and diclofenac acid salts from isotropic and anisotropic nonionic surfactant systems across rat skin. *Int. J. Pharm.* **212**:73-80 (2001).
162. G. Rafler and M. Jobmann. Controlled release systems of biodegradable polymers. 5th Communication: microparticle preparation by a salting-out process. *Drugs Made in Germany* **41**: 20-24 (1998).

163. T. Higuchi. Mechanism of sustained-release medication. Theoretical analysis of rate of release of solid drugs dispersed in solid matrices. *J. Pharm. Sci.* **52**:1145-1149 (1963).
164. S. E. Leucuta. Controlled release of nifedipine from gelatin microspheres and microcapsules: in vitro kinetics and pharmacokinetics in man. *J. Microencapsul.* **7**:209-217 (1990).
165. S. Mallick, K. Roy, A. Chakraborty and S. Saha. Mechanism of in vitro release kinetics of flurbiprofen loaded ethylcellulose micropellets. *Acta Pol. Pharm.* **59**:193-198 (2002).
166. <http://www.devicelink.com/mpb/archive/97/11/003.html>
167. <https://cop.ufl.edu/safezone/prokai/pha5100/6>.
168. S. N. Lloyd. Oral extended-release products. *Aust. Prescr.* **22**:88-90 (1999).
<http://www.australianprescriber.com/magazines/vol22no4/oral.htm>.
169. D. A. Alderman. Review of cellulose ethers in hydrophilic matrixes for oral controlled-release dosage forms. *Int. J. Pharm. Technol. Product Manuf.* **5**:1-9 (1984).
170. C. R. Young, J. J. Koleng and J. W. McGinity. Production of spherical pellets by a hot- melt extrusion and spheronization process *Int. J. Pharm.* **242**:87-92 (2002).
171. V. Batra, A. Bhowmick, B. K. Behera and A. R. Ray. Sustained release of ferrous sulfate from polymer-coated gum arabica pellets. *J. Pharm. Sci.* **83**:632-635 (1994).

172. G. M. Khan and Z. Jiabi. Formulation and in vitro evaluation of ibuprofen-carbopol 974P-NF controlled-release matrix tablets III: influence of co-excipients on release rate of the drug. *J. Control. Rel.* **54**:185-190 (1998).
173. J. L. Ford, M. H. Rubinstein, F. McCaul *et al.* Importance of drug type, tablet shape and added diluents on drug release kinetics from HPMC tablets. *Int. J. Pharm.* **40**:223-234 (1987).
174. J. J. Sousa, A. Sousa, M. J. Moura, F. Podczeczek and J. M. Newton. The influence of core materials and film coating on the drug release from coated pellets. *Int. J. Pharm.* **233**:111-122 (2002).
175. F. Sadeghi, J. L. Ford, M. H. Rubinstein and A. R. Rajabi-Siahboomi. Comparative study of drug release from pellets coated with HPMC or Surelease. *Drug Dev. Ind. Pharm.* **26**:651-660 (2000).
176. A. Gursoy and S. J. Cevik. Sustained release properties of alginate microspheres and tableted microspheres of diclofenac sodium. *J. Microencapsul.* **17**:565-575 (2000).
177. Y. Liu, J. B. Schwartz and R. L. Schnaare. A multimechanistic drug release approach in a bead dosage form and in vitro predictions. *Pharm. Dev. Technol.* **8**:163-173 (2003).
178. B. Narasimhan and R. Langer. Zero-order release of micro- and macromolecules from polymeric devices: the role of the burst effect. *J. Control. Rel.* **47**:13-20.
179. Calculations of drug release rates from controlled release devices. The slab. *Int. J. Pharm.* **2**:177-194 (1979).

180. Q. A. Thai, E. M. Oshiro and R. J. Tamargo. Inhibition of experimental vasospasm in rats with the periadventitial administration of ibuprofen using controlled-release polymers. *Stroke* **30**:140-147 (1999).
181. M. G. Papich. Principles of analgesic drug therapy. *Semin. Vet. Med. Surg. (Small Anim)* **12**:80-93 (1997).
182. D. A. Katzka, A. G. Sunshine and S. Cohen. The effect of nonsteroidal antiinflammatory drugs on upper gastrointestinal tract symptoms and mucosal integrity. *J. Clin. Gastroenterol.* **9**:142-148 (1987).
183. M. R. DiMatteo and D. D. DiNicola. Achieving patient compliance:the psychology of the medical practitioner's role. New York: *Pergamon Press*; 1982
184. K. E. Uhrich, S. M. Cannizzaro, R. S. Langer, and K. M. Shakesheff. Polymeric Systems for Controlled Drug Release. *Chem. Rev. (Washington, D. C.)* **99**:3181-3198 (1999).
185. F. Sadeghi, J. L. Ford, M. H. Rubinstein and A. R. Rajabi-Siahboomi. Study of drug release from pellets coated with Surelease containing hydroxypropylmethylcellulose. *Drug Dev. Ind. Pharm.* **27**:419-430 (2001).
186. R. S. Harland, C. Dubernet, J-P. Benoît and N. A. Peppas. A model of dissolution-controlled, diffusional drug release from non-swellable polymeric microspheres, *J. Control. Rel.* **7**:207-215 (1988).
187. S. Desai, S. Nadkarni, R. J. Wald, and G. A. De Brincat. Dual-release compositions of a cyclooxygenase-2 inhibitor. *PCT Int. Appl.* # **WO 0145706** (2001).

188. S. M. Lu and J-Y. Yu. Dimensionless presentation for drug release from a coated pure drug bead: 2. Experiment. *Int. J. Pharm.* **112**:117-124 (1994).
189. J. W. Moore and H. H.F lanner. Mathematical comparison of curves with an emphasis on in vitro dissolution profiles. *Pharm. Tech.* **20**: 64-74 (1996).
190. V. P. Shah, Y. Tsong and P. Sathe. In vitro dissolution profile comparison - statistics and analysis of the similarity factor, f2. *Pharm. Res.* **15**: 889-896 (1998).
191. V. P. Shah, Y. Tsong and P. Sathe and W. L. Roger. Dissolution Profile Comparison Using Similarity Factor, f2.
<http://www.dissolutiontech.com/DTresour/899Art/DissProfile.html>
192. <http://www.spwax.com/spcarnau.htm>
193. C. Tapia, G. Buckton and J. M. Newton. Factors influencing the mechanism of release from sustained release matrix pellets, produced by extrusion/spheronisation. *Int. J. Pharm.* **92**:211-218 (1993).
194. R. Chopra, G. Alderborn, J. M. Newton and F. Podczec. The influence of film coating on pellet properties. *Pharm. Dev. Technol.* **7**:59-68 (2002).
195. J. Akbuga. Preparation and evaluation of controlled-release furosemide microspheres by spherical crystallization. *Int. J. Pharm.* **53**:99-105 (1989).
196. J. L. Plummer, H. Owen, A. H. Ilsley and K. Tordoff . Sustained-release ibuprofen as an adjunct to morphine patient-controlled analgesia. *Anesth. Analg.* **83**:92-96 (1996).
197. A. Y. Lin, N. A. Muhammad, D. Pope and L. L. Augsburger. Study of crystallization of endogenous surfactant in Eudragit NE30D-free films and its

- influence on drug-release properties of controlled-release diphenhydramine HCl pellets coated with Eudragit NE30D. *AAPS PharmSci.* **3**:E14 (2001).
198. <http://www.rohmasia.com/HTML/process%20technologies.htm>
199. K. Lehman. Practical course in Film Coating of Pharmaceutical dosage forms with Eudragit[®]. http://www.rohmasia.com/HTML/practical_course_book.htm.
200. R. E. Robertson. Effect of free-volume fluctuations on polymer relaxation in the glassy state. *J. Polym. Sci. Polym. Symp.* **63**:173-183 (1978).
201. R. Bodmeier and O. Paeratakul. Propranolol HCl release from acrylic films prepared from aqueous latexes. *Int. J. Pharm.* **59**:197-203 (1990).
202. A. Gopferich and G. Lee. The influence of endogenous surfactant on the structure and drug-release properties of Eudragit NE30D-matrices. *J. Control. Rel.* **18**:133-144 (1992).
203. F. Podczek and B. E. Jones. The in vitro dissolution of theophylline from different types of hard shell capsules. *Drug Dev. Ind. Pharm.* **28**:1163-1169 (2002).
204. P. K. Heda, K. Muteba and L. L. Augsburger. Comparison of the formulation requirements of dosator and dosing disc automatic capsule filling machines. *AAPS PharmSci.* **4**:E17 (2002).
205. A. E. Lundqvist, F. Podczek and J. M. Newton. Compaction of, and drug release from, coated drug pellets mixed with other pellets. *Eur. J. Pharm. Biopharm.* **46**:369-79 (1998).

206. P. Mojaverian, P. H. Vlasses, S. Parker and C. Warner. Influence of single and multiple doses of oral ranitidine on the gastric transit of an indigestible capsule in humans. *Clin. Pharmacol. Ther.* **47**:382-388 (1990).
207. <http://www.capsugel.com/faq.html>.
208. <http://www.capsugel.com.br/pdf/conisnap.pdf>
209. R. Chopra, F. Podczeck, J. M. Newton and G. Alderborn. The influence of pellet shape and film coating on the filling of pellets into hard shell capsules. *Eur. J. Pharm. Biopharm.* **53**:327-333 (2002).
210. A. Hoffman, H. D. Danenberg, I. Katzhendler, R. Shuval, D. Gilhar and M. Friedman. Pharmacodynamic and pharmacokinetic rationales for the development of an oral controlled-release amoxicillin dosage form. *J. Control. Rel.* **54**:29-37 (1998).
211. <http://www.rjengineering.com/process.htm>.
212. <http://www.torpac.com/Reference/Torpac%20Dosing%20Guide.pdf>
213. Yamamoto, Taizo, Konishi and Hirokazu. Capsule filling machine. *US Patent # 6,499,279* (2002).
214. L. E. Small and L. L. Augsburger. Aspects of the lubrication requirements for an automatic capsule filling machine. *Drug Dev. Ind. Pharm.* **4**:345-372 (1978).
215. B. E. Jones. The filling of powders into two-piece hard capsules. *Int. J. Pharm.* **227**:5-26 (2001).
216. G. E. Reier, R. M. Cohn, S. Rock and F. Wagenblast. Evaluation of factors affecting the encapsulation of powders in hard gelatin capsules. I. Semiautomatic capsule machines. *J. Pharm. Sci.* **57**:660-666 (1968).

217. *Romaco capsule filling machine operation manual.*
218. K. Shah, L. L. Augsburger, L. E. Small and G. P. Polli, Gerald P. Instrumentation of a dosing disc automatic capsule filling machine. *Pharm. Technol.* **7**:42, 44, 46, 48, 52-4 (1983).
219. F. Podczeck. The development of an instrumented tamp-filling capsule machine I Instrumentation of a Bosch GKF 400S machine and feasibility study *Eur. J. Pharm. Biopharm.* **10**:267-274 (2000).
220. K. B. Shah, L. L. Augsburger and K. Marshall. Multiple tamping effects on drug dissolution from capsules filled on a dosing-disk type automatic capsule filling machine. *J. Pharm. Sci.* **76**:639-645 (1987).
221. B. Hauer, T. Remmele and H. Sucker. Rational development and optimization of capsule formulations with an instrumented dosing capsule filling machine. Part 2. Fundamentals of the optimization strategy. *Pharmazeutische Ind.* **55**:780-786 (1993).
222. L. L. Augsburger. Instrumented capsule filling machines. Methodology and application to product development. *S.T.P. Pharma* **4**:116-122 (1988).
223. D. J. Rowley, R. Hendry, M. D. Ward and P. Timmins. The instrumentation of an automatic capsule filling machine for formulation design studies. *Expo. Congr. Int. Technol. Pharm.* **5**:287-291 (1983).
224. F. Podczeck, S. Blackwell, M. Gold and J. M. Newton. The filling of granules into hard gelatine capsules. *Int. J. Pharm.* **188**:59-69 (1999).
225. K. Kurihara and I. Ichikawa. Effect of powder flowability on capsule-filling-weight-variation. *Chem. Pharm. Bull.* **26**:1250-1256 (1978).

226. http://www.romaco.com/Romaco_Group/products/default.asp?_fn=search
227. D. Lightfoot. Multiparticulate encapsulation equipment and process. *In Multiparticulate oral drug delivery*. I Ghebre-Sellassie (Ed.), Marcel Dekker Inc, NY, Vol 65, Ch. 8, pp 159-280 (1994).
228. J. M. Newton. Filling of hard gelatin capsules. *S.T.P. Pharma* **3**:880-885 (1987).
229. F. Podczeck and J. M. Newton. Powder filling into hard gelatin capsules on a tamp filling machine. *Int. J. Pharm.* **185**:237-254 (1999).
230. L. A. Felton, D. I. Garcia and R. Farmer. Weight and weight uniformity of hard gelatin capsules filled with microcrystalline cellulose and silicified microcrystalline cellulose. *Drug Dev. Ind. Pharm.* **28**:467-472 (2002).
231. J. M. Newton and F. N. Razzo. The influence of additives on the presentation of a drug in hard gelatin capsules. *J. Pharm. Pharmacol.* **29**:294-247 (1977).
232. Formulation of sustained-release products: dissolution and diffusion-controlled release from gelatin films, *Int. J. Pharm.* **20**:87-98 (1984).
233. W. J. Bowtle. Liquid filling of hard gelatin capsules: a new technology for alternative formulations. *Pharm. Technol. Eur.* **10**:84,86,88-90 (1998).
234. N. H. Shah, W. Phuapradit and H. Ahmed. Liquid/semi-solid filling in hard gelatin capsules: formulation and processing considerations. *Bulletin Technique/Gattefosse Report* **89**:27-38 (1996).
235. http://www.americanpharmaceuticalreview.com/industry_news/industry_news_heder.htm

236. H. Krasowski, W. Pfeifer, G. Marquardt and U. Klass. Automatic control by ultrasonic for the filling of pellets into hard gelatin capsules. *Pharmazeutische Ind.* **57**:328-332 (1995).
237. H. Moeller. In vitro release, bioavailability and in vivo release of propranolol from sustained-release preparations. *Acta Pharma. Technol.* **29**:287-294 (1983).
238. C. M. Adeyeye and J. C. Price. Chemical, dissolution stability and microscopic evaluation of suspensions of ibuprofen and sustained release ibuprofen-wax microspheres. *J. Microencapsulation* **14**:357-377 1997.
239. J. C. Tsao and T. S. Savage. High-performance liquid chromatographic determination of ibuprofen in bulk drug and tablets. *Drug Dev. Ind. Pharm.* **5**:1123-1131 (1985).
240. R. E. Gordon, W. T. Rosanske, D. E. Fonner, N. R. Anderson and G. S. Banker. Granulation technology and tablet characterization. In: Lieberman HA, Lachman L, Schwartz JB, eds. *Pharmaceutical dosage forms: Tablets*, New York: Marcel Dekker, 245-348 (1990).
241. M. F. L. Law and P. B. Deasy. Use of canonical and other analyses for the optimization of an extrusion-spheronization process of indomethacin. *Int. J. Pharm.* **146**:1-9 (1997).
242. C. R. Hicks. Fundamental concepts in the design of experiments, 4th edition. **Ch. 5**, pp 121-137 (1994).
243. D. A. Doornbos. Optimization in pharmaceutical sciences. *Pharmaceutisch Weekblad - Scientific Edition.* **3**:33-61 (1981).

244. G. Keppel. Design and analysis: *A researcher's handbook*, 3rd edition. Prentice Hall p. 482 (1991).
245. N. D. Eddington, M. Ashraf , L. L. Augsburger, J. L. Leslie, M. J. Fossler , L. J. Lesko, V. P. Shah and G. S. Rekhi. Identification of formulation and manufacturing variables that influence in vitro dissolution and in vivo bioavailability of propranolol hydrochloride tablets. *Pharm. Dev. Technol.* **3**:535-547 (1998).
246. J. Philippe (Ed.). *Les methodes statistiques en pharmacie et en chimie* (applications a la production et au controle), Masson, Paris, pp 195-223 (1967).
247. C. Ortigosa. La planification experimentale dans les sciences pharmaceutiques. *Lyon Pharm.* **42**:495-500 (1991).
248. M. K. Vuppala, D. Parikh and H. R. Bhagat. Application of powder-layering technology and film coating for manufacture of sustained-release pellets using a rotary fluid-bed processor. *Drug Dev.Ind. Pharm.* **23**:687-694 (1997).
249. K. Eichler. Current trends in solid dose manufacture. In: *Pharm.Manuf. Rev.* February, 1997.
250. J. M. Newton., S. R. Chapman and R. C. Rowe. The influence of process variables on the preparation and properties of spherical granules by the process of extrusion and spheronisation. *Int. J. Pharm.* **120**:101-109 (1995).
251. S. Watano, Y. Sato, K. Miyanami, Y. Ito, T. Kamata and N. Oda. Scale-up of agitation fluidized bed granulation. I. Preliminary experimental approach for optimization of process variables. *Chem. Pharm. Bull.* **43**:1212-1216 (1995).

252. T. Schaefer and O. Worts. Control of fluidized bed granulation. III. Effects of inlet air temperature and liquid flow rate on granule size and size distribution. Control of moisture content of granules in the drying phase. *Arch. Pharm. Chemi. Sci.* Ed. **6**:1-13 (1978).
253. Z. Ormos, K. Pataki and B. Csukas. Granulation in a fluidized bed. II. Effects of the amount of the binder on the physical properties of granules formed in a fluidized bed. *Hung J. Ind. Chem.* **1**:307-328 (1973).
254. E. S. Ghali, G. H. Klinger and J. B. Schwartz. Modified drug release from beads prepared from with combinations of two grades of microcrystalline cellulose. *Drug Dev. Ind. Pharm.* **15**:1455-1473 (1989).
255. R. E. O'Connor and J. B. Schwartz. Spheronization: II. Drug release from drug-diluent mixtures. *Drug Dev. Ind. Pharm.* **11**:1837-1857 (1985).
256. S. Watano, Y. Sato, K. Miyanami, T. Murakami, N. Nagami, Y. Ito, T. Kamata and N. Oda. Scale-up of agitation fluidized bed granulation. II. Effects of scale, air flow velocity and agitator rotational speed on granule size, size distribution, density and shape. *Chem. Pharm. Bull.* **43**:1217-1220 (1995).
257. D. Bains, S. L. Boutell and J. M. Newton. The Influence of Moisture Content on the Preparation of Spherical Granules of Barium Sulfate and Microcrystalline Cellulose. *Int. J. Pharm.* **69**:233-237 (1991).
258. A. M. Metha. Evaluation and Characterization of Pellets. In *Pharmaceutical Pelletization Technology*, Ghebre-Sellasie, I., Ed., Dekker, New York, 1989, 241-265.

259. J. Vertommen, A. Michoel, P. Rombaut and R. Kinget. Production of pseudoephedrine HCl pellets in a high shear mixer-granulator. *Eur. J. Pharma. Biopharm.* **40**:32-35 (1994).
260. D. Sonaglio, B. Bataille, C. Ortigosa and M. Jacob. Factorial Design in the Feasibility of Producing Microcel MC 101 Pellets by Extrusion/Spheronization. *Int. J. Pharm.* **115**:53-60 (1995).
261. J. Vertommen, P. Rombaut and R. Kinget. Shape and Surface Smoothness of Pellets Made in a Rotary Processor. *Int. J. Pharm.* **146**:21-29 (1997).
262. G. Zhang, J. B. Schwartz and R. L. Schnaare. Effect of spheronization technique on drug release from uncoated beads. *Drug Dev. Ind. Pharm.* **16**:1171-84 (1990).
263. S. C. Potter. Factors in the development of modified release pellets. *Drugs and Pharmaceutical Sciences.* **65**: 237, Chap. 10. I. Ghebre-Sellasie (Ed.).
264. A. Nokhodchi, P. Zakeri-Milani, H. Valizade and D. Hassan-Zadeh. Evaluation of microcapsules of acetyl salicylic acid prepared with cellulose acetate phthalate, ethylcellulose or their mixtures by an emulsion non-solvent addition technique. *Ars Pharmaceutica* **43**:135-147 (2002).
265. G. Zhang, J. B. Schwartz and R. L. Schnaare. Bead coating. I. Change in release kinetics (and mechanism) due to coating levels. *Pharm. Res.* **8**:331-335 (1991).
266. N. H. Shah, L. Zhang, A. Railkar, I. Trivedi, C. I. Patel, M. H. Infeld, A. W. Malick and L. K. Wong. Factors affecting the kinetics and mechanism of release of cilazapril from beadlets coated with aqueous and nonaqueous ethyl cellulose-based coatings. *Pharm. Technol.* **18**:140,142,144,146,148-9 (1994).

VII. ABSTRACT

The aim was to develop uncoated and coated ibuprofen microparticulates in a one-step fluid-bed machine with rotor-disk insert, for immediate and prolonged drug delivery. Feasibility studies using ibuprofen:Avicel[®] (RC-581; 50:50), sodium lauryl sulfate (1%) as surfactant and water as binder in FLM-15 Vector Flo-coater with 12" stainless-steel and waffle-disk inserts showed that amount of binder, plate type and the presence of surfactant affected most of spheroid characteristics. These variables were used in a 2x2x3 full factorial (replicated) experiment. Blocking was used to study batch-to-batch reproducibility of the process and product variables. Our results confirmed that the binder amount, plate-type and the presence of surfactant were important variables in rotor-disk spheronization. The amount of binder was the most critical. The batch with the most acceptable product characteristics was chosen as the optimized formulation, and used to statistically study the effects of other formulation variables *viz*, drug particle size (20 μm , 40 μm) and drug load (50%, 65%, 80%) in a 2x3 factorially designed (replicated) experiment. The two ibuprofen particle sizes and the three drug loads were spheronizable. However, spheronization of the higher drug load was more difficult and yielded larger sized microparticulates that consequently retarded drug release. The 65% drug load was therefore used for intermediate size scale-up, which resulted in spheroids with good product characteristics.

The optimized scaled-up batch was used in a 2x3 factorially designed (replicated) experiment to study the effects of polymer type (Surelease[®], Eudragit[®] NE-30D) and level (low, medium, high) on the developed microparticulates. Coating level was found to be inversely related to the drug release. The batch coated with the highest Surelease[®]

level yielded the most acceptable spheroid characteristics, including most prolonged release. The latter and the uncoated spheroids were encapsulated using a 2x2x3 experiment in Romaco Index-*K150i* machine. The average fill-weight of the encapsulated spheroids was mostly affected by the formulation type. Encapsulation of the microparticulates had no undesirable effects on the qualities of both the uncoated and coated pellets.

This study provides spheronized ibuprofen microparticulates that can be sold as ready-to-use modified ibuprofen to pharmaceutical companies owing to their lots of pharmaceutical market potentials.